The generation and analysis of transgenic *Arabidopsis* plants with improved capacity to recover from severe drought stress

by

Christopher Waterman

Thesis
Submitted to Flinders University
for the degree of

Doctor of Philosophy

College of Science and Engineering

September 2020

Table of contents

Table of figures

Table of tables

Declaration

I certify that this thesis does not incorporate without acknowledgement any material previously submitted for a degree or diploma in any university; and that to the best of my knowledge and belief it does not contain any material previously published or written by another person except where due reference is made in the text

……

Christopher Waterman

June 2020

I believe that this thesis is properly presented, conforms to the specifications for the thesis and is of sufficient standard to be, *prima facie,* worthy of examination

……

Prof. Kathleen Soole

June 2020

Summary

The alternative pathway (AP) is a non-phosphorylating respiratory pathway present in plant mitochondria as well as being found in lower eukaryotes and other organelles, such as the chloroplast. Flux through this pathway generates heat from the energy carried in, the electron carriers NAD(P)H and FADH2, rather than conserving the energy in ATP synthesis. Despite its seemingly wasteful nature, the AP plays an important role in stress tolerance and signalling. Although it clearly plays a role in general stress tolerance, how this benefit is conveyed is still unclear. Previous experimenters have highlighted the importance of alternative oxidase (AOX1a*)* in stress tolerance using RNAi and overexpressor (OEX) models under a range of stressors, with clear detriments and benefits being found respectively. Other research has also found this isoform is commonly co-expressed with another AP member, type II NADH dehydrogenase (NDB2) in response to many stressors, but far less is known regarding its role in stress tolerance. In this study we aimed to generate lines co-overexpressing both of these AP members and exposing them to a combined drought and light stress, determining their response using a variety of different methodologies.

Three dual OEX lines generated from individual insertion events all showed increased expression of *Ndb2* and *Aox1a* both at the transcriptional and protein level. Activity was assessed using isolated mitochondria and is the first example to show the Arabidopsis NDB2 to be NADH specific and calcium activated in a homologous expression system. Previous single *Ndb2* OEX lines generated in our lab have failed to show any changes to activity. Interestingly, the co-OEX model generated in our hands

were able to show significant increases in activity and further increases in the presence of AOX activators, highlighting the important connectedness these two AP members share.

Phenotype was assessed along with a number of biochemical and gas exchange measurements. Unlike the single OEX lines, the dual OEX lines showed minimal delay in growth milestones and were similar to the wildtype line under control conditions. There were minimal differences in the dual OEX lines compared to the wildtype line under control conditions. There was a small reduction in CO_2 assimilation rate in the double OEX lines compared to wildtype and single *Aox1a* OEX. Notably, oxidative damage marker TBARS, was reduced under control conditions in all transgenic lines tested compared to wildtype.

These lines were then tested under drought and light stress conditions to determine changes to tolerance and their ability to recover from stress. In our tests, both the single *Aox1a* OEX and dual OEX lines show clear advantage over both wildtype and single *Ndb2* OEX lines in their ability to recover from drought. With the addition of *Ndb2* OEX to the single *Aox1a* OEX line, the number of plants able to recover from drought significantly exceeded the single *Aox1a* OEX. Although gas exchange and stress marker measurements were made on these lines under stress, an answer for how the dual OEX is conveying the improvements to recovery was not clear.

A global transcriptomic approach was applied to investigate the potential pathways that could have contributed to the improved recovery. A clear shift in

signalling was demonstrated with a number of carbon and nitrogen metabolism pathways altered possibly linked also to a strong change in hormone signalling. Both single and dual OEX lines also showed upregulation of stress responsive pathways under control conditions suggesting these plants were primed for a general incoming stress. The large changes caused by altering expression of the AP highlighted the importance these genes have on controlling regulatory signals and their homeostatic role.

Acknowledgements

First, I would like to thank all my supervisors; Prof. Kathleen Soole, Assoc. Prof. Colin Jenkins, Prof. David Day and Dr Crystal Sweetman. I appreciate all your input, efforts, patience and willingness to improve myself and my work. Thank you for looking through my experimental data and reading my thesis. Thankyou especially to Kathleen and Crystal for your compassion and patience on a personal level. I would also like to thank Dr Peter Anderson and Dr Yuri Shavrukov for your thoughtful and friendly contributions to my experiments during our weekly lab meetings and morning tea.

Next, to all my friends inside the school of biological sciences, you've made this process all the more bearable. Thank you to Dr Arif Malik for all our quick lunches and love of the university, to Alex McDonald for all your thoughtful discussions (especially the ones off-topic), to Jason Smith for all your help especially with anything mathematical, to Barry Rainbird for your help in the lab and maintaining the office at sub-zero temperatures, to Lettee Dametto for all the shared laughter, to Lauren Philip-Dutton for sharing my frustrations within the lab. Thank you to all the lab members present and past including Carly Schramm, Vajira Wanniarachchi, Thanh Hai Tran, Hayden Burdett, Emma de Courcy-Ireland, Badr Alharthi, Nick Booth, Troy Miller, Shayne Faulkner, Motiur Rahman, Lam Nguyen, Nick Warnock and anyone else I forgot to mention.

I would like to thank my family and friends for all their support they've given me throughout my long candidature, you guys are awesome!

Last but definitely not least I'd like to thank my wonderful partner Dr Saira Ali. You are such an amazing, wonderful and kind human being. Your patience and compassion all throughout my PhD have been so important to me. I look forward to sharing our post PhD lives together and giving you the love and attention, you deserve.

I acknowledge the contribution of the Australian Government Research Training Program Scholarship for its contribution to my candidature.

Abbreviations

Acetyl-CoA	Acetyl coenzyme A
ADP	Adenosine di-phosphate
AGRF	Australian Genomic Research Facility
ANOVA	Analysis of variance
AOX	Alternative oxidase
AP	Alternative pathway
APX	Ascorbate peroxidase
ADP	Adenosine-diphosphate
AOX	Alternative oxidase
ATP	Adenosine triphosphate
BCA	Bicinchoninic acid
BLAST	Basic local alignment tool
BSA	Bovine Serum Albumin
Ca^{2+}	Calcium ion
CAC	Citric acid cycle
$CaCl_2$	Calcium chloride
cDNA	Complementary deoxyribonucleic acid
CO_2	Carbon Dioxide
COX	Cytochrome oxidase
DEPC	Diethylpyrocarbonate
dNTP	Deoxyribonucleotide
DTT	Dithiothreitol
EDTA	Ethylene di-amine tetra acetic acid
EGTA	Ethylene glycol tetra acetic acid
ETC	Electron transport chain
FADH	Flavin adenine dinucleotide
Fmol	Femtomoles
FW/DW	Fresh weight/Dry weight
GA	Glufosinate ammonium
gDNA	Genomic deoxyribonucleic acid
GR	Glutathione reductase
GO	Gene ontology
GPX	Glutathione peroxidase
GST	Glutathione S-transferase
H2O	Water
H_2O_2	Hydrogen Peroxide
IM	Intermembrane
IMS	Intermembrane space
Kb/Bp	Kilo base pair/Base pair
kDa	Kilodalton

KEGG	Kyoto Encyclopedia of Genes and Genomes
LB	Luria Broth
MDHAR	Monodehydroascorbate reductase
mETC	Mitochondrial electron transport chain
$MgCl_2$	Magnesium chloride
MPC	Mitochondrial pyruvate carrier
mRNA	Messenger Ribonucleic acid
MS	Murashige and Skoog
NAD+	Nicotinamide adenine dinucleotide (oxidised)
NADH	Nicotinamide adenine dinucleotide (reduced)
NAD-ME	Nicotinamide adenine dinucleotide malic enzyme
NADP+	Nicotinamide adenine dinucleotide phosphate (oxidised)
NADPH	Nicotinamide adenine dinucleotide phosphate (reduced)
NCBI	National Centre for Biotechnology Information
NDE/NDB	External type II NAD(P) dehydrogenases
NDH	Type II NAD(P)H dehydrogenases
NDI/NDA	Internal type II NAD(P) dehydrogenases
Ng	Nanograms
O.D.	Optical density
OEX	Overexpressor
O_2	Oxygen
OM	Outer membrane
PCD	Programmed cell death
PCR	Polymerase chain reaction
PDC	Pyruvate dehydrogenase complex
PEG	Polyethylene glycol
PEPCK	Phosphoenolpyruvate carboxykinase
pETC	Plant electron transport chain
Pi	Inorganic phosphate
PPi	Pixel per inch
qPCR	Quantitative polymerase chain reaction
RE	Restriction enzyme
RGR	Relative growth rate
RNA	Ribonucleic acid
RNAi	Ribonucleic acid interference
ROS	Reactive oxygen species
SDS-PAGE	Sodium dodecyl sulphate-Polyacrylamide gel electrophoresis
SEM	Standard error of the mean
SOD	Superoxide dismutase
Ta	Thermal annealing temperature
TAE	Tris-acetate-EDTA
TAIR	The Arabidopsis Information Resource
TCAC	Tricarboxylic acid cycle

TE	Tris-EDTA
UV	Ultraviolet
w/v	Weight/volume

Chapter 1

Introduction

1. Introduction

1.1. Plant respiration and the plant mitochondrial electron transport chain

The primary pathways for carbon and energy metabolism in plants occur through photosynthesis and respiration. Photosynthesis converts light energy received through light harvesting complexes bound within chloroplasts to drive the production of energy rich carbohydrates. Respiration can utilise these complex sugars to support and maintain plant growth through their supply of ATP and carbon intermediates. Respiration in plants occurs via three interconnected and tightly regulated pathways existing in the cytosol and mitochondria.

Respiration occurs firstly in the cytosol via a series of stepwise reactions. Glycolysis acts to consolidate several metabolic inputs into one pathway. From the perspective of energy production, glycolysis is primarily concerned with the formation of pyruvate and its transport and conversion into ATP in the mitochondria. The glycolytic pathway is a highly branched network, containing many offshoot anabolic pathways involved in the production of proteins, nucleic acids, adenylates, pyridine nucleotides and many other key components to survival. Thus, over accumulation of metabolites inhibiting the glycolytic pathway has potential to perturb systems both down and upstream and therefore may benefit from a bypass "valve" downstream, which at the detriment of energy conservation, provides a way of

removing the bottleneck built up within the pathway and hence allow for positive flux to anabolic reactions.

Pyruvate may enter the mitochondrial IM through mitochondrial pyruvate carriers (MPC), or through NAD-Malic enzyme (NAD-ME) or phosphoenolpyruvate carboxykinase (PEPCK) as malate. Malate can then be converted into pyruvate through NAD-ME or PEPCK. Arabidopsis doesn't contain mitochondrial localised NAD-ME and therefore pyruvate only enters through the MPC (Maier et al. 2011).Also no evidence seems to exist that PEPCK exist in *Arabidopsis* mitochondria. The formation of pyruvate may be considered the end product of glycolysis and represents a pivotal regulatory node in carbon metabolism. Pyruvate exists at a focal point between energising the tricarboxylic citric acid cycle (TCAC) through Acetyl-CoA formation and providing substrate for both fatty and amino acid biosynthesis as well as gluconeogenesis. The regulation of this equilibrium is maintained in part by the pyruvate dehydrogenase complex (PDC) present in the mitochondrial matrix. Transport of pyruvate across the outer membrane and into the mitochondria is facilitated by the passive diffusion through large non-discriminative voltage dependent anion channels enabling pyruvate to reach the intermembrane space (IMS) (Benz 1994; Schell et al. 2013). Movement of pyruvate across the IM and into the matrix is largely reliant on MPC. Only recently have three conserved MPC gene families been identified in yeast, drosophila and humans respectively (Bricker et al. 2012; Herzig et al. 2012). Upon transportation into the mitochondrial matrix, pyruvate is either oxidised into acetyl-coA or becomes a precursor to alanine or leucine and valine. It is

through the demand of adenylate and pyridines (among others) that allows for the activation or inactivation of the PDC and as such the amount of acetyl-coA formed, demonstrating both adenylate and pyridine nucleotides regulatory control over flux through the TCAC and thus respiration and biosynthesis of lipids and proteins (Shen & Atkinson 1970).

Enzymes of the TCAC are present in the mitochondrial matrix (except for succinate dehydrogenase, which is embedded in the IM). This cycle constitutes the second phase in respiration and allows unification of fatty acid, protein and carbohydrate metabolism. A new acetyl-CoA molecule is required for every new turn of the cycle and can be provided by the breakdown of pyruvate or fatty acids. Sugars, fats and proteins can also be metabolised to form intermediates of the TCAC, and with each turn of the TCAC, three NADH, one FADH2, one ATP and two CO_2 molecules are formed per molecule of acetyl-CoA. The energy from NADH and FADH2 is channelled through the mitochondrial electron transport chain (mETC) for production of ATP. Expression analysis of TCAC components consistently suggests that the majority of mitochondrial enzymes are expressed constitutively in most organs. Enzymes of the TCAC however, are highly sensitive to allosteric inhibition and post-translational regulation. The majority of the enzymes involved in the citric acid cycle are allosterically regulated by NADH and to a lesser extent ATP and acetyl-CoA (Oestreicher et al. 1973; Verniquet et al. 1991; Behal et al. 1997; Falk et al. 1998; Affourtit et al. 2001; Igamberdiev & Gardeström 2003; Studart-Guimaraes et al. 2005; Bunik & Fernie 2009; Araujo et al. 2012) adding to the hypothesis that the TCAC is regulated

primarily via redox and energy status. Furthermore, production of pyruvate is regulated via the PDC which again is strongly regulated via ATP, galvanising both the adenylate and pyridine nucleotides roles in regulating carbon flux. It is very likely that the control over carbon flux through NADH:NAD^+ and ATP:ADP ratios is partly a result of the organism's attempt to mitigate oxidative damage in the electron transport chain from over accumulation of said substrates (Murphy 2009). A result of the over accumulation of ATP and NADH are the non-regulated formation of reactive oxygen species (Sharma et al. 2012) which if left unkempt leads to oxidative damage of proteins, lipids and nucleic acids, eventually forcing the cell into programmed cell death.

1.2. Reactive oxygen species (ROS)

ROS is a collective term used to encompass various species of free oxygen radicals that form from the reduction of molecular oxygen. The term covers multiple different oxygen free radicals each with different levels of toxicity and stability. ROS are commonly used in cells as signalling molecules, as their overproduction can be used to signal instability in the mETC, chloroplast and peroxisomes and act to remediate cellular damage and prevent PCD where appropriate. Increased ROS formation is linked to the perturbation of the cell's respiration, allowing for changes in metabolism to occur based on disruptions to the respiratory pathway.

During the multiple electron transfer events that occur as a result of aerobic respiration, production of reactive oxygen species can occur. This is due to the spin of

both outer electrons in molecular O_2 being oriented in parallel. The parallel spins are inherently stable and are therefore not very reactive. However, if enough energy is supplied and one of the unpaired electrons becomes excited, spin orientation is changed, and reactive singlet oxygen is formed. Complexes I and III produce primarily superoxide anion, ($O_2^{-}\bullet$) a form of singlet oxygen, which either reduces cytochrome c or is converted to hydrogen peroxide (H_2O_2) and oxygen through a series of enzyme catalysed reactions. If concentrations of $O_2^{-}\bullet$ are maintained, $O_2^{-}\bullet$ can react with reduced Fe^{2+} and Cu^{+}, which can further react with H_2O_2 causing the formation of highly toxic hydroxyl radicals (OH•) or peroxynitrite, both of which are powerful, indiscriminate oxidants (Turrens 2003). These powerful oxidants, if left to accumulate cause further oxidation of lipids, proteins and nucleic acids resulting in irreparable damage and eventually apoptosis of the cell.

There are two primary conditions that have been identified in isolated mitochondria that allow for the significant production and efflux of ROS. The first is a high NADH:NAD+ ratio present within the mitochondrial matrix (high redox potential). This leads to instability in the flavin moiety of complex I, causing undue production of superoxides (Hansford et al. 1997; Kudin et al. 2004; Kussmaul & Hirst 2006). The other conditions favourable to ROS generation are a highly reduced ubiquinol pool, in the presence of a high proton motive force with very low ATP synthesis (Hansford et al. 1997; Korshunov et al. 1997; Brand et al. 2004). Although complex III has long been associated with ROS production, Murphy (2009) and colleagues have suggested that complex III role in ROS production *in vivo* is negligible

compared with that of complex I although further research would be required to confirm this.

1.1.1 Enzymatic detoxification of reactive oxygen species

Plants have evolved multiple enzymatic and non-enzymatic scavenging and detoxification pathways to mitigate the accumulation of ROS species. Non-enzymatic antioxidants include ascorbate, glutathione, tocopherol, alkaloids, flavonoids and carotenoids (Gechev et al. 2006), of which ascorbate and glutathione act as ROS buffers, minimising accumulation of ROS. To do this, both glutathione and ascorbate are oxidised by ROS to form their oxidised counterparts. To maintain optimal levels of ROS scavenging, high ratios of reduced to oxidised glutathione and ascorbate need to be preserved. This is sustained through the recycling pathway of ascorbate-glutathione cycle and glutathione peroxidase cycle (Figure 1.1) which catalyses the reformation of reduced ascorbate and glutathione through ascorbate peroxidase (APX), monodehydroascorbate reductase (MDHAR), dehydroascorbate reductase (Corpas et al.), glutathione reductase (GR), (Affourtit et al. 2001) glutathione S-transferase (GST) and glutathione peroxidase (GPX) utilising NADPH as a reductant (Gechev et al. 2006). Both cycles however only detoxify H_2O_2 and therefore rely on superoxide dismutase (SOD) to convert singlet oxygen to H_2O_2 and thus are limited by the activity of SOD. These detoxification systems work downstream of ROS production and therefore do not act to stem the flow of ROS formation. Thus, a means to minimise the active source of ROS and the conditions that favour them are key to dealing with oxidative stress.

Image removed due to copyright restriction. Original can be viewed online at https://www.annualreviews.org/doi/abs/10.1146/annurev.arplant.55.031903.141701

Figure 1.1 Four pathways of ROS detoxification utilising enzyme and substrate cycling.

Superoxide dismutase (SOD) converts superoxide into hydrogen peroxide and forms the first line of defence against ROS. Catalase (CAT) can then convert hydrogen peroxide (H_2O_2) into water and oxygen. Hydrogen peroxide can also be detoxified via the Ascorbate-Glutathione cycle. Ascorbate peroxidase (APX) with the provision of ascorbate, is able to reduce hydrogen peroxide into water and monodehydroascorbate (MDA). MDA can then be recycled under the presence of NAD(P)H and MDA reductase (MDAR) back into ascorbate. Dehydroascorbate can form spontaneously from MDA but is again converted by DHA reductase with the help of GSH (glutathione) back into ascorbate. Oxidised glutathione (GSSG) is produced as a result and is converted back into reduced glutathione via glutathione reductase and NAD(P)H. This constitutes the Ascorbate-Glutathione cycle. The glutathione peroxidase cycle utilises reduced glutathione (GSH) and glutathione peroxidase GPX) to detoxify hydrogen peroxide, converting it to water and oxidising glutathione. Glutathione is then recycled via NAD(P)H and glutathione reductase back into reduced glutathione. (Apel & Hirt 2004)

Though the majority production of H_2O_2 appears to occur in the peroxisome and chloroplast (Foyer & Noctor 2003), ROS is still considered a significant molecule in mitochondrial signalling as its function in retrograde intracellular signalling (Ng et al. 2013b) and mediating cell hypersensitive response (Lam et al. 2001) are crucial to alleviating redox imbalances and stressors.

An AP of the mETC that may aid in monitoring cellular energy and redox imbalances has been seen in all plants to date as well as some fungi and protists. Although the role the pathway plays may vary greatly depending on host species and the particular isoform in question, preliminary transgenic studies in model plants have shown increased abiotic tolerances and reduced ROS formation in lines overexpressing particular components of the AP (Kowaltowski et al. 2009; Saha et al. 2016)

1.3. The AP of the mETC

The AP is an electron-funnelling pathway ubiquitous to all plants as well as some fungi, protists and animals. In *A.thaliana* there are two small gene families of a terminal oxidase (*Aox1, Aox2*) which with the provision of O_2, can accept electrons from ubiquinone, passing them onto oxygen to form H_2O and heat. In conjunction with the *Aox* family, type II NAD(P)H dehydrogenases form another part of the AP. Situated on both the inner and outer layers of the inner membrane of the mitochondria, type II NAD(P)H dehydrogenases present a mechanism for electrons from NAD(P)H present in the mitochondrial IMS and matrix to reduce ubiquinone

(Douce et al. 1973) (Figure 1.2). Unlike the cytochrome pathway (CP), the AP is not proton motive and its activity is not inhibited by the typical mitochondrial respiratory inhibitors cyanide and antimycin A (Moore et al. 1978). The substrate specificity and cofactor binding has yet to be confirmed for each of the type II dehydrogenases, but research in bacterial membrane models suggest at least a partial affinity towards Ca^{2+} for one of the external type II dehydrogenases and a preference towards NADH and/or NADPH (Geisler et al. 2007). However, attempts to measure individual type II dehydrogenases *in vivo* through RNAi knockdown mutants often results in up regulation of other AP components (Smith et al. 2011), hindering the ability to identify the biochemical properties of individual mitochondrial type II dehydrogenases.

Multiple key cofactors are produced during photosynthesis and respiration and can act as regulators to processes such as protein, lipid and nucleic acid synthesis. Cofactors such as NAD(P)H and ATP are often feedback inhibitive towards their own formation and can regulate their own over accumulation. Feedback inhibition can often lead to upstream inhibition of important anaplerotic reactions, reducing the cells capacity to maintain carbon anabolism under cell perturbation. Therefore under conditions that induce photosynthesis and respiration inhibition, the AP may aid in control of carbon and adenylate homeostasis as well as reducing the formation of ROS by mediating the redox status of the mitochondria (Rychter et al. 1992; Maxwell et al. 1999; Smith et al. 2009; Smith et al. 2011).

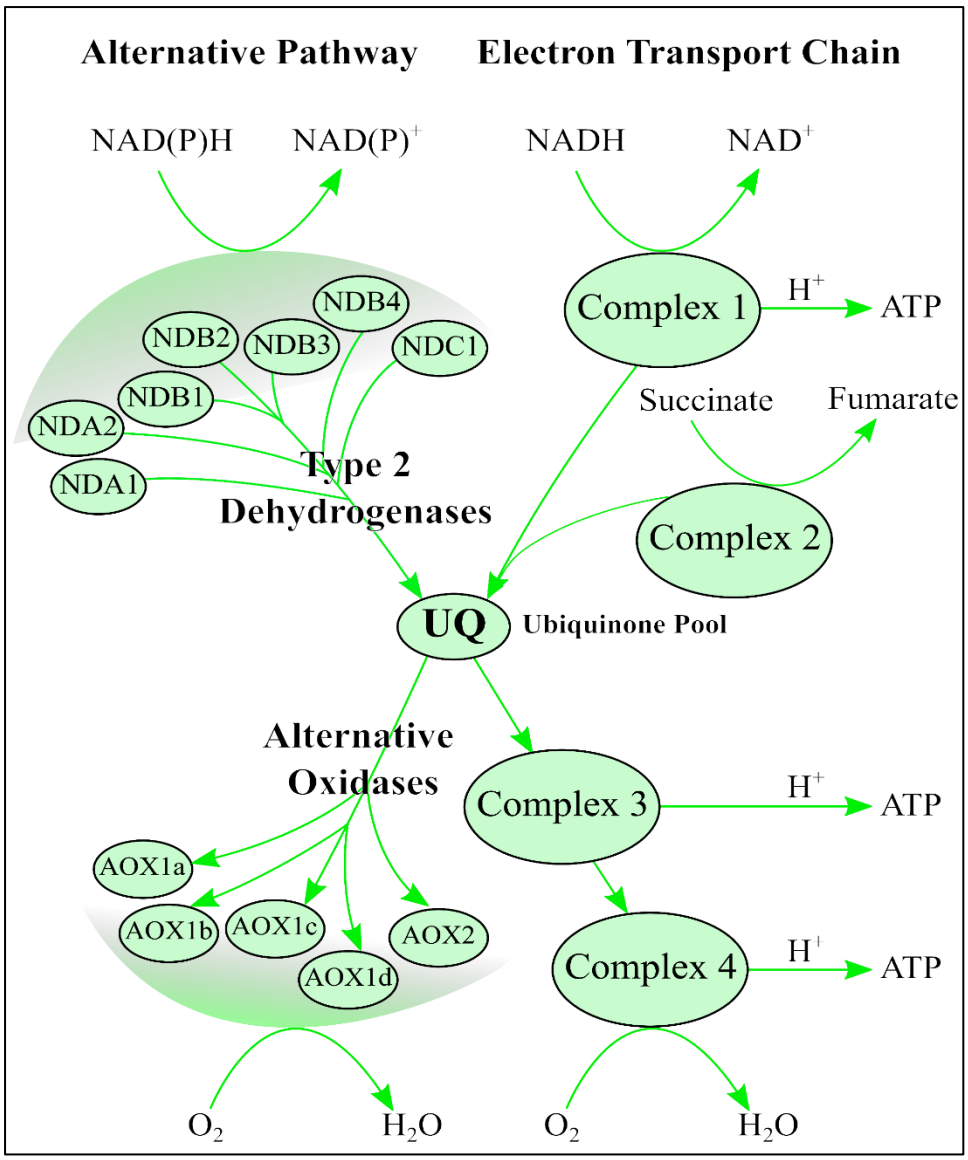

Figure 1.2 Diagram of mitochondrial electron transport pathways present in the IMS that oxidise NAD(P)H and reducing oxygen into water

1.4. Alternative oxidase

AOX is a semi-integral protein embedded within the inner mitochondrial membrane. The AOX proteins have been identified as diiron carboxylate proteins based on the conservation of four carboxylate residues and two histidine amino acids forming a unique iron binding motif, essential for activity (Albury et al. 2002; Moore & Albury 2008). The relatively small sized proteins (32-36kDa) transcribed from nuclear genes catalyse the four-electron reduction of O_2 to water coupled to the oxidation of ubiquinol. This reaction occurs prior to complex III, permitting AOX to form an additional branching point within the ETC, partitioning electrons between itself and cytochrome oxidase. As previously mentioned, AOX is non-proton motive so significant decreases in ATP yield can occur as a result of its activity, even more so if electrons enter the mETC through the type II NAD(P)H dehydrogenases. As such, AOX is optimally positioned within the mETC to provide a great deal of flexibility regarding the coupling of ETC flux to ATP formation and carbon metabolism. The partitioning of electrons between the two pathways likely allows for reconciliation of the cell's demand for ATP versus the turnover rate of pyridine nucleotides and the supply carbon intermediates upstream (Vanlerberghe 2013b) (Del-Saz, Ribas-Carbo et al. 2018).

1.4.1. Origins and diversification of alternative oxidase

The *Aox1* gene family is present in both eudicot and monocots, but the *Aox2* gene family has not been found in any monocots screened to date suggesting an

evolutionary divergence and specialised roles for *Aox* (Considine et al. 2002). Interestingly, only recently have both *Aox* gene families been discovered in gymnosperms, suggesting that both *Aox* families were present prior to the divergence of dicots and monocots and that the lack of *Aox2* in monocots is due to gene deletion events (Frederico et al. 2009).

The alternative oxidase was first noticed as a result of the thermogenic properties of the *Arum lily* (James & Beevers 1950) although observations had previously been made on cyanide insensitive respiration in tomato plants as early as 1919 (Clayton 1919). The spadix of thermogenic plants undergo a controlled and sustained burst of uncoupled respiration, releasing energy within the mitochondrial chemiosmotic gradient as heat, volatilising odorous compounds to attract insect pollinators. Thermogenesis is the first and only definitive role confirmed for AOX (Wagner et al. 2008). As the majority of plants are non-thermogenic, AOX must play other roles, with many conserved isoforms being confirmed in numerous kingdoms ranging from plants to the more recent identification in primitive animals (McDonald et al. 2009). As such, the role of AOX has become the subject of much interest as preliminary research suggests it may have significant regulatory power over carbon, adenylate and ROS production in plants.

1.1.2 Suggested roles for alternative oxidase

The only confirmed role for the AOX protein has been the production of heat from uncoupled respiration. However, as research progresses many more roles have

been suggested for AOX, particularly because of its critical positioning within respiration, and it is likely to perform many different roles.

1.4.1.1. Metabolic homeostasis

Mitochondria are the centre of non-photosynthetic metabolism and play an important role in balancing the supply of ATP production with the turnover of pyridine nucleotides and the supply of upstream metabolic intermediates. Adjusting the partitioning of electron flow to COX or AOX may allow plant cells to better align their cellular needs based on environmental conditions. A recent review by Vanlerberghe (2013b) and Selinski, Scheibe et al. (2018) has outlined many possible roles for the alternative oxidase, mostly regarding adaptation to abiotic and biotic stressors. It is likely that metabolic homeostasis is also controlled in conjunction with the type II NAD(P)H dehydrogenases as multiple researchers have shown enhanced co-expression of these DH under numerous conditions (Clifton et al. 2005; Smith et al. 2009; Yoshida et al. 2009; Smith et al. 2011).

Recent studies involving measurements of chloroplastic function and *aox* mutants have suggested AOX is involved in protecting the photosynthetic ETC by minimizing the inhibition to repair of photosystem II (PSII) caused by overproduction of ROS (Zhang et al. 2011). Further to this, inhibition experiments utilising salicylhydroxamic acid (SHAM) and high light conditions showed that inhibition of the AOX pathway under high light led to rapid accumulation of excess NADPH reductant in the chloroplast, resulting in over-reduction of photosystem 1 electron

acceptor side (Zhang et al. 2011). In agreement with the previous study, electron flow through to PSII was reduced along with oxygen evolution and thylakoid ΔpH. At the same time, inhibition of AOX lead to the inhibition of non-photochemical quencher (NPQ) induction. Therefore, the mechanism of AOX to alleviate photoinhibition may be by preventing over reduction of PSI acceptor side, minimizing inhibition of NPQ and thus reducing over accumulation of ROS in the chloroplast (Zhang et al. 2012a; Zhang et al. 2012b). ROS production from the photosynthetic ETC is likely to occur at either PSI or PSII. ROS production at PSI and PSII is promoted under conditions of stress, generally characterised by stomatal closure, a concomitant reduction in activity of the Calvin cycle due to reduced CO_2 and ATP availability and the simultaneous increase in NADPH:NADP+ ratios (Corpas et al. 2015; Gupta & Igamberdiev 2015). This relationship between ROS production, photosynthetic status and NADPH was illustrated by Vishwakarma et al. (2014) via *AtAox1a* knockout mutants. When placed under optimal light conditions, alterations to photosynthesis, NADPH ratios and O_2 uptake were not changed. While under conditions of high light, P700 reduction state of PSII was increased compared to wildtype along with an increase in the ratio of NADPH:NADP+. This also led to the increased production of ROS species and oxidative damage by-product, malondialdehyde (MDA) in *AtAox1a* knockouts compared to wildtype.

1.4.1.2. Signalling homeostasis

Aerobic respiration inherently leads to the production of ROS, but while overproduction of ROS leads to damaging cellular effects, discreet levels of ROS are known to play a role in organelle signalling. ROS signalling has been implicated in programmed cell death (PCD), often to isolate and limit damage to surrounding tissue (Gadjev et al. 2008; Petrov et al. 2015). As a toxic by-product of respiration and more specifically a reflection of the state of respiration, ROS has also been shown to act as a signal to limit the over production of itself. A recent study by Ng et al. (2013b) had illustrated cleaving of ANAC017 transcription factor as a result of H_2O_2 led to the retrograde signalling of *Aox* and a return of normal ROS production. ROS has also been implicated in signalling of *Aox* induction in perturbed mitochondrial ETC, resulting in reduced ROS production and improved photosynthetic activity (Vishwakarma et al. 2014). As such, ROS is important in providing a signal to reflect the state of respiration and this signal can ultimately be received and curtailed by expression of *Aox*.

Although there is much less evidence to suggest a regulatory link between *Aox* and reactive nitrogen species, preliminary research has shown that transgenic *Nicotiana tabacum* with reduced AOX resulted in increased nitric oxide formation (Cvetkovska & Vanlerberghe 2012). Further to this, *A.thaliana* seedlings grown in phosphate limiting conditions were shown to require NO to induce AOX expression and resulted in an altered phenotype when AOX was not induced (Royo et al. 2015). It should also be noted that more recently, analysis of highland barley treated with

UV-B radiation and NaCl illustrated a mutual regulation of photosynthesis and stomatal movement with the AP and glucose-6-phoshate dehydrogenase (G6DPH), through modulation of homeostasis of NADPH. It was suggested that G6PDH activity was acting to modulate the availability of NADPH and thus the activities of monodehydroascorbate reductase and glutathione reductase of the ascorbate-glutathione antioxidant cycle. It was also inferred that upregulation of AOX was important for removing excess NADPH reductant (Zhao et al. 2015)

1.4.2. Regulation of alternative oxidase

The presence of AOX in respiration is clearly a compromise between mETC efficiency and aligning the cell with current biochemical demands. As such, AOX's "wasteful" nature requires a regulatory process that prevents the unnecessary use of AOX. AOX is controlled both at the transcriptional and post-translational level, allowing plants to regulate levels of AOX capacity and activity. It is worth noting that as AOX is regulated post-translationally, abundance (capacity) of AOX protein is not always indicative of electron flux through AOX (activity).

1.4.2.1. Genetic regulators of alternative oxidase

Aox in plants is commonly comprised of two gene families separated and grouped historically by order of discovery (Whelan et al. 1996), but as more sequence data was made available, *Aox* was separated into two subfamilies and grouped based on protein sequence similarity (Clifton et al. 2006b). More recently, a more comprehensive analysis of *Aox* phylogeny confirmed that *Aox* is comprised of 2

subfamilies but can be broken down further into 4 major phylogenetic clades *Aox1a*–c/1e, *Aox1d*, *Aox2a*–c and *Aox2d*. Additionally it was also found that not all eudicots encode an *Aox* multigene family (Costa et al. 2014). Typically, expression of *Aox1* genes are associated with a response to an abiotic or biotic stress or a perturbation to the mETC. Interestingly, transcript analysis of *A.thaliana* plants treated with plastid disruptive compounds showed significant upregulation of *Aox2*; this was also seen for soybean *Aox1*, suggesting that AOX's role in plastids is not determined by gene family (Djajanegara et al. 2002; Fu et al. 2012). AOX2 may however play a role in germination, fertility and gametophyte development and function, as has been indicated in studies performed on *A.thaliana* and *Glycine max* respectively (Saisho et al. 2001; Chai et al. 2010a; Chai et al. 2010b). As such it is likely that there are many genetic controls regulating the expression and localisation of AOX within the plant and cell.

As both gene families are encoded within the nucleus of the cell, retrograde signalling from the mitochondria to the nucleus is required to induce transcription. Numerous headways have been made into identifying the genetic regulators of *Aox* induction via the use of cytochrome pathway inhibitors, which have been shown to induce *Aox* transcription. Nuclear-localised cyclin-dependent kinase E1 (CDKE1) was found to be a regulatory component of *Aox* (Ng et al. 2013a). Interestingly, as CDKE1 is associated with cell division and was found to interact with KIN10 (a known integrator of signals for growth, energy metabolism and stress). Baena-González et al. (2007b); Ng et al. (2013b) hypothesised that CDKE1 may act as a switching signal between growth and a stress response. Further to this, tobacco suspensions cultures

grown on nutrient limited media with inhibited *Aox* expression did not experience inhibition of growth whereas plants with normal *Aox* essentially stopped growing (Baena-González & Sheen 2008). Characterisation of the *A.thaliana* promoter region identified a strong repressor element which was identified to bind transcription factor ABSCISIC ACID INSENSITIVE4 (ABI4) (Giraud et al. 2009). Interestingly, ABI4 has previously been implicated in chloroplastic retrograde signalling, which, as suggested by Giraud et al. (2009), may provide a link between mitochondrial and chloroplastic signalling systems. Identification of the WRKY15 transcription factor was found via mutagenesis of the promoter region of *AtAox1a* (Dojcinovic et al. 2005b). OEX mutants of WRKY15 resulted in the abolishment of a mitochondrial stress response to osmotic stress, suggesting WRKY15 is another negative regulator of *Aox* (Vanderauwera et al. 2012b). As outlined previously, ANAC017 transcription factor, which is bound to the endoplasmic reticulum (ER), was found to induce expression of *AtAox1a*. It was illustrated that activation of ANAC017 was through cleavage of a consensus rhomboid protease sequence present within ANAC017. It was hypothesised, based on fluorescent protein labelling, mitochondria may position themselves close to the endoplasmic reticulum using F-actin to transfer the ROS signal to the ER embedded ANAC017 (Ng et al. 2013b).

1.4.2.2. Biochemical regulators of alternative oxidase

AOX plant proteins are a 32-34 kDa protein belonging to a group of non-heme diiron carboxylate family of proteins. The conserved regions of AOX consist of six

amino acids that coordinate two iron molecules within a conserved four-helix-bundle conformation (Moore et al. 1995; Siedow & Umbach 1995). Only recently has the structure for AOX been identified via crystallisation, however, the AOX analysed was from the parasitic protist *Trypanosoma brucei* (Shiba et al. 2013). As such, inferences about plant AOX may be limited in their predictive ability.

AOX proteins from *G.max* were identified as a pool of covalently-linked and non-covalently-linked homodimers (Umbach & Siedow 1993). Interestingly, the conformation of the AOX homodimer plays a significant role in the activity of the AOX protein; non-covalently linked AOX homodimers are considered reduced and active, whereas covalently linked dimers are deemed oxidised and less active. The covalent interaction between the two monomers is a result of two conserved cysteine residues facing the matrix allowing the formation of a disulfide bond between the two monomers (Rhoads et al. 1998). Notably, the conversion of AOX from its oxidised form to its reduced form is facilitated by the presence thioredoxin h (Gelhaye et al. 2004). It was hypothesised that NADPH was required by thioredoxin h to reduce AOX and that this was provided by the oxidation of TCA intermediates, specifically isocitrate and malate (Vanlerberghe et al. 1995) (Figure 1.3). Interestingly, *Lycopersicon esculentum* contains an AOX isoform without the conserved cysteine residues, and instead has replaced Cys1 with a serine residue preventing the AOX from forming a disulfide bridge and forming the inactive AOX homodimer (Holtzapffel et al. 2003).

When AOX has been converted into its reduced form, allosteric regulation of AOX with specific α-keto acids can act to fine tune activity. Pyruvate has been shown

Image removed due to copyright restriction. Original can be viewed online at http://6e.plantphys.net/topic12.03.html

Figure 1.3 AOX activation through a balance of redox status and the presence of 2-oxoglutaric acids (pyruvate in this case) http://6e.plantphys.net/topic12.03.html

in multiple species to be an activator of AOX activity (Millar et al. 1993; Vanlerberghe et al. 1995; Millar et al. 1996; Carré et al. 2011). It has been illustrated that due to a substitution of the Cys1 residue with a serine residue, allosteric activation of AOX no longer occurs via pyruvate but rather succinate (Holtzapffel et al. 2003; Grant et al. 2009). Thus, it seems that Cys1 is crucial to the covalent interaction between AOX monomers and allosteric regulation.

Apparent Km values measured for AOX in *Cucumis melo* roots showed AOX appears to have a Km for O_2 between 20-30 μM whereas the reported COX Km is much lower at 0.1 μM. Additionally, the reported Vmax values for COX were significantly higher than that of AOX (Kano et al. 1977). However, the reported COX Km was not actually measured and AOX measurements were hampered by the presence of multiple terminal oxidases. As such, the data may not a reflect a real-world Km/Vmax value, however it could be suggested that a lower Km value coupled with a high Vmax, may allow AOX to remain inactive until the system becomes perturbed. More accurate measurements were performed by Millar et al. (1994). They reported values of 0.14 μM for COX and 1.7 μM for AOX in soybean roots and cotyledons.

The combined regulation of AOX through covalent modification via redox status (NADPH/thioredoxin h) and allosteric activation via carbon status (pyruvate) may allow for the plant to accumulate AOX regardless of respiratory state, providing a means to immediately adjust partitioning of electrons based on redox or carbon status. Further to this, isotope discrimination of plants with enhanced expression of AOX did not necessarily see the same increase in AOX activity as was seen in AOX

capacity (Guy & Vanlerberghe 2005; Dahal et al. 2015b).This is supported by Millar et al. (1998), Noguchi et al. (2005) and Ribas-Carbo et al. (2005), where a concomitant increase in AOX in activity was not proportional to an increase in AOX protein. Again, demonstrating the importance of the post-translation regulatory mechanisms.

1.5. Plant Type II NADPH dehydrogenases

In addition to the AOX family of proteins, several type II NAD(P)H DH are embedded within the mitochondrial inner membrane and make up the second component of the AP. Type II plant NAD(P)H DH are a small, single polypeptide (~55Kda to 70Kda) family that provide an additional branching point where electrons can enter the mETC. Some type II DH are dual targeted to either the chloroplast (NDC1) or peroxisomes, (NDA1, NDA2 and NDB1), but less research exists around organelle specific activity in these organelles (Carrie et al. 2008; Xu et al. 2013). Type II DH have been found across many species including plants, fungi, (Michalecka et al. 2003) protists (Biagini et al. 2006) and an extensive range of bacteria (Melo et al. 2004). Unlike the proton motive Complex I of the mETC, type II NAD(P)H DH do not couple the oxidation of NAD(P)H to the translocation of protons. Therefore, alongside the AOX family, the type II NAD(P)H DH are able to form a route for electrons that bypasses all proton motive steps. Besides their non-proton motive mechanism, they're also differentiated from type I NAD(P)H DH due to an insensitivity to complex I inhibitors rotenone, piercidin A and capsaicin. *Solanum tuberosum* and *Oryza sativa*

have also been predicted, based on protein sequence, to have isoforms localised on either side of the mitochondrial IM (Michalecka et al. 2003).

1.5.1. Localisation of type II NAD(P)H dehydrogenase

From analysis of the *A.thaliana* genome, in comparison to the previously identified type II DH of *S.Cerevisiae* and *E.coli* and potato, a total of seven isoforms were identified based on sequence homology (Michalecka et al. 2003). Phylogenetic analysis suggested that four of the isoforms were localised to the outer side of the mitochondrial IM and the other three were present on the matrix-facing side (Finnegan et al. 2004; Millar et al. 2011). The type II DH in *A.thaliana* were differentiated into three groups labelled NDA, NDB and NDC based on the presence and absence of conserved motifs as suggested by Michalecka et al. (2003). AtNDA and AtNDB both share two conserved putative ADP-binding motifs however AtNDB differs from AtNDA and AtNDC due to the presence of a unique calcium binding EF-hand motif. NDC contains only one ADP-binding motif (Michalecka et al. 2003). AtNDA1-2 proteins have all been illustrated to be localised to the inner side of the IM along with AtNDC, while AtNDB1-4 were all shown to be localised to the external side of the IM (Elhafez et al. 2006). Unlike the AOX proteins, the type II DH are targeted to more than one location within the cell. As has been shown in *A.thaliana* (Carrie et al. 2008), *O.sativa* (Xu et al. 2013) and *S.tuberosum* (Rasmusson & Agius 2001), specific isoforms lead to the dual targeting of the type II DH. AtNDA proteins tagged with fluorescent protein markers at both the N- and C-terminal were visualised in

both the peroxisome and mitochondria, agreeing with previous results (Carrie et al. 2008). Additionally, OsNDA1 lacking PTS1 was shown to only target the mitochondria whereas *OsNDA2* containing PTS1 was localised to both the mitochondria and peroxisome (Xu et al. 2013). Results for AtNDB were consistent with previous literature (Carrie et al. 2008) and NDA results, whereby NDB1 was targeted to the peroxisome and mitochondria due to PTS1 whereas both AtNDB2 and AtNDB4 are only targeted to the mitochondria. Interestingly, the NDC protein was shown to be targeted to both the mitochondria and plastid but only in *A.thaliana* and *O.sativa* and not in the lower plant *Physcomitrella*. It was thus inferred that targeting to the mitochondria of NDC1 arose later on in evolution (Xu et al. 2013). Therefore, it was shown that the localisation of these proteins to the mitochondria, peroxisome or plastid is due to targeting via N-terminal and C-terminal target tags.

1.1.3 Substrate specificity, calcium activation and optimal pH

The type II NAD(P)H DH of *A.thaliana* have previously been recombinantly expressed as fusion proteins embedded within *E.coli* membranes to test for catalytic dependency. Only three of the external DH were tested as AtNDB3 is considered too lowly expressed to be worthy of any significance. AtNDB2 and AtNDB4 both oxidised NADH but small amounts of NAD(P)H oxidation were observed suggesting they may utilise both with different efficiencies. AtNDB2 NADH oxidation appeared to be stimulated by the addition of calcium whereas the small amount of NADPH oxidation appeared to be activated with the addition of calcium. AtNDB1 appears to oxidise both NADH and NADPH but much higher values were seen for NADPH. AtNDB1

also appears to require the presence of calcium to oxidise NAD(P)H (Geisler et al. 2007).

In addition to the testing of NAD(P)H and calcium, pH was also tested for its effects on NAD(P)H oxidation. Both AtNDB2 and AtNDB4 did not appear to be affected by the change in pH, though, the minimal NADPH oxidation significantly decreased with the increase in pH. AtNDB1 calcium independent NAD(P)H oxidation appeared to rapidly decrease with the increase in pH but calcium dependent oxidation was significantly slower (Geisler et al. 2007). It has been suggested that cytosolic pH could act as an activator on external NAD(P)H oxidation (Hao et al. 2015).

Numerous studies exist utilising transgenic mutant plants with altered levels of *Ndb1* (Michalecka et al. 2004; Wallström et al. 2014a) and *AtNda1*/*AtNda2* (Wallström et al. 2014b) but none exist on the NDB2 protein *in planta*. Suppression of *AtNdb4* lead to the co-expression of other AP components, particularly *AtAox1a* and *AtNdb2,* hindering the ability to define catalytic specificity *in vivo* (Smith 2010; Smith et al. 2011). As such further work is needed to isolate the individual substrate specificities, activities and co-factors required.

1.1.4 The use of transgenic plants to elucidate the AP pathway function

The suppression and OEX of mitochondrial external type II NAD(P)H DH in *A.thaliana* and *Nicotiana sylvestris* has confirmed the previous results in *E.coli* membranes (Michalecka et al. 2004; Geisler et al. 2007; Liu et al. 2008; Wallström et al. 2014a). Suppression of either the *S.tuberosum* and *A.thaliana* NDB1 resulted in a significant increase in NADPH:NADP ratio in rosettes and a loss of NADPH

oxidation. Furthermore, *AtNDB1* suppression significantly decreased biomass but did not change leaf maximum quantum efficiency, carbon assimilation or respiration. Suppression did, however, reduce quantities of four major sugars, TCA intermediates and amino acids. It was hypothesised by Wallström et al. (2014a) that changes to NADP:NADPH ratios were changing metabolism, resulting in a decrease in TCAC intermediates and a build-up of upstream metabolites, including sugars. In contrast, leaf maximum quantum efficiency of photosystem II, CO_2 assimilation rates and total respiration were similar to that of wildtype as were transcripts of central respiratory genes. OEX of *StNdb1* led to the co-upregulation of *Aox* and uncoupling protein, in contrast to the Arabidopsis *ndb1* mutant (Michalecka et al. 2004; Wallström et al. 2014a). Increased electron flux into the UQ pool may have induced AOX expression.

Transgenic models have been produced also of the *AtNDA proteins.* Suppression of both proteins resulted in a growth retardation, an increase in NAD(P)H:NAD(H) ratios in rosettes, and elevated levels of lactate and alanine (Wallström et al. 2014b). It may be possible that due to an increase in mitochondrial NADH levels caused by *AtNDA* suppression, metabolism at the PDC was significantly affected causing accumulation of fermentative products and a growth retardation (Igamberdiev & Gardeström 2003; Noctor et al. 2007). So, it seems that *AtNDA* proteins may be involved in dealing with accumulation of NADH in the matrix and preventing inhibition of the PDC.

Attempts have also been made to characterise the AtNDB2 and AtNDB4 proteins using both suppressive and constitutive transgenic models. Suppression of

AtNdb4 led to the co-upregulation of both *AtAox1a* and *AtNdb2,* masking the effects of reduced AtNDB4. This led to a significant lowering or ROS and an altered growth phenotype (Smith et al. 2011). Additionally, RNAi plants also showed better growth rates under saline stress and lower shoot Na content, which is most likely a reflection of the upregulation of *AtAox1a* and *AtNdb2* which has been seen before (Smith et al. 2009).Therefore a combination of multiple OEX inserts could be a useful in determining the functions of Type II NAD(P)H DH *in vitro.*

The upregulation of *AtAox1a* and *AtNdb2* in *Atndb4* RNAi lines, as well as wildtype under saline stress, suggests that these two AP components may be mutually involved in tolerating saline stress. Unpublished research from our lab has suggested that OEX of *AtNdb2* was able to confer both an increased resistance to saline stress resulting in an improved growth phenotype in both normal and stress conditions. Therefore, it could be reasoned that the overexpression of both these components could provide further gains to saline tolerance and would be useful to investigate.

1.2 Aims

The aim of this project was to utilise a combination of transgenic *A.thaliana* plants in which particular genes were either over-expressed or decreased, with the expectation of better understanding components of the AP, particularly the type II NAD(P)H dehydrogenases. Previous research from Smith et al. (2009) and Smith et al. (2011) have illustrated the potential for the AP in improving stress tolerances in *A.thaliana,* specifically the *AtAoxa1* and *AtNdb2* genes. However further research is

required to better understand the mechanisms in which these tolerances are conferred and how they may be applied in important crop species. As such this project aims to utilise a combination of *AtAox1a* and *AtNdb2* dual OEX lines in *A.thaliana* to increase our understanding of the type II NAD(P)H dehydrogenases in plants and identify potential exploitable functions provided by the AP.

Transgenic plants overexpressing the *AtAox1a* gene have previously been generated by Umbach et al. (2005). Plants containing an OEX construct for the *AtNdb2* gene have been generated in our lab and characterised by Sweetman et al. (2019). It has previously been shown in *A.thaliana* overexpressing *AtAox1a* (Smith et al. 2009) gene that there was a growth advantage in lines under salt stress. This was also witnessed in *Atndb4* RNAi lines, where we see the upregulation of both *AtAox1a* and *AtNdb2* and the same yield advantage under stress (Smith et al. 2011). It is expected that these lines in combination with a new line overexpressing *AtAox1a* and *AtNdb2* together, will better demonstrate whether the increased tolerance conferred by the AP is due to either *AtAox1a* or *AtNdb2* or both. Additionally, it is hoped that OEX of both constructs will further increase the stress tolerance seen in individual OEX lines and allow an increased understanding of the role NDB2 protein and activity.

Chapter 2

Materials and Methods

2 Methods

2.1 Reagents

For a comprehensive list of reagents, suppliers and protocols for recipes please see Appendix A. Unless otherwise stated, autoclaved MilliQ water was used in all molecular techniques.

2.2 Plant Growth Conditions

A.thaliana plants grown in the Sanyo controlled environment cabinet were exposed to 16 hours light at 100-120 μmol m^{-2} s^{-1} and 6 hours of dark at 22°C and 20°C respectively; humidity could not be monitored or adjusted in these cabinets. *A.thaliana* plants grown in the PC2 glasshouse were maintained at 22°C and 20°C respectively, relative humidity at 60% with lighting conditions subject to seasonal variations (200-1200 μmol m^{-2} s^{-1}) and shade cloths employed for summer seasons. *A.thaliana* plants maintained in the walk-in PC2 growth room were maintained at 23°C with 16 hours of 120 μmol $m^{2-}s^{1}$ and 8 hours of dark. Relative humidity was maintained at 60%. Plants maintained in the PC2 LED growth chambers were maintained at 20°C with 16 hours of 120 μmol $m^{2-}s^{1}$ light containing a mixture of red and blue (Figure A7.1); humidity could not be controlled in these cabinets. Soil used for *A.thaliana* experiments was prepared by the South Australian Research & Development Institute (Table A7.1). Unless otherwise stated, sterile media used in plant growth comprised of ½ strength MS media, 2% sucrose (w/v) and 0.8% (w/v) agar or 2% (w/v) phytagel in cases requiring increased media clarity.

2.3 General lab methods

2.3.1 Agarose gel electrophoresis

Agarose gel electrophoresis was performed according to the methods described by Sambrook et al. (1989). Depending on the size of the expected product 0.8-2.0% (w/v) agarose gels were used. Agarose was dissolved in TAE buffer (A7.2.1) and heated in a microwave then supplemented with GelRed™ (Biotium, U.S.A.). Promega 6X loading dye and DNA ladders (1 kB and 100 bp) were used. Samples were loaded in 5 µl aliquots and run in gel systems BioRad Mini Sub® DNA Cell, BioRad Mini Sub® Cell GT, BioRad Wide Mini Sub® Cell (BioRad, U.S.A.) and an Easy Cast Gel Electrophoresis System Model#B1 (Owl Scientific, U.S.A.). The power pack used for the gel systems were either a BioRad Power Pack 300 (BioRad, U.S.A.) or an EC570 (E-C apparatus, U.S.A.). Typical run conditions were 100 V over 60 minutes. Visualising was done via the BioRad EZ Imager (BioRad, U.S.A.)

2.3.2 Plasmid purification

Plasmid purification was performed using the Wizard Plus SV miniprep DNA purification system according to the manufacturers protocol (Promega, U.S.A.). Bacterial cultures were centrifuged in 50 ml falcon tubes at 3893 g for 10 minutes at 4°C using a Sigma 3-16PK centrifuge (Sigma Aldrich, U.S.A.) Plasmid DNA was eluted from spin columns in 100 µl aliquots of sterile MilliQ water and stored at -20°C until required.

2.3.3 gDNA extraction

DNA extractions were performed per methods provided by Sambrook et al. (1989) with an additional RNase treatment included. Leaf samples were placed in 1.5ml microfuge tubes and snap frozen in liquid nitrogen. Tissue (50-100mg) was then ground in microfuge tubes under liquid nitrogen using a plastic pestle. DNA extraction buffer (A7.2.2) was added (500 µl) to microfuge tubes and vortexed. SDS was added (35 µl of 20% w/v) and incubated at 65°C for five minutes in a Solid-State Dry Block Heater (Ratek Instruments, Australia). Extraction solutions were then mixed with 130 µl of 5 M potassium acetate and incubated on ice for five minutes. The extraction mix was centrifuged at 15,000 g for ten minutes (Eppendorf 5415c centrifuge, Crown Scientific, Australia) and the supernatant treated with 75 µl of 10µg/ml RNase A (Promega, U.S.A.) at 37°C for 30 minutes. Isopropyl alcohol (640 µl) and of 3M sodium acetate (60 µl) were used to precipitate DNA at -20°C for ten minutes. The solution was centrifuged at 15,000 g for ten minutes and the opaque pellet was washed with 300 µl of 70% (v/v) ethanol and centrifuged at 15,000 g for five minutes. The dried, pelleted DNA was resuspended in 50 µl of water and stored at -20°C until required. Concentration and purity were then determined using the NanoDrop™1000 Spectrophotometer (Thermo-Scientific, USA).

2.3.4 RNA extraction

Extraction of RNA from *A.thaliana* leaves was performed according to the methods outlined by MacRae (2007). Approximately 100 mg of leaf tissue was ground into a fine powder under liquid nitrogen using a ceramic mortar and pestle. TRIzol-

like reagent (A7.2.3) was added in 1 ml to ground powder and immediately vortexed until mixed thoroughly. Leaf suspensions were centrifuged at 12,000 g for 5 min at 4°C. The resulting supernatant was transferred to a new 1.5 ml microfuge tube and mixed vigorously by hand with 200 µl of chloroform for 20 seconds. Samples were incubated for 3 minutes at room temperature and centrifuged for 15 minutes at 12,000 g. The upper aqueous phase was collected and mixed with 500 µl of isopropyl alcohol for a 10-minute precipitation step at room temperature. After centrifuging at 12,000 g for 10 minutes at 4°C, the resulting pellet was rinsed with 1 ml of 75 % (v/v) ethanol, centrifuged again at 12,000 g for 10 minutes at 4°C then allowed to air dry in a sterile bio-cabinet. The pellet was re-suspended in 20 µl of RNase-free water. DNA was removed using the RQ1 RNase-free DNase according to the manufacturers protocol (Promega, Australia) using 10 µl of RNA and the RNA stored at -20°C until required. RNA quantity was checked using the NanoDrop™1000 Spectrophotometer (Thermo-Scientific, USA) and integrity checked by running on an agarose gel.

2.4 Generation and characterisation of transgenic *A.thaliana* plants with enhanced expression of *Aox1a* and *Ndb2*

2.4.1 Seed Sterilisation

Prior to plating on sterile media, seeds were sterilised in a solution of 2% sodium hypochlorite and 0.01% (v/v) tween-20 with mechanical shaking for 15 minutes. Seeds were then briefly centrifuged in a micro-centrifuge and the sterilisation solution removed by pipette. Seeds were then washed in equal volumes of sterile

Milli-Q at least five times. All washing steps were performed in the bio-cabinet to prevent contamination.

2.4.2 Seed plating and sowing

All seeds sown on sterile media were performed in the bio-cabinet using sterile pipette tips. Seeds were added to the top of the media and any residual solution left to dry before sealing with 3M™ Micropore tape. Seeds were vernalised for 72 hours at 4°C in the dark before being transferred into light. Seeds directly sown on soil did not require sterilisation but were still vernalised. Seeds sown on soil including seedlings transferred to soil from media were maintained under high humidity for the first two weeks of germination using plastic domes or cling wrap.

2.4.3 Electroporation of *Ndb2*over-pEarlygate into *Agrobacterium*

Prior to electroporation, duplicate electroporation cuvettes (50 x 2 mm gap, Cell Projects) were placed on ice for 10 minutes and allowed to cool. Glycerol stocks of electrocompetent GV3101:pMP90 *Agrobacterium tumefaciens* cells and pEarlygate-*Ndb2*over plasmid were placed on ice and allowed to thaw (10 minutes). Once thawed, 20 µl of competent cells were carefully mixed by pipette with 1 µl of pEarlygate-*Ndb2*over plasmid and transferred into the electro cuvette, ensuring the solution contained no bubbles and formed a bridge between both electrodes. Electroporation was performed with the following conditions; low range set to 200 Ω, high range set to 500 Ω, 24 µF and 2kV held for ~ 1 second (Gene Pulser® II, Pulse controller plus and Capacitance extender plus BioRad, U.S.A.). A pre-chilled aliquot of 200 µl LB broth (A7.2.4) was then mixed into the electro-cuvette and allowed to incubate at 30°C

for 2 hours. Post incubation, 50 and 100 µl aliquots were spread-plated on pre-warmed LB agar plates (A7.2.4) containing 25 µg/ml rifampicin, 50 µg/ml gentamycin and 100 µg/ml spectinomycin and allowed to incubate at 30°C for 2 days.

2.4.4 PCR screening of pEarlygate-*Ndb2*over

The pEarlygate plasmid was gratefully received from Dr Ian Dry (CSIRO Agriculture & Food, Urrbrae, S.A.) and the *Ndb2* OEX construct generated in our lab by Dr. Crystal Sweetman. Prior to dipping, the pEarlygate was screened for the *Ndb2* OEX construct with the primers outlined in table A7.4. Colonies growing on LB agar containing the above listed antibiotics were propagated in 30 ml LB media also containing the same selective antibiotics. *A.tumafacien* cultures were grown over two days at 30°C with shaking. DNA plasmid was extracted using the Promega Wizard® Plus SV Miniprep DNA purification system. Extracted plasmids were analysed for DNA concentration using the NanoDrop™ 1000 spectrophotometer and stored at -20°C until ready for use. PCR amplification was performed using the Promega GoTaq® Flexi DNA polymerase kit. Reagent concentrations were as follows and were per 50 µl reaction: 10 µl GoTaq Flexi buffer, 2 mM MgCl, 0.2mM dNTP's, 0.4 µM forward and reverse primer (Table A7.4), 1.25 units Taq polymerase, 1 µl DNA template (<10 ng). Thermal cycler conditions were initial melt for 5 minutes at 95°C; 35 cycles of 95°C for 30 seconds, 60°C for 30 seconds and 72°C for 30 seconds; final extension at 72°C for 5 minutes.

2.4.5 Screening XX1 *Aox1a*over lines prior to transformation

Prior to transformation, *Aox1a*over background line XX1 was screened for the *Aox1a*Over cDNA construct. The primers were designed to bind within exons of *Aox1a*. Because the construct contained the cDNA version of *Aox1a*, which excludes the introns, it could be discriminated from the endogenous gDNA version of the gene. (Table A7.4). Thermal cycler conditions were initial melt for 2 minutes at 95°C; 35 cycles of 95°C for 30 seconds, 58°C for 30 seconds and 72°C for 1.5 minutes; final extension at 72°C for 5 minutes. Additionally, it was found that setting heating ramp rates to 0.5°C/second was crucial for amplification. If this setting is unavailable, it was also found that utilising a gradient PCR setting achieved the same result. PCR reactions were stored at -20°C until required.

2.4.6 Plant *Agrobacterium* transformation

XX1 *A.thaliana* lines were grown as per conditions outlined in section 2.2. Plant lines were grown and selected based on a positive result seen in the PCR screen of the cDNA insert. A sterile loop was picked from an *A.tumefaciens* pEarlygate-*Ndb2*over glycerol stocks maintained at -80°C and cultured in duplicates in 35 ml of LB media containing 25 μg/ml rifampicin, 50 μg/ml gentamycin and 100 μg/ml spectinomycin. Cultures were incubated for two days at 30°C with shaking and $O.D._{600}$ was determined on the second day. Cultures were pelleted at 3893 g for 5 minutes at 4°C and resuspended in 5% (w/v) sucrose. A 1:10 dilution (1 ml) was used to measure $O.D._{600}$ using a Beckman DU640 spectrophotometer. The remaining culture was adjusted to $O.D._{600}$ 0.8-1 and Silwett L-77 added at 0.05% (v/v). Plants were then dipped

into the Agrobacterium solution, ensuring all flowers were covered and any residual solution gently shaken off (Clough & Bent 1998). Plants were then kept in the dark under humidity domes for two days to allow for recovery. Once matured, siliques were captured in brown paper bags and dried at 37°C for at least two weeks. Seeds were separated from dried plant material by using a tea strainer and stored in 1.5 ml microfuge tubes at 4°C in humidity-controlled containers in the dark.

2.4.7 Selective marker screening of plants containing the *Ndb2*over construct

Preliminary confirmation of the newly inserted *Ndb2*over construct was performed via selective marker screening. Plants were selected via the *bar* resistance gene associated with the pEarlygate plasmid. Plants were plated on MS media (see appendix) containing 5 μg/ml glufosinate ammonium (GA) and after two weeks were scored for resistance. Wildtype seed were included on all plates as a control for the efficacy of the GA. Plants demonstrating resistance were transferred to soil for gDNA screening and seed collection.

2.4.8 Genomic screen of *Ndb2*over construct in transformants

To confirm the presence of the inserted OEX construct, gDNA was extracted as per Section 2.3.3 and PCR was performed as per Section 2.4.4. PCR reagent concentrations were per 20 μl reaction: 4 μl GoTaq Flexi buffer, 2.5 mM MgCl, 0.2mM dNTP's, 0.4 μM forward and reverse primer, 1.25 units Taq polymerase, 1 μl DNA template (<0.5 μg/50 μl). Thermal cycler conditions were initial melt for 2 minutes at 95°C; 35 cycles of 95°C for 30 seconds, 52°C for 30 seconds and 72°C for 30 seconds;

final extension at 72°C for 5 minutes. Plants shown to be resistant and containing the *Ndb2*over construct were allowed to grow and collected for seed.

2.4.9 Determination of insert copy number via segregation ratio analysis

To determine insert copy number in each transformant, segregation ratio analysis was employed. T2 seeds were plated on MS media containing 5 μg/ml GA at roughly 100 seeds per square petri dish. After two weeks, seedlings were scored as resistant or susceptible. Plant lines showing a ratio of 3:1 resistant: susceptible plants were assumed to contain a single insertion of the *Ndb2*over construct. Chi-square analysis was performed to determine statistical significance.

2.4.10 Confirmation of homozygosity in T3 seed lines

Prior to characterisation, confirmation of homozygosity was confirmed. T3 seeds were plated on MS media containing 5 μg/ml GA and allowed to grow for 2 weeks. Seed lines were scored for resistance or susceptibility. If all seedlings that germinated were resistant, this line was deemed homozygous.

2.4.11 Transcriptional screening of transgenics with increased *AtAox1a* and *AtNdb2* expression

RNA (1 μg, extracted as per Section 2.3.4) was reverse transcribed using the iScript™ cDNA synthesis kit (BioRad) in 20 μl volumes according to the manufacturers protocol and diluted 1:10 with sterile MilliQ water. Transcript abundance was quantified from cDNA using the KAPA SYBR-fast qPCR Universal ReadyMix system (Geneworks, Australia). qRT-PCR standards were prepared using end point PCR and nanodrop quantification. Four qPCR standard dilutions were

included in each run, in triplicate (10^{-2}, 10^{-4}, 10^{-6} and 10^{-8} fmol/µl). qPCR was performed on the CFX96™ Real Time PCR Detection System (BioRad). Reactions were performed in10 µl. volumes containing 2X KAPR Sybr Fast, 0.2 µM of forward and reverse primers and 1 µl of 1:5 diluted cDNA. Amplification conditions for *Aox1a* and reference genes Ubiquitin and Protein phosphatase2A (*Pdf2)* were initial melt for 1 minute at 95°C; 39 cycles of 95°C for 5 seconds and 58°C for 10 seconds. Amplification conditions for *Ndb2* were initial melt for 1 minute at 95°C; 39 cycles of 95°C for 5 seconds and 61°C for 15 seconds. Melt curve analysis was pre-set for all samples at 50^0C to 95^0C in increments of 0.5^0C. For each cDNA sample, the concentration of each target gene was calculated from the standard curve. A normalisation factor was calculated from the geometric mean of the two reference genes. Relative transcript levels for the gene of interest (i.e. *Aox1a*) were calculated as the concentration of *Aox1a*, divided by the normalisation factor. Three biological replicates were each measured in triplicate technical replicates.

2.4.12 Isolation and purification of mitochondria

Mitochondria were isolated based on the adaption of the method by Neuburger et al. (1982), Sweetlove et al. (2007) and Juszczuk et al. (2007). All steps were performed at 4°C. *A.thaliana* shoot tissue (~20g) was extracted from plate grown seedlings after 21 days of growth grown as per Section 2.2. Shoot tissue was weighed and rinsed in distilled water. Tissue was then homogenised in 150 ml of isolation media (A7.2.5) using a Polytron blender (Kinematica, Australia) at four bursts of 8000 rpm for 2 seconds each. The homogenate was then filtered through two layers of miracloth and

centrifuged at 1100 g for 5 minutes. at 4°C. The supernatant was centrifuged again at 18,000g for 20 minutes at 4°C. The pellets were gently re-suspended with small paintbrushes and a glass mortar and pestle in wash media containing BSA (A7.2.5). The homogenate was then layered onto a prepared discontinuous Percoll gradient containing 60, 45, 28 and 5% (v/v) Percoll (Table A7.2). The gradients were then centrifuged at 30,000g for 45 minutes at 4°C in a SW 32 Ti swinging bucket rotor. The centrifuge brake was off until the last 500 rpm of deceleration for which the slowest brake setting was applied. Top layers of Percoll were removed using an aspirator and the mitochondrial band sitting at the interface between 28 and 45 %(v/v) Percoll was gently pipetted into 40 ml centrifuge tubes. After diluting in wash media containing BSA, the mitochondrial band was centrifuged at 31,000g for 20 minutes at 4°C, with a slow brake over 5 minutes. The pellet was resuspended and diluted in wash media without BSA and centrifuged at 31,000g for 20 minutes at 4°C. The final pellet was resuspended in 2 ml of wash media without BSA and the protein kept on ice till further use. Protein concentrations were determined using the BCA protein assay (Bradford 1976) as per manufacturers (ThermoFisher) instructions and all NAD(P)H and oxygen electrode assays were performed on the same day of preparation.

2.4.13 Detection of AOX, NDB2 and reference protein PORIN using SDS-PAGE and immunoblotting

Isolated mitochondrial samples were mixed with equal volumes of 2X denaturing loading buffer (A7.2.6) and boiled at 100°C for 5 minutes. Boiled samples were then centrifuged at max speed for 5 minutes to removed precipitated proteins.

Samples (10 ug) were loaded onto a 10% (v/v) polyacrylamide resolving and 4% (v/v) stacking SDS-PAGE gel (A7.2.6). Each gel was run using the SDS-PAGE running buffer (A7.2.6) and included either the Precision Plus Protein™ Kaleidoscope™ Prestained Protein Standards or Precision Plus Protein™ Dual Colour Standards (BioRad). Running conditions were always maintained at 170 V constant for approximately 70 minutes using the PowerPac™ Basic Power Supply and Mini-PROTEAN Tetra Vertical Electrophoresis Cell (BioRad). The separated proteins were transferred to nitrocellulose membrane using the Mini Trans-Blot® Cell (BioRad). Nitrocellulose membrane (General Electrics), Whatman filter papers, sponges and the SDS-PAGE gels were incubated at room temperature in a solution of transfer buffer (A7.2.6) for 15 minutes. The SDS-PAGE gel was sandwiched against the nitrocellulose using a piece of equal size filter paper and sponge on both sides of the sandwich. All bubbles were removed before being placed within the tank buffer system. The transfer was then run at 60 V at 4°C for 2 hours. Post transfer, the membranes were incubated in blocking buffer (A7.2.6) for an hour at room temperature on a gyrating platform. The blocking buffer with the appropriate antibody solution was added (Table A7.3). Each primary antibody incubation was left overnight at 4°C on a shaking platform. A minimum of three, 10-minute washes with 15 ml TBS-T (A7.2.6) was used to remove the primary antibody. The appropriate secondary antibody conjugated to a horseradish peroxidase (Table A7.3) was then added to fresh blotting buffer and the membrane allowed to incubate at room temperature for a minimum of 1 hour. The secondary was then washed away using a minimum of three 10-minute, 15 ml washes

of TBS-T. Proteins were then visualised using the Clarity Western ECL Substrate by adding 1ml of each reagent to 15ml of water and allowing the blot to incubate for 1 minute with shaking in the dilute solution. The blot was then imaged using the ChemiDoc XRS+ imaging system. Each membrane was probed sequentially with three primary antibodies. To ensure all protein bands could be recognised and quantified, the lowest concentration proteins were detected first, i.e. anti-AOX, then anti-NDB2 and finally anti-PORIN, which gave the most intense band.

2.4.14 Quantification of NAD(P)H oxidation in isolated mitochondria of transgenic dual *Aox1a/Ndb2* OEX lines

NAD(P)H oxidation was quantified by following the change in absorbance at 340 nm. All measurements of NAD(P)H oxidation were performed on freshly isolated mitochondria as per Section 2.3.12. Apart from Figure 3.10, all measurements were performed on an Olis Modernized Aminco™ DW-2 spectrophotometer. Measurements were performed at 25°C and utilised 50 μg of protein per sample. Measurements were taken using either oxygen as an electron acceptor or supplemented with 0.04 mM decylubiquinone. Isolated mitochondria (100 μl) were incubated in a solution containing 860 μl of standard reaction media (A7.2.5), 0.5 mM EGTA (for calcium independent rates) or 1 mM $CaCl_2$ (for calcium-activated rates), 0.2 mM NAD(P)H and 1 mM ADP. A stable, linear rate was then taken. The following was added in order and a linear rate taken after each subsequent addition: 1 mM dithiothreitol (DTT), 5 mM pyruvate (AOX activator), 10mM succinate (to look for further activation of the mitochondrial electron transport chain through Complex II),

0.5 mM potassium cyanide (KCN, a COX inhibitor) and 0.12 mM propyl gallate (PG, an AOX inhibitor). Rates were calculated using slopes of the lines generated by Olis Spectral Works software.

2.4.15 Determining oxygen consumption rates and electron transport chain capacity of transgenic dual *Aox1a*/*Ndb2* OEX lines

Oxygen consumption was measured polarographically using the Oxygraph Plus chambers (Hansatech Oxygraph, Norfolk, England). Measurements were performed at 25°C and on the same day of mitochondrial isolation. Each assay contained 100 µg of protein and was incubated with the same SRM as section 2.4.14. The same volumes and concentrations of SRM and inhibitors/activators were again used for oxygen consumption measurements and in similar orders as section 2.4.14. The only difference was when determining COX and AOX capacity. COX capacity was measured as the PG-insensitive, KCN-sensitive rate of oxygen consumption, while AOX capacity was measured as the KCN-insensitive, PG-sensitive rate of oxygen consumption.

2.5 Plant response to high light and drought stress

2.5.1 Boyes growth analysis on MS media

Phenotypic characterisation of new transgenics was performed using the Boyes et al. (2001) method. Growth analysis on MS media utilised the same growth conditions and media as outlined in Section 2.2 containing 2% (w/v) phytagel. To test the effects of using sucrose as a supplementary carbon source over CO_2 when growing plants in sealed containers, phenotypic analysis on MS media was performed with

and without 2% (w/v) sucrose. Seeds were sown in a single row along the top of a square petri dish with 10 mm gaps between each seed. Each plate had two replicates of each line and were vernalised at 4°C in the dark for 3 days. Plates were positioned vertically in custom made racks to ensure roots would grow downwards, and repositioned daily to minimise positional effects between plates. Seedlings were then monitored every day for growth stages including radicle emergence, cotyledon emergence, cotyledons fully opening and length of the primary root. On the 14th day, growth stage measurements ceased, and the number of rosette leaves and secondary root hairs were counted under a dissecting microscope.

2.5.2 Boyes growth analysis on soil

Growth analysis on soil utilised the same conditions and medium outlined in section 2.2. Seeds were sown directly onto soil and vernalised for three days at 4°C in the dark. Once seeds had germinated, plants were monitored every second day and the growth stages recorded. Rosette radius was measured every second day starting on the 14th day until the growth stage at which the first flower buds became visible. At this stage, a selection of plants was harvested, and the fresh/dry weights recorded. Dry weights were measured after plants had been incubated at 80°C for a minimum of 48 hours or until dry. Once bolting had occurred, measurements of bolt height were recorded every second day and were used to indicate when approximately 50% of flowers had been produced. It's expected that 50% of flower production coincides with a plateauing of bolt height. Before harvesting, plant stems were counted for the number of branches on main bolt and number of side bolts. Plants were then harvested

at this point ensuring both rosette and stem weight were weighed separately. Relative growth rates (RGR) for rosettes were calculated using the DW data obtained at the first growth stage harvest. Stem RGR were calculated on the assumption of DW was zero on bolt emergence using the equation obtained from Evans (1972). $RGR=(\ln W_2-\ln W_1)/(t_2-t_1)$ where W_1 and W_2 are the dry weights at two different time points and t_2-t_1 are the corresponding days of harvest.

2.5.3 Moderate light and drought experiment with recovery

To test the effects of a combined moderate light and drought stress on the newly generated transgenics, a new method not using hydroponics and mannitol was devised by another member of the lab that utilised soil. The pots utilised were custom made 63 mm diameter pots lacking drainage holes, to prevent loss of soil when watering. Soil was completely dried before adding to pots (114 g). Pots were then watered to 163 g (minus pot weight) (0.43 ml per g soil) and seeds sown directly into the pot. Seeds were then vernalised on soil for 3 days at 4°C in the dark. Plants were grown for 4 weeks under control conditions with the same lighting intensity, day/night length and temperatures as outlined in Section 2.2. Water was then withheld for selected plants for the following seven days. Control pots continued to be watered as normal. As soil content weight was known, water content could be carefully maintained every day by measuring pot weights. Due to slight positional effects on evaporation rates in the growth cabinet, all "drought" pots were topped up with a minimal volume of water, to maintain equal water contents between pots. This allowed for a consistent drought stress across all samples. After seven days, "drought"

plants were transferred to moderate light conditions (~300 μmol m^{-2} s^{-1}) and water content was maintained at an equal minimum, as previously mentioned. This was labelled as a moderate light and drought (MLD) treatment. Triplicate biological samples of control and MLD plants were immediately frozen in liquid nitrogen for use in biochemical analysis and stored at -80°C until required. Triplicates of both control and MLD samples were also harvested every day for seven days after exposure to moderate light and weighed for fresh/dry/turgid weights. Turgid weights were determined by submerging the freshly harvested sample in water for 24 hours, removing excess water via brief centrifugation in a salad-spinner and dabbing with paper towel, and then weighing. Plants were then measured for dry weights as per Section 2.5.2. Samples that didn't undergo destructive measurements were rewatered to 163 g pot weight to determine recovery rates. Each line was scored and photographed for recovery rates one week after re-watering.

2.5.4 MDA quantification

Quantification of MDA was achieved following the spectrophotometric TBARS reactive method outlined by Hodges et al. (1999) and Singh et al. (2012). Approximately 50-100 mg of frozen and homogenised leaf tissue was vortexed with 1 ml of 80% (v/v) ethanol and centrifuged at 16,000 g for 15 minutes. The supernatant was split into 400μl and mixed with an equal volume of either TBA+ or TBA- solution (A7.2.7). Samples were heated to 96°C for 30 minutes and then quickly cooled on ice. The solution was centrifuged at 9500 g for 10 minutes and 100 μl of both TBA+/- were

measured at 440, 532 and 600 nm. MDA was then quantified using the equation outlined by Hodges et al. (1999).

2.5.5 Anthocyanin quantification

Anthocyanins were quantified by a method adapted from Nakata et al. (2013) and Rabino and Mancinelli (1986). Some methods utilise an acidified ethanol solution to extract anthocyanins, however Oancea et al. (2012) has shown ethanol alone to be more effective. As such, 100 mg of liquid nitrogen frozen ground tissue was vortexed in 1 ml of 80% (v/v) ethanol and centrifuged at 16,000 g for 15 minutes. Anthocyanins were quantified from the remaining supernatant by measuring absorbance at 530 and 657 nm as outlined by Rabino and Mancinelli (1986).

2.5.6 Gas exchange analysis

Photosynthesis measurements were performed on whole rosettes after 29 days of growth under standard conditions. All measurements were made at least four hours into the lighting period and were completed four hours before completion of lighting period. All measurements were made using the LI-6400 XT portable photosynthesis system (LICOR, Nebraska) connected to the whole plant Arabidopsis chamber (6400-17) and RGB LED light source (6400-18A). For all light curve measurements, the leaf fan was set to fast, flow rate was 500 μmol s^{-1}, 400 μmol CO_2 mol^{-1} reference stream, 20% relative humidity and 20°C block temperature. Light source was a mixture of red and blue in a 0.75 and 0.25 ratio respectively to mimic the growth conditions found in the growth chamber. Photosynthetic light curves were generated using PAR values of 1500, 1000, 600, 400, 250, 120, 60, 40, 20, 10 and 0 μmol

m^{-2} s^{-1} measured in order of highest to lowest. Each intensity was measured for a minimum/maximum of 3 to 6 minutes respectively. Sampling was performed after 3 minutes when the stability parameters of photosynthesis, conductance and flow were stable or until 6 minutes was reached, whichever came first. Leaf area was determined using the image analysis program ImageJ (Schneider et al. 2012) and photographed images with a known scale included.

2.6 Transcriptomic analysis of *Arabidopsis* plants

2.6.1 RNA extraction and cDNA preparation

Total RNA was extracted from shoot tissue using the Bioline Isolate II RNA Plant kit. RNA quality was assessed using the Perkin Elmer LabChip GX Touch 24 with RNA quality scores cut off set at >8. mRNA was purified and cDNA prepared using the Truseq Stranded mRNA HT Sample Prep Kit (Illumina).

2.6.2 RNA sequencing quality control and sequence data evaluation

RNA sequencing services were provided by Flinders Genomics Facility, Adelaide, Australia. cDNA libraries were analysed with the Perkin Elmer LabChip GX Touch 24 using the High Sensitivity DNA kit producing average fragment size of 268 bp. Libraries were sequenced using the Illumina NextSeq 500 to generate single-end reads of 75 bp. Raw sequence reads were then processed using the following pipeline: (1) remove reads with sequence quality scores less than Q30; (2) remove adapter/overrepresented sequence and cross species contamination; (3) remove reads with final lengths less than 30 bp. The quality of the cleaned reads was assessed using FastQC.

2.6.3 Read mapping and post alignment quality control

The cleaned sequence reads were then aligned and mapped against the *Arabidopsis* genome (Ensembl, TAIR10) using Tophat aligner (v2.1.1) with bowtie aligner (v2.3.3). Total number of reads was compared to number of mapped reads to determine the percentage of mapped reads to total reads.

2.6.4 Differential expression analysis

DESeq2 was used for statistical analysis of differential expression and provided normalised gene counts, $\log_2$ fold change, Wald statistics, p-values and p-adjusted values. To account for very low or zero read counts for certain genes, a mean of normalized reads counts was calculated from the three replicates for each individual gene. Base means lower than 25 in both groups to be compared were considered too error prone to be useful and were removed. Genes were then filtered based on p-adjusted values <0.01 and $\log_2$ fold changes greater than 1 or less than -1.

2.6.5 Gene ontology term enrichment

Gene ontology was performed using the "GO term enrichment for plants" provided by The Arabidopsis Information Resource (TAIR), www.arabidopsis.org/aboutarabidopsis.html (Berardini et al. 2015) utilising the PANTHER classification system (Thomas et al. 2003; Thomas et al. 2006). Gene lists entered in PANTHER were previously filtered according to 2.6.4. A summary of the settings used in PANTHER are highlighted in table 2.1

2.6.6 KEGG pathway analysis

Pathway analysis was performed using the Kyoto Encyclopedia of Genes and Genomes (KEGG) mapper, search and colour pathway tool (Kanehisa & Goto 2000; Kanehisa 2019; Kanehisa et al. 2019). Pathways were mapped using the organism specific search mode with the *A.thaliana* database.

Table 2.1 Summary of selections used in PANTHER classification system tool for PANTHER overrepresentation test

Criterium/datasets	Selected criterium/datasets
Analysis type	PANTHER Overrepresentation Test (Released 13/11/2018)
Annotation version and release data	GO Ontology database (Released 15/11/2018_
Reference list	Arabidopsis thaliana (all genes in database)
Annotated data set	- GO cellular component complete - GO biological process complete - GO molecular function complete
Test type	Fisher's exact test with false discovery rate

Chapter 3

Generation and characterisation of Arabidopsis lines overexpressing *AtAox1a* and *AtNdb2*

Data from this chapter is part of the published work in Sweetman, C., Waterman, C. D., Rainbird, B. M., Smith, P. M. C., Jenkins, C. L., Day, D. A., & Soole, K. L. (2019). AtNDB2 is the main external NADH dehydrogenase in mitochondria and is important for tolerance to environmental stress. *Plant physiology*, pp-00877.

Written text in this chapter is my own, however some figures are the collaborative work of another author of the paper.

3 Generation and characterisation of Arabidopsis lines overexpressing *AtAox1a* and *AtNdb2*

3.1 Co-expression of *Aox1a* and *Ndb2* gene in response to stress

Co-expression of AP components has been shown under a multitude of conditions. The internal type II NAD(P)H DH *Nda1* has been seen under multiple occasions to be responding diurnally to light. This has also been seen in the co-expression of *Ndc1* gene and the *Aox2* gene in *A.thaliana* (Escobar et al. 2004). While Elhafez et al. (2006) and Michalecka et al. (2003) did not find evidence concurring with Escobar et al. (2004). However, they did find that *Ndb2* was regulated diurnally along with another AP member, *Nda1* (albeit weakly), which concurs with Smith et al. (2004). Although the evidence for *Aox1a* having a form of diurnal regulation is tentative (Escobar et al. 2004; Elhafez et al. 2006; Rasmusson & Escobar 2007; Lee et al. 2010) it is clear at least that the *Aox1a* gene responds to illumination and especially an overabundance of light in *A.thaliana* (Yoshida et al. 2009; Yoshida et al. 2011a). Alongside the expression of *Nda1* and *Ndb2*, the AP may be forming a complete bypass

for both sides of the membrane for electrons from reductants to flow. Many other forms of co-expression exist in the AP as well. As shown by Elhafez et al. (2006) analysis of microarray data from Genevestigator, an extensive list of chemical and environmental treatments result in the co-expression of *Nda2, Ndb2 and Aox1a.* Interestingly, not all treatments that resulted in co-expression had all three mentioned genes upregulated. In fact, the majority of the conditions resulted only in *Aox1a* and *Ndb2* co-expression. Several shared cis-acting regulatory elements (CAREs) were identified in the promoter regions of both *Aox1a* and *Ndb2* that were responsive to both hydrogen peroxide and rotenone in both genes.

The co-expression of *Aox1a* and *Ndb2* is most evident in the analysis of Genevestigator's Affymetrix and mRNA seq data bases (Figure 3.1 and 3.2). Using the co-expression tool in Genevestigator, a single gene can be selected and commonly co-expressed genes responding to perturbations across the database can be visualised. Searching against *Aox1a* in both Affymetrix and mRNA-seq databases, it was shown that *Ndb2* was the 5th and 2nd most co-expressed gene alongside *Aox1a,* respectively; highlighting the many shared roles these two genes have in responding to stress.

3.1.1 Investigating *Aox1a* for potential benefits in an OEX model

While a number of studies have demonstrated the importance of *Aox1a* via T-DNA and RNAi modifications (Watanabe et al. 2008; Strodtkötter et al. 2009; Yoshida et al. 2011b; Gandin et al. 2012), the ability to exploit these genes under a transgenic OEX promoter has been investigated far less (especially in *A.thaliana)*. OEX lines generated by Umbach et al. (2005) highlighted the role of *Aox1a* in reducing the

damaging effects of ROS by measuring a by-product of lipid peroxidation, however no phenotypical measurements were made. A low temperature study (Fiorani et al. 2005) identified for the first time a phenotypical vegetative growth phenotype in lines overexpressing *Aox1a.* OEX lines showed appreciable increases in a number of areas including leaf area, number of leaves and rosette diameter. These effects were even more pronounced under the cold stress, providing evidence for the potential of *Aox1a* to be used as a marker for improved growth and stress but also as a method to transgenically improve commercial plants. These benefits weren't constrained to low temperature acclimation either. Salinity treatments applied to an *Aox1a* OEX saw noticeable increases in growth rates under stress compared to wildtype (Smith et al. 2009). Interestingly, a decrease was seen in growth rates for the *Aox1a* OEX under normal conditions, an observation in disagreement with Fiorani et al. (2005). Fortunately, further experiments by Smith identified a new approach that seemingly minimises the growth penalty under normal conditions but maintains the improved resilience.

3.1.2 Exploiting the co-expression of stress responsive genes

RNAi experiments on the *Ndb4* gene were performed by (Smith et al. 2011) in an attempt to determine the substrate specificity of NDB4. The reduced expression of *Ndb4* led to a significant upregulation of *Aox1a, Ndb2* and *Nda1* genes under normal conditions. Interestingly, the downregulation of the *Ndb4* led to a significant improvement in the plants growth rate in roots and shoots under both normal and

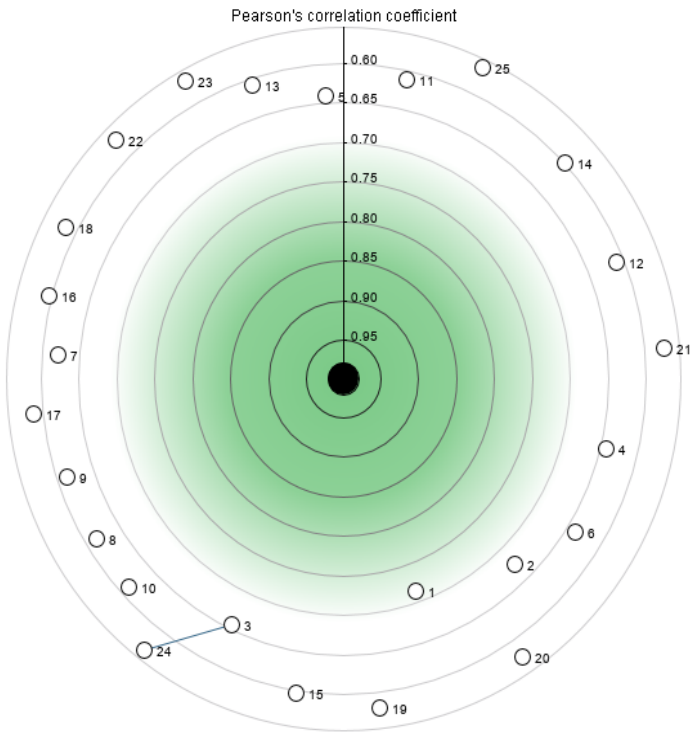

Showing 25 measure(s) of top 27 most correlated gene(s)

	Score	Gene	Description
1	0.71	NAC13	NAC domain-containing protein 13 [Source:UniProtKB/Swiss-Prot;Acc:F4IED2]
2	0.67	AT2G41730	
3	0.66	CYP81D8	cytochrome P450, family 81, subfamily D, polypeptide 8 [Source:TAIR;Acc:AT4G37370]
4	0.64	UGT74E2	UDP-glycosyltransferase 74E2 [Source:UniProtKB/Swiss-Prot;Acc:Q9SYK9]
5	0.64	NDB2	External alternative NAD(P)H-ubiquinone oxidoreductase B2, mitochondrial [Source:UniProtKB/Swiss-Prot;Acc:Q94BV7]
6	0.64	SOT12	Cytosolic sulfotransferase 12 [Source:UniProtKB/Swiss-Prot;Acc:P52839]
7	0.62	UGT73B5	UDP-glycosyltransferase 73B5 [Source:UniProtKB/Swiss-Prot;Acc:Q9ZQG4]
8	0.62	ZAT12	Zinc finger protein ZAT12 [Source:UniProtKB/Swiss-Prot;Acc:Q42410]
9	0.61	OXI1	Serine/threonine-protein kinase OXI1 [Source:UniProtKB/Swiss-Prot;Acc:Q9LSF1]
10	0.61	BZIP60	bZIP transcription factor 60 [Source:UniProtKB/Swiss-Prot;Acc:Q9C7S0]
11	0.61	AT3G50910	
12	0.61	AT5G43450	
13	0.61	AT5G13200	
14	0.60	UGT73C6,UGT73C5	UGT73C6:UDP-glycosyltransferase 73C6 [Source:UniProtKB/Swiss-Prot;Acc:Q9ZQ95], UGT73C5:UDP-glycosyltransferase 73C5 [S...
15	0.60	SAP12	Zinc finger AN1 domain-containing stress-associated protein 12 [Source:UniProtKB/Swiss-Prot;Acc:Q67YE6]
16	0.60	NAC102	NAC domain-containing protein 102 [Source:UniProtKB/Swiss-Prot;Acc:Q8H115]
17	0.59	AT4G24160	
18	0.59	NAC053	NAC domain-containing protein 53 [Source:UniProtKB/Swiss-Prot;Acc:Q949N0]
19	0.58	SRO2	Probable inactive poly [ADP-ribose] polymerase SRO2 [Source:UniProtKB/Swiss-Prot;Acc:Q9ZUD9]
20	0.57	NFXL1	NF-X1-type zinc finger protein NFXL1 [Source:UniProtKB/Swiss-Prot;Acc:Q9SY59]
21	0.57	GSTU9	Glutathione S-transferase U9 [Source:UniProtKB/Swiss-Prot;Acc:Q9FUT0]
22	0.57	BCS1	cytochrome BC1 synthesis [Source:TAIR;Acc:AT3G50930]
23	0.57	AT5G42050	
24	0.57	AT4G39670	
25	0.57	AT4G27585,AT5G5...	

Figure 3.1 Co-expression analysis of *AtAox1a* using Genevestigator Affymetrix Arabidopsis ATH1 genome array data

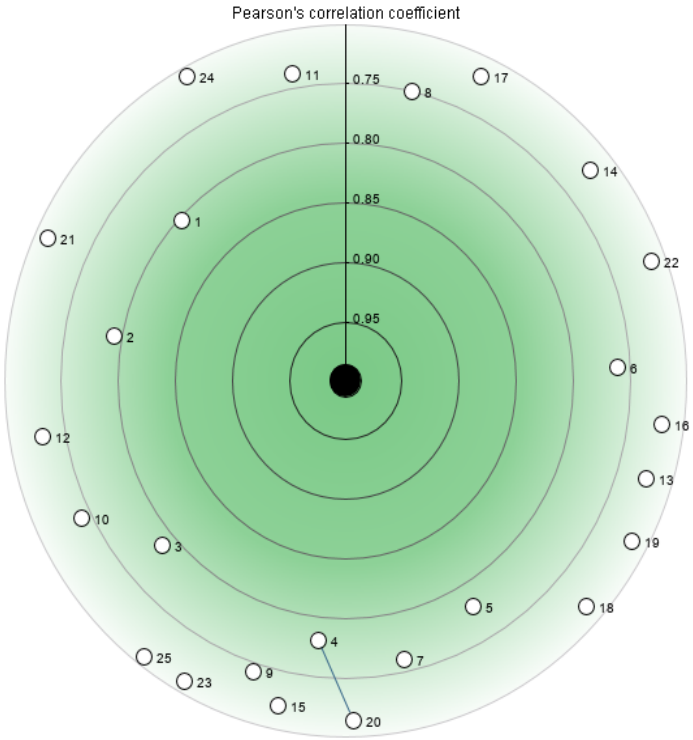

Showing 25 measure(s) of top 25 most correlated gene(s)

	Score	Gene	Description
1	0.80	ABCC3	ABC transporter C family member 3 [Source:UniProtKB/Swiss-Prot;Acc:Q9LK64]
2	0.79	NDB2	External alternative NAD(P)H-ubiquinone oxidoreductase B2, mitochondrial [Source:UniProtKB/Swiss-Prot;Acc:Q94BV7]
3	0.79	PMAT1	Phenolic glucoside malonyltransferase 1 [Source:UniProtKB/Swiss-Prot;Acc:Q940Z5]
4	0.78	ALA10	Phospholipid-transporting ATPase 10 [Source:UniProtKB/Swiss-Prot;Acc:Q9LI83]
5	0.78	CYP81D8	cytochrome P450, family 81, subfamily D, polypeptide 8 [Source:TAIR;Acc:AT4G37370]
6	0.76	AT3G55410	
7	0.76	OXI1	Serine/threonine-protein kinase OXI1 [Source:UniProtKB/Swiss-Prot;Acc:Q9LSF1]
8	0.75	AT2G41730	
9	0.74	AT4G22530	
10	0.74	SBT3.5	Subtilisin-like protease SBT3.5 [Source:UniProtKB/Swiss-Prot;Acc:Q9MAP7]
11	0.74	AT4G12735	
12	0.73	AT5G56350	
13	0.72	RPI1	Probable ribose-5-phosphate isomerase 1 [Source:UniProtKB/Swiss-Prot;Acc:Q9C998]
14	0.72	PA200	proteasome activating protein 200 [Source:TAIR;Acc:AT3G13330]
15	0.72	ABCG40	ABC transporter G family member 40 [Source:UniProtKB/Swiss-Prot;Acc:Q9M9E1]
16	0.72	AT5G51830	
17	0.72	BEH3	BES1/BZR1 homolog protein 3 [Source:UniProtKB/Swiss-Prot;Acc:O49404]
18	0.72	SAP12	Zinc finger AN1 domain-containing stress-associated protein 12 [Source:UniProtKB/Swiss-Prot;Acc:Q67YE6]
19	0.72	AT2G39650	
20	0.71	AT4G39670	
21	0.71	AT4G00500	
22	0.71	AT5G08300	
23	0.71	NAC081	Protein ATAF2 [Source:UniProtKB/Swiss-Prot;Acc:Q9C598]
24	0.71	GAPC1	Glyceraldehyde-3-phosphate dehydrogenase GAPC1, cytosolic [Source:UniProtKB/Swiss-Prot;Acc:P25858]
25	0.71	AT4G08555	

Figure 3.2 Co-expression analysis of *AtAox1a* using Genevestigator mRNA-Seq gene level *A.thaliana* data

saline conditions. This change in phenotype was suggested to be a result of an initial stress early in development resulting from the *ndb4* RNAi. Triggering an induction of *Aox1a* and *Ndb2,* it was suggested that this resulted in a positive growth phenotype through the reduction of ROS. It was hypothesised that the main benefit seen in these lines could be conferred through a transgenic OEX of the *Aox1a* and *Ndb2* genes.

3.2 Aims

The aims of this chapter were to generate at least 3 single insertion homozygous lines overexpressing both *Aox1a* and *Ndb2*. These lines would be made from the previously generated and characterised XX1 *Aox1a* OEX lines(Umbach et al. 2005) that utilised a CaMV35s promoter. This same OEX promoter would be used for the OEX of *Ndb2* in these lines. These lines could then be characterised at the phenotypic level for any altered differences in growth characteristics. It was hypothesised that a dual OEX plant would be more similar to the *ndb4* RNAi phenotype rather than the single *Aox1a* OEX phenotype but still retain the improved stress resilience. Characterising these lines and how they differ to previous transgenics may be informative about the post-translational regulation of the AP under non stressed conditions. Previous attempts at isolating the substrate specificity of the external type II NAD(P)H dehydrogenases has been difficult due to other interfering isoforms or lacking confidence due to expression in a heterologous system. These experiments aim to provide further evidence of the substrate used by *Ndb2* and any change in activity resulting from calcium activation.

These experiments aimed to insert the *Ndb2* OEX construct into *Aox1a* OEX lines (XX1), confirm its presence through antibiotic selective screening and PCR screening. Transgenics would then be screened for single insertions through mendelian genetics and the antibiotic selective marker. These lines could then be tested for levels of OEX through a combination of transcript and protein measurements. Combined with an existing *ndb2* T-DNA line, substrate specificity was tested as well as a number of enzymatic treatments aiming to test the changes in electron flux through the ETC and AOX activation changes. The comprehensive phenotypic analysis laid out by Boyes et al. (2001) was used to characterise phenotypic changes.

3.3 Results

3.3.1 Generating *AtAox1a* and *AtNdb2* dual OEX lines

3.3.1.1 Preliminary confirmation of *Aox1a* OEX lines and *Ndb2* OEX vector pEarlygate100

The empty OEX vector pEARLYGATE100 was obtained through Dr. Ian Dry's laboratory and the *AtNdb2* OEX construct had been generated and inserted in lab by Dr. Crystal Sweetman using the gateway cloning procedure. The presence of the *AtNdb2* construct was previously confirmed from plasmids extracted from *E.coli* post transformation and sequencing performed to ensure the sequence had not been unintentionally altered. The purified pEARLYGATE100+*AtNdb2* OEX plasmid was transformed into *A.tumefaciens* via electroporation and the resulting bacterium spread plated on to LB agar containing the selective antibiotic BASTA. Colonies grown after two days at 28°C were inoculated into LB broth containing the appropriate selective agents and allowed to proliferate for a further two days. Plasmids were extracted and purified from the resulting broth and a PCR for the *AtNdb2* cDNA construct using qPCR designated primers was performed. The *AtNdb2* construct was successfully amplified from two different *A.tumefaciens* colonies, showing a 182bp PCR product in the *A.tumefaciens* colonies as well as the original *E.coli* plasmid (positive control)(Figure 3.3).

Before the *Aox1a* OEX plants could be dipped with the pEARLYGATE100+*AtNdb2* OEX plasmid, the presence of the original *Aox1a* OEX

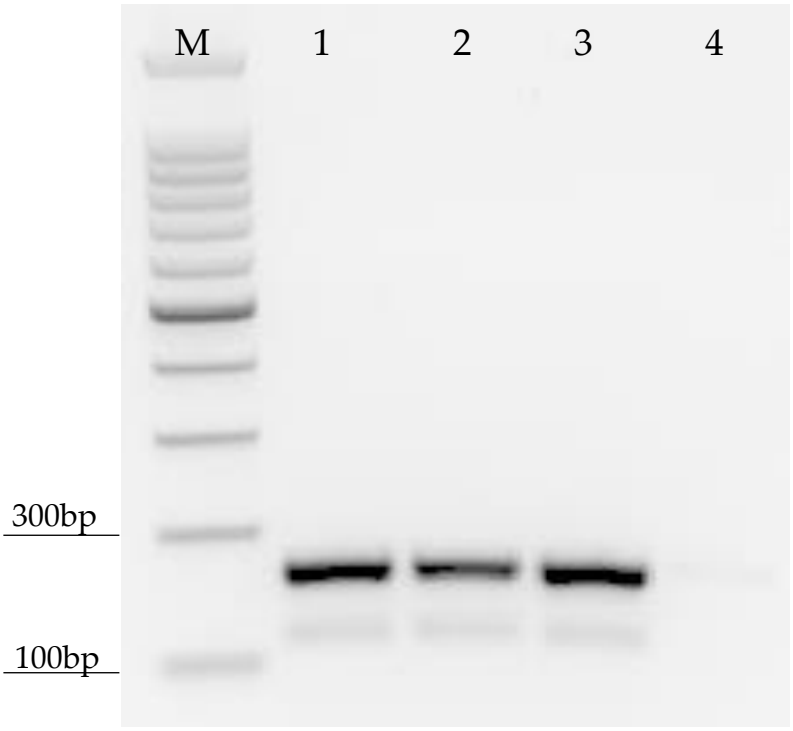

Figure 3.3 PCR confirmation for the presence of the *Ndb2* construct within pEARLYGATE100 OEX plasmid

PCR was performed on plasmid DNA extracted from transformed *A.tumefaciens* or transformed *E.coli.* Primer set used were *Ndb2* specific qPCR FWD/REV primer set as seen in Table A7.4. PCR was performed as described in methods section 2.4.4. Expected product size was 182bp.

Marker	Thermo Scientific GeneRuler Express DNA ladder
Lane 1	*Ndb2*over plasmid from *A.tumefaciens* colony 1
Lane 2	*Ndb2*over plasmid from *A.tumefaciens* colony 2
Lane 3	*Ndb2*over plasmid from *E.coli* (positive control)
Lane 4	No template control (negative control)

construct firstly needed to be confirmed. Three potential lines were chosen for dipping including the auto-active E14 line containing the site directed glutamate residue alteration as well as the non-auto-active lines XX1 and X6 (Umbach et al. 2005). Several replicates of each line were grown for dipping, with leaf tissue sampled for gDNA extraction. PCR was performed on the extracted gDNA using cDNA discernible (qPCR) primers that would amplify differing product sizes depending on the presence of either the gDNA or cDNA gene/construct. All transgenics showed a strong single band of 1100 bp, the expected size of the amplified cDNA construct (Figure 3.4). Majority also showed another single, but distinctly lighter band at around 1600 bp. Amplification of the genomic *AtAox1a* gene results in a 1600 bp product highlighted in the wildtype sample. An unexpected 500 bp product was amplified in the sample containing the *Aox1a* OEX plasmid which was not expected. As this product does not overlap with the expected products, this result was ignored. Unfortunately, the positive control did not produce the expected band size of 1100 bp. However, the differentiation seen in the gel photo as well as the future experiments highlighting the massively increased *Aox1a* expression confirm these lines are *Aox1a* OEX lines.

3.3.1.2 Generation and confirmation of transgenic A.thaliana containing OEX constructs for *AtNdb2* and *AtAox1a*

The newly constructed pEARLYGATE100+*AtNdb2* OEX plasmid was then dipped with the three different *Aox1a* OEX transgenics lines and the seed collected. Seeds were then plated on to ½ strength MS media containing the herbicide BASTA.

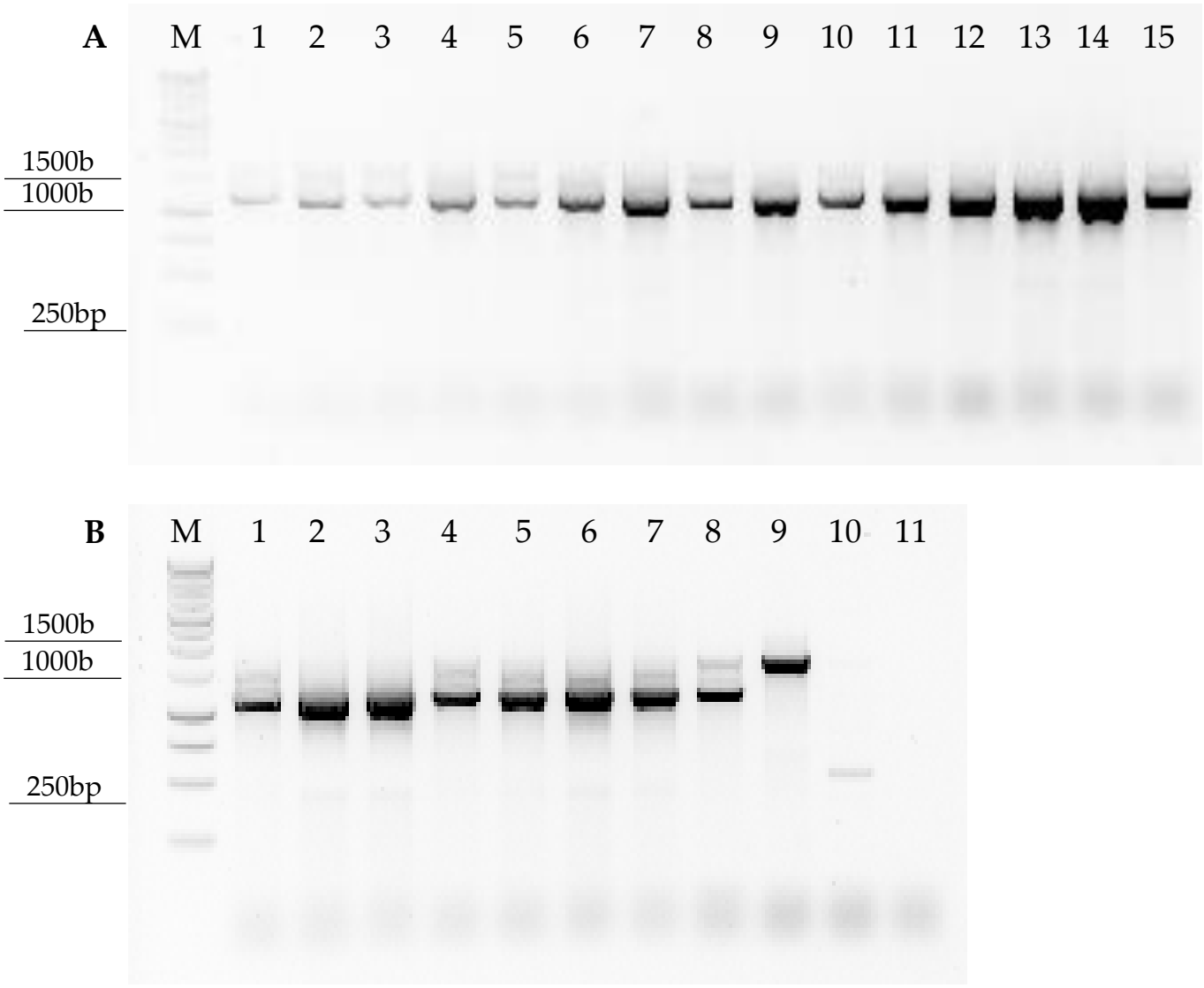

Figure 3.4 PCR confirmation for the presence of the *Aox1a* cDNA OEX construct within the XX1, E14 and X6 *Aox1a* OEX lines

gDNA was extracted from *A.thaliana* and construct amplified using *Aox1a* cDNA specific qPCR primers PCR was performed on gDNA extracted from either transformed or wildtype *A.thaliana* and plasmid extracted from *E.coli.* Primer set used were *Aox1a* cDNA specific FWD/REV primer set as seen in Table A7.4 PCR was performed as described in methods section 2.4.5. Expected product size was 1100bp for cDNA present in transgenics and 1600bp for the wildtype gDNA

Row 1	
Marker	1kB Promega ladder
Lane 1	*Aox1a*over E14 replicate 1
Lane 2	*Aox1a*over E14 replicate 2
Lane 3	*Aox1a*over E14 replicate 3
Lane 4	*Aox1a*over E14 replicate 4
Lane 5	*Aox1a*over E14 replicate 5
Lane 6	*Aox1a*over E14 replicate 6
Lane 7	*Aox1a*over E14 replicate 7
Lane 8	*Aox1a*over E14 replicate 8
Lane 9	*Aox1a*over XX1 replicate 1
Lane 10	*Aox1a*over XX1 replicate 2
Lane 11	*Aox1a*over XX1 replicate 3
Lane 12	*Aox1a*over XX1 replicate 4
Lane 13	*Aox1a*over XX1 replicate 5
Lane 14	*Aox1a*over XX1 replicate 6

Row 2	
Marker	1kB Promega ladder
Lane 1	*Aox1a*over X6 replicate 1
Lane 2	*Aox1a*over X6 replicate 2
Lane 3	*Aox1a*over X6 replicate 3
Lane 4	*Aox1a*over X6 replicate 4
Lane 5	*Aox1a*over X6 replicate 5
Lane 6	*Aox1a*over X6 replicate 6
Lane 7	*Aox1a*over X6 replicate 7
Lane 8	*Aox1a*over X6 replicate 8
Lane 9	Wildtype
Lane 10	pEARLYGATE100 *Aox1a* OEX plasmid
Lane 11	No template control

Plants able to germinate and successfully grow on the media were considered positive transformants and transferred to soil for seed collection. Once seeds had been collected, a known amount of seed was again plated onto ½ strength MS media containing BASTA and a segregation ratio analysis performed. To determine the number of insertion events that occurred in each transgenic line, the ratio of resistant to non-resistant seedlings was determined. Combined with the chi-square statistic, a statistical prediction regarding the number of *AtNdb2* OEX insertion events could be made. If plants lines demonstrated a chi squared value of <3.84 for a 3:1 ratio these were considered to contain only a single insertion. A number of lines demonstrated only a single insertion event and were used for further analysis (P1, P5, P6, P8, P9, P10, P11, P12, P15, P16, P17 P18 and P20) (Table 3.1) (it should be noted that although seeds were collected for X6 and E14 dual OEX, no analysis was included in this thesis).

Further PCR confirmation was required to confirm the presence of the *Ndb2* construct and not simply the selection marker. Amplification of extracted gDNA from T2 plants was performed using a combination of CaMV35S and *Ndb2* specific primers. The presence of the *Ndb2* OEX construct was assumed when there was amplification of a 280 bp PCR product. As these primers used sites specific to the transgenic insertion, no product was expected to be amplified in wildtype lines. All putative transgenics displayed the expected 280 bp product for the *Ndb2* OEX construct (Figure 3.5).

To ensure the presence of the *Ndb2* OEX construct was stably inherited across

Table 3.1 Determining the gene copy number of *Ndb2* OEX constructs inserted into the *Aox1a* OEX (XX1) lines in T2 seedlings

Antibiotic resistant T1 plants were used for seed collection and the resulting T2 seeds plated on MS media containing 5 μg/ml glufosinate ammonium. Chi square values below 3.84 were considered to be single insertion events based on a p-value of 0.05.

Plant Line	Resistant (alive)	Non-resistant (dead)	Ratio	Chi-squared value
P1	66	28	2.35	**1.02**
P2	17	58	0.29	107.21
P3	92	5	18.4	19.99
P4	86	6	14.3	16.75
P5	65	21	3.09	**0.05**
P6	54	25	2.16	**1.67**
P7	83	5	16.6	17.52
P8	50	24	2.08	**1.96**
P9	62	26	2.38	**0.97**
P10	76	18	4.22	**1.85**
P11	64	23	2.78	**0.06**
P12	78	15	5.2	**3.70**
P13	81	7	11.57	13.64
P14	79	12	6.58	7.04
P15	42	22	1.90	**3**
P16	53	24	2.2	**1.75**
P17	67	27	2.48	**0.60**
P19	74	20	3.7	**0.80**
P20	77	17	4.52	**2.55**

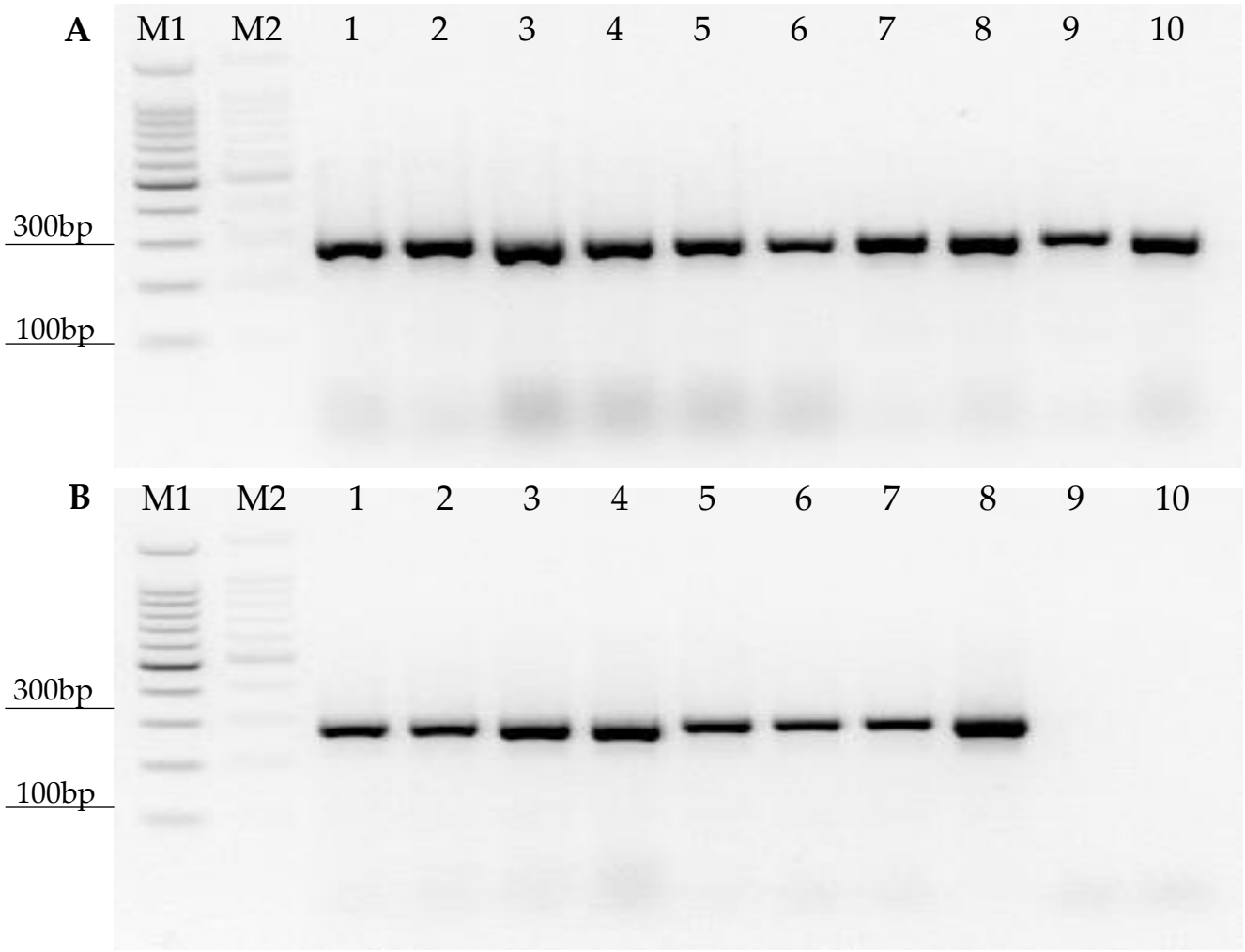

Figure 3.5 PCR confirmation for the presence of the *Ndb2* OEX construct within the XX1 *Aox1a* OEX lines.

gDNA was extracted from T2 dual *Aox1a*/*Ndb2* OEX lines and constructs amplified using CaMV35S FWD and *Ndb2*RNAi (-att) REV primer set as seen in Table A7.4. PCR was performed as described in methods section 2.4.8. Expected product size was 280bp for transformants and no product for wildtype

Row 1	
Marker 1	100bp Promega ladder
Marker 2	100bp Promega ladder
Lane 1	XX1/*Ndb2* OEX T2 5.2
Lane 2	XX1/*Ndb2* OEX T2 6.1
Lane 3	XX1/*Ndb2* OEX T2 8.1
Lane 4	XX1/*Ndb2* OEX T2 9.1
Lane 5	XX1/*Ndb2* OEX T2 9.2
Lane 6	XX1/*Ndb2* OEX T2 10.1
Lane 7	XX1/*Ndb2* OEX T2 11.1
Lane 8	XX1/*Ndb2* OEX T2 11.2
Lane 9	XX1/*Ndb2* OEX T2 12.1
Lane 10	XX1/*Ndb2* OEX T2 12.2

Row 2	
Marker 1	100bp Promega ladder
Marker 2	100bp Promega ladder
Lane 1	XX1/*Ndb2* OEX T2 15.1
Lane 2	XX1/*Ndb2* OEX T2 15.2
Lane 3	XX1/*Ndb2* OEX T2 16.1
Lane 4	XX1/*Ndb2* OEX T2 16.2
Lane 5	XX1/*Ndb2* OEX T2 17.1
Lane 6	XX1/*Ndb2* OEX T2 17.2
Lane 7	XX1/*Ndb2* OEX T2 20.1
Lane 8	pEARLYGATE100 *Ndb2* OEX plasmid
Lane 9	Wildtype
Lane 10	No template control

generations, T3 transgenic lines were tested for homozygosity of the selective marker associated with the *Ndb2* OEX construct. To test for homozygosity, approximately >100 T3 seeds were plated onto ½ strength MS media containing BASTA. T3 lines that showed 100% resistance to the herbicide were homozygous for the insert. Lines with <100% resistance were heterozygous for the insert and were again grown to seed. These T4 seeds would again be tested for homozygosity. If seedlings were again found to be heterozygous, the process was repeated until homozygosity was achieved. In the first series of transgenic lines collected, a total of nine lines were found to be homozygous with another nine lines heterozygous (Table 3.2)

A final genomic confirmation was performed on the new single insertion, homozygous T3 dual *Aox1a*/*Ndb2* OEX lines. Gene specific PCR was performed for both the *AtNdb2* and *AtAox1a* OEX constructs. In all seven lines tested, all were shown to be positive for both the *AtNdb2* (Figure 3.6) and *AtAox1a* (Figure 3.7) constructs. A false positive for the wildtype during an *AtNdb2* OEX construct screen was present. To combat this, a second screen utilising a combination of *AtNdb2* specific qPCR primers and mRNA instead of gDNA resulted in the same dual OEX lines being identified as positive transformants without a false positive seen in the wildtype (Figure 3.8).

mRNA was extracted from the seven positively identified dual OEX transformants and cDNA was synthesised for use in qRT-PCR. All lines examined for *AtNdb2* transcript abundance showed a varied but consistent increase in the *AtNdb2*

Table 3.2 Determining homozygosity of T3 dual *Aox1a*/*Ndb2* OEX lines via selective antibiotic screening

Antibiotic resistant T2 plants were collected for seed and plated on glufosinate ammonium . Lines that produced only 100% resistant seedlings were considered homozygous. ~100 seeds were plated per line.

Fully resistant (homozygous)	<100% resistant (heterozygous)
5.2	1.1
6.1	6.2
9.1	8.1
10.1	9.2
11.2	11.1
12.2	15.1
15.2	16.1
17.1	16.2
20.1	17.2

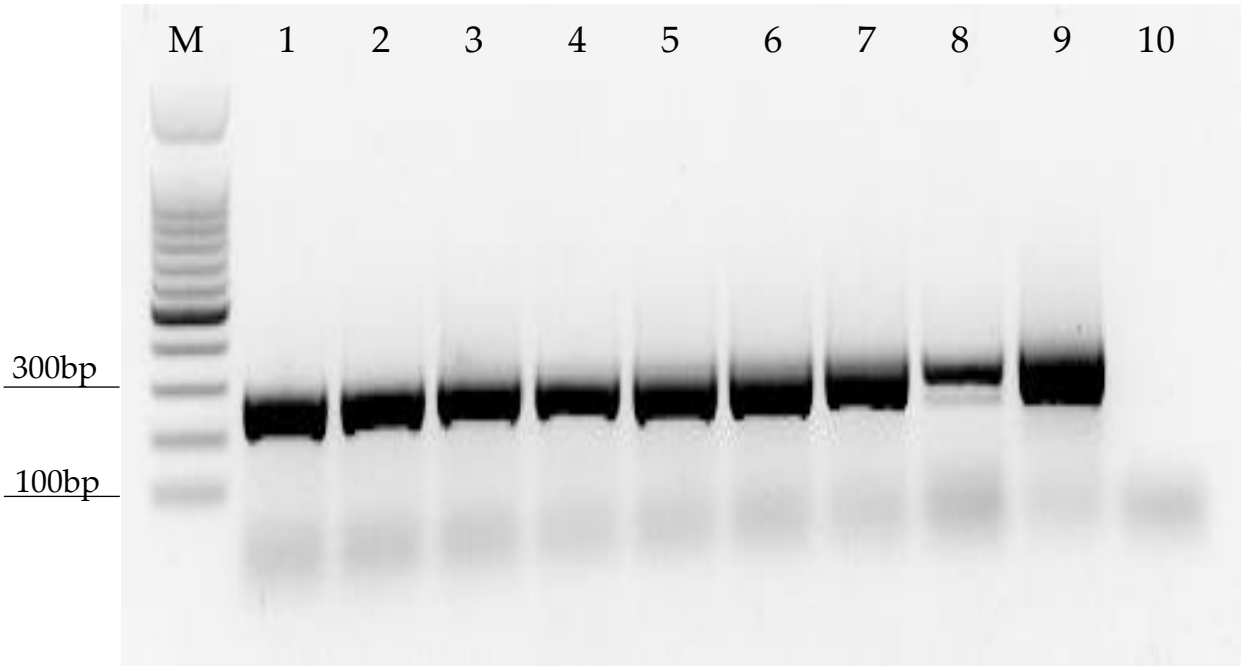

Figure 3.6 PCR confirmation for the presence of the *Ndb2* OEX construct within the *Aox1a*/*Ndb2* dual OEX lines.

gDNA was extracted from T3 dual *Aox1a*/*Ndb2* OEX lines and constructs amplified using CaMV35S FWD and *Ndb2*RNAi (-att) REV primer set as seen in Table A7.4. PCR was performed as described in methods section 2.4.8. Expected product size was 280bp for transformants and no product for wildtype

Marker	Promega 100bp ladder
Lane 1	XX1/*Ndb2* OEX T3 5.1
Lane 2	XX1/*Ndb2* OEX T3 5.2
Lane 3	XX1/*Ndb2* OEX T3 6.1
Lane 4	XX1/*Ndb2* OEX T3 11.2
Lane 5	XX1/*Ndb2* OEX T3 12.2
Lane 6	XX1/*Ndb2* OEX T3 15.2
Lane 7	XX1/*Ndb2* OEX T3 17.1
Lane 8	Wildtype
Lane 9	pEARLYGATE100 *Ndb2* OEX plasmid
Lane 10	No template control

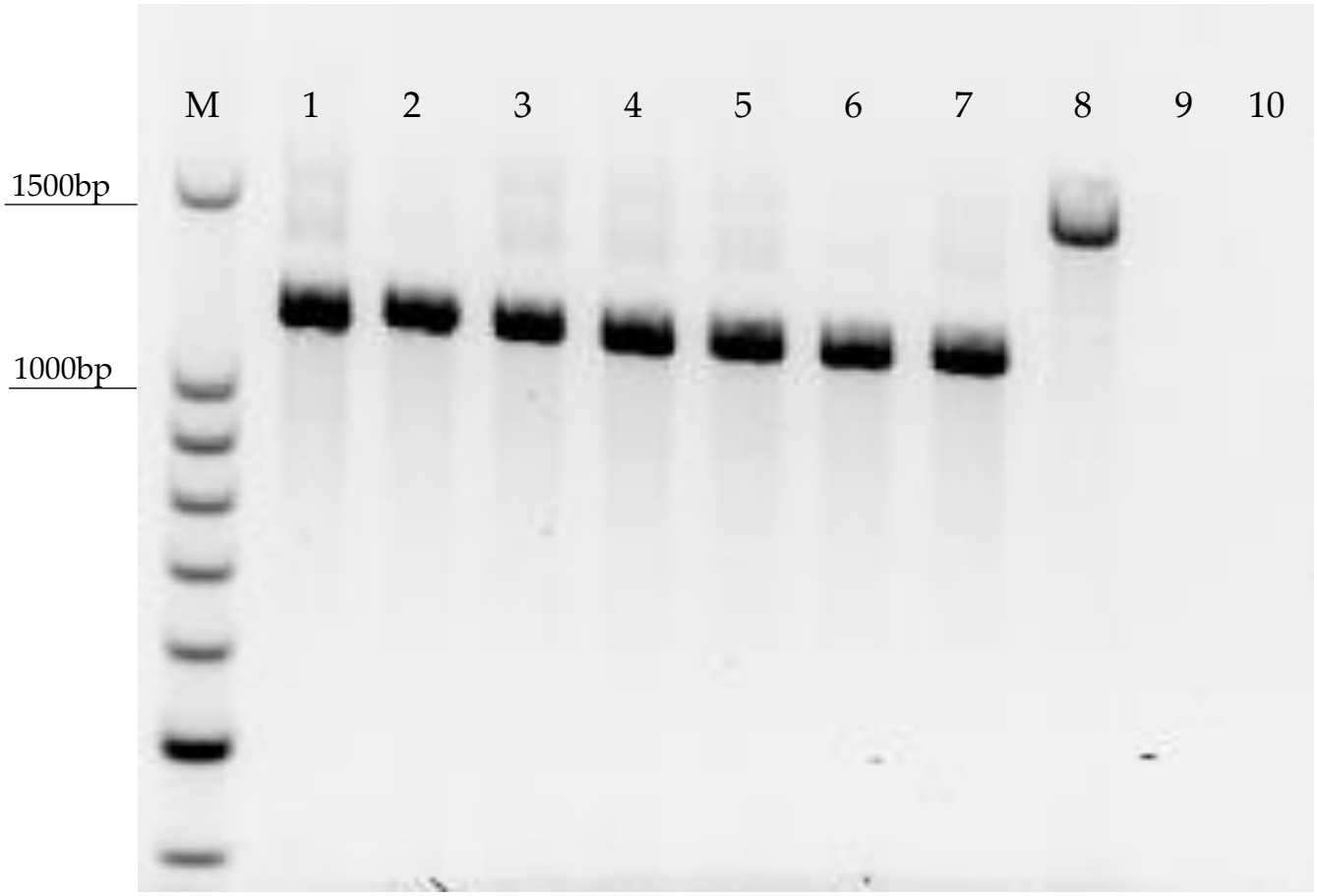

Figure 3.7 PCR confirmation for the presence of the *Aox1a* OEX construct within the dual T3 *Aox1a*/*Ndb2* OEX lines.

gDNA was extracted from T3 dual *Aox1a*/*Ndb2* OEX lines and constructs amplified using *Aox1a* cDNA specific primer set as seen in Table A7.4. PCR was performed as described in methods section 2.4.5. Expected product size was 1100 bp for transformants and 1600bp product for wildtype

Marker	Promega 100bp ladder
Lane 1	XX1/*Ndb2* OEX T3 5.1
Lane 2	XX1/*Ndb2* OEX T3 5.2
Lane 3	XX1/*Ndb2* OEX T3 6.1
Lane 4	XX1/*Ndb2* OEX T3 11.2
Lane 5	XX1/*Ndb2* OEX T3 12.2
Lane 6	XX1/*Ndb2* OEX T3 15.2
Lane 7	XX1/*Ndb2* OEX T3 17.2
Lane 8	Wildtype
Lane 9	pEARLYGATE100 *Aox1a* OEX plasmid
Lane 10	No template control

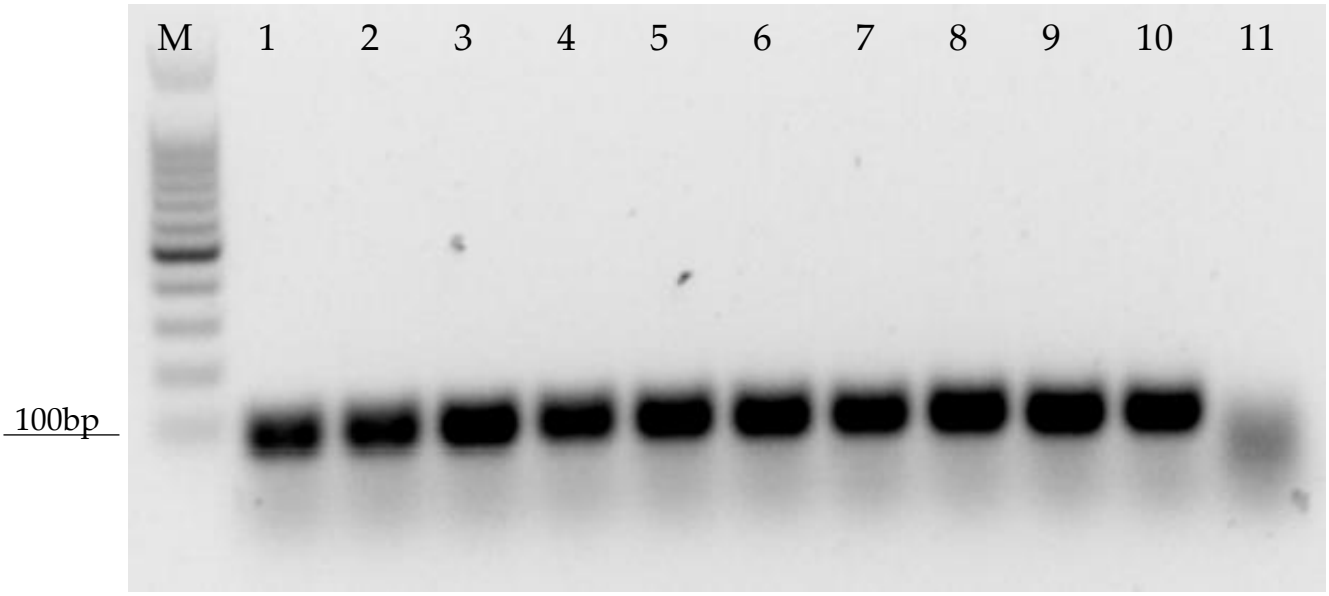

Figure 3.8 PCR confirmation for the presence of the *Ndb2* OEX construct within the *Aox1a*/*Ndb2* dual OEX lines.

mRNA was extracted from T3 dual *Aox1a*/*Ndb2* OEX lines and constructs amplified using and *Ndb2* qPCR FWD/RWD primer set as seen in Table A7.4. PCR was performed as described in methods section 2.4.8. Expected product size was 100bp for transformants and no product for wildtype

Marker	Promega 100bp ladder
Lane 1	XX1/*Ndb2* OEX T3 5.1
Lane 2	XX1/*Ndb2* OEX T3 5.2
Lane 3	XX1/*Ndb2* OEX T3 6.1
Lane 4	XX1/*Ndb2* OEX T3 9.1
Lane 5	XX1/*Ndb2* OEX T3 11.2
Lane 6	XX1/*Ndb2* OEX T3 12.2
Lane 7	XX1/*Ndb2* OEX T3 15.2
Lane 8	XX1/*Ndb2* OEX T3 17.1
Lane 9	XX1/*Ndb2* OEX T3 17.2
Lane 10	XX1/*Ndb2* OEX T3 20.1
Lane 11	Wildtype

transcript (Figure 3.9). The three lines showing the greatest increase in *AtNdb2* transcript were selected for protein and enzymatic analysis (lines 5.2 , 6.1 and 15.2).

3.3.1.3 Protein and enzymatic characterisation of dual *AtAox1a* and *AtNdb2* *OEX lines*

To determine the change to NDB2 related activity, mitochondria were fractionated and isolated from seedlings grown on MS media. Isolated mitochondria were initially tested in a Dynamica HALO DB-20 UV-VIS double beam spectrophotometer.to determine the change to NAD(P)H oxidation but were later tested in an Olis Modernized Aminco™ DW-2. External NADH oxidation was measured in the presence of either calcium chloride (to mimic the effects of calcium activation) or EGTA (a calcium chelator). NADH oxidation was also measured in the presence of oxygen or with the addition of decylubiquinone (DCQ) which acts as a ubiquinone analog and an additional electron acceptor. In preliminary measurements of external NADH oxidation rates in three dual *Aox1a*/*Ndb2* OEX lines, there was difficulty in reducing noise within measurements, likely due to the spectrophotometer used and its inability to measure highly turbid samples. Regardless, external NADH oxidation from a single replicate was still measured in the wildtype control and three putative *Aox1a*/*Ndb2* dual OEX lines. In the presence of oxygen and calcium, external NADH oxidation doubled only in line 5.2 but was reduced by more than half in the presence of EGTA (Figure 3.10a). Line 6.1 showed similar NADH oxidation under the presence of calcium but close to double in the presence of EGTA. In the other dual OEX line, 15.2, there were decreases in NADH

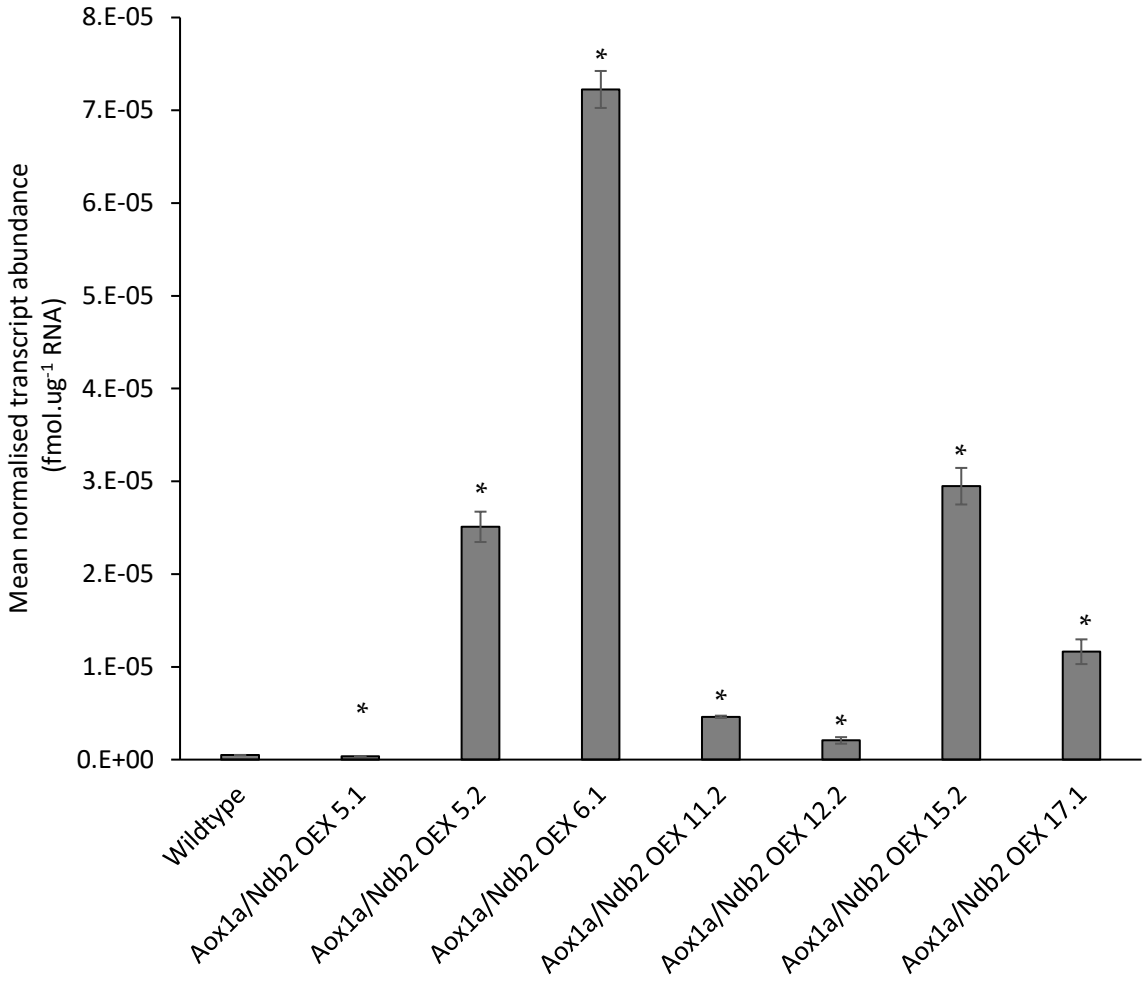

Figure 3.9 Identifying T3 dual *Aox1a*/*Ndb2* OEX transformants with the highest *Ndb2* transcript abundance

Mean normalised transcript abundance of *Ndb2* in six different dual *Aox1a*/*Ndb2* OEX lines each coming from separate insertion events determined via qRT-PCR. Constructs were amplified using *AtUbiquitin* and *AtProtein phosphatase2A* (*PDF2*) qPCR primer set as seen in Table A7.4. qRT-PCR was performed as described in methods section 2.4.11. Transcript abundance was normalised to references genes *AtUbiquitin* (*Ubq)* and *AtProtein phosphatase2A* (*Pdf2*). Values are mean +/- SE N=3 * denotes significance of $p<0.05$ determined via unpaired, two-tailed t-test against wild type .

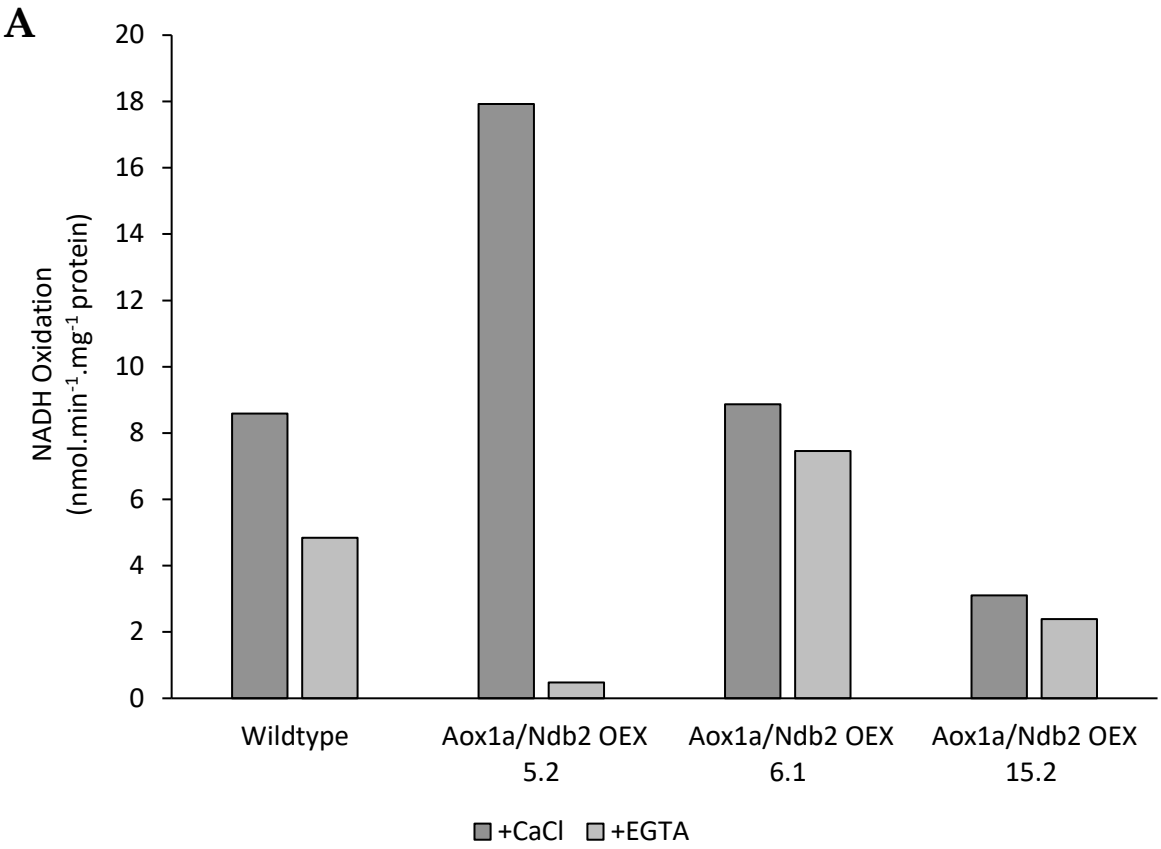
A
NADH Oxidation (nmol.min-1.mg-1 protein)
0
2
4
6
8
10
12
14
16
18
20
Wildtype
Aox1a/Ndb2 OEX 5.2
Aox1a/Ndb2 OEX 6.1
Aox1a/Ndb2 OEX 15.2
+CaCl
+EGTA

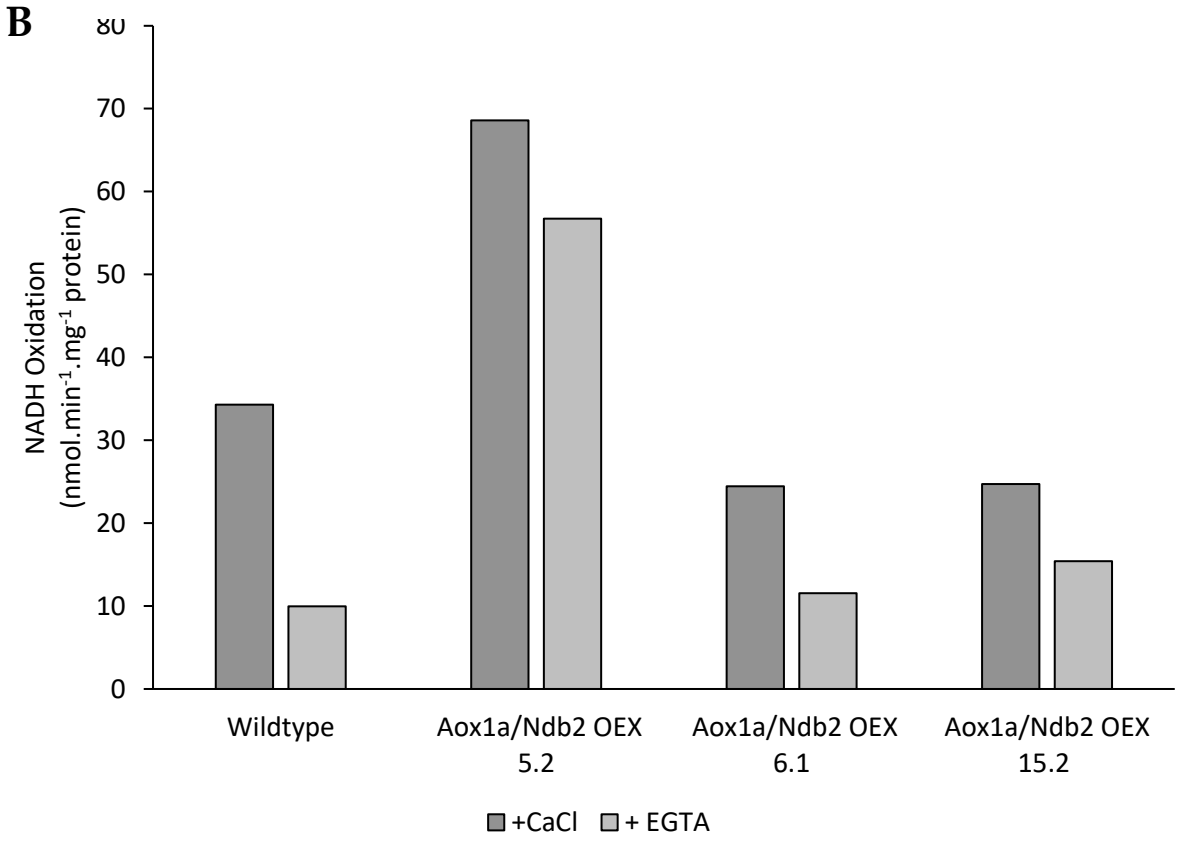
B
NADH Oxidation (nmol.min-1.mg-1 protein)
0
10
20
30
40
50
60
70
80
Wildtype
Aox1a/Ndb2 OEX 5.2
Aox1a/Ndb2 OEX 6.1
Aox1a/Ndb2 OEX 15.2
+CaCl
+ EGTA

Figure 3.10 External mitochondrial membrane NADH activity of dual *Aox1a*/*Ndb2* OEX lines in isolated mitochondria.

NADH oxidation rates were measured using isolated, intact mitochondria from 21-day old seedlings grown in ½ strength MS media. NADH oxidation was measured at 340 nm in the presence of ADP (1 mM), NADH (0.2 mM), CaCl (1 mM) or EGTA (0.5mM). Oxidation rates were measured to oxygen (A) or to DCQ (0.5 mM)(B). Oxidation rates were first measured through to oxygen and then in the presence of decylubiquinone. Spectrophotometer used was a Dynamica HALO DB-20 UV-VIS double beam spectrophotometer. N=1

oxidation in both the presence of calcium and EGTA. When tested in the presence of DCQ a mostly similar trend was seen however the rates of reaction were all largely increased. Compared to wildtype under the same conditions, line 5.2 again showed a doubling in the presence of calcium (Figure 3.10b). Conversely, the reaction rate in the presence of EGTA was at least five times higher than that of the wildtype, a trend not seen when measured in the presence of oxygen. Line 6.1 and 15.2 both showed decreases in reaction rate in the presence of DCQ and calcium but were marginally higher in the presence of EGTA. Measurements of external NADPH oxidation were attempted but due to very noisy and low rates of reaction, a confident measurement of external NADPH oxidation was not achieved and was not presented. Isolated mitochondria were then measured for changes to AOX, NDB2 and PORIN.

To determine whether the changes (or lack thereof) to NADH oxidation correlated with changes to protein levels, isolated mitochondria were separated and quantified using SDS-PAGE and western blot. Isolated mitochondria were probed for PORIN as a reference protein to normalise both AOX and NDB2 too (Figure 3.11). Under the presence of reducing agents, DTT and β-mercaptoethanol, AOX and PORIN antibodies produced single bands of sizes 35 and 30 kDa respectively. The NDB2 probe used however produces multiple bands. As the calculated size of NDB2 is 60 kDa, it was assumed the band at 60 kDa represents the NDB2 protein. In future results, a different NDB2 antibody is used that produces a single band at 60 kDa. The quantity

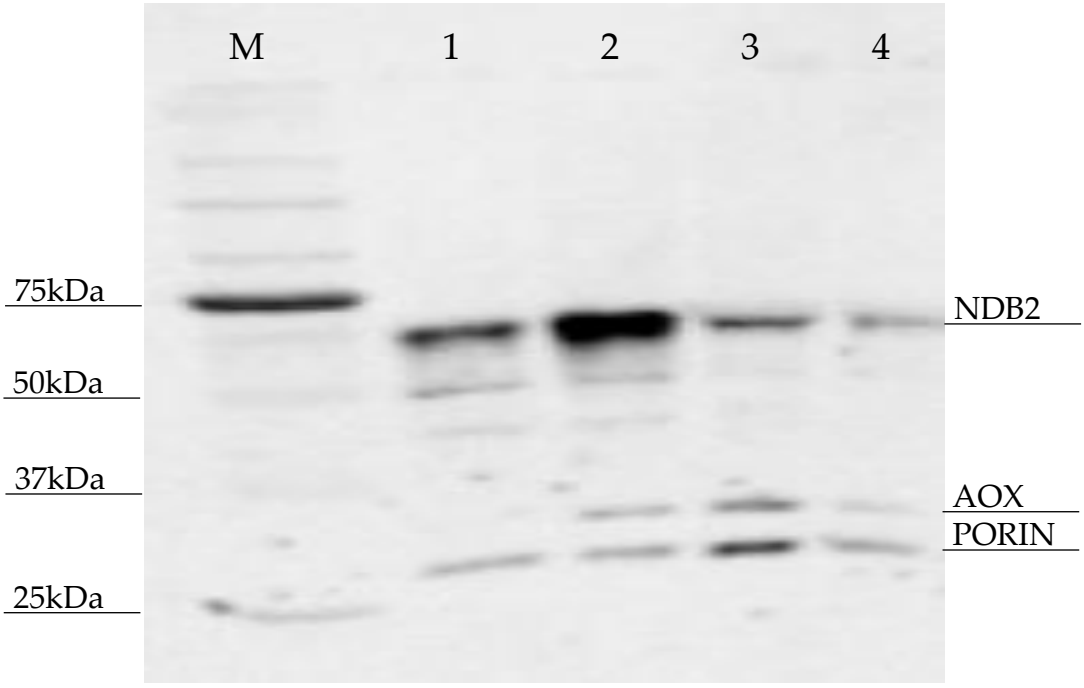

Figure 3.11 Western blot of isolated mitochondria extracted from wildtype and *Aox1a*/*Ndb2* dual OEX seedlings grown for 21 days on MS media.

Seedlings were grown for 21 days on ½ strength MS media and 2%(w/v) sucrose. Isolated mitochondria were separated on a 10% SDS PAGE, transferred to nitrocellulose membrane and blotted for AOX, NDB2 and mitochondrial reference protein PORIN. Expected protein sizes were 60, 35 and 30kDa for NDB2, AOX and PORIN respectively. Isolated mitochondria were assayed for total protein concentration using the BCA protein assay and 1 μg was loaded per sample.

Marker 1	Promega Precision Plus Protein Kaleidoscope Prestained Protein Standard
Lane 1	Wildtype
Lane 2	XX1/*Ndb2* OEX T2 5.2
Lane 3	XX1/*Ndb2* OEX T2 6.1
Lane 4	XX1/*Ndb2* OEX T2 15.2

of AOX, PORIN and NDB2 were determined using pixel analysis in ImageLab. Based on a single replicate, AOX was seen to be increased in all dual OEX lines with the highest amount seen in line 5.2 (Figure 3.12). NDB2 protein was only seen to be upregulated in 5.2 and downregulated in 6.1 and 15.2 correlating with the trends seen in NADH oxidation. (Figure 3.10). Therefore, only one of the three tested dual OEX lines had increased NDB2 content and related activity.

To increase the number of biological replicates of dual *Aox1a*/*Ndb2* replicates, other lines were tested for increased NAD(P)H oxidation rates. Mitochondria were once again isolated from seedlings and the external NAD(P)H oxidation rates were measured. Both 5.2 and 6.1 lines were included again as positive and negative controls respectively. Two more dual *Aox1a*/*Ndb2* OEX were included (11.2 and 12.2) as well as the *Aox1a* OEX background line (XX1), a *ndb2* T-DNA line (330) as well as an *aox1a* T-DNA line (084). External NADH oxidation was measured again with the addition of either calcium chloride or EGTA in the presence of oxygen or DCQ. It should be noted that these experiments now utilised the Olis Modernized Aminco™ DW-2 spectrophotometer. A spectrophotometer that is optimised for measuring turbid samples such as isolated mitochondrial samples. In agreement with previous results, the 6.1 *Aox1a*/*Ndb2* dual OEX line showed a decrease in external NADH oxidation compared to wildtype under all conditions. (Figure 3.13). The same was seen for an additional dual OEX line 12.2. The 11.2 line showed minor differences in NADH oxidation compared to 6.1 and 12.2. (Figure 3.13a) In the presence of either oxygen or

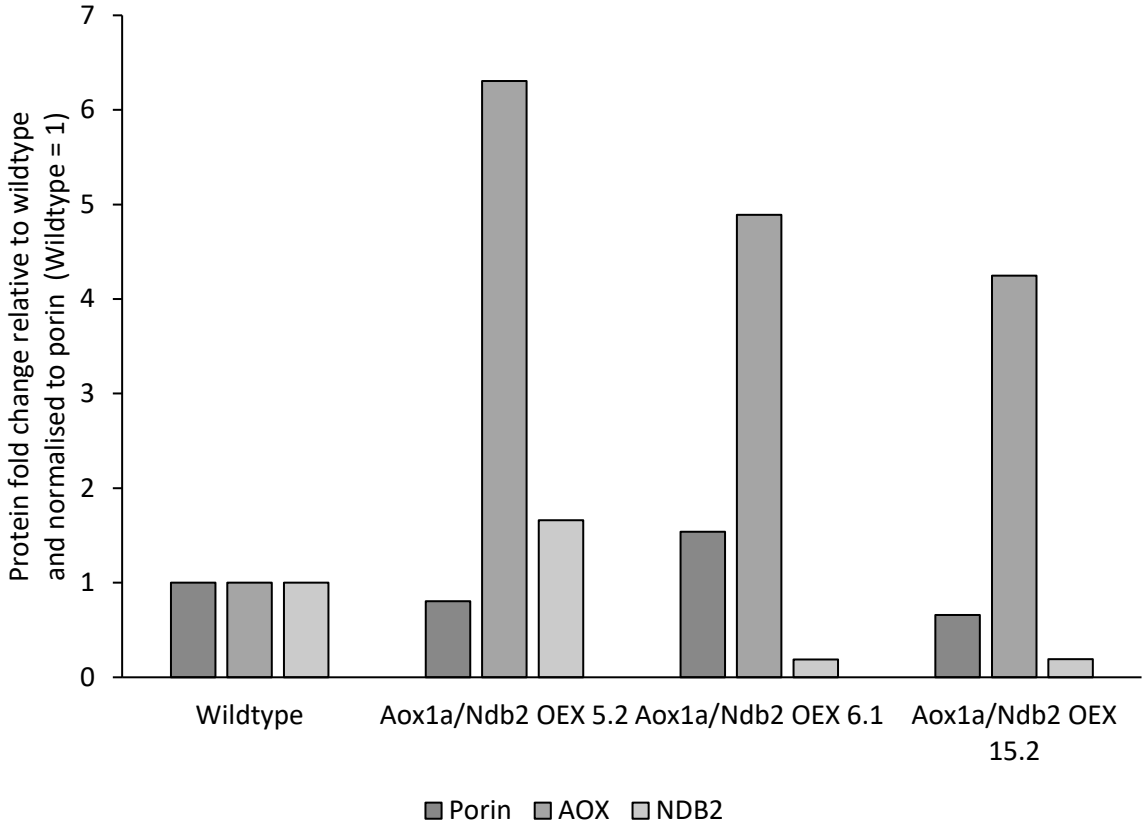

Figure 3.12 Protein abundance of AOX and NDB2 in isolated mitochondria from dual *Aox1a*/*Ndb2* OEX lines under control conditions

Samples were normalised to PORIN and digital quantification performed using ImageLab version 5.2.1. Wildtype values were set to 1. N=1

A

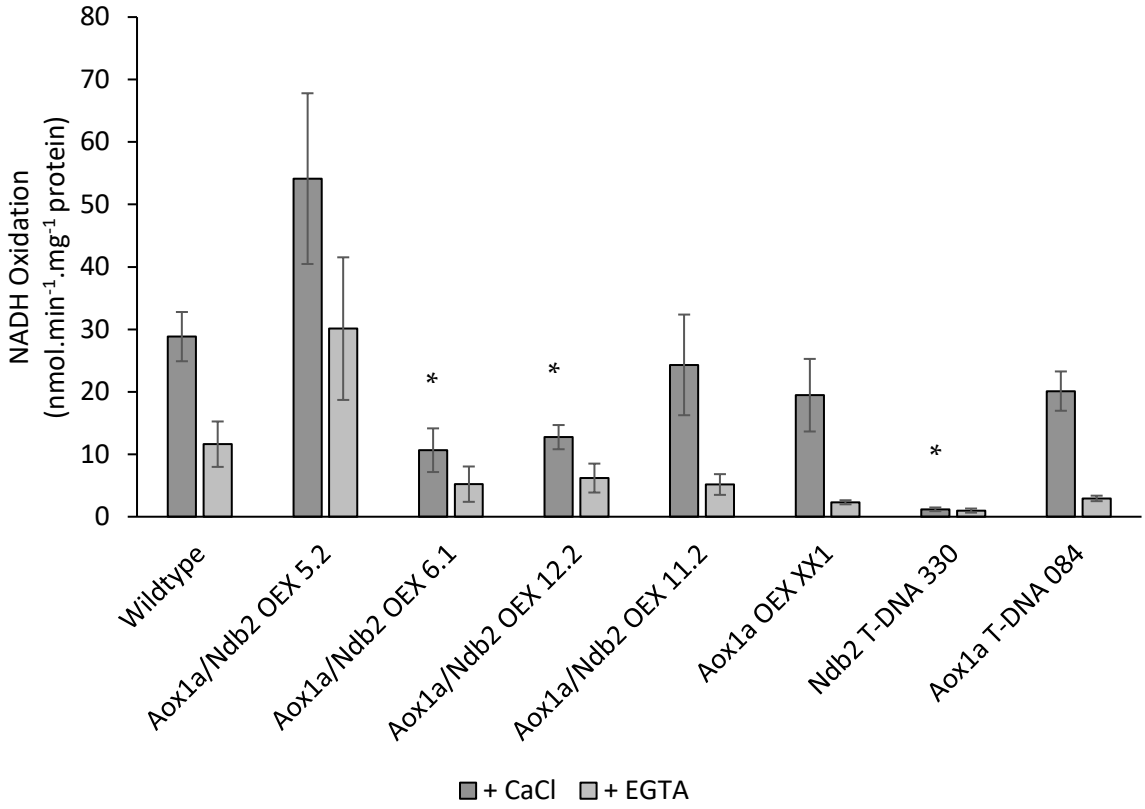
NADH Oxidation (nmol.min-1.mg-1 protein)
80
70
60
50
40
30
20
10
0
*
*
*
Wildtype
Aox1a/Ndb2 OEX 5.2
Aox1a/Ndb2 OEX 6.1
Aox1a/Ndb2 OEX 12.2
Aox1a/Ndb2 OEX 11.2
Aox1a OEX XX1
Ndb2 T-DNA 330
Aox1a T-DNA 084
+ CaCl
+ EGTA

B

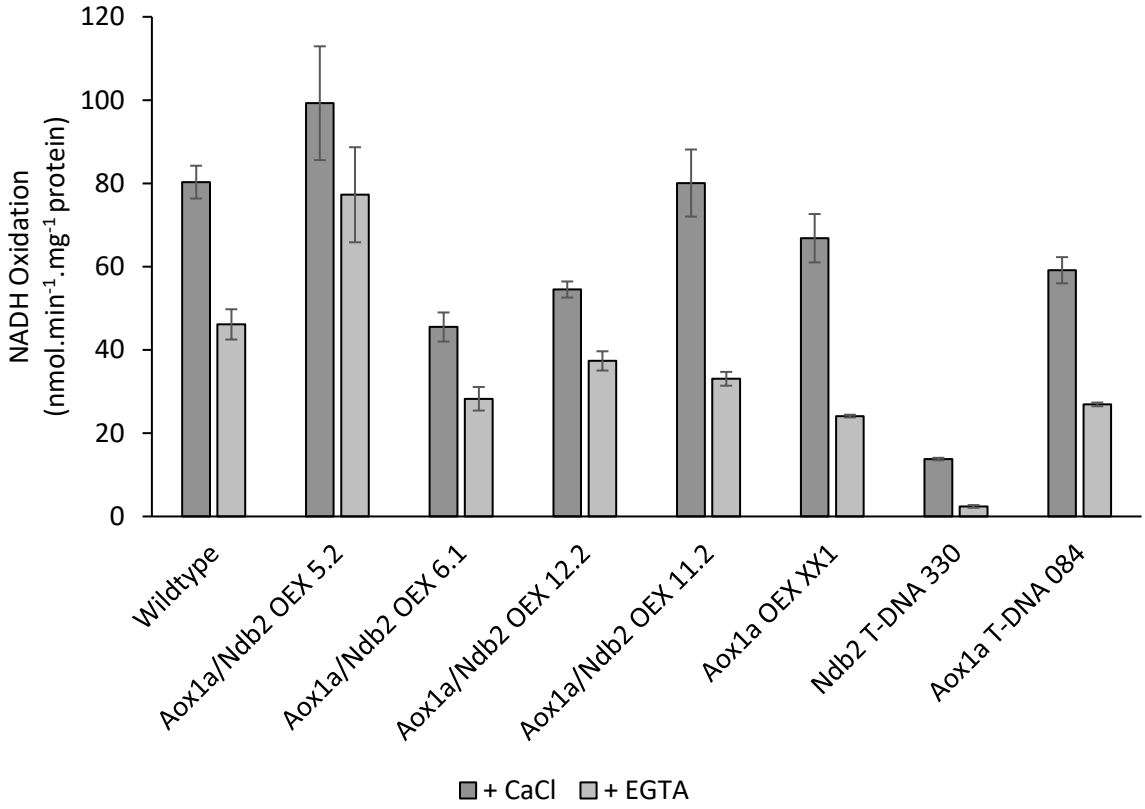
NADH Oxidation (nmol.min-1.mg-1 protein)
120
100
80
60
40
20
0
Wildtype
Aox1a/Ndb2 OEX 5.2
Aox1a/Ndb2 OEX 6.1
Aox1a/Ndb2 OEX 12.2
Aox1a/Ndb2 OEX 11.2
Aox1a OEX XX1
Ndb2 T-DNA 330
Aox1a T-DNA 084
+ CaCl
+ EGTA

Figure 3.13 External mitochondrial membrane NADH activity of a single *Aox1a* OEX line, dual *Aox1a*/*Ndb2* OEX lines, an *ndb2* T-DNA line and a *aox1a* T-DNA line in isolated mitochondria

NADH oxidation rates were measured using isolated, intact mitochondria from 21-day old seedlings grown in ½ strength MS media. NADH oxidation was measured at 340 nm in the presence of ADP (1 mM), NADH (0.2 mM), CaCl (1 mM) or EGTA (0.5mM). Oxidation rates were measured to oxygen (A) or to DCQ (0.5 mM)(B). Spectrophotometer used was an Olis Modernized Aminco™ DW-2. Values are mean +/- SE N=3. * denotes significance of $p<0.05$ determined via unpaired, two-tailed t-test against wild type

DCQ and calcium, 11.2 showed no change in NADH oxidation rates compared to wildtype. There however is a small decrease in NADH oxidation in 11.2 when EGTA is added. The 5.2 line, which was used as a positive control, demonstrated again that the rate of external NADH oxidation was increased under all conditions. Interestingly, both the single *Aox1a* OEX and *aox1a* T-DNA had reduced rates of NADH oxidation under all conditions compared to wildtype, similar to majority of the dual OEX lines. Most notable however was the *ndb2* T-DNA line which showed almost a complete absence of all external NADH oxidation (Figure 3.13). Of the five tested dual OEX transformants, only the 5.2 line has shown to have increased external NADH activity and NDB2 protein content. External membrane localised NADPH oxidation was also measured in isolated mitochondria under the same conditions as above. NADPH oxidation is notably lower in all lines compared to NADH oxidation but did not show any significant differences between any lines (Figure 3.14). The 5.2 line which had previously shown increases in NADH activity showed no changes in activity compared to wildtype under any conditions. Due to the no or low levels of activity detected in tested samples, some samples have only 1 or 2 replicates leading to large variation within the dataset (Figure 3.14a). When DCQ was added, activity was substantially higher, allowing for three replicates from all samples to be measured (Figure 3.14b). Again, there was no significant difference in either calcium or EGTA treated samples suggesting the OEX of NDB2 does not alter the rate of NADPH oxidation.

A

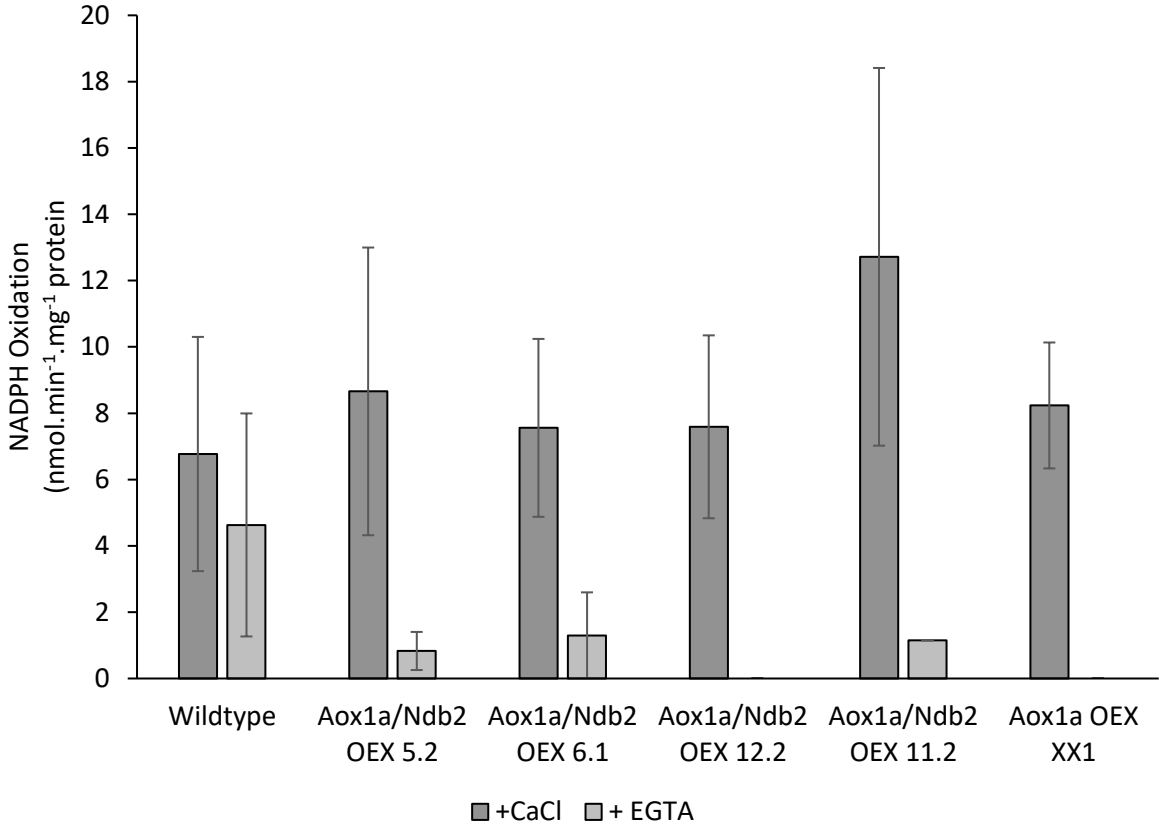
NADPH Oxidation (nmol.min-1.mg-1 protein
20
18
16
14
12
10
8
6
4
2
0
Wildtype
Aox1a/Ndb2 OEX 5.2
Aox1a/Ndb2 OEX 6.1
Aox1a/Ndb2 OEX 12.2
Aox1a/Ndb2 OEX 11.2
Aox1a OEX XX1
+CaCl
+ EGTA

B

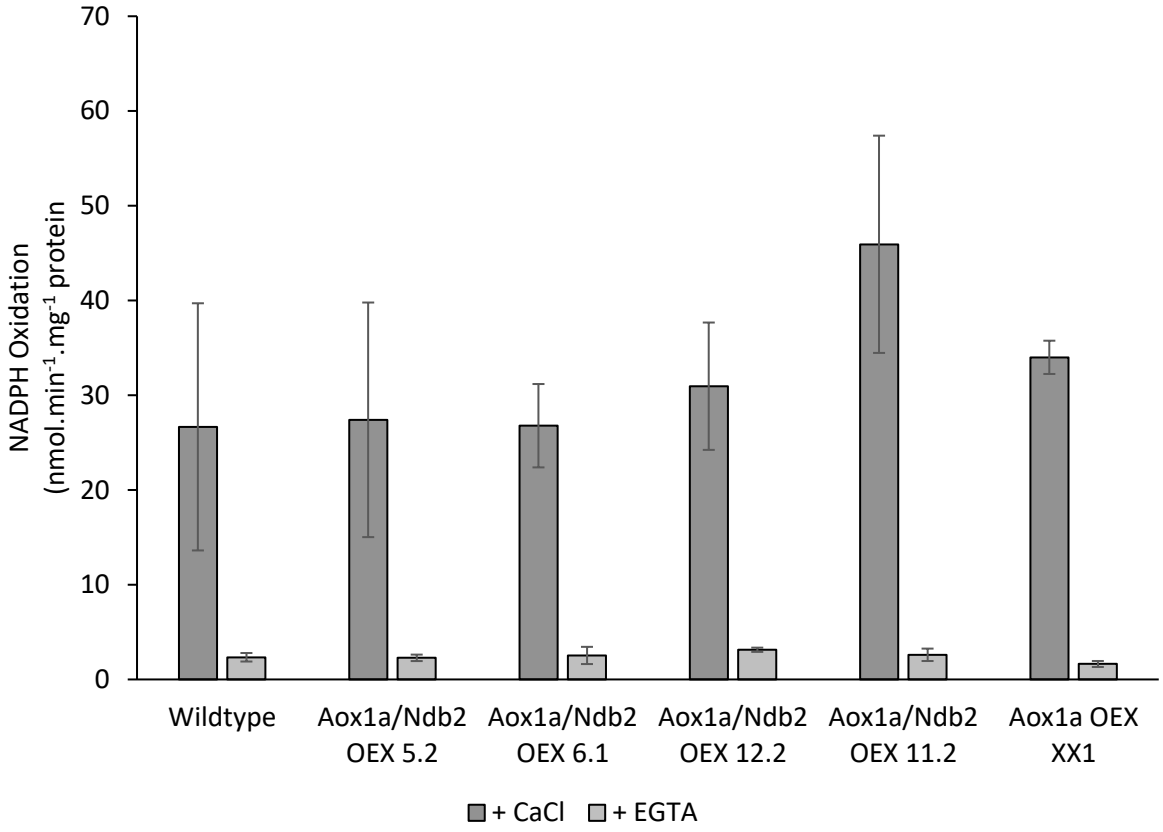
NADPH Oxidation (nmol.min-1.mg-1 protein
70
60
50
40
30
20
10
0
Wildtype
Aox1a/Ndb2 OEX 5.2
Aox1a/Ndb2 OEX 6.1
Aox1a/Ndb2 OEX 12.2
Aox1a/Ndb2 OEX 11.2
Aox1a OEX XX1
+ CaCl
+ EGTA

Figure 3.14 External mitochondrial membrane NADPH activity of a single *Aox1a* OEX line and dual *Aox1a*/*Ndb2* OEX lines in isolated mitochondria.

NADPH oxidation rates were measured using isolated, intact mitochondria from 21-day old seedlings grown in ½ strength MS media. NADPH oxidation was measured at 340 nm in the presence of ADP (1 mM), NADPH (0.2 mM), CaCl (1 mM) or EGTA (0.5mM). Oxidation rates were measured to oxygen (A) or to DCQ (0.5 mM)(B). NADPH activity in the presence of EGTA with oxygen as the electron acceptor was undetectable in line 12.2 and XX1. Line 6.1 and 11.2 in the presence of EGTA with oxygen as the electron acceptor did not have measurable changes in oxidation in two of the replicas. Spectrophotometer used was an Olis Modernized Aminco™ DW-2. N=3 unless otherwise mentioned. Values are mean +/- SE N=3

Quantification of NDB2, AOX and PORIN protein was once again undertaken with western blotting. A replicate from the 5.2 line was used as both a positive controlfor NDB2 upregulation but also as a measure to normalise to allow for comparison between the two separate blots (Figure 3.15 and Figure 3.16). AOX detection was varied and produced unexpected results. Apart from the wildtype and two T-DNA lines, all dual OEX lines were generated from the same background *Aox1a* OEX line (XX1) and should have similar OEX of AOX. AOX protein was not detected in two of the XX1 mitochondrial isolates (Figure 3.15) The *ndb2* T-DNA line showed similar increases in AOX to the lines OEX AOX. The *aox1a* T-DNA line also had higher a content of AOX compared to the XX1 OEX line. Regular inconsistencies were also seen in the other samples (Figure 3.16). Wildtype had increased AOX expression in one replicate, a result not normally seen when plants are grown under normal conditions. Whereas the 6.1 dual OEX line had no detectable AOX protein despite showing similar levels to the 5.2 line previously (Figure 3.11).

Difficulties also arose when attempting to measure NDB2 protein. High quantities of NDB2 in the 5.2 positive control (Figure 3.15) were reassuring but were not replicated across blots (Figure 3.16). Compared to other lines, 5.2 had the most NDB2 content (Figure 3.15) but was the only line to show an accompanying increase in related activity (Figure 3.13). The same increase in NDB2 content in 5.2 was not seen in the other blot (Figure 3.16). The 11.1 dual OEX line showed slightly higher NDB2 content compared to 5.2 but had no change to activity when measured for NADH

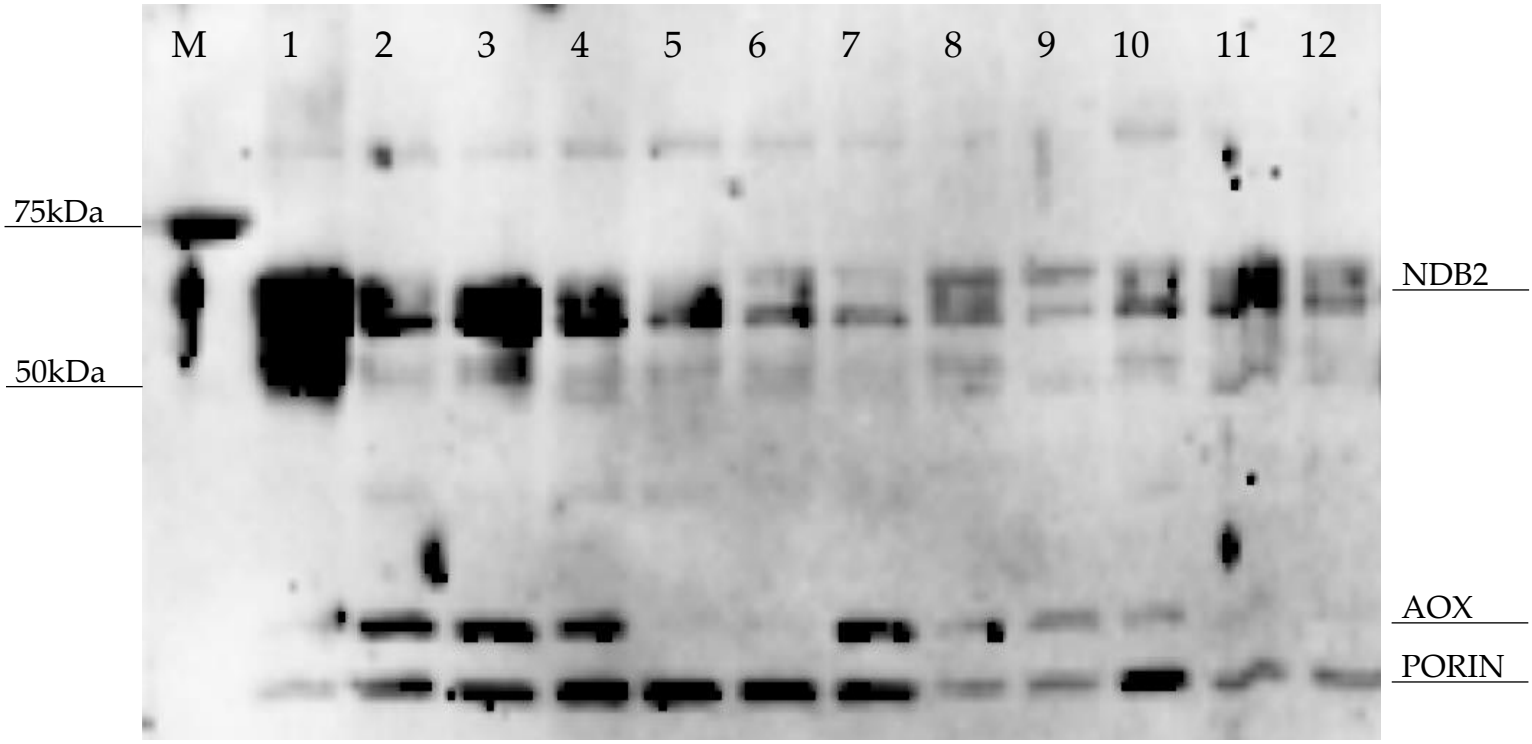

Figure 3.15 Western blot of isolated mitochondria extracted from wildtype and *Aox1a*/*Ndb2* dual OEX seedlings grown for 21 days on MS media.

Seedlings were grown for 21 days on ½ strength MS media and 2%(w/v) sucrose. Isolated mitochondria were separated on a 10% SDS PAGE, transferred to nitrocellulose membrane and blotted for AOX, NDB2 and mitochondrial reference protein PORIN. Expected protein sizes were 60, 35 and 30kDa for NDB2, AOX and PORIN respectively. Isolated mitochondria were assayed for total protein concentration and 1 μg was loaded per sample.

Marker 1	Promega Precision Plus Protein Kaleidoscope Prestained Protein Standard
Lane 1	XX1/*Ndb2* OEX 5.2 replicate 1
Lane 2	XX1/*Ndb2* OEX 12.2 replicate 1
Lane 3	XX1/*Ndb2* OEX 12.2 replicate 2
Lane 4	XX1/*Ndb2* OEX 12.2 replicate 3
Lane 5	XX1 OEX replicate 1
Lane 6	XX1 OEX replicate 2
Lane 7	XX1 OEX replicate 3
Lane 8	330 *ndb2* T-DNA replicate 1
Lane 9	330 *ndb2* T-DNA replicate 2
Lane 10	330 *ndb2* T-DNA replicate 3
Lane 11	084 *aox1a* T-DNA replicate 1
Lane 12	084 *aox1a* T-DNA replicate 2

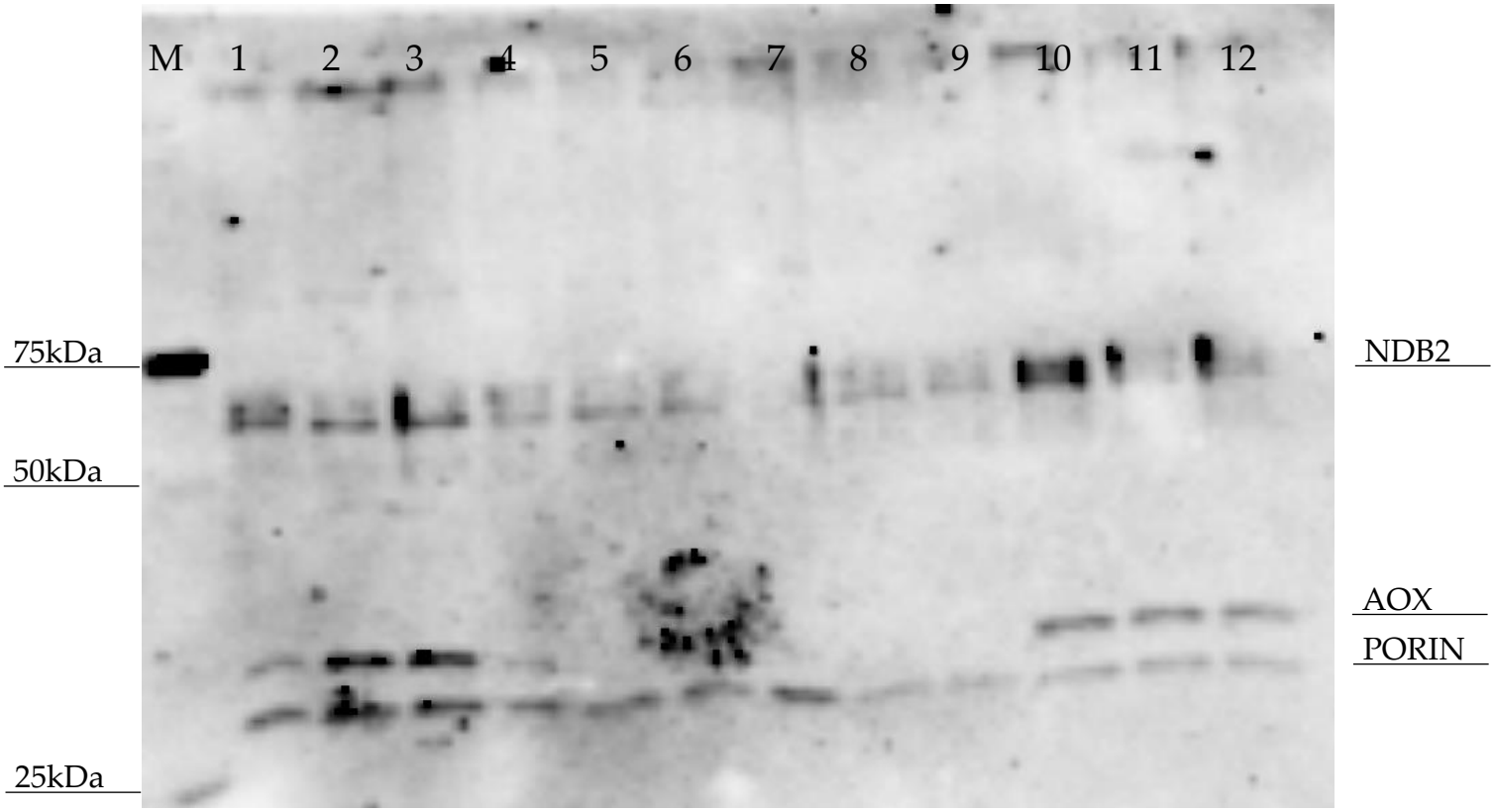

Figure 3.16 Western blot of isolated mitochondria extracted from wildtype and *Aox1a*/*Ndb2* dual OEX seedlings grown for 21 days on MS media.

Seedlings were grown for 21 days on ½ strength MS media and 2%(w/v) sucrose. Isolated mitochondria were separated on a 10% SDS PAGE, transferred to nitrocellulose membrane and blotted for AOX, NDB2 and mitochondrial reference protein PORIN. Expected protein sizes were 60, 35 and 30kDa for NDB2, AOX and PORIN respectively. Isolated mitochondria were assayed for total protein concentration and 1 μg was loaded per sample.

Marker 1	Promega Precision Plus Protein Kaleidoscope Prestained Protein Standard
Lane 1	XX1/*Ndb2* OEX 5.2 replicate 1
Lane 2	XX1/*Ndb2* OEX 5.2 replicate 2
Lane 3	XX1/*Ndb2* OEX 5.2 replicate 3
Lane 4	Wildtype replicate 1
Lane 5	Wildtype replicate 2
Lane 6	Wildtype replicate 3
Lane 7	XX1/*Ndb2* OEX 6.1 replicate 1
Lane 8	XX1/*Ndb2* OEX 6.1 replicate 2
Lane 9	XX1/*Ndb2* OEX 6.1 replicate 3
Lane 10	XX1/*Ndb2* OEX 11.1 replicate 1
Lane 11	XX1/*Ndb2* OEX 11.1 replicate 2
Lane 12	XX1/*Ndb2* OEX 11.1 replicate 3

oxidation (Figure 3.13). Based on the western blots inability to highlight increased AOX protein in the *Aox1a* OEX and the inconsistent detection of AOX and NDB2 in the dual OEX line 5.2, it was reasoned that there would be minimal confidence in any conclusions made based on the western blots. It was also reasoned that as none of the new dual OEX lines tested showed any increase in NADH oxidation when compared to the wildtype , that these lines were not overexpressing the NDB2 protein and would not be included in further analysis. In further experiments, a newly designed NDB2 antibody was used that permitted only a single protein product to be detected at the expected size.

Transcript abundance of *Ndb2* in two new dual OEX lines were again tested for increased transcript abundance relative to wildtype. Significantly increased *Ndb2* expression was seen across both the new dual OEX lines (Figure 3.17). Coupled with the similar increases seen in 5.2, it was expected that these lines were overexpressing the *Ndb2* gene. To provide further evidence of upregulated expression of *Ndb2*, protein content in isolated mitochondria was measured. The fold change of NDB2 protein highlights across all lines that that the increase in transcript abundance does not necessarily follow protein (Figure 3.18). NDB2 protein was increased across all new dual OEX lines; protein content was increased by 80 to 110-fold compared to wildtype whereas transcript was only upregulated 5 to 8-fold (Figure 3.19 and 3.17). Also notable was the trending increase of AOX protein compared to both the wildtype and especially the *Aox1a* background OEX line. However large variation among replicates

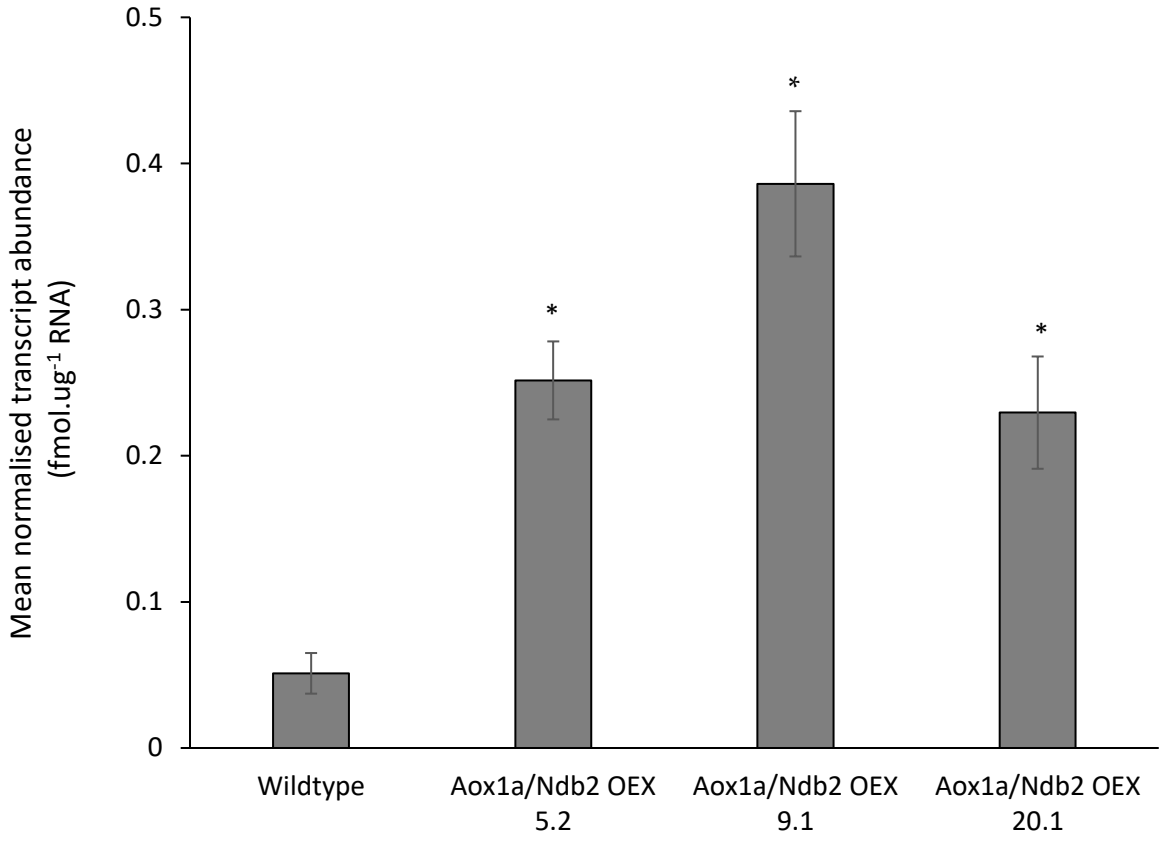

Figure 3.17 Identifying new T3 dual *Aox1a*/*Ndb2* OEX transformants in attempt to find lines with corresponding increases in protein and localised external membrane NAD(P)H oxidation.

Mean normalised transcript abundance of *Ndb2* in two new dual *Aox1a*/*Ndb2* OEX lines (9.1 and 20.1) each coming from separate insertion events determined via qRT-PCR. Transcript abundance was normalised to references genes *AtUbiquitin* and *AtProtein phosphatase2A* (*PDF2*). Values are mean +/- SE N=3. * denotes significance of $p<0.05$ determined via unpaired, two-tailed t-test against wild type

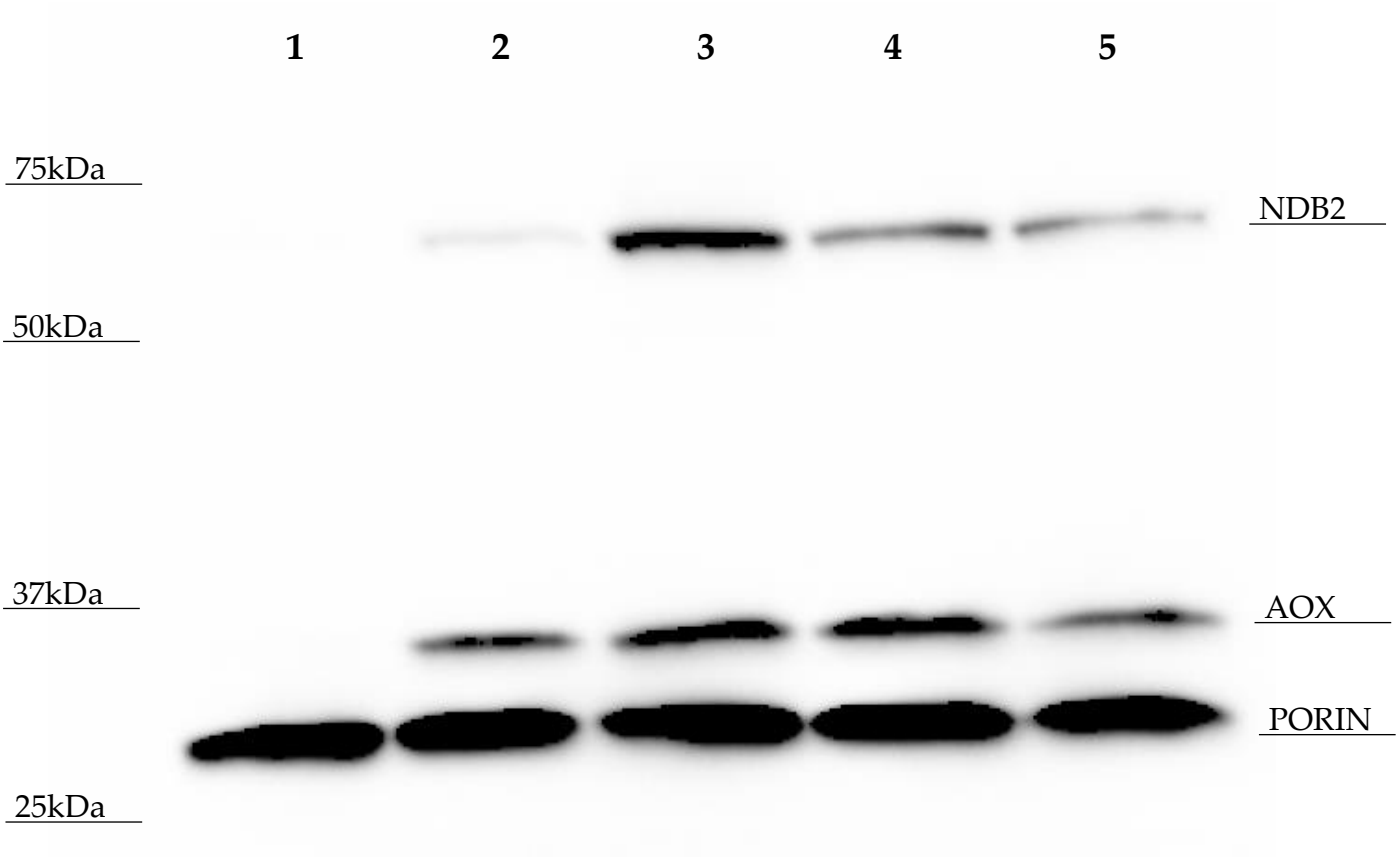

Figure 3.18 Western blot of isolated mitochondria extracted from wildtype and *Aox1a*/*Ndb2* dual OEX seedlings grown for 21 days on MS media.

Seedlings were grown for 21 days on ½ strength MS media and 2%(w/v) sucrose. Isolated mitochondria were separated on a 10% SDS PAGE, transferred to nitrocellulose membrane and blotted for AOX, NDB2 and mitochondrial reference protein PORIN. Expected protein sizes were 60, 35 and 30kDa for NDB2, AOX and PORIN respectively. Isolated mitochondria were assayed for total protein concentration and 1 μg was loaded per sample

Lane 1	Wildtype
Lane 2	*Aox1a* OEX XX1
Lane 3	XX1/*Ndb2* OEX 5.2
Lane 4	XX1/*Ndb2* OEX 9.1
Lane 5	XX1/Ndb2 OEX 20.1

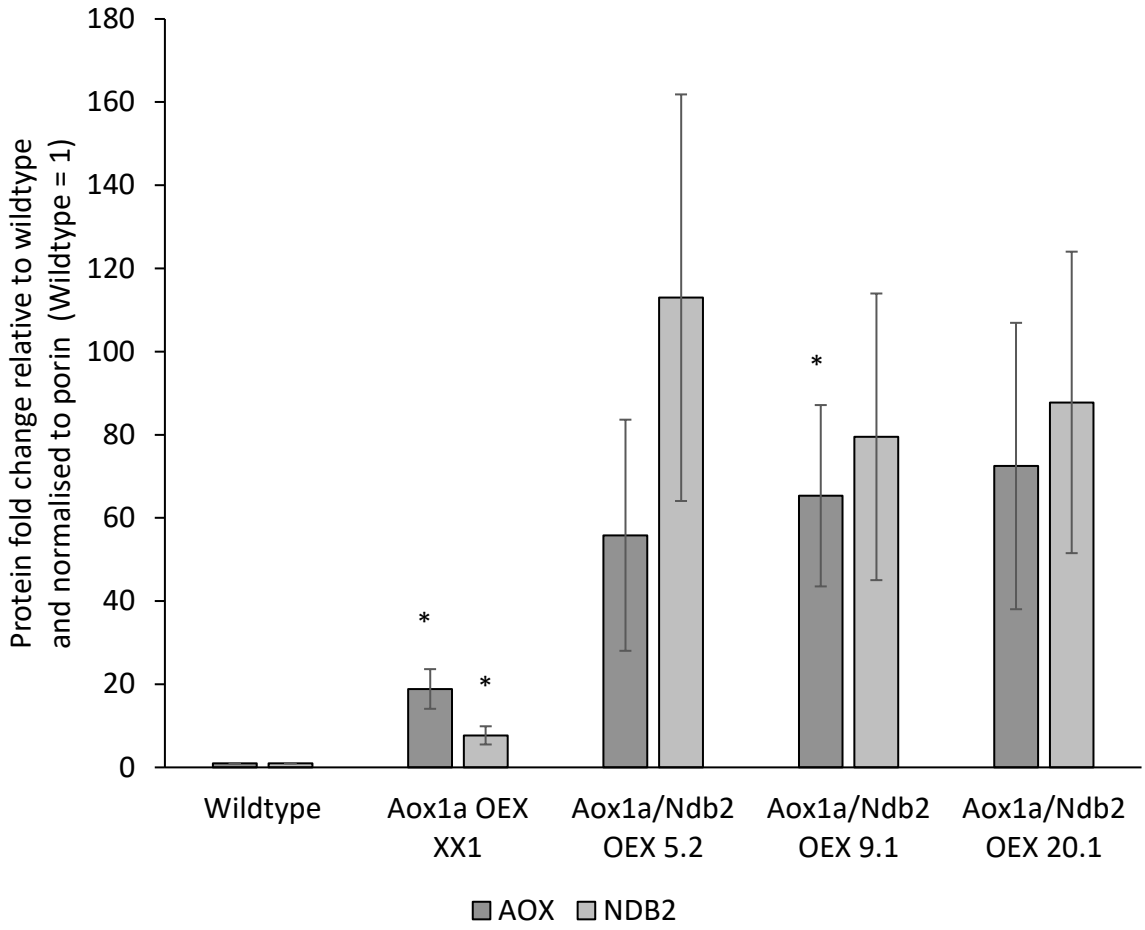

Figure 3.19 Protein abundance of PORIN, AOX and NDB2 in isolated mitochondria from dual *Aox1a*/*Ndb2* OEX lines under control conditions

Seedlings were grown for 21 days on ½ strength MS media and 2%(w/v) sucrose. Samples were normalised to PORIN and digital quantification performed using ImageLab 5.2.1. Wildtype values were set to 1. Values are mean ± SE N=3. * denotes significance of $p<0.05$ determined via unpaired, two-tailed t-test against wild type

makes it difficult to form confident conclusions.

To confirm this, further enzymatic activity in isolated mitochondria was assessed. NADH oxidation in the presence of calcium was markedly increased across all new dual OEX lines compared to both the wildtype and single *Aox1a* OEX (Figure 3.20a).The 9.1 line had the smallest increase in NADH oxidation compared to wildtype, whereas 20.1 had similar levels to the 5.2 line. Addition of AOX activators DTT and pyruvate caused a 3 to 4-fold increase in activity in the dual OEX. The massive increase in electron flux seen with the addition of AOX activators suggested the capacity of the ETC was at capacity before AOX activation. Competition of the ubiquinone pool was tested by adding an additional substrate. All lines tested including wildtype had trended towards a decrease in NADH oxidation, suggesting complex II was outcompeting NDB2 for the ubiquinone pool. Almost complete inhibition was seen with the addition of cytochrome c inhibitor cyanide in wildtype lines, while all *Aox1a* OEX lines maintained substantial activity (10-60-fold). Only when combined with AOX inhibitor propyl gallate was there an almost complete removal of activity across all lines. Similar trends across all treatments were seen in NADH + EGTA experiments albeit with less activity and larger variation. All lines showed increased NADH activity and a significant increase with the addition of AOX activators (Figure 3.20b). These same measurements were performed in the presence of NADPH. NADPH activity did not display any statistical difference between lines however, there does appear to be decreases in line 20.1 and particularly 9.1 in the

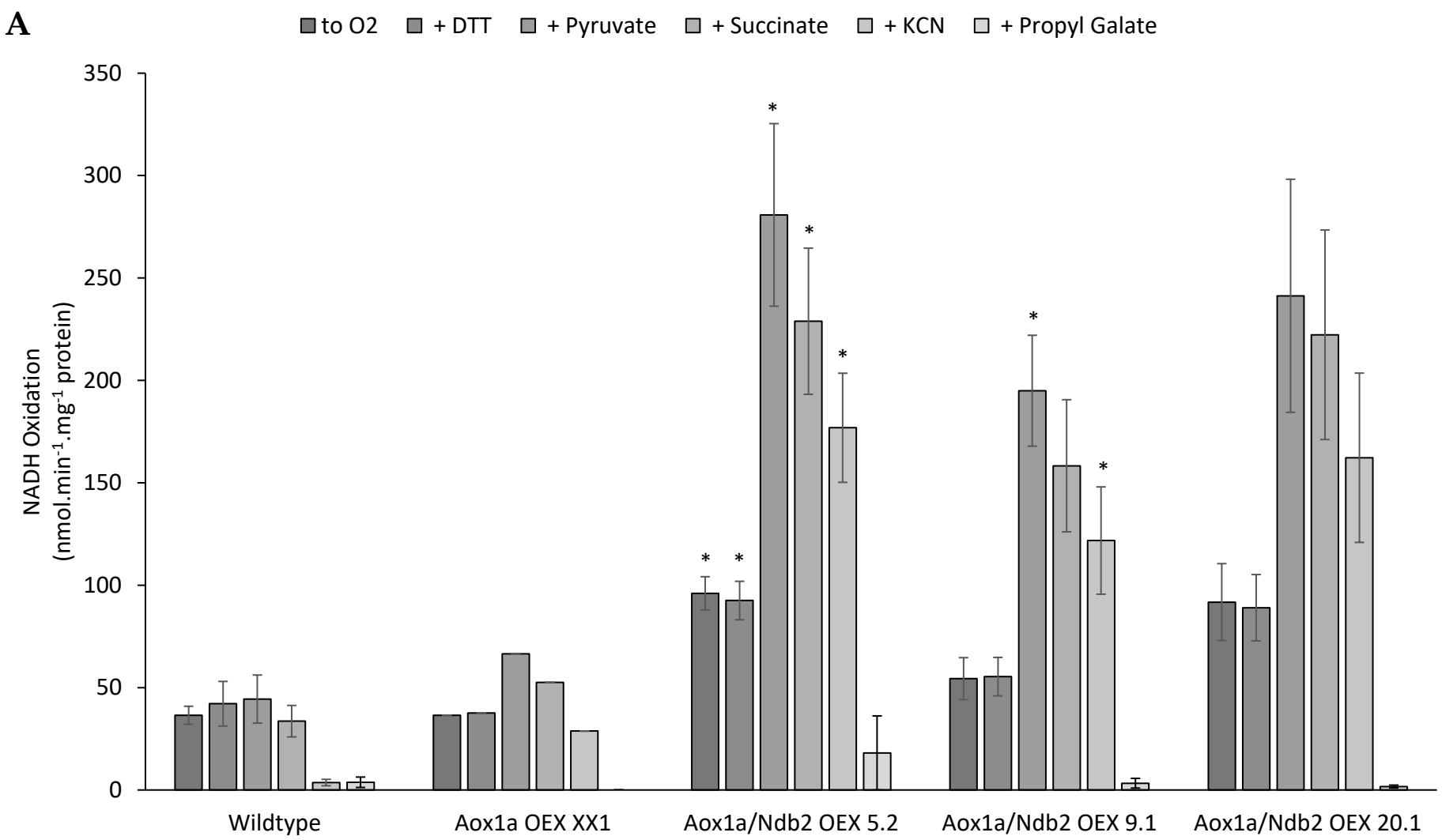
A
to O2
+ DTT
+ Pyruvate
+ Succinate
+ KCN
+ Propyl Galate
NADH Oxidation
(nmol.min-1.mg-1 protein)
350
300
250
200
150
100
50
0
Wildtype
Aox1a OEX XX1
Aox1a/Ndb2 OEX 5.2
Aox1a/Ndb2 OEX 9.1
Aox1a/Ndb2 OEX 20.1

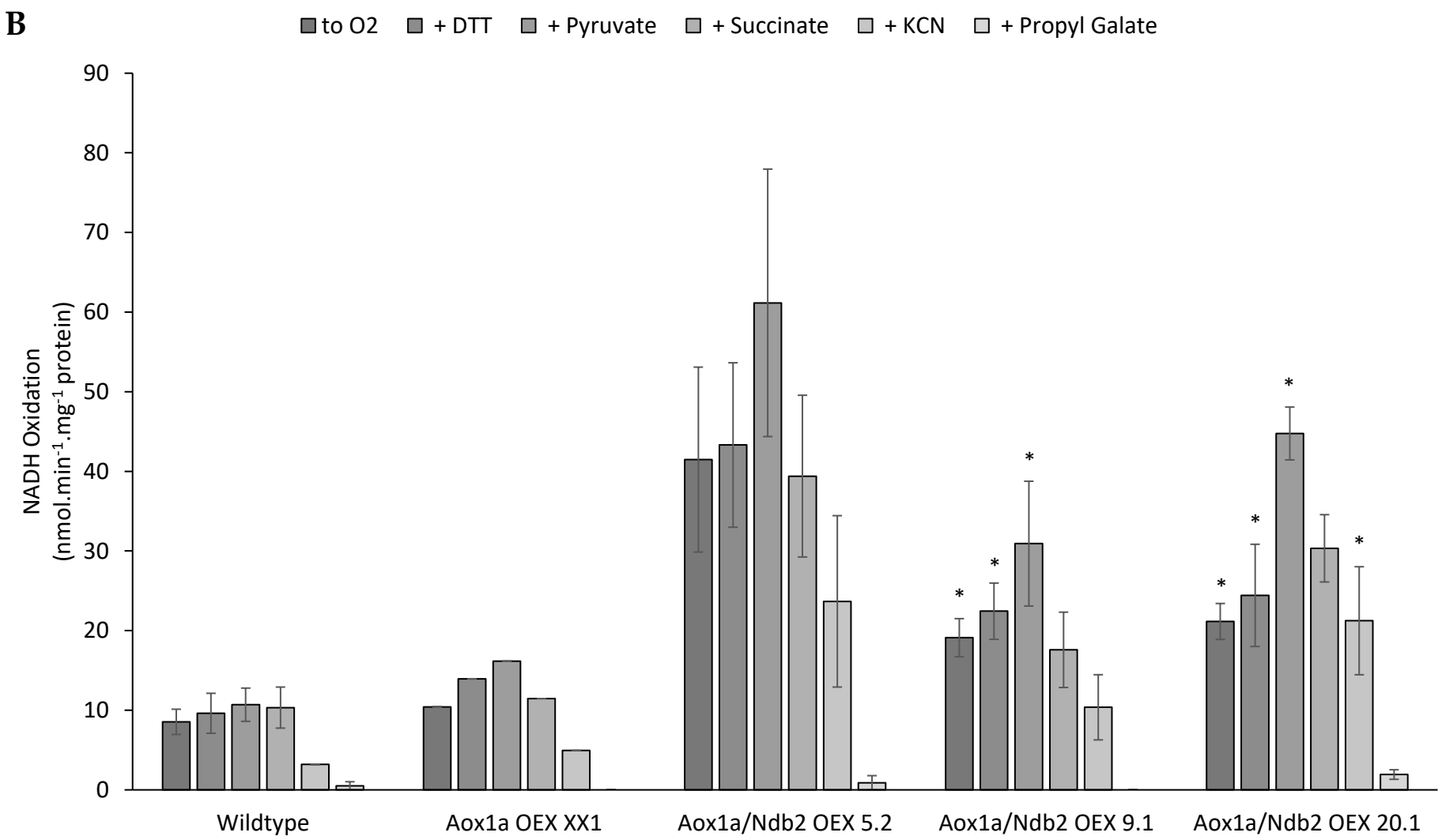
B
to O2
+ DTT
+ Pyruvate
+ Succinate
+ KCN
+ Propyl Galate
NADH Oxidation
(nmol.min-1.mg-1 protein)
90
80
70
60
50
40
30
20
10
0
Wildtype
Aox1a OEX XX1
Aox1a/Ndb2 OEX 5.2
Aox1a/Ndb2 OEX 9.1
Aox1a/Ndb2 OEX 20.1

Figure 3.20 External mitochondrial membrane NADH activity and activation of a single *Aox1a* OEX line and dual *Aox1a*/*Ndb2* OEX lines in isolated mitochondria under the presence of CaCl or EGTA

NADH oxidation rates were measured using isolated and intact mitochondria from 21-day old seedlings grown in ½ strength MS media. NADH oxidation was measured at 340 nm in the presence of ADP (1 mM), NADH (0.2 mM), CaCl (1 mM)(A) or EGTA (0.5mM)(B). Subsequent additions of activators and inhibitors were made in order of DTT (1 mM), pyruvate (5 mM)(AOX activators), succinate (10mM)(complex II substrate), potassium cyanide(0.5 mM)(complex 4 inhibitor) and propyl gallate (0.12 mM)(AOX inhibitor). Spectrophotometer used was an Olis Modernized Aminco™ DW-2. Values are mean +/- SE N=3 * denotes significance of $p<0.05$ determined via unpaired, two-tailed t-test against wild type

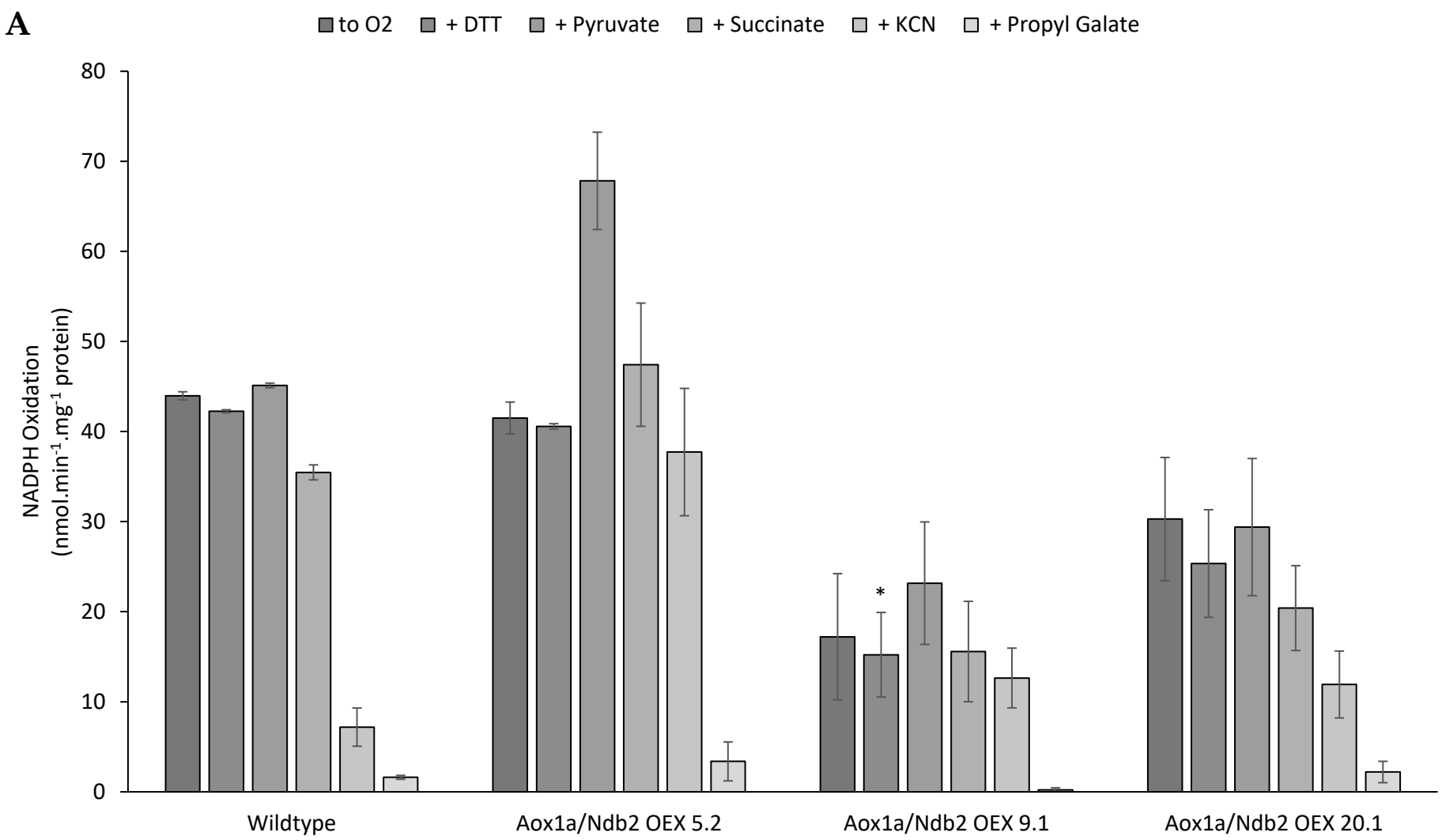
A
to O2
+ DTT
+ Pyruvate
+ Succinate
+ KCN
+ Propyl Galate
NADPH Oxidation
(nmol.min-1.mg-1 protein)
80
70
60
50
40
30
20
10
0
*
Wildtype
Aox1a/Ndb2 OEX 5.2
Aox1a/Ndb2 OEX 9.1
Aox1a/Ndb2 OEX 20.1

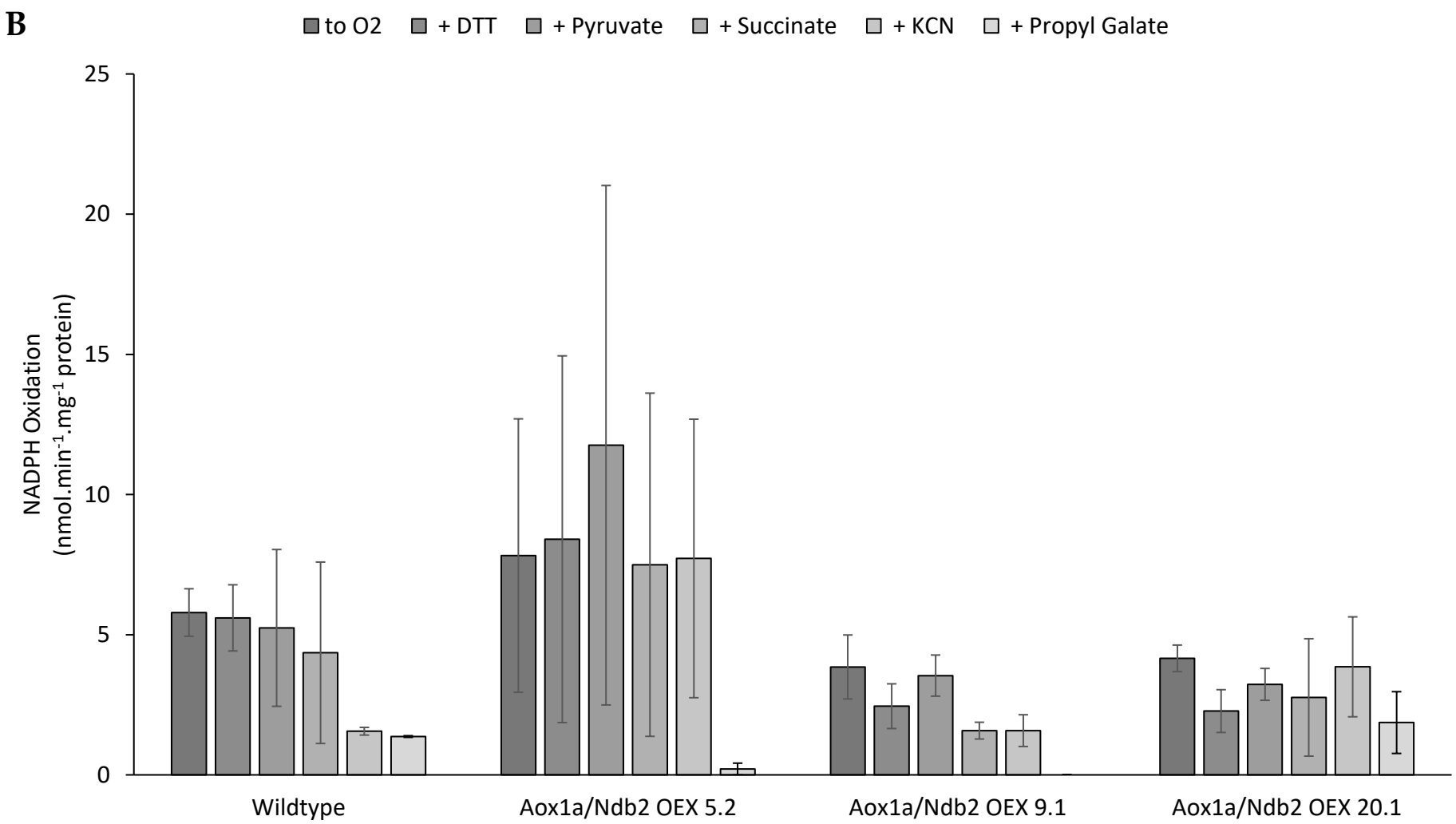
B
to O2
+ DTT
+ Pyruvate
+ Succinate
+ KCN
+ Propyl Galate
NADPH Oxidation
(nmol.min-1.mg-1 protein)
25
20
15
10
5
0
Wildtype
Aox1a/Ndb2 OEX 5.2
Aox1a/Ndb2 OEX 9.1
Aox1a/Ndb2 OEX 20.1

Figure 3.21 External mitochondrial membrane NADPH activity and activation of dual *Aox1a*/*Ndb2* OEX lines in isolated mitochondria under the presence of CaCl or EGTA

NADPH oxidation rates were measured using isolated and intact mitochondria from 21-day old seedlings grown in ½ strength MS media. NADPH oxidation was measured at 340 nm in the presence of ADP (1 mM), NADPH (0.2 mM), CaCl (1 mM)(A) or EGTA (0.5mM)(B). Subsequent additions of activators and inhibitors were made in order of DTT (1 mM), pyruvate (5 mM)(AOX activators), succinate (10mM)(complex II substrate), potassium cyanide(0.5 mM)(complex 4 inhibitor) and propyl gallate (0.12 mM)(AOX inhibitor). Spectrophotometer used was an Olis Modernized Aminco™ DW-2. Values are mean +/- SE N=2 (Wildtype and 5.2) N=3 (9.1 and 20.1). * denotes significance of $p<0.05$ determined via unpaired, two-tailed t-test against wild type

presence of calcium (Figure 3.21a). Whereas in the presence of EGTA, all lines appeared much more similar albeit very low and in one case with large amounts of variation across samples (Figure 3.21b) Comparing the changes to calcium dependent and independent rates of oxidation, all new dual OEX lines clearly show increased rates of calcium-dependent NADH oxidation while maintaining similar levels of calcium-independent activity compared to wildtype (Figure 3.22). In the presence of NADPH, line 5.2 showed similar rates of calcium-dependant and independent rates of reaction, whereas 9.1 and 20.1 showed decreases in calcium dependent activity albeit not statistically significant.

As the plants had previously demonstrated a limitation through the ETC without the presence of activators (Figure 3.20a), it could be reasoned that the measured activity was still rate limited by the electron flow and not representative of maximal activity. To test this, the final product of the electron transport chain (oxygen) was measured using an oxygen electrode. Of all the lines tested, only wildtype showed an increase in oxygen consumption after succinate was added demonstrating that all three lines were still rate limited and that the true NADH oxidation capacity was higher than measured (Figure 3.23) To determine the changes to the capacity of the electron transport chain, AOX and COX capacity were determined. There was no statistical difference between COX capacities of wildtype and the dual OEX lines however they did tend to trend towards a decrease (Table 3.3). COX capacity in the single *Aox1a* OEX appeared slightly down compared to wildtype. AOX capacity was

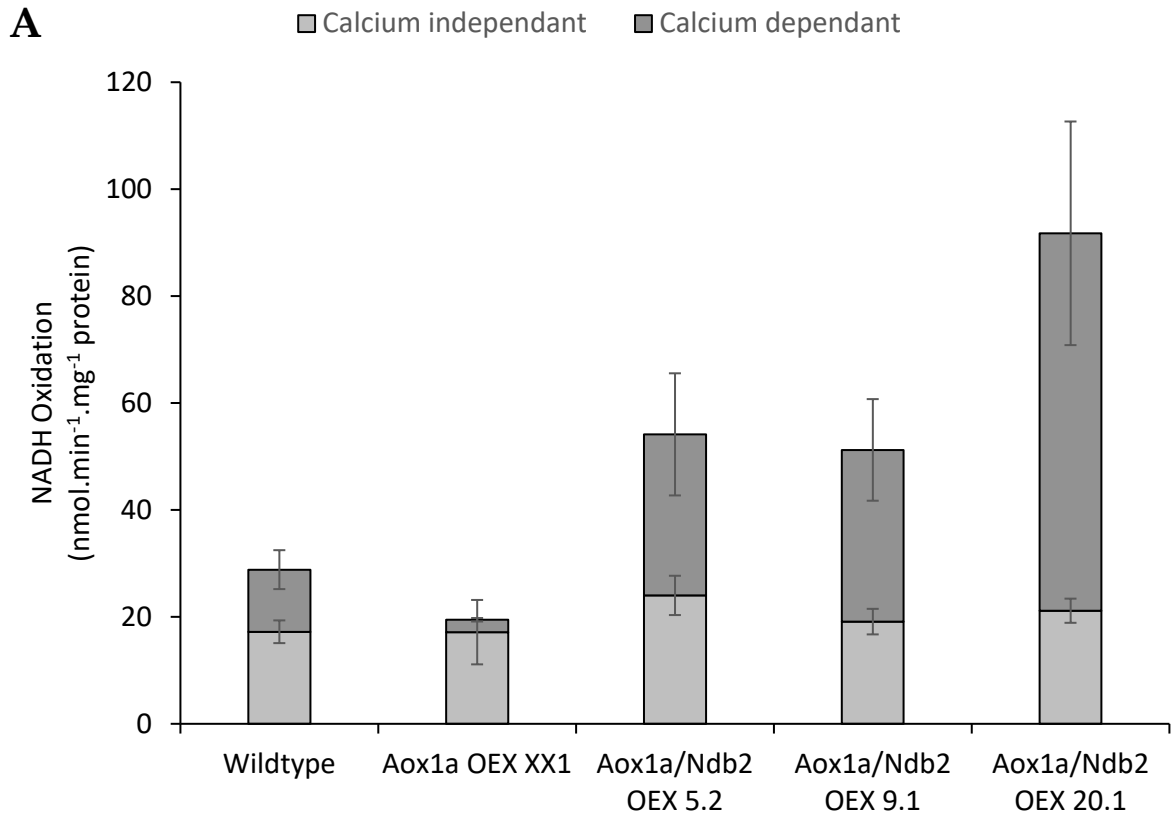
A
Calcium independant
Calcium dependant
NADH Oxidation (nmol.min-1.mg-1 protein)
120
100
80
60
40
20
0
Wildtype
Aox1a OEX XX1
Aox1a/Ndb2 OEX 5.2
Aox1a/Ndb2 OEX 9.1
Aox1a/Ndb2 OEX 20.1

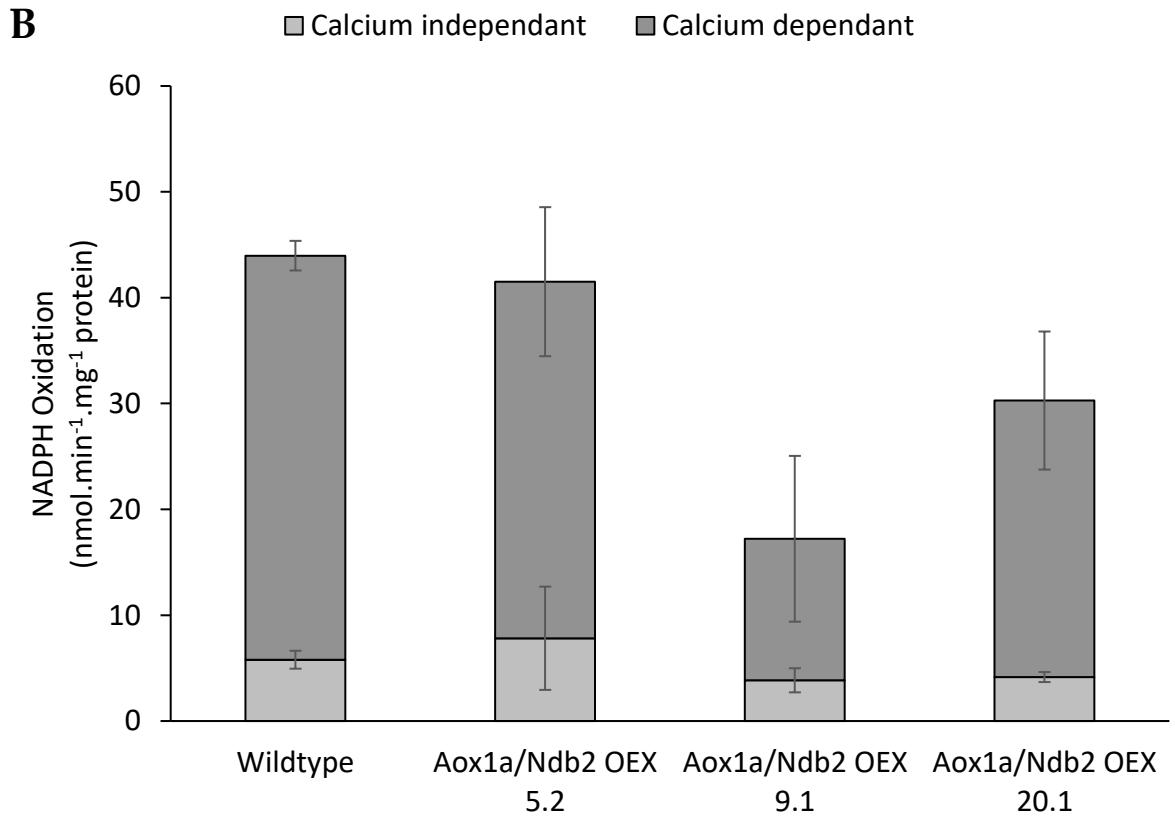
B
Calcium independant
Calcium dependant
NADPH Oxidation (nmol.min-1.mg-1 protein)
60
50
40
30
20
10
0
Wildtype
Aox1a/Ndb2 OEX 5.2
Aox1a/Ndb2 OEX 9.1
Aox1a/Ndb2 OEX 20.1

Figure 3.22 Calcium dependence of the external membrane located NDB2 protein

NAD(P)H oxidation rates were measured using isolated and intact mitochondria from 21-day old seedlings grown in ½ strength MS media. NAD(P)H oxidation was measured at 340 nm in the presence of ADP (1 mM), NAD(P)H (0.2 mM), CaCl (1 mM)or EGTA (0.5mM). A) NADH oxidation calcium dependence, B) NADPH oxidation calcium dependence Spectrophotometer used was an Olis Modernized Aminco™ DW-2. Values are mean +/- SE N=3 (NADH oxidation), N=2 (NADPH oxidation) (Wildtype and 5.2) N=3 (9.1 and 20.1)

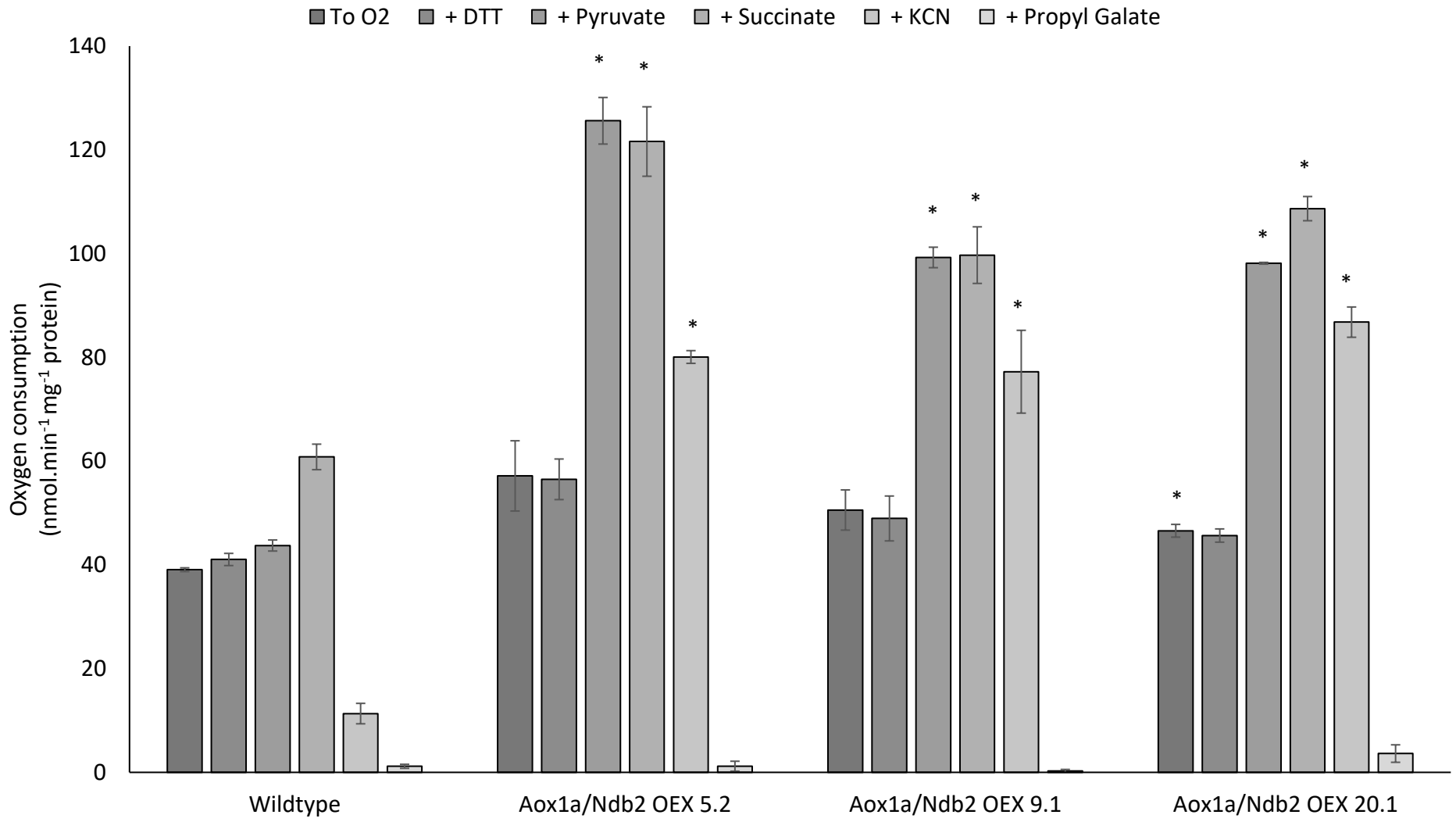
To O2
+ DTT
+ Pyruvate
+ Succinate
+ KCN
+ Propyl Galate
Oxygen consumption (nmol.min-1 mg-1 protein)
140
120
100
80
60
40
20
0
Wildtype
Aox1a/Ndb2 OEX 5.2
Aox1a/Ndb2 OEX 9.1
Aox1a/Ndb2 OEX 20.1

Figure 3.23 Oxygen consumption of intact isolated mitochondria from dual *Aox1a*/*Ndb2* OEX lines in the presence of NADH and electron transport chain activators and inhibitors

Oxygen consumption rates were measured using isolated and intact mitochondria from 21-day old seedlings grown in ½ strength MS media. Reactions were performed in the presence of ADP (1 mM), NADH (0.2 mM) and CaCl (1 mM). Subsequent additions of activators and inhibitors were made in order of DTT (1 mM), pyruvate (5 mM) (AOX activators), succinate (10 mM), potassium cyanide (0.5 mM) (Complex IV inhibitor) and propyl gallate (0.12 mM) (AOX inhibitor). Oxygen consumption was monitored polarographically using Oxygraph Plus chambers coupled to O_2View software (Hansatech Oxygraph, Norfolk, England). Values are mean +/- SE N=2 (Wildtype and 5.2) N=3 (9.1 and 20.1).* denotes significance of $p<0.05$ determined via unpaired, two-tailed t-test against wild type

Table 3.3 Electron transport chain capacity of dual *Aox1a*/*Ndb2* OEX lines in the presence of propyl gallate or potassium cyanide

AOX and COX capacity were determined through first exposing intact isolated mitochondria to ADP (1 mM), NADH (0.2 mM) and CaCl (2 mM), DTT (1 mM), and pyruvate (5 mM). Additions of either propyl gallate (COX capacity) or potassium cyanide (AOX capacity) were made in different oxygen chambers. Oxygen consumption was monitored polarographically using Oxygraph Plus chambers coupled to O_2View software (Hansatech Oxygraph, Norfolk, England) Values are mean +/- SE N=2 (Wildtype, XX1 and 5.2) N=3 (9.1 and 20.1). * denotes significance of $p<0.05$ determined via unpaired, two-tailed t-test against wild type.

	Oxygen consumption (nmol.min^{-1} mg^{-1} protein)	
	COX capacity	AOX capacity
Wildtype	41.28 ± 6.21	10.17 ± 1.97
Aox1a OEX XX1	18.31 ± 1.19	22.56 ± 3.32 *
Aox1a/*Ndb2* OEX 5.2	34.88 ± 9.20	78.89 ± 1.23 *
Aox1a/*Ndb2* OEX 9.1	23.98 ± 2.44	76.94 ± 7.98 *
Aox1a/*Ndb2* OEX 20.1	27.40 ± 0.77	83.16 ± 2.92 *

significantly increased across all dual OEX lines in a similar manner (8-fold).whereas the single *Aox1a* OEX had only a 2-fold increase.

3.4 Discussion

Much of the focus around the alternative respiratory system in plants has centered around the alternative oxidase enzyme. Of the most interest is the crucial, stress responsive *Aox1a* isoform. Known to be required to maintain an adequate stress response to a variety of different stressors (Fiorani et al. 2005; Giraud et al. 2008; Smith et al. 2009), *Aox1a* has been exploited using transgenic approaches to provide an overall improved stress response in multiple studies (Fiorani et al. 2005; Smith et al. 2009; Smith et al. 2011; Li et al. 2013; Liu et al. 2014). Far less is known about the type II NAD(P)H dehydrogenases that make up the rest of the AP. Of the seven isoforms found in *A.thaliana*, at least two are stress responsive (Elhafez et al. 2006) with *Ndb2* responding together with *Aox1a* to a variety of stressors (Clifton et al. 2005). Recent experiments silencing the *Ndb4* isoform highlighted an unexpected concomitant upregulation of *Aox1a* and *Ndb2* leading to plants with improved salt tolerance compared to wildtype. To investigate this conferred tolerance further, plants were generated overexpressing both the *Aox1a* and *Ndb2* genes. These lines were first generated using a combination of end point PCR selection and selective marker screening. Transgenic lines were then characterised for changes at the molecular level and in the following chapter, these lines were characterised at the phenotypical level including their response to a moderate light and drought stress.

The *Aox1a* OEX background line (XX1) chosen was sourced from the Siedow lab (Umbach et al. 2005). This line contains the *Aox1a* cDNA construct controlled by

the CaMV 35S promoter under a kanamycin selection marker. Unlike the other *Aox1a* transgenics produced by Umbach et al. (2005), these do not contain any modifications to the two regulatory cysteine residues and as such acts similar to a wildtype *AtAox1a.* Although dual OEX lines were generated using the auto-active version produced by Umbach et al. (2005), these were not analysed in these experiments. The *Ndb2* construct was amplified from cDNA and inserted in the gateway compatible pEARLYGATE100 plasmid (Earley et al. 2006) containing the selective marker for glufosinate ammonium (BASTA) and controlled by the CaMV 35S promoter. As previously stated, the XX1 line was generated with the kanamycin selective marker. Having the BASTA selective marker for *Ndb2* allows for an easy, high throughput method for determining putative transgenics from wildtype lines without interference from the previous selective marker. These putative transgenics could then be confirmed for insertion and homozygosity through a combination of end point PCR and Mendelian genetics.

It was important that all transgenics selected for analysis contained a single insertion event and was homozygous for this insertion. Additional insertion events are a liability, potentially resulting in insertion events occurring within genes and confounding results. Moreover, homozygosity of the transgenes is difficult to determine, as selection marker testing would not be able to differentiate between a plant containing insertion events that are both homozygous or homo- or hemizygous. This would result in unstable inheritance of the transgene. The number of insertion events was first determined through the progeny of the T2 lines. If T1 parents were

hemizygous for a single insertion event, then the ratio of their progeny should be 3:1 or 16:1 for dual insertion events. A total of 13 single insertion lines were identified, of which 9 were continued to homozygous state. Complementary confirmation of the insertion was performed through end point PCR to ensure the transgene was inserted and not just the selection marker.

To achieve the greatest effect resulting from OEX, lines with the highest transcript expression of *Ndb2* were selected for further analysis (Figure 3.9). Large variation was seen amongst the different lines however this is not un-expected. OEX with the CaMV 35S promoter has been shown to produce variation up to 100 fold (Holtorf et al. 1995). Attempts to try and correlate the transcript abundance with protein expression or enzymatic activity were mostly unsuccessful. NADH was expected to be the main substrate of NDB2 based on previous heterologous expression in *Escherichia coli* (Geisler et al. 2007). Initially, this was partially confirmed as the 5.2 line showed increased NADH oxidation (Figure 3.10). However, two additional lines (6.1 and 15.2) showed no changes to NADH oxidation. DCQ was utilised in separate NADH experiments, as it may provide an additional electron acceptor site for pathways that are impeded and has shown to produce faster rates (Bénit et al. 2008). With the addition of DCQ, the same trend was seen for lines 6.1 and 15.2, albeit with increased rates of oxidation. 5.2 was similar but with much higher rates of NADH oxidation in the presence of EGTA. This may be indicative of calcium's role and interaction with ubiquinone in NDB2. Ubiquinone has been shown to interact with calcium and may act as a transporter across the IMM (Bogeski et al. 2011) however

very little is known about DCQ's comparability to ubiquinone. The same trend was seen in *Solanum tuberosum* NDB1 isoform which might indicate the response is specific to the class of enzyme rather than the specific isoform. Due to the single wavelength capability of the spectrophotometer, limiting resolution and accurate measurements of turbid samples (Osmundsen & Bremer 1977; Osmundsen 1981), no NADPH oxidation measurements could be made nor were additional replicates produced. Future experiments were made with a more appropriate dual wavelength Olis Modernized Aminco™ DW-2 spectrophotometer allowing the capture of NADPH oxidation. Regardless, protein measurements of NDB2 and AOX were still made. AOX content was similar across the dual OEX lines, indicating the artificial upregulation of NDB2 does not lead to increases in AOX. It is interesting that the common co-expression of *Aox1a* and *Ndb2* is not brought on by an increase in *Ndb2* transcript .With the lack in response of *Aox1a* to unbridled expression of *Ndb2*, it was inferred that NDB2s activity is regulated post-transcriptionally preventing a stress response from excess NDB2 activity. Regardless, extra lines were required to build confidence in the changes seen in line 5.2. A minimum of three transgenic lines was required to ensure the differences occurring from dual OEX in 5.2 were not resulting from the insertion event.

An additional two lines (12.2 and 11.2) showing increased transcript abundance were tested for increased NDB2 protein and associated activity. The 5.2 and 6.1 line were included as positive and negative controls respectively. Both new lines had no significant increase in NAD(P)H oxidation under any condition. This is not the first

example of a transgene controlled by CaMV35s promoter being post translationally silenced in plants (Dehio & Schell 1994; Ingelbrecht et al. 1994; Elmayan & Vaucheret 1996; English et al. 1996).Vaucheret et al. (1998) has suggested post-transcriptional transgene silencing could be an example of an epigenetic defence mechanism against invading pathogens that have integrated in to the host genome. They also suggested that higher rates of transcription coupled with the homology of the transgene to the host gene can contribute to co-suppression. However, as the 5.2 line showed the strongest transcript abundance as well as sharing the same construct as all other lines, the location of the insertion seems to be key here. Interestingly, the background line XX1 showed no significant changes to NAD(P)H oxidation indicating the suppression of activity in the dual OEX lines was not a result of the *Aox1a* OEX either. Most notable however was the almost complete elimination of NADH oxidation in the *ndb2* T-DNA line. The transcripts of other external facing isoforms were measured (data not shown) and found to show no compensatory increases. This is the first known experiment to show NDB2 to be the main external facing, NADH oxidising alternative type II dehydrogenase. The small portion of remaining NADH oxidation was likely attributable to NDB4, based on heterologous expression in *E.coli* (Geisler et al. 2007).

Attempts were again made to quantify NDB2 protein abundance but with uncertain results. Neither the NDB2 nor the AOX antibody produced consistent results. The *Aox1a* OEX did not show increased AOX protein and in fact could not be detected in two of three replicates. The *ndb2* T-DNA produced similar levels of NDB2 protein to all other lines despite being almost mostly knocked down in activity and

transcript (Sweetman et al. 2019). The 5.2 line was just as inconsistent. Although seemingly showing far more NDB2 protein in the initial blot (Figure 3.15) these results were not replicated across blots (Figure 3.16). In future experiments, a newly designed NDB2 antibody was utilised that was confirmed to produce a single protein band from isolated mitochondria. As such, little confidence was held in these blots, but with the complimenting evidence found from protein activity, none of the newly tested lines were considered NDB2 OEX.

New lines were again tested for changes to *Ndb2* transcript abundance, protein and activity. *Ndb2* transcript was upregulated in both of the two new lines tested (9.1 and 20.1). More importantly was that the NDB2 was upregulated at the protein level in both new lines across all replicates, measuring similar levels of protein to the 5.2 line. Protein concentrations were very high at 80-110-fold, much higher than was first measured in 5.2. This could be explained by the previous antibodies inability to accurately detect the NDB2 protein and the very low detection of NDB2 in wildtype samples amplifying the fold change seen in the dual OEX lines. However, the NDB2 protein has the second lowest turnover rate of all mitochondrial proteins (Nelson et al. 2013) which may explain the accumulation of NDB2 protein. These are the first lines (apart from 5.2) that show increased NDB2 at the protein level. Measurements of NADH oxidation were also as expected with increased activity across all lines. As NDB2 is often upregulated along with AOX1A, it was suggested that the concomitant expression may regulate the activity of NDB2 through ETC flux. Previous experiments have highlighted the importance of redox status and-2-oxoglutaric acid accumulation

in the activation of AOX1A (Vanlerberghe et al. 1995; Millar et al. 1996; Hoefnagel et al. 1998; Gelhaye et al. 2004). To mimic these conditions and to demonstrate the potentially true activity of NDB2, DTT and pyruvate were used as a reducing agent and 2-oxoglutaric acid, AOX activator respectively (Figure 1.3). The function of DTT is to reduce the disulfide bond formed between the AOX1A monomers, allowing pyruvate access to the activation site. DTT did not result in any change to activity. Although reduction of the disulfide bonds to a potentially more active enzyme, its only with the addition of the 2-oxoglutaric acids in which AOX is activated (Umbach et al. 2006). It should also be noted that the reducing agent was hypothesised by Hoefnagel et al. (1998) to not just reduce the disulfide bond but to maintain this state which could otherwise be oxidised and inactivated by AOX substrate, ubiquinone. A massive increase in activity was seen with the addition of pyruvate, up to 7-fold over that of wildtype, highlighting what was expected; that the NDB2 activity was hindered by total flux through the ETC which AOX has partial control over. The addition of succinate was useful in determining complex II and NDB2s competition for the ubiquinone pool. Although not significant, there are trends within each line showing small decreases to NADH oxidation indicating complex II appears to outcompete NDB2 for the ubiquinone pool. It should be noted that later experiments measuring oxygen consumption, indicate no change in most cases to electron transport flux when succinate is added indicating complex II higher affinity for ubiquinone under substrate saturation. In agreement with the literature (Geisler et al. 2007), the NDB2 protein is NADH specific calcium stimulated. In fact, both the 9.1 and

20.1 line seemed to show a reduced NADPH oxidation rate. The only suspected external NADPH type II dehydrogenases are NDB1 and NDB4. Neither gene was seen to be dysregulated in 5.2 in future RNA-seq experiments, albeit 5.2 the only line not showing differences to NADPH oxidation. Smith et al. (2011) *ndb4* RNAi lines demonstrated the ability of *Ndb2* to be upregulated in response to *Ndb4* silencing. Whether *Ndb4* was responding directly to *Ndb2* transcript or an indirect product is not known. It may also be another mitochondrial NADPH-dependent enzyme such as glutathione reductase, NADPH oxidase or thioredoxin h, the latter being crucial to regulation of AOX (Gelhaye et al. 2004).

The capacity of the COX and AOX pathway were determined polarographically using Clark Brother's oxygen electrode. Although not significant, all three lines had less COX capacity compared to wildtype, with the lowest being in line 9.1. The single *Aox1a* OEX had even lower COX capacity than the dual OEX. Previous experimenters have seen the opposite effect in *Nicotiana tabacum* overexpressing the *NtAox1a* whereby the COX capacity tended to trend upwards in these lines albeit with no statistical significance (Pasqualini et al. 2007). COX capacity values were similar in this study to the results presented here. The slight reduction in COX capacity in XX1 may suggest the increased AOX capacity is causing dysregulation in the traditional pathway, resulting in down regulation or inhibition of the COX pathway. However, in future RNA-seq experiments, none of the COX pathway proteins are seen to be down regulated. XX1 shares very similar amounts of AOX protein but shows a quarter of the AOX capacity to those of the dual OEX lines.

This seems to suggest the AOX capacity of XX1 is actually a measure of the NADH flux through the ETC. This is backed up by similar levels of COX capacity. Therefore, the reduction in COX capacity is most likely an indication of reduced activity upstream of COX i.e. complex 1, NADH specific type II dehydrogenases and/or complex II.

In summary, three lines were found to have increased transcript and protein expression of *Aox1a* and *Ndb2*, concomitant with an external membrane, mitochondrial localised NADH, calcium stimulated activity. Alongside the *ndb2* T-DNA, the dual OEX demonstrated NDB2 to be the major NADH oxidising external facing type II dehydrogenase, capable of oxidising large quantities of NADH when paired with the co-expressed AOX1A protein. These combined data provide substantial molecular evidence for the successful dual OEX of *Aox1a* and *Ndb2* in *A.thaliana.* To determine the effects at the phenotypic level, and the response to the common Australian stress of too little water and too much light, these lines were assessed further in future experiments.

Chapter 4

A phenotypic investigation into the role of *AtAox1a* and *AtNdb2* in response to increased light and drought stress

Data from this chapter is part of the published work in Sweetman, C., Waterman, C. D., Rainbird, B. M., Smith, P. M. C., Jenkins, C. L., Day, D. A., & Soole, K. L. (2019). AtNDB2 is the main external NADH dehydrogenase in mitochondria and is important for tolerance to environmental stress. *Plant physiology*, pp-00877.

Written text in this chapter is my own, however some figures are the collaborative work of another author of the paper.

4 A phenotypic investigation into the role of AOX1a and NDB2 in response to increased light and drought stress

4.1 Phenotyping of transgenic plants overexpressing *AtAox1a/AtNdb2*

While many studies have investigated the effects of altering *Aox1a* expression on stress tolerance (Maxwell et al. 1999; Fiorani et al. 2005; Umbach et al. 2005; Pasqualini et al. 2007; Giraud et al. 2008; Murakami & Toriyama 2008; Watanabe et al. 2008; Smith et al. 2009; Zhang et al. 2011; Fu et al. 2012; Gandin et al. 2012; Zhang et al. 2012b; Li et al. 2013; Liu et al. 2014), far fewer have considered the type II dehydrogenases (Michalecka et al. 2003; Escobar et al. 2004; Michalecka et al. 2004; Carrie et al. 2008; Smith et al. 2011; Wallström et al. 2014a) and none have used a combined transgenic model, nor specifically investigated the role of NDB2, a stress-responsive dehydrogenase confined to the outside of the mitochondrial inner membrane. Furthermore, a comprehensive characterisation of *Aox1a* OEX lines under

control conditions has not yet occurred. The majority of studies of *AtAox1a* OEX lines under standard conditions has focused on minimal differences compared to wildtype whether at the phenotypic level or the biochemical level (Fiorani et al. 2005; Umbach et al. 2005; Smith et al. 2009; Florez-Sarasa et al. 2011; Liu et al. 2014). The experiments described in this chapter aimed to collect a more comprehensive phenotypic analysis using the Boyes et al. (2001) methodology, with a focus on both single *Aox1a* OEX and newly generated dual *Aox1a*/*Ndb2* OEX lines.

The phenotype of the previously generated *Aox1a* OEX lines (Umbach et al. 2005), especially the XX1 line, has not been reported in detail. Smith et al. (2009) highlighted a slight growth rate decrease in all *AtAox1a* OEX lines measured (XX1, X6 and E9) in both roots and shoots in hydroponics under control conditions, while Fiorani et al. (2005) showed a number of *Aox1a* OEX lines to have more and bigger leaves. To account for this gap in our knowledge, a comprehensive phenotypic analysis would be useful to understanding whether the OEX of *Aox1a* alters the phenotype.

4.1.1 Drought and light stress

Although agriculture accounts for a relatively small amount of Australian GDP and employment (Jackson 2018) (2.7% and 2.5 % respectively), its contribution to exports are over five times that and accounts for the majority of the land use in Australia. Periods of extended drought can have massive effects on the gross farm production (GFP) (Figure 4.1) not just for plants but for livestock as well. Currently,

Image removed due to copyright restriction. Original can be viewed online at www.abs.gov.au

Figure 4.1 Total estimated gross farm production loss in periods of extended drought in Australia

"Periods shown in chart refer to years in which pre-drought peak and post-drought trough in real gross farm product occurred (not financial years). (2017-2018 is from March quarter 2017 through March quarter 2018. Source Australian Bureau of Statistics"- (Eslake 2018)

Image removed due to copyright restriction. Original can be viewed online at www.bom.gov.au/

Figure 4.2 Rainfall deficiencies in Australia between the 16 month period of 1st April 2018 to 31st July 2019 (Meteorology 2019)

large parts of Australia are seeing significant deficiencies in rainfall compared to average rainfall rates (Figure 4.2) With future projections of climate change resulting in further extreme weather and climate events (King et al. 2017), action is required to improve our food security through development of more hardy crops.

Drought and an excess of light often coincide with summer, compounding the stress effect on plants. Generally, when C3 plants are grown on well-irrigated lands and under excessive light, the majority of the incoming photons are dissipated as heat (>50%); photosynthesis only incorporates between 20-30% of these photons while the remainder is made up of photorespiration and fluorescence. However, when exposed to a moderate or severe drought stress, anywhere from 70-90% of the total light absorbed is thermally dissipated and the rest of the absorbed energy is mostly used in photorespiration, exacerbated by the extreme summer heat (Flexas & Medrano 2002). Maximising potential gains in photosynthetic efficiency is a reasonable approach to maximising growth and tolerance under excess light and drought.

4.1.2 Plant molecular processes in response to drought and excess light

Due to their sessile nature, plants are often exposed to multiple stressors at once and must adapt accordingly. Although drought and high light stress are two distinctly different stressors, they often occur together in the summer months coupled with excessive heat. In these typical summer conditions plants prevent excess water loss through adjusting stomatal gas exchange. The reduction in both H_2O and CO_2 within the leaf cells resulting from stomatal closure sees downregulation of the photosynthetic components which would otherwise contribute to wasteful and

damaging photorespiration and photooxidation (Osakabe et al. 2014). Photorespiration is the process in which oxygen is assimilated by RUBISCO instead of carbon dioxide. This process is wasteful and is a by-product of RUBISCO's preferential oxygenase activity also exacerbated by increases in ambient temperature. However, there are some evidence that suggests that photorespiration is useful to prevent photooxidation through dissipation of excess photons (Kozaki & Takeba 1996; Eisenhut et al. 2017). Photooxidation is the process in which the photosynthetic apparatus under excessive light conditions contributes to a pool of reaction oxygen species. This occurs through the direct donation of energy or electrons to oxygen from over-whelmed photosystems (Foyer et al. 1994).

Together, these processes limit growth of plants exposed to these conditions and contribute to early senescence and cell death. To combat these processes, plants can modify hormone signalling, adjust metabolism and alter regulation of transcription to adapt. An example of this would be the transcriptional upregulation of ascorbate peroxidase under high light responding to the redox state of plastoquinone, a key intermediary of the photosynthetic apparatus (Karpinski et al. 1997). A crucial ROS scavenger, a loss of function *Apx* mutant exhibited higher degradation of photosynthetic components indicating a role in minimising the effects of excess ROS (Davletova et al. 2005; Li et al. 2009) while a gain of function mutant *alx8* with significantly higher levels of *Apx2* expression was more drought tolerant and had higher water use efficiency in *A.thaliana*(Rossel et al. 2006; Wilson et al. 2009; Estavillo et al. 2011). However, the OEX phenotype results in a severely altered leaf

shape, delayed flowering time and development (Wilson et al. 2009). It is obvious that the modification of some established systems of control, especially constitutive expression, can lead to improvements in stress tolerance albeit with a significant penalty under optimal conditions. Thus, it is important to identify pathways that can be exploited to improve stress tolerance without a significant growth penalty under optimal growth conditions.

4.1.3 A role for AOX in drought and excess light tolerance

AOX is a protein well positioned to fit this role since mitochondria have been implicated in oxidation of excess photosynthetic and photorespiratory reductant(Atkin et al. 2000). *Aox1a* is vital to providing an adequate abiotic and biotic stress response in Arabidopsis. *Aox1a* OEX experiments have shown increased stress tolerance with either no or small negatives changes to growth rates compared to wildtype under control conditions (Fiorani et al. 2005; Smith et al. 2009). Due to the complex network of post-translational regulation, the potentially wasteful effects of OEX of *Aox1a* may be minimised or prevented completely. In the hands of Giraud et al. (2008), plants deficient in *Aox1a* were seen to be more susceptible to moderate light and drought stress. *Aox1a* deficient plants were smaller, had increased anthocyanin content, altered metabolic profile and photosynthetic parameters. While both Bartoli et al. (2005) and Dahal et al. (2014) established through a combination of AOX inhibitors and RNAi knockdowns that upregulation of *Aox* is capable of maintaining photosynthetic redox states and photosynthetic efficiency. It was hypothesised by Dahal et al. (2014) that AOX maintained an electron sink, through respiration within

the mitochondria, to prevent feedback inhibition of upstream photosynthetic components, specifically the chloroplastic ATP synthase, leading to a limit in photosynthetic capacity. Others have shown that without AOX, high levels of ROS build up in plants causing higher oxidative cellular damage, cell death and earlier downregulation of key ROS scavenging transcripts, leading to less drought tolerant lines (Wang & Vanlerberghe 2013). It is likely that these two effects are linked, as photosynthesis becomes impaired, an electron sink is required for the excess reductant. Without the ability to remove excess reductant through AOX, plants will see dysregulated levels of ROS, leading to damage and death of the cell, adding to the effects of inhibited photosynthesis. The response of *Aox1a* OEX lines in drought and excess light is quite different from that of the mutant *aox1a* lines. *Aox1a* OEX lines maintain higher rates of CO_2 assimilation and lower rates of non-photochemical quenching (NPQ) and cyclic electron transport (Dahal et al. 2014). AOX OEX in severe drought conditions leads to slightly higher ROS scavenging activities in the chloroplast (Dahal et al. 2015b). While this may be interpreted as increased ROS generation, Smith et al. (2009) measured significantly less ROS in cell culture under salinity stress, which would also likely mimic a lack of gas exchange. However, it is notoriously difficult to make reliable ROS measurements (Foyer & Noctor 2003). The increased respiration from AOX was suggested to remove an ATP turnover limitation in the chloroplast, which was inhibiting the Mehler reaction.

Manipulation of AOX expression represents a promising biotechnological approach to improving plant stress tolerance with the attraction of a limited effect on

plant growth under optimal conditions. However, little information exists on the effects of OEX of *Aox1a* on plant phenotype under optimal conditions. Knowing whether there are wasteful effects under optimal growth conditions affecting plant growth is crucial to implementing GMO crops as an economically viable crop.

4.1.4 *Aox1a and Ndb2* co-expression

While there exist numerous examples of *Aox1a* OEX leading to improved tolerance, few studies exist incorporating the type II NAD(P)H dehydrogenases. Suppression of the internal type II dehydrogenases (*Nda1* and *Nda2*) demonstrated the importance of the internal dehydrogenases in maintaining NAD(P)(H) redox status, carbon status (sugar content) and metabolite levels; resulting in smaller plants (Wallström et al. 2014b). Suppression of an external type II dehydrogenase *Ndb1*, results in a similar response, with NADPH redox status, carbon status and metabolite levels all being altered, again resulting in smaller plants (Wallström et al. 2014a). Due to the co-localisation of these proteins, it was also difficult to discern whether the effects on phenotype result from changes occurring within the mitochondria, chloroplast and/or peroxisome. *ndb4* RNAi experiments performed by Smith et al. (2011), which resulted in the upregulation of both *Aox1a* and *Ndb2* as well as *Aox1b* (mitochondrial targeted) and *Nda1* (mitochondrial and chloroplast targeted) saw plant lines with larger leaves, faster growth rates and reduced ROS accumulation under both optimal and saline conditions. This was hypothesised to be a result of the co-upregulation of *Aox1a* and *Ndb2* reasoned from the fact that both the T-DNA and RNAi lines share similar phenotypes but only share increases in *Aox1a, Ndb2* and

Aox1b. Aox1b is unlikely to provide any additional benefit under high light conditions as previous experimenters have not seen any light regulation of *Aox1b* (Zhang et al. 2010). Unlike the response seen in the single *Aox1a* OEX lines, the *ndb4* RNAi lines resulted in plants without a growth penalty under normal conditions. Whether the increase in growth rates is reproducible and the same stress tolerance improvement is seen in drought and excess light remains to be seen.

4.2 Aims

The aim of this chapter is to identify whether the OEX of *Aox1a* and *Ndb2* alters the phenotype of plants grown under optimal conditions compared to that of wildtype and single *Aox1a* OEX. Specifically, whether the dual OEX prevents the reduced growth rate under normal conditions of the single *Aox1a* OEX that was seen by Smith et al. (2009) and Smith et al. (2011). Additionally, the improvements resulting from indirect upregulation of *Aox1a* and *Ndb2* seen by Smith et al. (2011) would need to be replicated by constitutive expression of *Aox1a* and *Ndb2* in *A.thaliana* to conclude whether the origin of stress tolerance originated from increased *Aox1a*/*Ndb2* expression or another gene(s) (e.g., *Aox1b)*.

4.3 Results

4.3.1 Sucrose is important to growth on plates and should not be removed

Phenotypic analysis of transgenics was performed according to the methods outlined by Boyes et al. (2001) with minor changes. Plants grown on agar were measured for germination, early seedling development and root growth traits. Plants grown on soil were more extensively evaluated including measurements of leaf growth development, stem and floral development and growth rates. According to Boyes et al. (2001), plants should be grown on agar containing only MS salts and phytagel (gelling agent), but I found that the lack of sucrose resulted in large variations in germination, seedling development and root growth (Figure 4.3, 4.4 and 4.5). Without sucrose, many seeds did not germinate (Figure 4.3) and reached growth milestones at significantly different time points compared to those grown on sucrose. (Figure 4.4). Root length was the most strongly affected by the lack of sucrose with large variation amongst each line with significantly less root length across all lines compared to those on sucrose (Figure 4.5). Due to the exceptional variation in measurements and germination resulting from a lack of sucrose, data collected from plants grown on media without sucrose are not considered reliable and won't be presented.

4.3.2 Boyes phenotypic analysis of transgenic dual *Aox1a*/*Ndb2* OEX under control conditions in MS media

Two of the three dual OEX lines and the *Ndb2* OEX developed cotyledons significantly later compared to wildtype (Figure 4.4A). This trend continued into

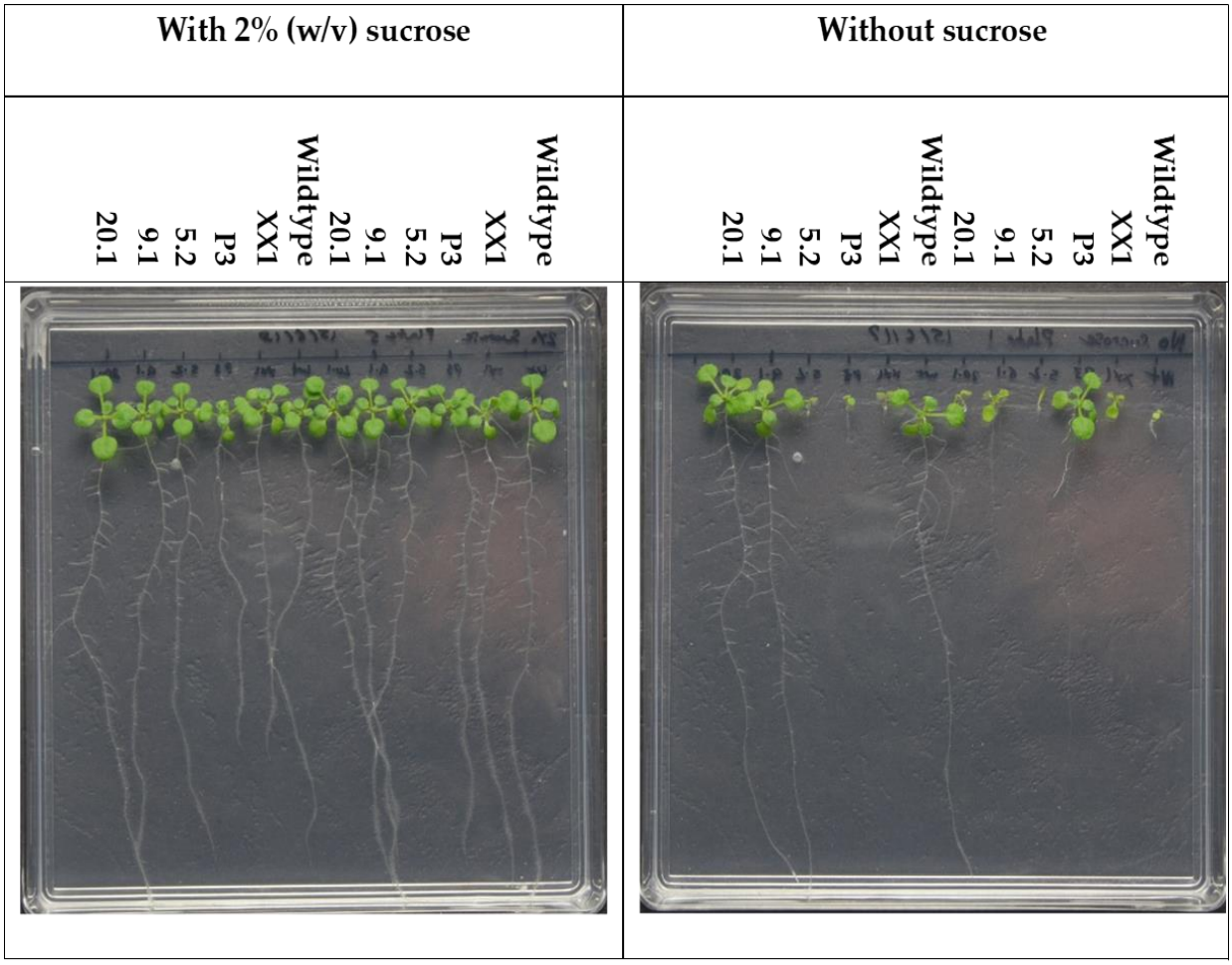

Figure 4.3 Phenotyping of transgenics on MS media after 14 days growth

Growth stage development and root morphology was determined under control conditions. Lines assessed were wildtype, *Aox1a* OEX XX1, *Ndb2* OEX P3, *Aox1a*/*Ndb2* OEX 5.2, 9.1 and 20.1. Plant order from left to right is as follows: 20.1, 9.1 5.2, P3, XX1, wildtype, 20.1, 9.1 5.2, P3, XX1 and wildtype. Plates were grown for 14 days at 16 hours light at 100-120 μmol m^{-2} s^{-1} and 6 hours of dark at 22°C and 20°C respectively.

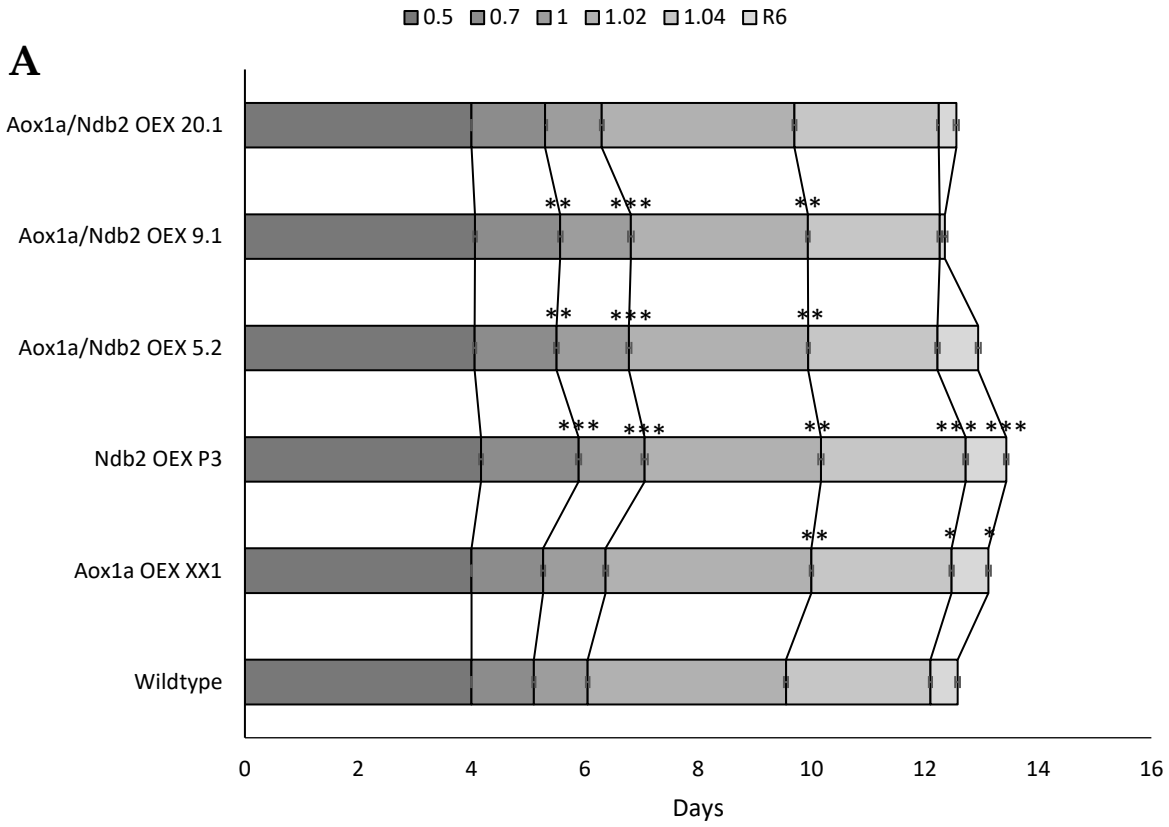
0.5
0.7
1
1.02
1.04
R6
A
Aox1a/Ndb2 OEX 20.1
Aox1a/Ndb2 OEX 9.1
Aox1a/Ndb2 OEX 5.2
Ndb2 OEX P3
Aox1a OEX XX1
Wildtype
0
2
4
6
8
10
12
14
16
Days

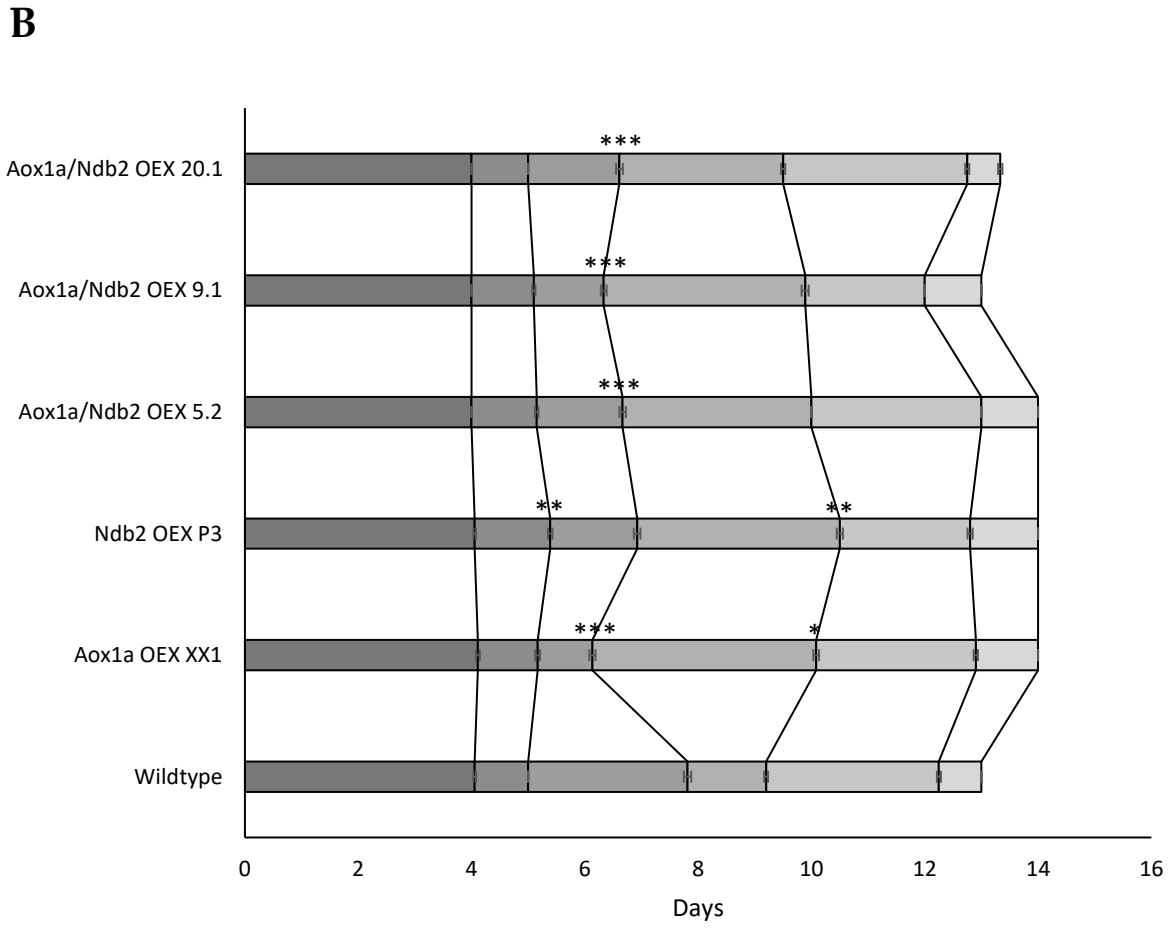
B
Aox1a/Ndb2 OEX 20.1
Aox1a/Ndb2 OEX 9.1
Aox1a/Ndb2 OEX 5.2
Ndb2 OEX P3
Aox1a OEX XX1
Wildtype
0
2
4
6
8
10
12
14
16
Days

Figure 4.4 Growth stage analysis of transgenic OEX lines grown in MS media with and without sucrose

Plants were grown for 14 days and assessed daily for growth stages. Plants were grown on ½ strength MS media and (A) 2% (w/v) sucrose or (B) 0% sucrose. Growth stages are as follows: 0.5, radicle emergence; 0.7, cotyledon emergence; 1, cotyledons fully open; 1.02, 2 rosette leaves >1 mm; 1.04, 4 rosette leaves >1 mm and R6, more than 50% of seedlings have primary roots greater than 6 cm. Values are mean +/- S.E. (with sucrose) N=20, Wildtype and 20.1; N=19, XX1; N=18, P3 and 5.2; N=16, 9.1; (without sucrose) N=20, 5.2, 9.1 and 20.1; N=18, Wildtype, XX1 and P3. * denotes significance of $p<0.05$, ** denotes significance of $p<0.01$, *** denotes significance of $p<0.001$ determined via unpaired, two-tailed t-test against wild type.

rosette development where all lines, including XX1, had slower rosette emergence. With the emergence of the 2nd set of rosette leaves and the final growth milestone, only the single OEX lines XX1 and P3 retained slower development. A similar trend occurred with root length. Throughout all eight days of root length measurements, the single OEX lines XX1 and P3 had significantly reduced root length compared to wildtype whereas all three dual OEX lines had very similar root lengths compared to wildtype (Figure 4.5A). Despite significant differences between lines during development, all lines were almost identical in terms of number of rosettes after the 14-day growth period (Figure 4.6A). The number of secondary roots followed a similar trend as root length: while only P3 was reduced significantly, XX1 was also lower than all the dual OEX lines and trended towards being lower than wildtype (Figure 4.6B). From these results, it seems the initial delay in leaf development was not exclusive to either the single or dual OEX lines. Delayed early leaf development was seen in the dual OEX lines and the *Ndb2* OEX, but these plants caught up during later leaf development. However, the single OEX lines continued to show delayed leaf development after the initial two rosettes. This later stage developmental delay was also evident in root measurements, with the single OEX lines showing smaller root lengths and secondary roots.

4.3.3 Boyes phenotypic analysis of transgenic dual *Aox1a*/*Ndb2* OEX under control conditions in soil

While growth in MS media allowed easy measurements of early leaf

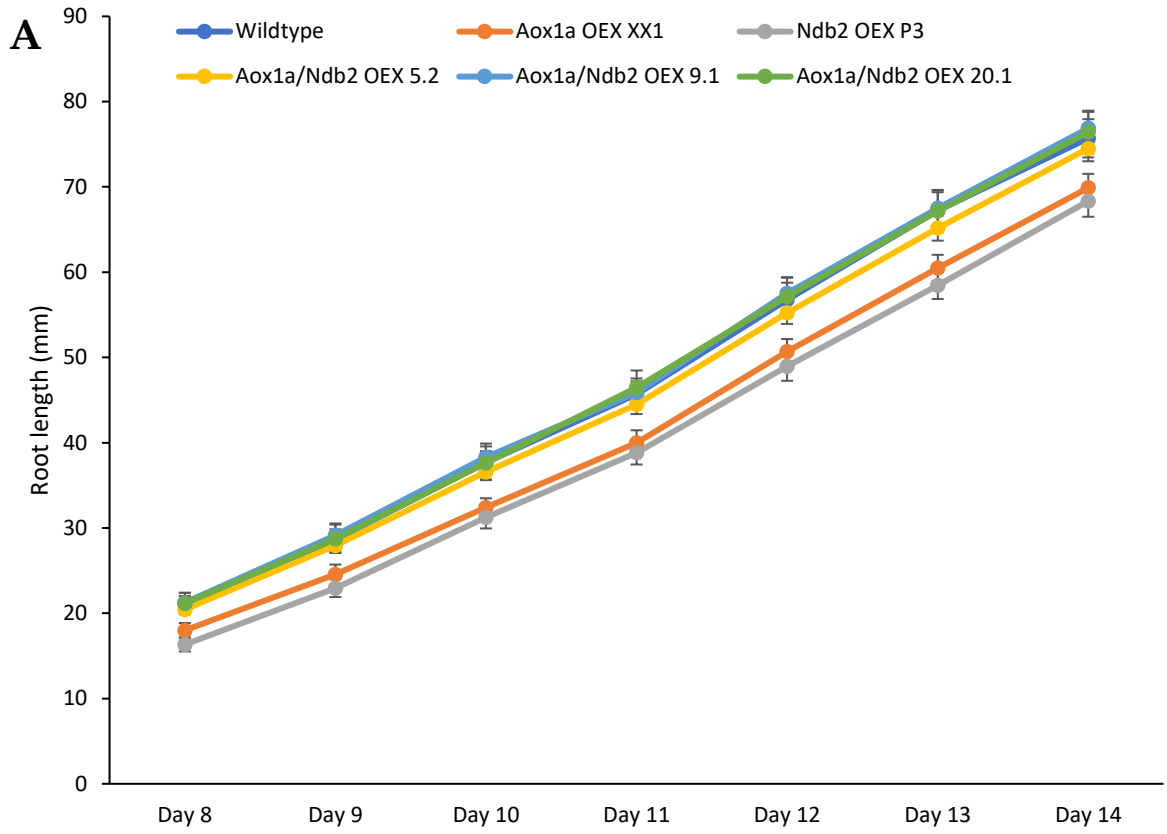
A
Wildtype
Aox1a OEX XX1
Ndb2 OEX P3
Aox1a/Ndb2 OEX 5.2
Aox1a/Ndb2 OEX 9.1
Aox1a/Ndb2 OEX 20.1
Root length (mm)
0
10
20
30
40
50
60
70
80
90
Day 8
Day 9
Day 10
Day 11
Day 12
Day 13
Day 14

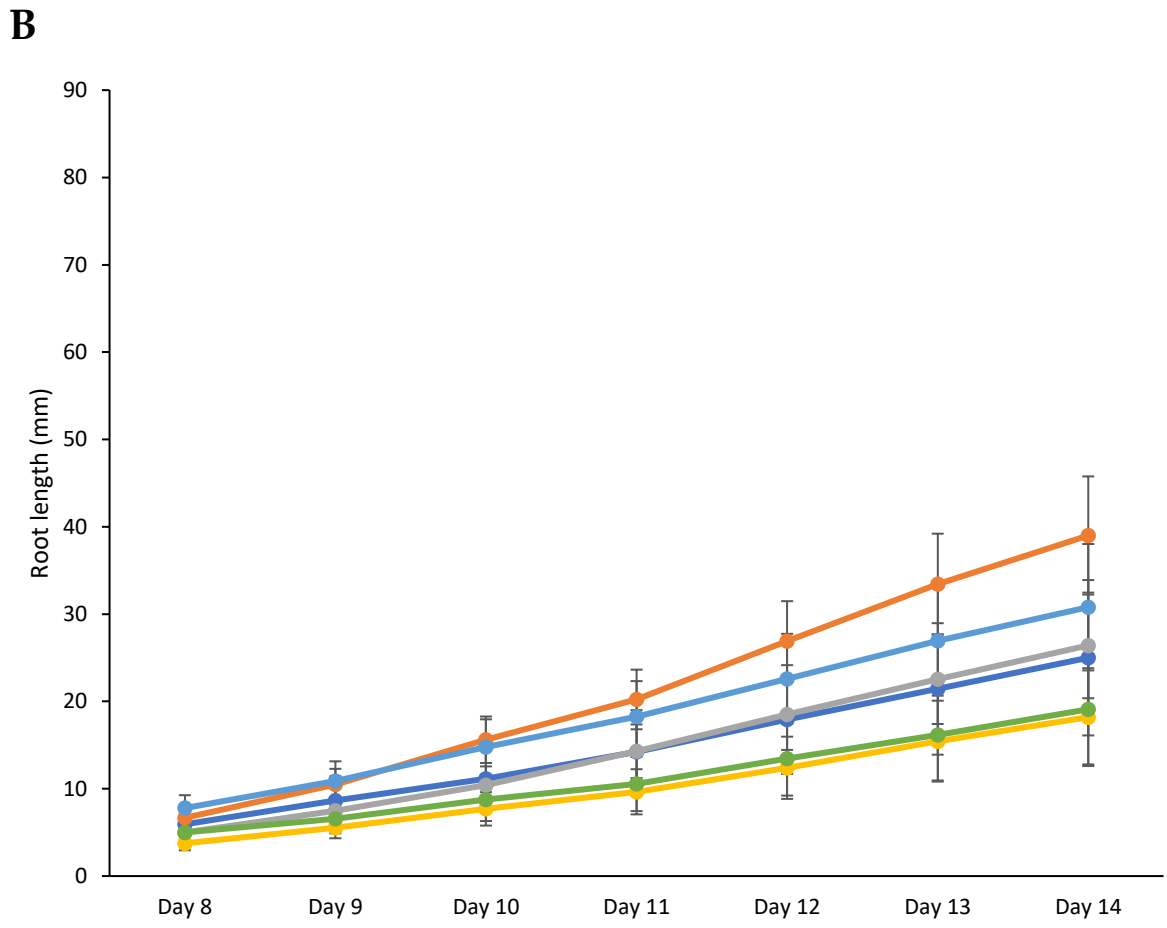
B
Root length (mm)
0
10
20
30
40
50
60
70
80
90
Day 8
Day 9
Day 10
Day 11
Day 12
Day 13
Day 14

Figure 4.5 Root length measurements of transgenic OEX lines grown in MS media with and without sucrose

Roots measurements were made daily. (A) ½ strength MS media and 2% (w/v) sucrose or (B) no sucrose. Values are mean +/- S.E. (with sucrose) N=20, Wildtype; N=19, 20.1; N=18, XX1, P3 and 5.2; N=16, 9.1; (without sucrose) N=20, 5.2 and 20.1; N=19, 9.1; N=18, XX1; N=17, P3; N=14. Significance was determined via unpaired, two-tailed t-test against wild type. Values found to be statistically significant were: (with sucrose) Day 8, XX1 <0.05, P3 <0.001; Day 9, XX1 <0.01, P3 <0.001; Day 10, XX1 <0.01, P3 <0.01; Day 11, XX1 <0.01, P3 <0.01; Day 12, XX1 <0.01, P3 <0.05; Day 12, XX1 <0.01, P3 <0.01; Day 12, XX1 <0.05, P3 <0.01; Day 13, XX1 <0.05, P3 <0.01; Day 14 XX1 <0.05, P3 <0.05.

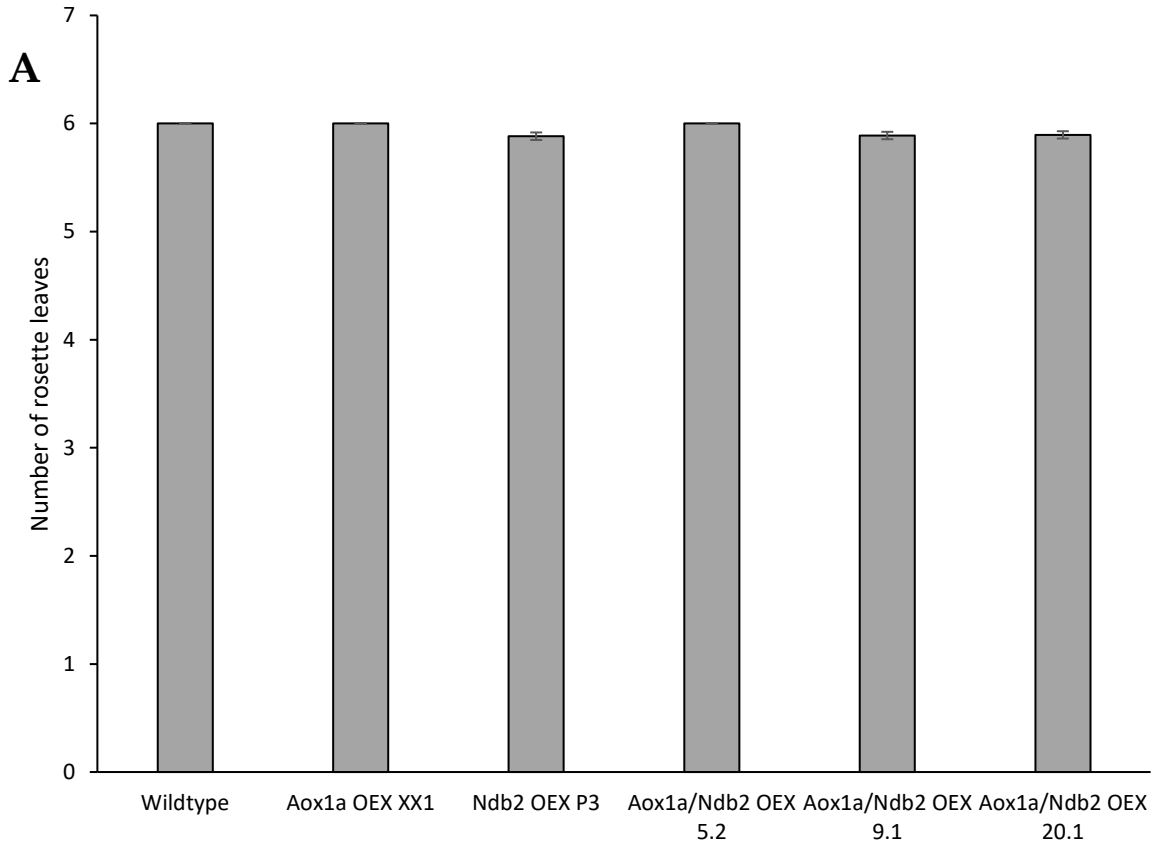
A
Number of rosette leaves
0
1
2
3
4
5
6
7
Wildtype
Aox1a OEX XX1
Ndb2 OEX P3
Aox1a/Ndb2 OEX 5.2
Aox1a/Ndb2 OEX 9.1
Aox1a/Ndb2 OEX 20.1

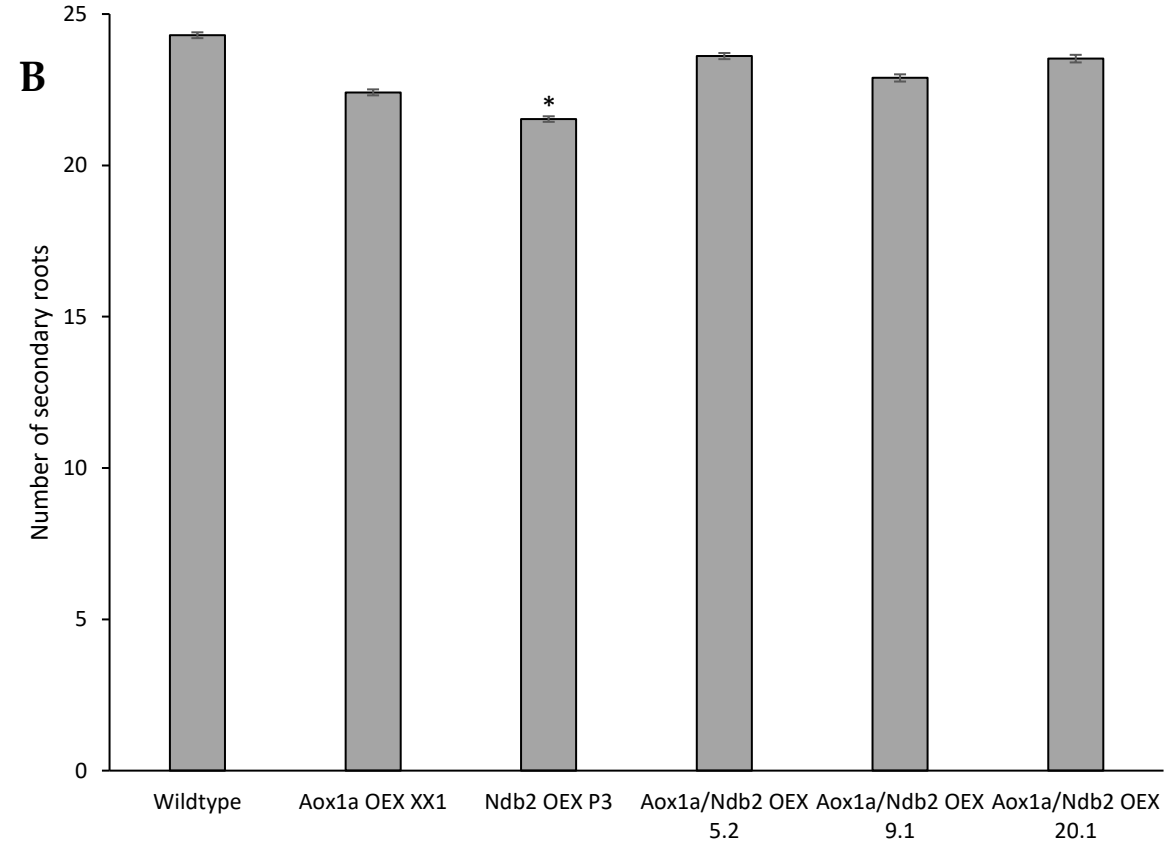
B
Number of secondary roots
0
5
10
15
20
25
*
Wildtype
Aox1a OEX XX1
Ndb2 OEX P3
Aox1a/Ndb2 OEX 5.2
Aox1a/Ndb2 OEX 9.1
Aox1a/Ndb2 OEX 20.1

Figure 4.6 Secondary root hairs and rosette numbers of transgenic OEX lines grown in MS media containing 2% (w/v) sucrose

Number of rosette leaves (A) and secondary root hair count (B) was performed 14 days after sowing on MS media. Values are mean +/- S.E. N=20, Wildtype; N=19, 20.1; N=18, XX1, 5.2 and 9.1; N=17, P3. * denotes significance of $p<0.05$ determined via unpaired, two-tailed t-test against wild type.

development and roots, analysis in soil focuses on longer developmental time frames, stem/floral development and leaf/stem growth rates. When plants were grown in soil, rosette growth milestone delays were strongest and most prevalent in the single OEX lines (Figure 4.7). Almost all time points for these lines were significantly retarded whereas the dual OEX lines had far less delayed growth stages, with any significant delays being far smaller than in the single OEX lines. This continued further into the flowering growth stages. The first flower buds emerged significantly later in the single OEX lines, with P3 also being behind in flower opening while XX1 was also slowed in terms of overall flower production (Figure 4.8). None of the dual OEX lines experienced retardation in their shift to flower production or emergence. With the consistent delay in growth stages and reduced root growth, it was not surprising that both the single OEX lines were also significantly and consistently smaller in terms of rosette size (Figure 4.9). Both lines were consistently smaller across the whole MS media experiment except for the last timepoint. Both the single OEX lines were slower reaching bolting, due to the delayed start, the stems were significantly and consistently smaller across all timepoints (Figure 4.10). It should be noted that by the end of stem measurements, the difference between the single OEX lines and wildtype was less pronounced, suggesting accelerated later growth. This was similar to what was seen in rosette size across time. As such, it was interesting to note that there was no change in stem bolt numbers in the single OEX lines (Figure 4.11) despite the significant delay to bolting and reduced stem height. Unexpectedly, this trend was not reflected in weight measurements. Neither of the two single OEX lines showed any

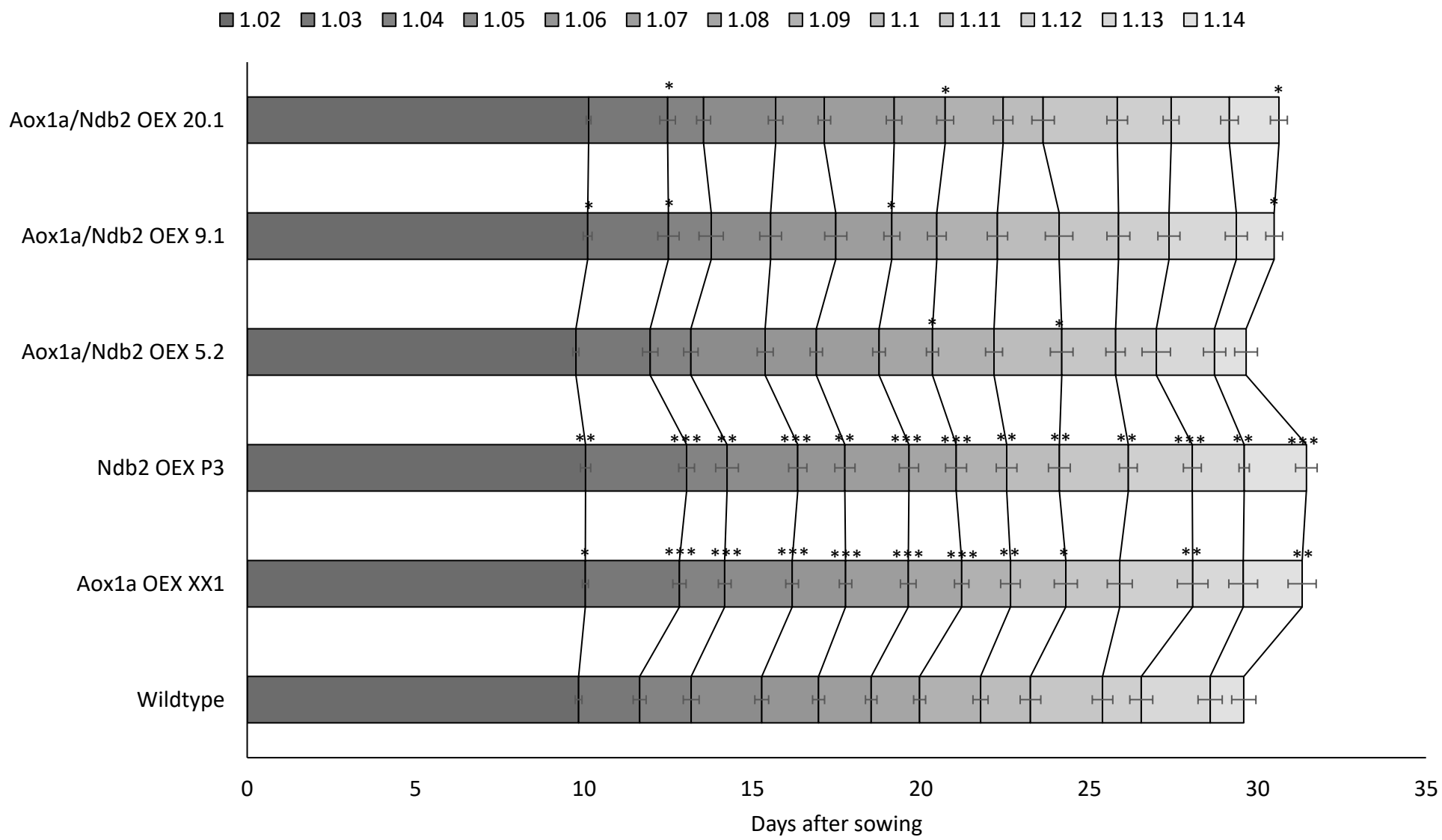
1.02
1.03
1.04
1.05
1.06
1.07
1.08
1.09
1.1
1.11
1.12
1.13
1.14
Aox1a/Ndb2 OEX 20.1
Aox1a/Ndb2 OEX 9.1
Aox1a/Ndb2 OEX 5.2
Ndb2 OEX P3
Aox1a OEX XX1
Wildtype
0
5
10
15
20
25
30
35
Days after sowing

Figure 4.7 Rosette growth stage analysis of transgenic OEX lines grown in soil

Plants were grown for 48 days or until growth milestone 6.50 was reached and assessed every second day for growth stages. Plants were germinated and grown on soil. Growth stages are as follows: 1.02-1.14, 2-14 rosettes >1 mm in length. Values are mean +/- S.E. N=28, Wildtype and 9.1; N=27, XX1, 5.2 and 20.1; N=20, P3. * denotes significance of $p<0.05$, ** denotes significance of $p<0.01$, *** denotes significance of $p<0.001$ determined via unpaired, two-tailed t-test against wild type.

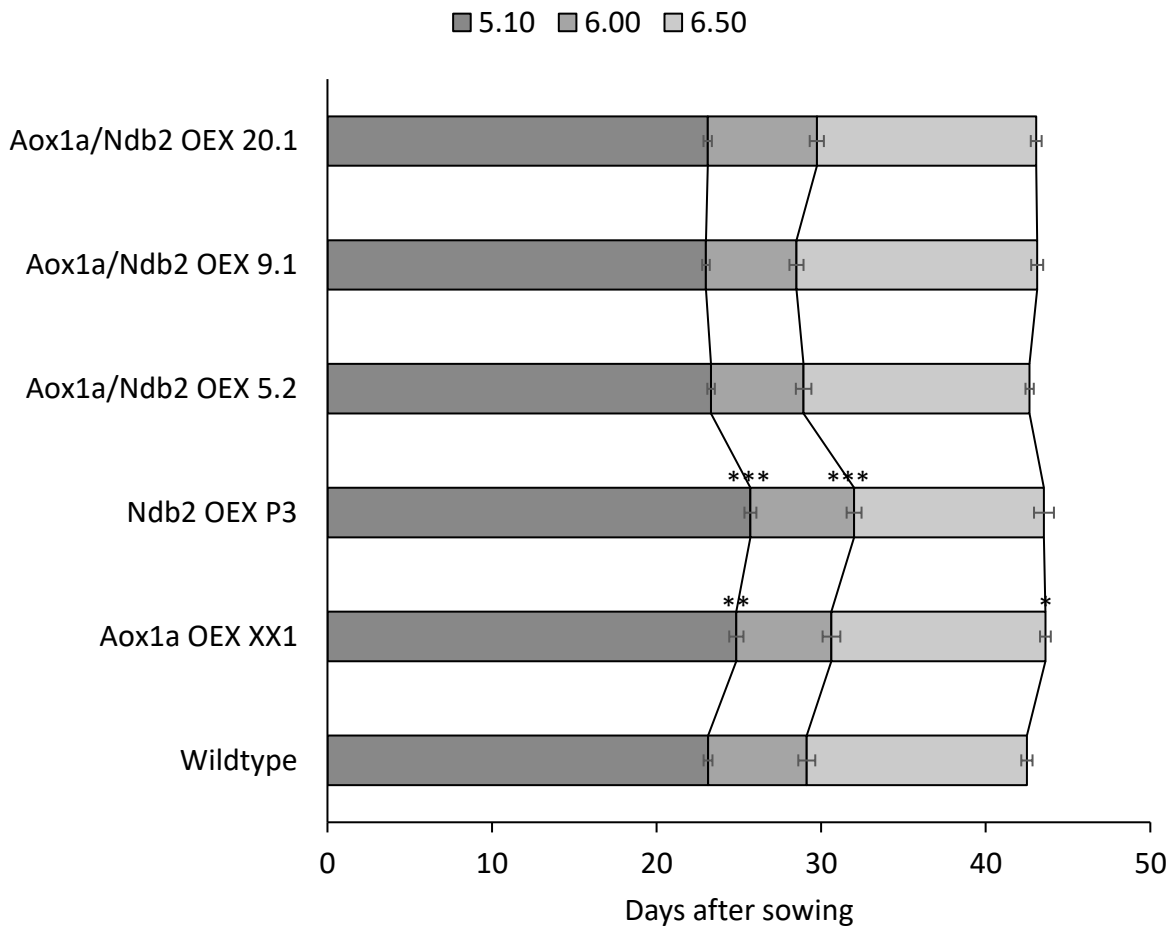

Figure 4.8 Flower growth stage analysis of transgenic OEX lines grown in soil

Plants were grown for 48 days or until growth milestone 6.50 was reached and assessed every second day for growth stages. Growth stages are as follows: 5.10, first flower buds visible; 6.00, first flowers open; 6.50, 50% of flower buds to be produced have opened. Values are mean +/- S.E. N=16, Wildtype, XX1, 9.1; N=15, 5.2 and 20.1; N=13, P3. * denotes significance of $p<0.05$, ** denotes significance of $p<0.01$, *** denotes significance of $p<0.001$ determined via unpaired, two-tailed t-test against wild type.

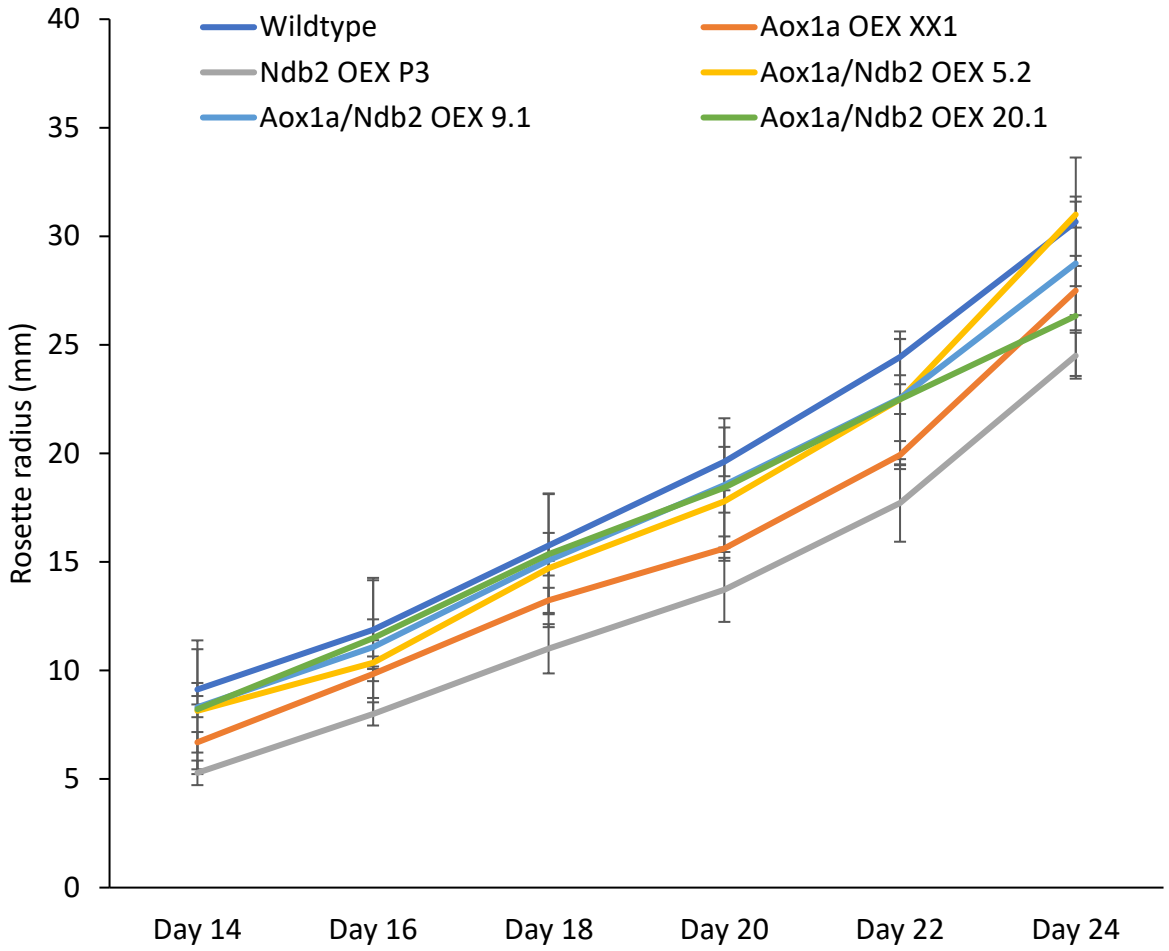

Figure 4.9 Timeline of rosette radius growth rate in transgenic OEX lines grown in soil

Rosette radius was recorded every second day, 14 days after sowing and continued until growth stage 5.10 (first flower buds visible). Values are mean +/- S.E. N=16, Wildtype; N=14, 5.2 and 20.1; N=13, XX1 and 9.1; N=7, P3. Significance was determined via unpaired, two-tailed t-test against wild type. Values found to be statistically significant were: Day 14, XX1, P3, <0.001, 5.2 <0.05; Day 16, XX1 <0.01, P3 <0.001, 5.2 <0.05; Day 18, XX1, P3 <0.01; Day 20, XX1 <0.001, P3 <0.01, 5.2 <0.05; Day 22, XX1 0.001, P3 0.01 determined via unpaired, two-tailed t-test against wild type.

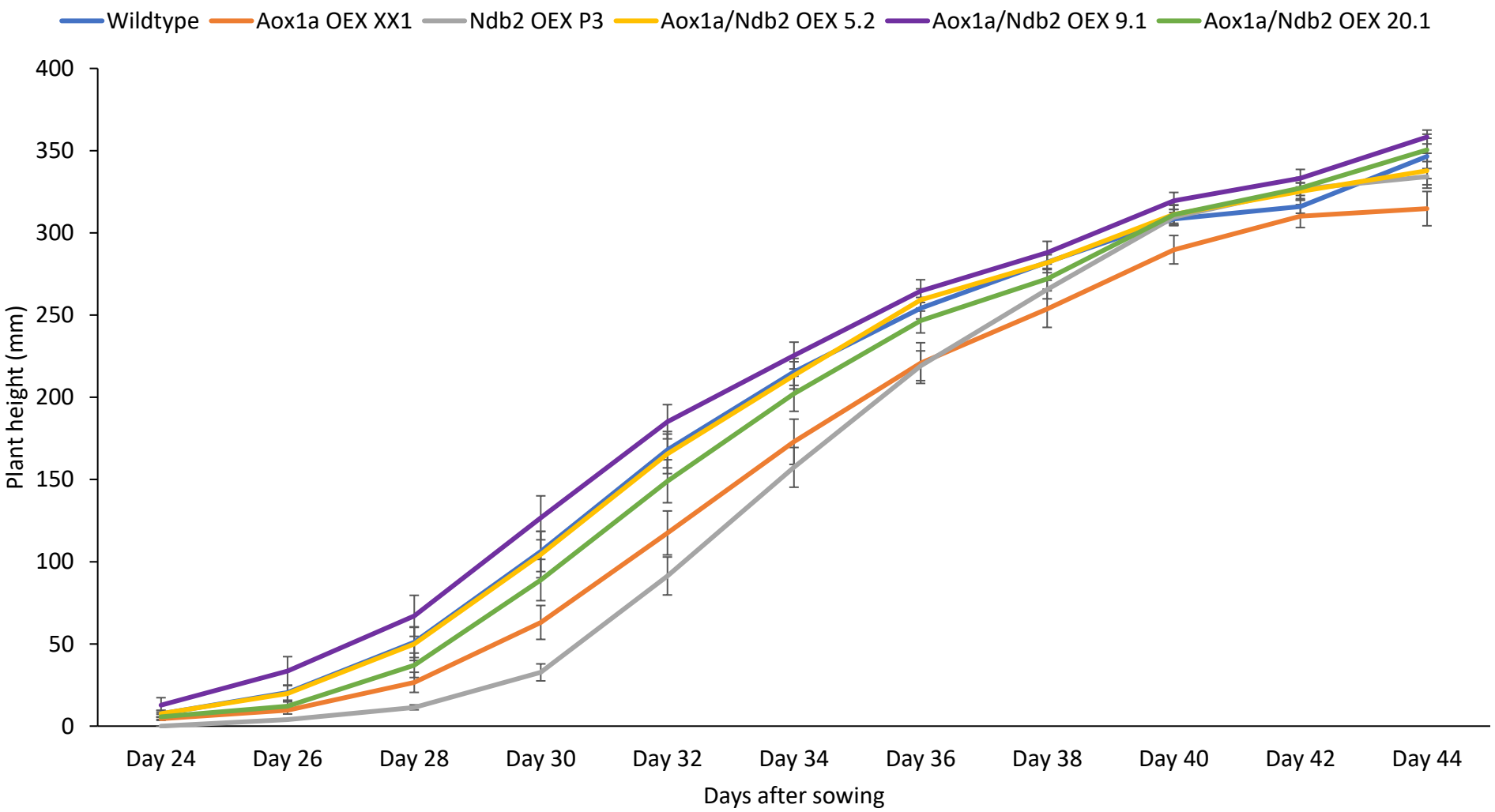
Wildtype
Aox1a OEX XX1
Ndb2 OEX P3
Aox1a/Ndb2 OEX 5.2
Aox1a/Ndb2 OEX 9.1
Aox1a/Ndb2 OEX 20.1
Plant height (mm)
0
50
100
150
200
250
300
350
400
Day 24
Day 26
Day 28
Day 30
Day 32
Day 34
Day 36
Day 38
Day 40
Day 42
Day 44
Days after sowing

Figure 4.10 Plant height timeline of transgenic OEX grown in soil

Plant height was recorded as soon as bolts had emerged and measured every second day after. Measurements were stopped at growth milestone 6.50 (50% of flower buds to be produced have opened). The time at which plant height began plateauing was used as an indirect measure of milestone 6.50 (Boyes et al. 2001).Values are mean +/- S.E. N=16, Wildtype, XX1, 9.1; N=15, 5.2 and 20.1; N=12, P3. Day 26, XX1 <0.05, P3 <0.01; Day 28, XX1 <0.05, P3 <0.001; Day 30, XX1 <0.05, P3 <0.001; Day 32, XX1 <0.01, P3 <0.001; Day 34, XX1 <0.05, P3 <0.001; Day 36, XX1 <0.05, P3 <0.01; Day 38, XX1 <0.05, P3 <0.05; Day 42, 9.1<0.05; determined via unpaired, two-tailed t-test against wild type.

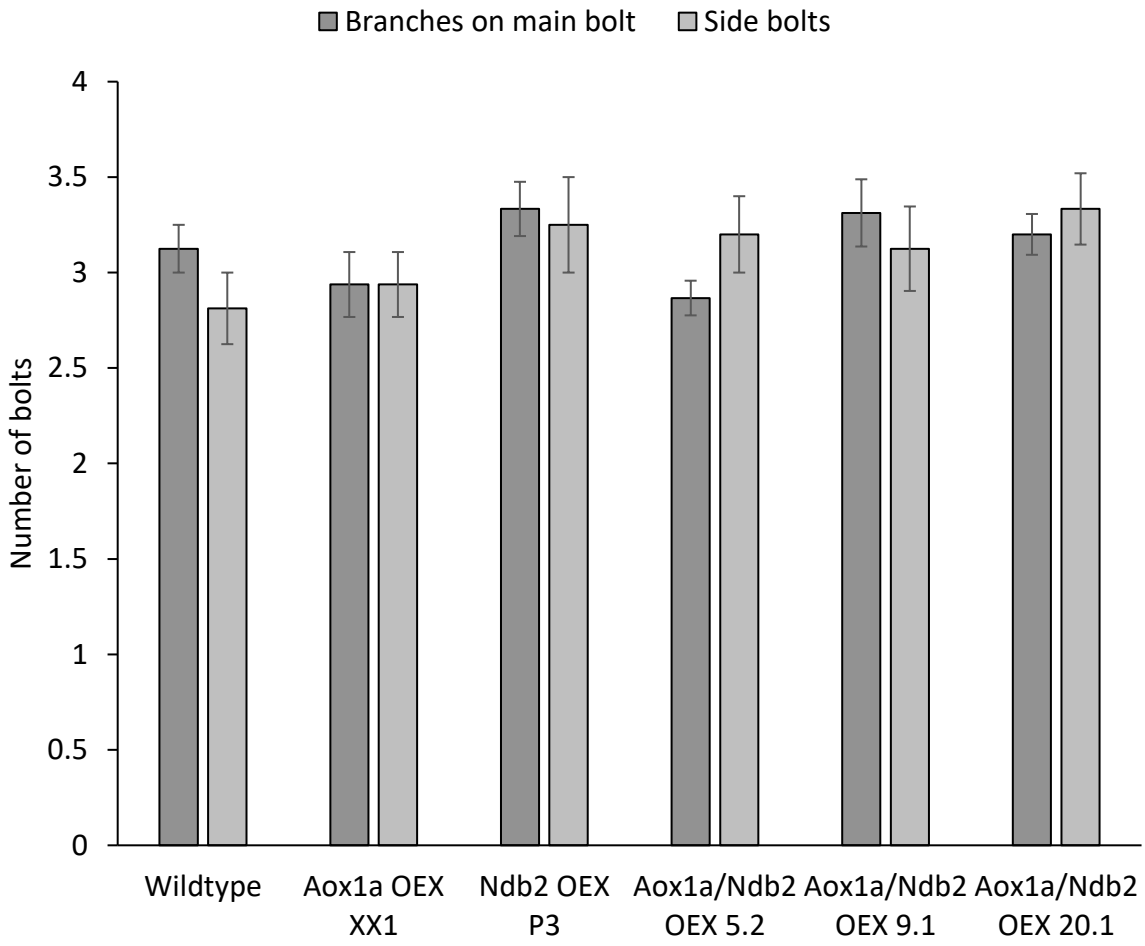

Figure 4.11 Stem and branching growth of transgenic OEX grown in soil

Plants were grown in soil until they had reached growth milestone 6.50 (50% of flower buds to be produced have opened or the time at which plant height began plateauing was used as an indirect measure of milestone). Side bolts were considering stem tissue that did not come off the initial stem. Branches on the main bolt were considered any branch point that came off the first stem bolt. Values are mean +/- S.E. N=16, Wildtype, XX1, 9.1; N=15, 5.2 and 20.1; N=12, P3.

difference in fresh or dry weight after growth milestone 5.10 was reached (first flower buds visible), although two dual OEX lines 9.1 and 20.1 were both significantly lighter in fresh and dry weights compared to wildtype but not to either of the single OEX lines. (Figure 4.12).

A selection of plants was maintained until they had reached the growth milestone of 6.50 (50% of flower buds to be produced have opened or the time at which plant height began plateauing was used as an indirect measure of the milestone) and were again measured for fresh weights and dry weights. Unexpectedly, both the P3 and XX1 had either significantly higher rosette fresh weight or no difference at all respectively (Figure 4.13), whereas the dual OEX 9.1, had significantly lower fresh weight. This trend was less pronounced in the dry weights, as the *Ndb2* OEX P3 maintained the increased dry weight but 9.1 showed no difference. Although not significant, both P3 and 9.1 again followed the same trend in stem fresh weights. The second lot of fresh and dry weight measurements enabled the calculation of relative growth rates. Similar to the trend above, the single OEX P3 has a significantly faster rosette and stem growth rate (Figure 4.14). This was the only line that showed any significant changes in growth rates. It appears there are significant differences between transgenics under control conditions, with a number of trends being consistent across measurements. The single OEX lines, especially the *Ndb2* OEX, had significant growth delays across rosette and flowering development but not during germination. Interestingly, this phenotype was not replicated in any of the dual OEX

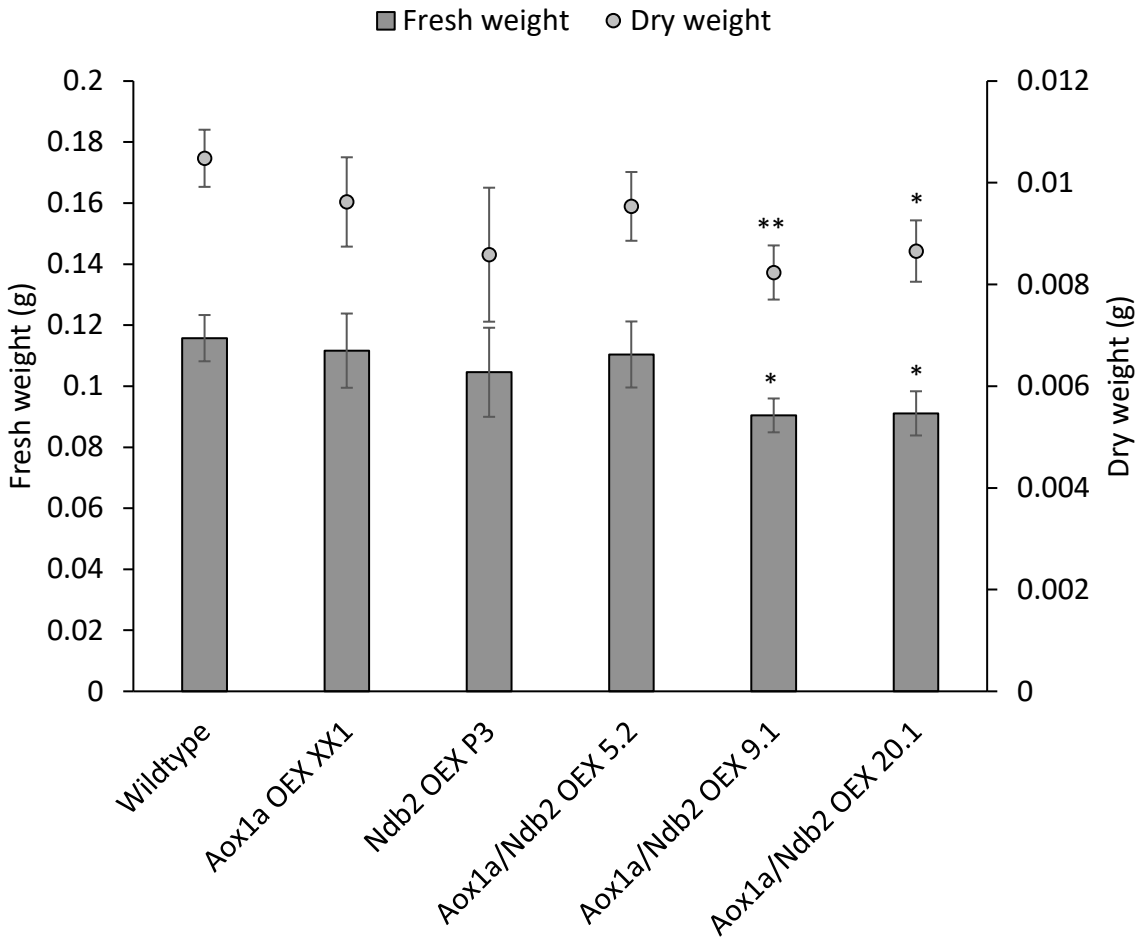

Figure 4.12 Rosette fresh and dry weight in transgenic OEX lines grown in soil

Plants were grown in soil until they had reached growth milestone 5.10 (first flower buds visible). Shoots were then removed and weighed for fresh weight. Dry weights were taken from shoots incubated at >80°C for 48 hours. Values are mean +/- S.E. N=16, Wildtype; N=14, 5.2 and 20.1; N=13, XX1 and 9.1; N=7, P3. * denotes significance of $p<0.05$, ** denotes significance of $p<0.01$ determined via unpaired, two-tailed t-test against wild type.

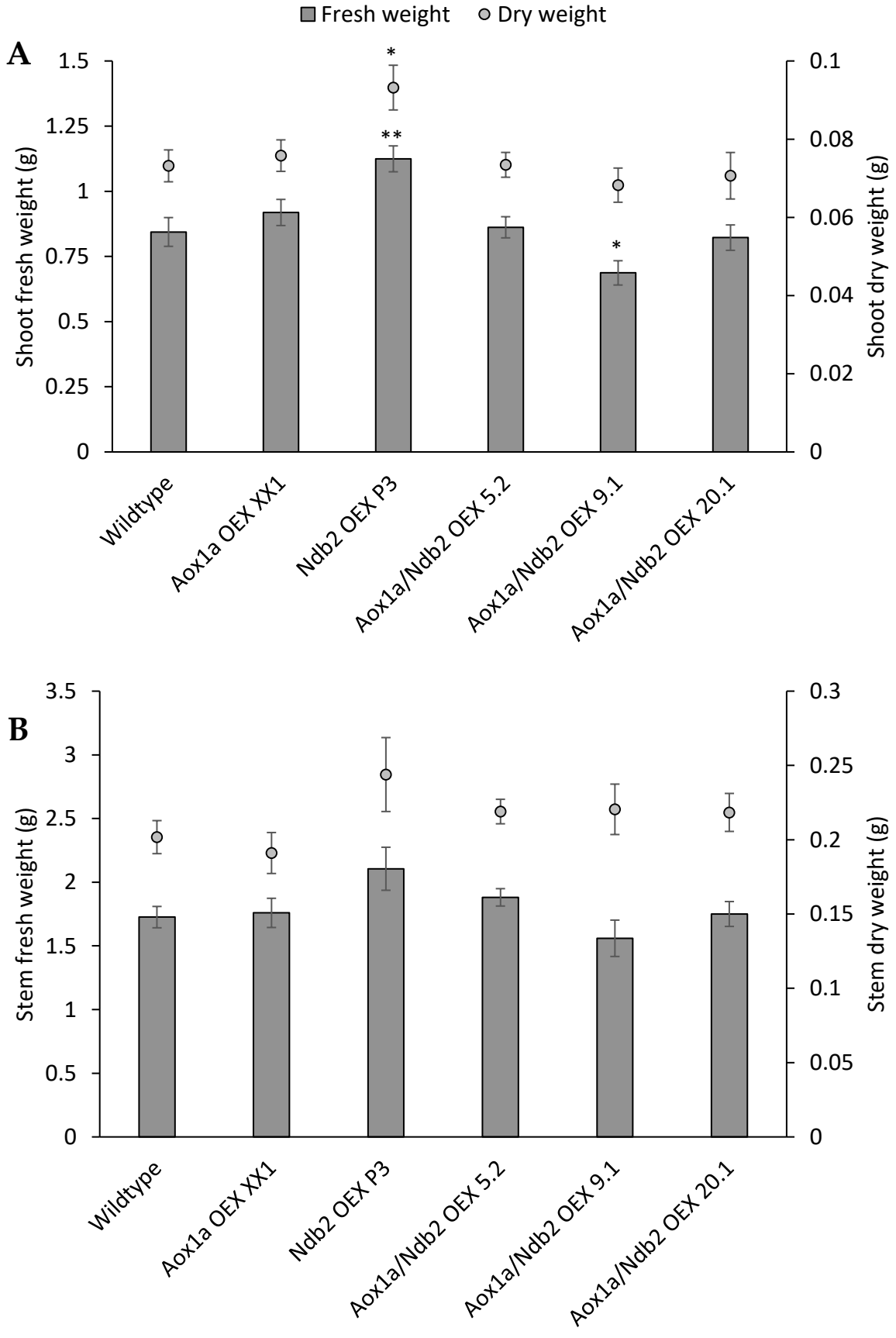
A
Fresh weight
Dry weight
Shoot fresh weight (g)
Shoot dry weight (g)
1.5
1.25
1
0.75
0.5
0.25
0
0.1
0.08
0.06
0.04
0.02
0
*
**
*
Wildtype
Aox1a OEX XX1
Ndb2 OEX P3
Aox1a/Ndb2 OEX 5.2
Aox1a/Ndb2 OEX 9.1
Aox1a/Ndb2 OEX 20.1
B
Stem fresh weight (g)
Stem dry weight (g)
3.5
3
2.5
2
1.5
1
0.5
0
0.3
0.25
0.2
0.15
0.1
0.05
0
Wildtype
Aox1a OEX XX1
Ndb2 OEX P3
Aox1a/Ndb2 OEX 5.2
Aox1a/Ndb2 OEX 9.1
Aox1a/Ndb2 OEX 20.1

Figure 4.13 Fresh and dry weights of rosettes and stems of transgenic OEX grown in soil under control conditions

Plants were grown until they had reached growth milestone 6.50 (50% of flower buds to be produced have opened or the time at which plant height began plateauing was used as an indirect measure of milestone). Shoots (A) and whole stems including siliques (B) were separated and fresh weights were measured separately. Dry weights were taken from tissue incubated at >80°C for 48 hours. Values are mean +/- S.E. N=16, Wildtype; N=14, 5.2 and 20.1; N=13, XX1 and 9.1; N=7, P3. * denotes significance of $p<0.05$, ** denotes significance of $p<0.01$ determined via unpaired, two-tailed t-test against wild type.

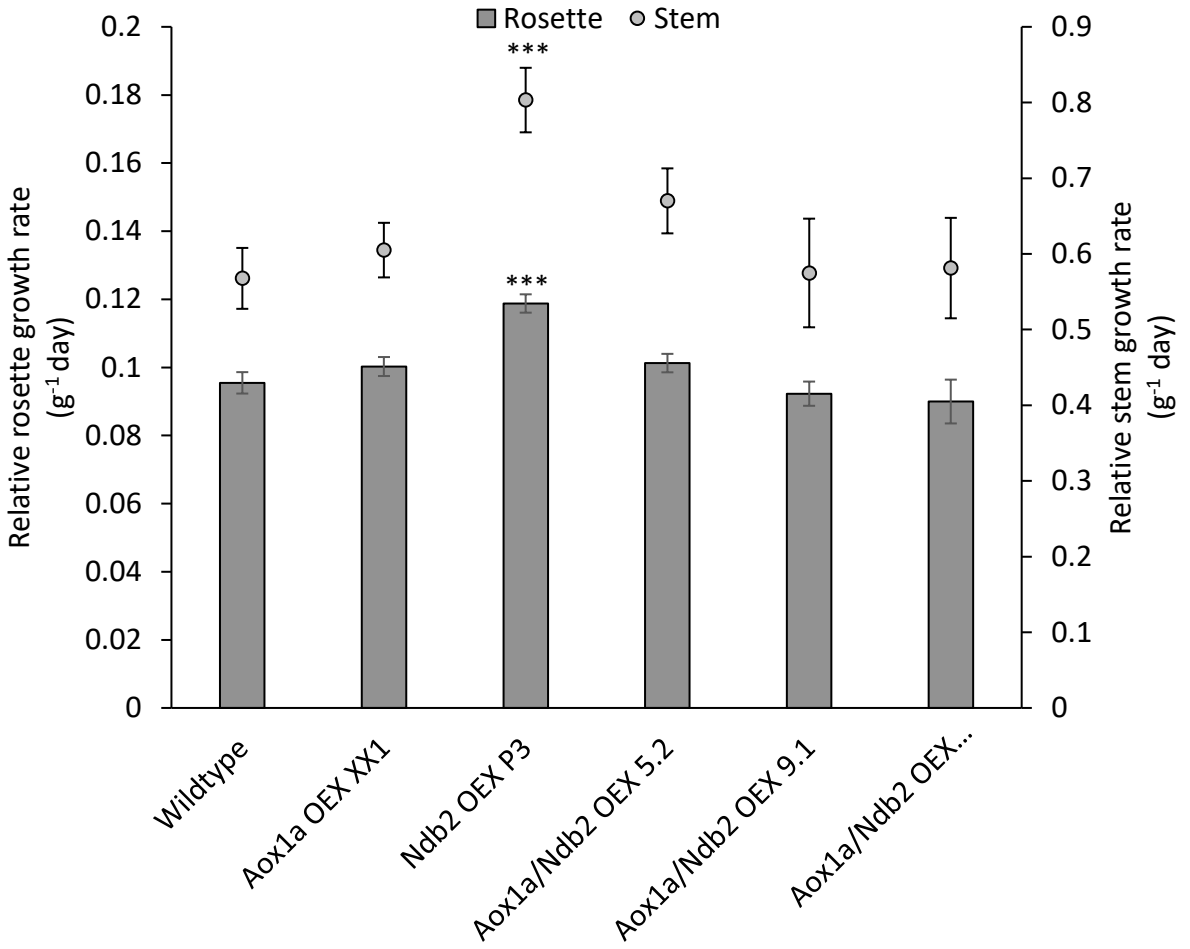

Figure 4.14 Relative growth rates of rosettes and stems during flowering period of transgenic OEX grown in soil

Relative growth rates were calculated from the dry weights measurements obtained at growth milestone 5.10 and 6.50 using the calculation outlined by Hoffmann and Poorter (2002). Values are mean +/- S.E. N=16, Wildtype, XX1 and 9.1; N=15, 5.2 and 20.1; N=12, P3. *** denotes significance of $p<0.001$ determined via unpaired, two-tailed t-test against wild type.

lines. Additionally, the single OEX lines produce slightly smaller roots and rosettes and less secondary roots, and although stem heights did eventually reach similar values, both single OEX lines lagged behind the other lines. Again, this phenotype was not replicated in any of the dual OEX lines. It is interesting to note that despite the delay in rosette and flowering, and smaller rosette and root sizes earlier in growth, the *Ndb2* OEX had similar fresh and dry weights while two of the dual OEX lines appear to have significantly smaller fresh and dry weights than the wildtype. However, due to the sampling method employed in the Boyes et al. (2001) method, plants are not sampled at the same time point, rather they're sampled based on when they reach a particular milestone. As the first fresh/dry weight measurements were taken based on when plants begun flowering, those plants that flowered earlier had less time for vegetative growth. Both lines 9.1 and 20.1 had one less day of vegetative growth compared to all other lines (Figure 4.12, values not shown). Although 20.1 fresh and dry weights were similar in later weight analysis, the 9.1 line was again significantly smaller. Strangely, the *Ndb2* OEX had both an increase in fresh and dry shoot weights and similar stem height despite the earlier delay in development. The faster relative growth rates of both the stem and shoots in the *Ndb2* single OEX allowed them to catch up after 44 days of growth. However, again, the sampling method recommends measurements to be taken on different days and thus measurements of growth rates are made at different start and end points and over different lengths of time. Due to the sigmoidal growth curve of most plants, the

difference between a single day's growth can be significant and may likely affect the growth rate measured.

4.3.4 Moderate light and drought stress of transgenic plants

From the phenotypic analysis of the newly generated dual overexpressing transgenics as well as the parent line XX1 and single *Ndb2* OEX line P3, a clear difference in growth has been demonstrated under control conditions. To determine whether these differences translated into increased stress tolerance, plant lines were exposed to a combination stress of drought and moderately excessive light. Data from several separate experiments performed with the MLD stress are presented with any differences between experimental designs stated.

Initially, many lines were included to determine the effects of MLD on biomass and plant water content. This also allowed a separate experiment to compare biomass under control conditions with the previous phenotypical analysis. In partial contradiction to what was seen previously, fresh and dry weights of dual OEX lines 9.1 and 20.1 were not lower than wildtype (Figure 4.15A, Figure 4.12 and 4.13A). The *Ndb2* OEX line P3 had increased fresh weight (Figure 4.15A), but in the previous experiment both the dry and fresh weights were significantly increased (Figure 4.13A). When these same plant lines were exposed to an MLD stress, most lines appeared similar in fresh and dry weight (Figure 4.15B). Two of the *Ndb2* OEX lines (P3 and P9) were, however, significantly smaller in terms of biomass, in contrast to what was seen under control conditions (at least partially).

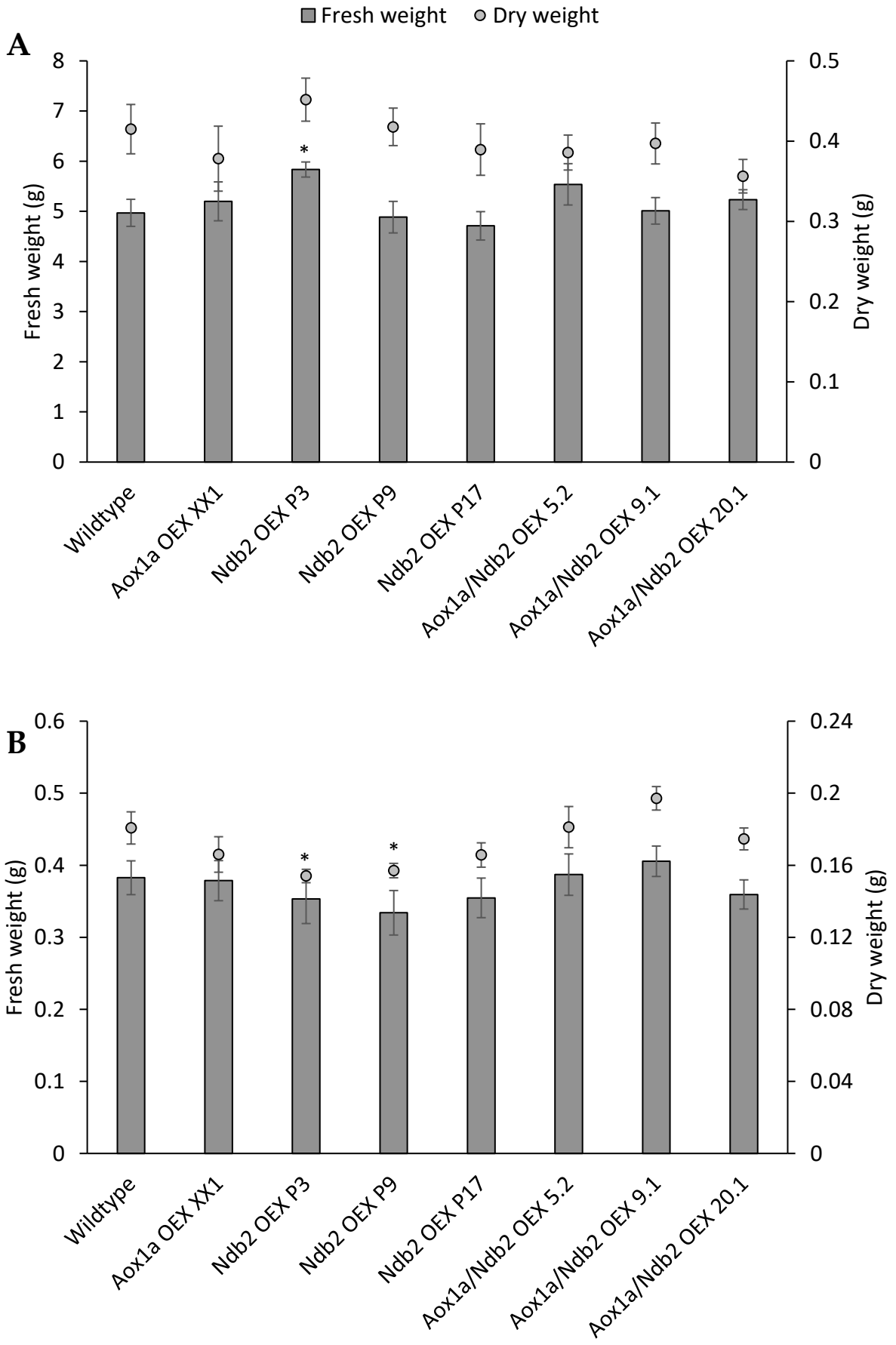
A
Fresh weight
Dry weight
Fresh weight (g)
Dry weight (g)
0
1
2
3
4
5
6
7
8
0
0.1
0.2
0.3
0.4
0.5
*
Wildtype
Aox1a OEX XX1
Ndb2 OEX P3
Ndb2 OEX P9
Ndb2 OEX P17
Aox1a/Ndb2 OEX 5.2
Aox1a/Ndb2 OEX 9.1
Aox1a/Ndb2 OEX 20.1
B
Fresh weight (g)
Dry weight (g)
0
0.1
0.2
0.3
0.4
0.5
0.6
0
0.04
0.08
0.12
0.16
0.2
0.24
*
*
Wildtype
Aox1a OEX XX1
Ndb2 OEX P3
Ndb2 OEX P9
Ndb2 OEX P17
Aox1a/Ndb2 OEX 5.2
Aox1a/Ndb2 OEX 9.1
Aox1a/Ndb2 OEX 20.1

Figure 4.15 Fresh and dry weights of rosettes of transgenic OEX and T-DNA grown in soil exposed to control or MLD conditions

Plants were grown in soil 28 days under well-watered conditions according to section 2.5.2. Water was then withheld for 6 days, followed by another 7 days of drought with a moderate light exposure of 300 μmol m^{-2} s^{-1}. Fresh weights were taken from plants on the 41st day of optimal growth (A) or the 7th day of MLD (B) and measured immediately. Dry weights were taken from tissue incubated at >80°C for 48 hours. Values are mean +/- S.E. Control N=11, wildtype, 5.2, 9.1 and 20.1; N=9, XX1; N=8, P17, N=7, P3; N=5, P9. MLD N=9, 9.1; N=8, wildtype, 5.2 and 20.1; N=6, XX1; N=5, P17; N=3, P3 and P9. * denotes significance of $p<0.05$ determined via unpaired, two-tailed t-test against wild type of the same weight type.

The water content relative to dry weight was calculated to determine whether differences between lines were caused by differences between biomass and water accumulation. Under both control and MLD conditions, the majority of lines showed no difference compared to wildtype (Figure 4.16), with the exception of the dual OEX lines 5.2 and 20.1. Both showed a minor but statistically significant increase compared to wildtype, but similar dry weights. Although the P3 and P9 lines had increased water content under MLD conditions, this was not deemed statistically significant due to the large variation and small differences seen between lines, although the variation obfuscated by the small error bars resulting from the large replicate numbers.

To determine the effects of altering AP expression on photosynthesis, especially under MLD, plants were assessed for gas exchange using the LICOR 6400-XT. Plants measured in the LICOR required growth in a pot specifically designed for the gas exchange apparatus. As a result, the pots were smaller and had holes in the base, preventing some control over the soil content and increasing water evaporation through the soil. Regardless, plants were grown for a similar period under control conditions and transitioned to a drought simulation and then a combined MLD simulation. Due to the smaller size of pots and increased exposure, the drought and MLD exposures were shorter (3 and 5 days respectively) compared to previous experiments (6 and 7 days respectively).

There was a significant and consistent separation between wildtype and the dual OEX lines as well as the *aox1a* T-DNA at the highest PAR (Figure 4.17A).

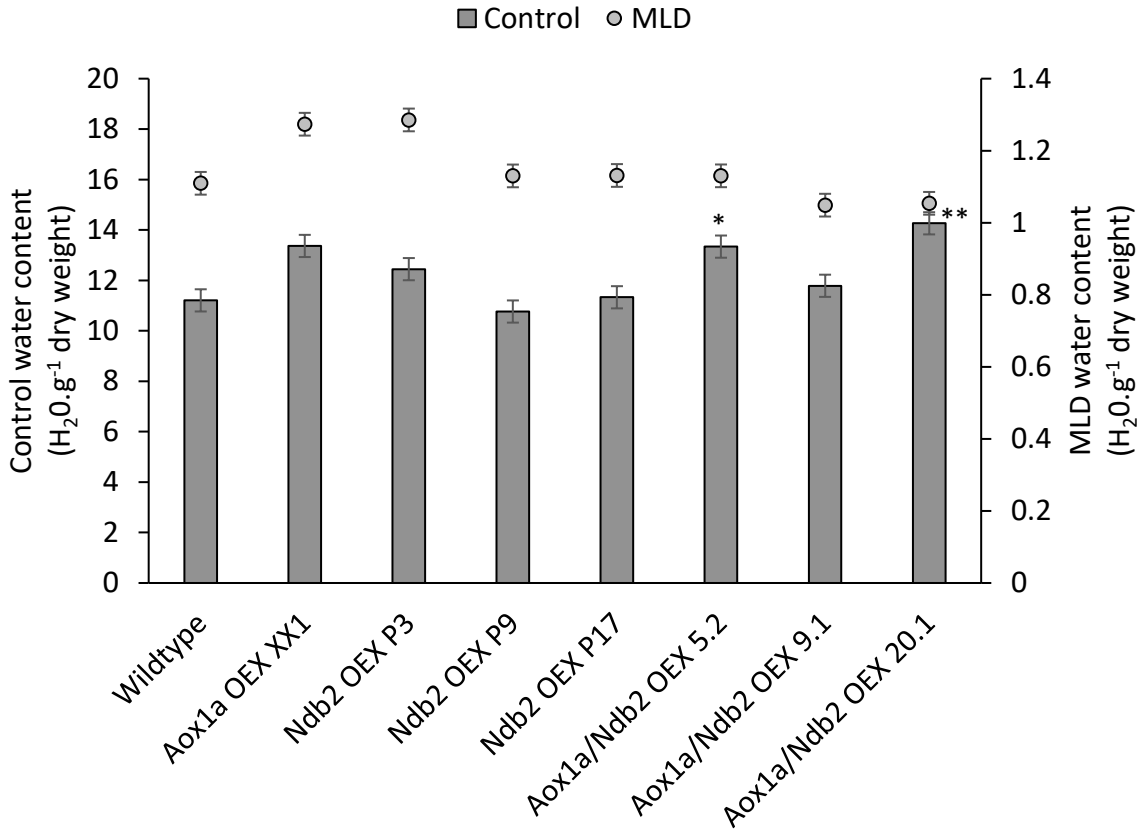

Figure 4.16 Water content in transgenic OEX and T-DNA lines exposed to moderate light and drought measured on the 7th day of MLD stress

Plants were grown in soil 28 days under well-watered conditions according to section 2.5.2. Water was then withheld for 6 days, followed by another 7 days of drought with a moderate light exposure of 300 μmol m^{-2} s^{-1}. Plants were sampled on the 41st day of optimal growth (control) or the 7th day of MLD. Values are mean +/- S.E. Control N=11, wildtype, 5.2, 9.1 and 20.1; N=9, XX1; N=8, P17, N=7, P3; N=5, P9. MLD N=9, 9.1; N=8, wildtype, 5.2 and 20.1; N=6, XX1; N=5, P17; N=3, P3 and P9. * denotes significance of $p<0.05$, ** denotes significance of $p<0.01$ determined via unpaired, two-tailed t-test against wild type.

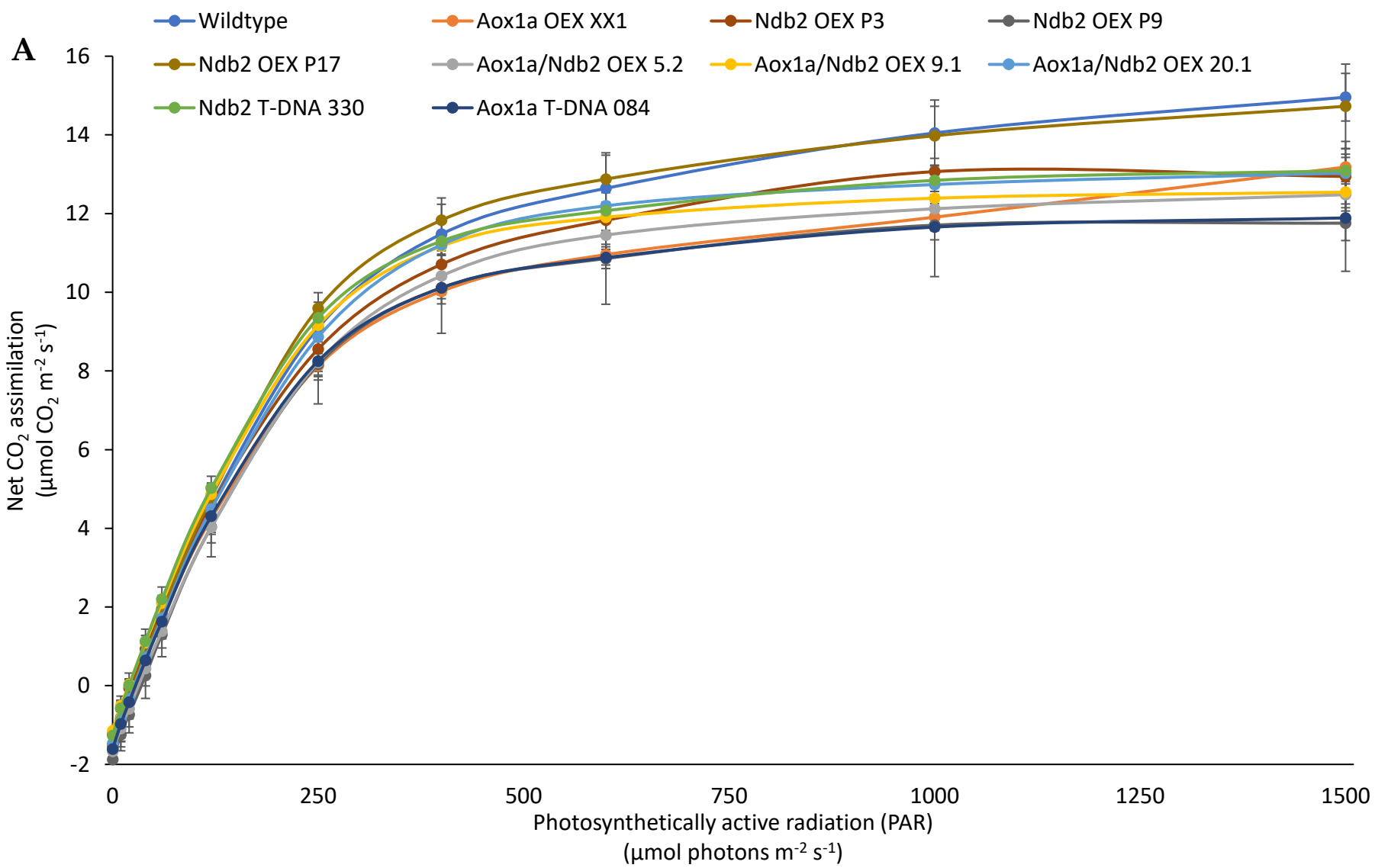
A
Wildtype
Aox1a OEX XX1
Ndb2 OEX P3
Ndb2 OEX P9
Ndb2 OEX P17
Aox1a/Ndb2 OEX 5.2
Aox1a/Ndb2 OEX 9.1
Aox1a/Ndb2 OEX 20.1
Ndb2 T-DNA 330
Aox1a T-DNA 084
Net CO_2 assimilation (μmol CO_2 m^{-2} s^{-1})
16
14
12
10
8
6
4
2
0
-2
0
250
500
750
1000
1250
1500
Photosynthetically active radiation (PAR)
(μmol photons m^{-2} s^{-1})

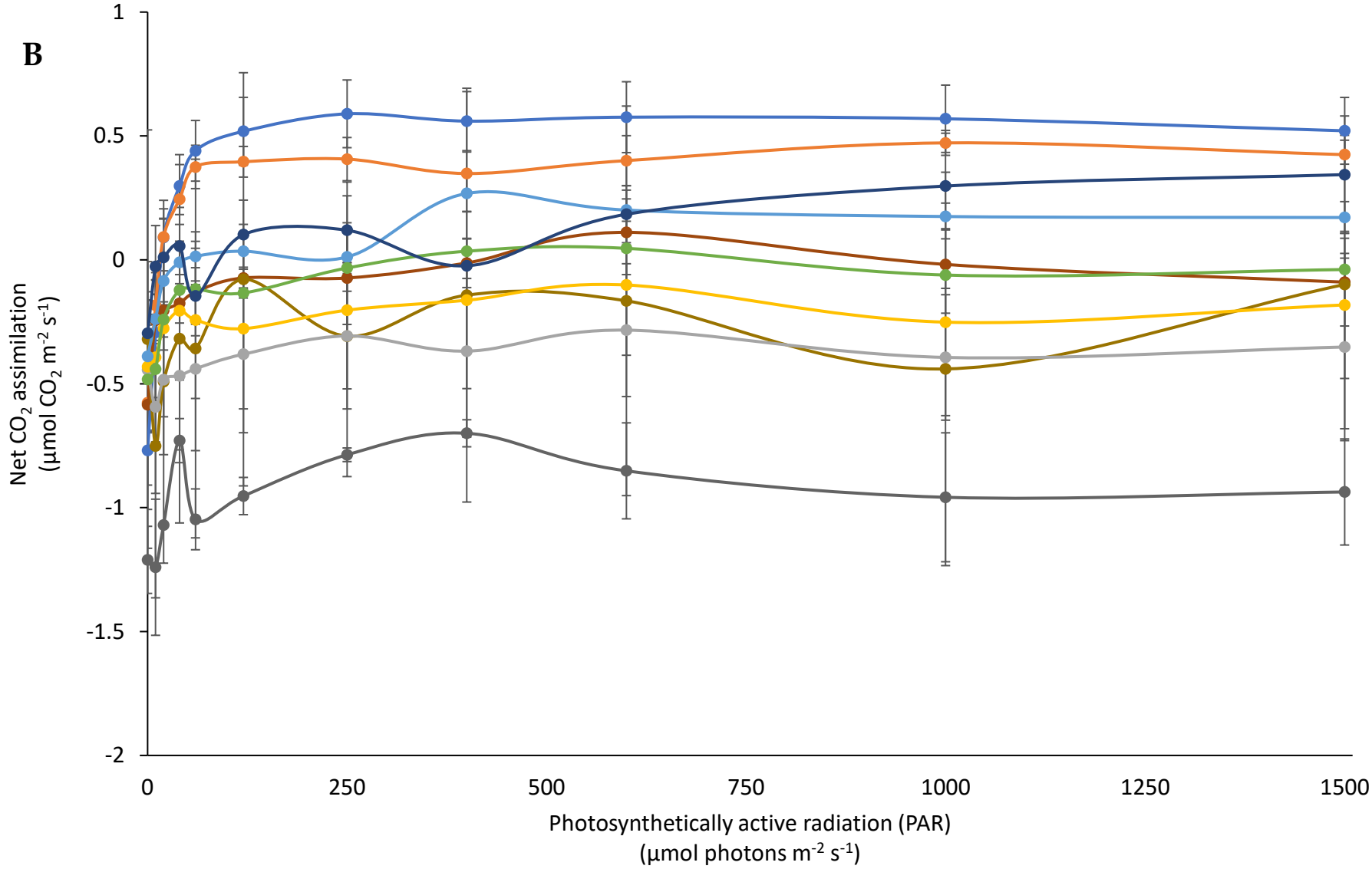
B
1
0.5
0
-0.5
-1
-1.5
-2
Net CO_2 assimilation
(µmol CO_2 m^{-2} s^{-1})
0
250
500
750
1000
1250
1500
Photosynthetically active radiation (PAR)
(µmol photons m^{-2} s^{-1})

Figure 4.17 Light response curve of CO_2 assimilation in transgenic OEX and T-DNA lines grown under control and moderate light and drought conditions

Plants were grown in soil for 29 days under well-watered conditions according to section 2.5.2. Water was then withheld for 3 days, followed by another 5 days of drought with a moderate light exposure of 300 μmol m^{-2} s^{-1}. Each line was measured in quadruplicate for control (A) conditions and (B) MLD stress. Plants were evaluated for CO_2 assimilation according to section 2.5.6. Values are mean +/- S.E N=4. PAR 1500 control, 5.2, 9.1, 20.1 and 084 <0.05; PAR 1500 MLD, P3 and 330 <0.05; PAR 1000 MLD, 5.2, 20.1 and 330; PAR 600 MLD, P9, 5.2 and 330 <0.05; PAR 400 MLD, P3, P9, 5.2 and 330 <0.05; PAR 250 MLD, P3, P9, 5.2, 20.1 and 330 <0.05; PAR 120 MLD, P3, P9, 5.2, 20.1 and 330 <0.05; PAR 60 MLD, P3, P9, 5.2 20.1 and 330 <0.05; PAR 40 MLD, P3, P9 and 330 <0.05; PAR 20 MLD, P9 and 330 <0.05; determined via unpaired, two-tailed t-test against wild type.

Although not significant, the trend within the data suggests that wildtype plants had a greater CO_2 assimilation capacity over all other lines except P17. It's also interesting to note that wildtype, P17 and XX1 did not plateau at 1500 PAR, suggesting they may potentially have room for higher CO_2 assimilation rates. The same measurements were performed for plants exposed to MLD conditions. The majority of the plant lines reached a maximal CO_2 assimilation rate between 60-120 PAR and fluctuated around that mark (Figure 4.17B). CO_2 assimilation rate was greatest in wildtype plants compared to most other lines, although not consistently across all time points. Two of the dual OEX lines, two of the single *Ndb2* OEX lines and the *ndb2* T-DNA were significantly lower than the wildtype. It should be noted that due to the very low measurable gas exchange occurring in MLD samples, there was significant variation between replicates in most lines, making it difficult to form confident conclusions. From the same CO_2 measurements performed under control conditions (Figure 4.17A), the level of respiration occurring in the light can be extrapolated. Respiration in the light (day respiration) was found to be significantly higher in 2 of 3 *Ndb2* OEX lines, with the third also higher, but not significantly so (Figure 4.18A). Although the dual OEX lines and T-DNA lines had slightly elevated day respiration rates than wildtype, these differences were not statistically significant. Day respiration in the single *Aox1a* OEX was the most similar to wildtype. Due to difficulties in obtaining consistent results in MLD samples, respiration in the light was not measured in MLD samples. Respiration measured in the dark saw increases in CO_2 output across most lines compared to day measurements albeit with greater variation between replicates.

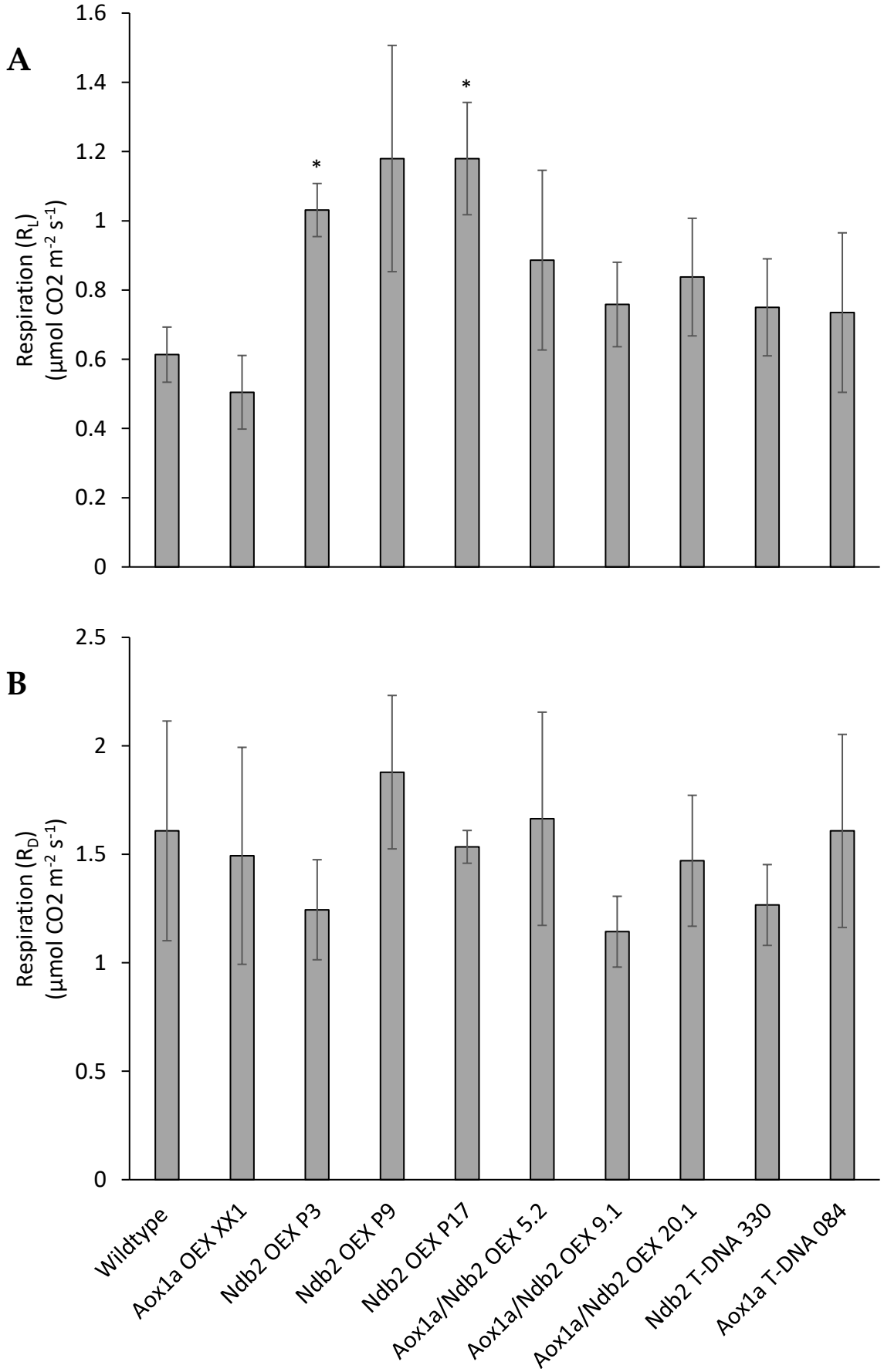
A
Respiration (R_L) (µmol CO2 m^{-2} s^{-1})
1.6
1.4
1.2
1
0.8
0.6
0.4
0.2
0
*
*
B
Respiration (R_D) (µmol CO2 m^{-2} s^{-1})
2.5
2
1.5
1
0.5
0
Wildtype
Aox1a OEX XX1
Ndb2 OEX P3
Ndb2 OEX P9
Ndb2 OEX P17
Aox1a/Ndb2 OEX 5.2
Aox1a/Ndb2 OEX 9.1
Aox1a/Ndb2 OEX 20.1
Ndb2 T-DNA 330
Aox1a T-DNA 084

Figure 4.18 Respiration measured in the light (A) or dark (B) of control plants using the Kok method

Plants were grown in soil for 29 days under well-watered conditions according to section 2.5.2. Each plant line was then measured in quadruplicate. Respiration in the light was calculated from the y-intercept of CO_2 assimilation values obtained between 40 and 120 PAR. Values are mean +/- S.E N=4. * denotes significance of $p<0.05$ determined via unpaired, two-tailed t-test against wild type.

(Figure 4.18B). There were no significant differences found between lines.

The LICOR6400-XT is also capable of measuring H_2O content present in the air, allowing for simultaneous measurements of transpiration rates during light response curves. Under control conditions, all *Ndb2* single OEX lines as well as the *aox1a* T-DNA had significantly higher transpiration (Figure 4.19A). This trend was consistent across all light intensities measured. For all other lines, a significant decrease in transpiration was detected, mostly at the higher light intensities, but this difference was much smaller than that seen for the *Ndb2* single OEX lines. In contrast, under MLD conditions, a mostly opposite trend was seen. Wildtype and XX1 both maintained and reached a higher transpiration rate than all other lines (Figure 4.19B). The *Ndb2* single OEX lines as well as the *aox1a* T-DNA lines were all significantly lower than wildtype and generally grouped together as they did under control conditions. However, in contrast with control conditions, the dual OEX lines did not group with wildtype under MLD. Additionally, it was unusual that several lines displayed negative transpiration rates across most of the light intensities, indicating that more water vapour was being absorbed within the chamber than was being released. It should also be noted that due to the length of time required to measure gas exchange, only eight samples could be measured per day. As a result, lines were sowed in pairs and staggered to allow for measurement of 10 different lines with the same number of days of growth. These pairs (1. Wildtype and XX1, 2. 5.2 and 9.1, 3. 20.1 and 330, 4. 084 and P3, 5. P9 and P17) tend to group together in the MLD transpiration measurements, suggesting that the differences seen between lines may be a result of the experimental

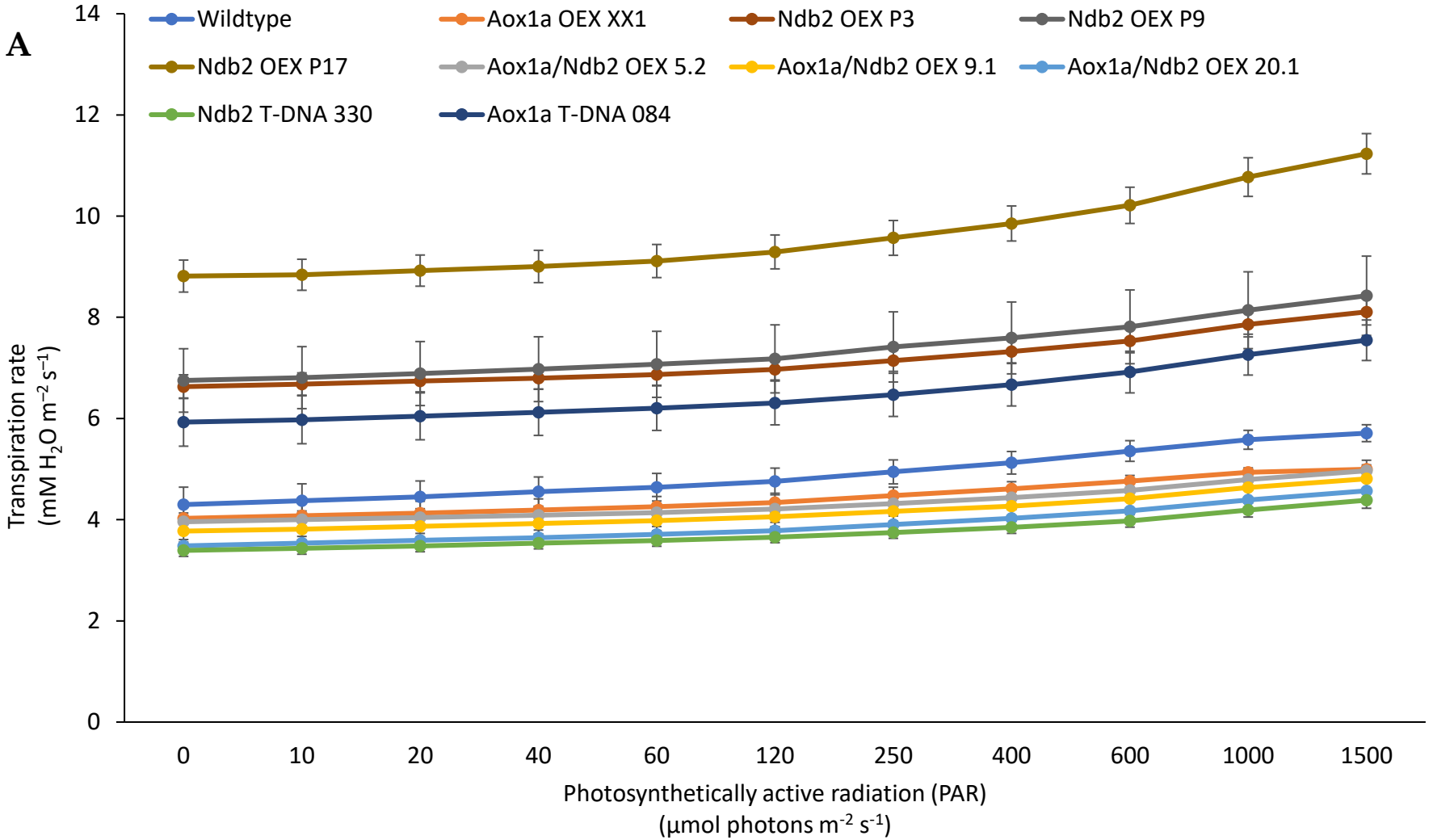
A
Wildtype
Aox1a OEX XX1
Ndb2 OEX P3
Ndb2 OEX P9
Ndb2 OEX P17
Aox1a/Ndb2 OEX 5.2
Aox1a/Ndb2 OEX 9.1
Aox1a/Ndb2 OEX 20.1
Ndb2 T-DNA 330
Aox1a T-DNA 084
Transpiration rate (mM H_2O m^{-2} s^{-1})
0
2
4
6
8
10
12
14
0
10
20
40
60
120
250
400
600
1000
1500
Photosynthetically active radiation (PAR)
(µmol photons m^{-2} s^{-1})

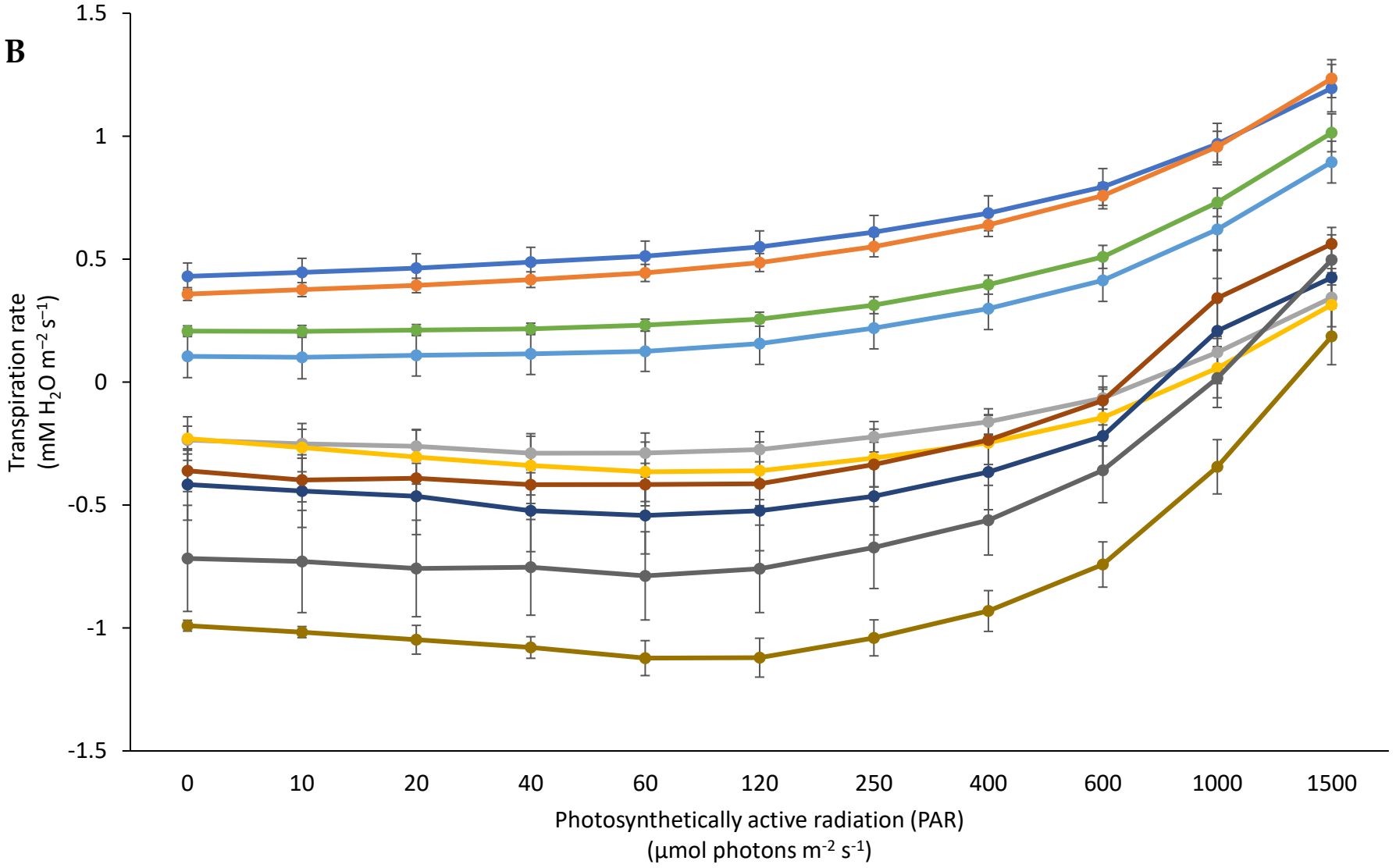
B
1.5
1
0.5
0
-0.5
-1
-1.5
Transpiration rate
(mM H2O m−2 s−1)
0
10
20
40
60
120
250
400
600
1000
1500
Photosynthetically active radiation (PAR)
(µmol photons m-2 s-1)

Figure 4.19 Light response curve of transpiration in transgenic OEX and T-DNA lines grown under control and moderate light and drought conditions

Plants were grown in soil for 29 days under well-watered conditions according to section 2.5.2. Water was then withheld for 3 days, followed by another 5 days of drought with a moderate light exposure of 300 μmol m^{-2} s^{-1}. Each line was measured in quadruplicate for control (A) conditions and (B) MLD stress. Plants were evaluated for transpiration according to section 2.5.6. Values are mean +/- S.E N=4. PAR 1500 control, XX1, P9, 5.2, 9.1 and 084 <0.05; 20.1 and 330 <0.01; P3 and P17 <0.001; PAR 1000 control, XX1, P9, 5.2, 9.1 and 084 <0.05; 20.1 and 330 <0.01; P3 and P17 <0.001; PAR 600 control, P9, 5.2, 9.1 and 084 <0.05; 20.1 and 330 <0.01; P3 and P17 <0.001; PAR 400 control, P9, 9.1 and 084 <0.05; 20.1 and 330 <0.01; P3 and P17 <0.001; PAR 250 control, P9, 9.1, 20.1 and 084 <0.05; 330 <0.01; P3 and P17 <0.001; PAR 120 control, P9, 20.1, 330 and 084 <0.05; P3 and P17 <0.001; PAR 60 control, P9, 20.1, 330 and 084 <0.05; P3 and P17 <0.001; PAR 40 control, P9, 20.1, 330 and 084 <0.05; P3 <0.01; P17 <0.001; PAR 20 control, P9, 330 and 084 <0.05; P3 <0.01; P17 <0.001; PAR 10 control, P9 and 084 <0.05; P3 <0.01; P17 <0.001; PAR 0 control, P9 and 084 <0.05; P3 <0.01; P17 <0.001; PAR 1500 MLD, P9, 20.1 and 330 <0.05; 9.1 and 084 <0.01; P3, P17 and 5.2 <0.001; PAR 1000 MLD, P9, 20.1 and 330 <0.05; 9.1 and 084 <0.01; P3, P17 and 5.2 <0.001; PAR 600 MLD, P9 and 20.1 <0.05; 9.1, 330 and 084 <0.01; P3, P17 and 5.2 <0.001; PAR 400 MLD, P9 and 20.1 <0.05; 9.1, 330 and 084 <0.01; P3, P17 and 5.2 <0.001; PAR 250 MLD, P9 <0.05; 9.1,20.1, 330 and 084 <0.01; P3, P17 and 5.2 <0.001; PAR 120 MLD, P9 and 20.1 <0.05; P17, 9.1, 330 and 084 <0.01; P3 and 5.2 <0.001; PAR 60 MLD, P9 and 20.1 <0.05; 9.1, 330 and 084

<0.01; P3, P17 and 5.2 <0.001; PAR 40 MLD, 20.1 and 330 <0.05; P9 , P17 and 084 <0.01; P3, 5.2 and 9.1<0.001; PAR 20 MLD, 20.1 and 330 <0.05; P9 , P17 and 084 <0.01; P3, 5.2 and 9.1<0.001; PAR 10 MLD, P3, 20.1 and 084 <0.05; P9 , P17 and 9.1 <0.01; 5.2 <0.001; PAR 0 MLD, P17 <0.05; P3, P9, 5.2 and 9.1 <0.01; 084 <0.001; determined via unpaired, two-tailed t-test against wild type.

design, despite attempts to keep experimental conditions constant, with the same settings utilised on the LICOR6400-XT, same growth conditions and experimental design for each line tested.

Although the previous measurements under MLD demonstrated small differences between lines in terms of biomass accumulation, a stress-tolerant phenotype was not clear. To investigate the response to stress in more detail, plant lines were exposed to the same MLD stress as above, but some plants were re-watered at the end of the stress to determine their ability to recover. Due to the large number of plants required to run these experiments and the spacial limitations in the growth cabinets, this study was performed twice with different plant lines in each experiment.

In initial recovery experiments the dual OEX lines showed substantially greater ability to recover after the MLD treatment (Figure 4.20A). The AOX parent line, XX1, also demonstrated an improvement in recovery over the wildtype line albeit slightly less pronounced than the dual OEX. When assessed for water content, both the above lines showed slightly higher values under both control and MLD conditions (Figure 4.20C). This trend was also present in the single *Ndb2* OEX lines, although these lines did not show an improvement in recovery ability.

In subsequent experiments, all three dual OEX lines were exposed to the same MLD conditions and assessed for recovery. Only the single *Aox1a* OEX and dual OEX lines were able to recover from the MLD stress (except one wildtype plant) (Figure 4.21). Quantification of survival rates highlighted the dual OEX lines significantly

Image removed due to copyright restriction. Original can be viewed online at http://www.plantphysiol.org/content/181/2/774

Figure 4.20 Effect of drought and moderate light treatment on transgenic OEX and T-DNA lines under control and moderate light drought conditions

Plants were grown in soil for 32 days under well-watered conditions according to section 2.5.2. Water was then withheld for 6 days, followed by another 7 days of drought with a moderate light exposure of 300 μmol m^{-2} s^{-1}. Plants were then either harvested, or re-watered and returned to control growth conditions to check recovery. (A) Photos of representative plants grown under control conditions (left), at the end of the drought and moderate light treatment (middle), and after two weeks of recovery (right). (B) Dry weights and (C) water contents of plants harvested at the end of the drought and moderate light treatment (n = 4 ± S.E.M.). * denotes significance of $p<0.05$ determined via unpaired, two-tailed t-test against wild type.

Collaborative work of Crystal Sweetman and myself, adapted from (Sweetman et al. 2019)

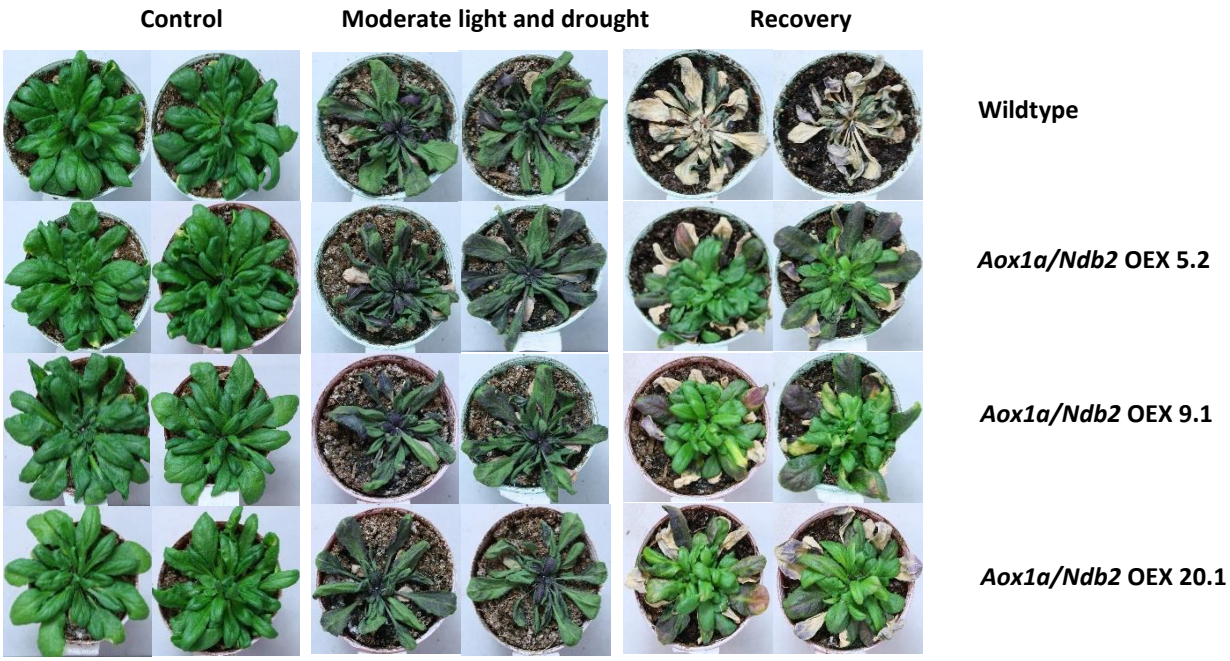

Figure 4.21 Effect of extended drought and moderate light treatment on plants overexpressing *AtNdb2* and *AtAox1a*

Plants of wildtype and dual OEX lines were grown in a controlled temperature After 33 days, water was withheld. After a further 6 days, plants were transferred to increased light (300 μmols.m^{-2}.sec^{-1}), with drought continued in the same manner for a further 7 days, at which point plants were either harvested or re-watered and returned to control growth conditions to check recovery. Photos of representative plants grown under control conditions (left), at the end of the drought and moderate light treatment (middle), and after 11 days of recovery (right).

Table 4.1 Survival rates of dual *Aox1a*/*Ndb2* OEX plants watered for recovery at the end of the drought and moderate light treatment.

Plants of wildtype and dual OEX lines were grown in a controlled temperature growth cabinet. After 33 days, water was withheld. After 6 days, plants were transferred to moderate light (300 μmols.m^{-2}.sec^{-1}), with drought continued in the same manner for a further 7 days, at which point plants were re-watered and returned to control growth conditions to check recovery. Survival was scored 11 days after re-watering. *$p<0.01$ (Chi-squared test, (df=1).

Line	Recoverable	Non-recoverable	% survival
Wildtype	1	11	9
***Aox1a* OEX XX1**	2	1	66*
***Ndb2* OEX P3**	0	9	0
***Ndb2* OEX P17**	0	3	0
***Aox1a/Ndb2* OEX 5.2**	7	6	54*
***Aox1a/Ndb2* OEX 9.1**	11	1	92*
***Aox1a/Ndb2* OEX 20.1**	6	2	75*

better ability to recover from MLD stress (Table 4.1). OEX of *Aox1a* alone (line XX1) also conferred an increase in stress tolerance, but the relatively small number of replicates for this line makes it difficult to determine whether differences between it and the dual OEX are significant. It is interesting to note that not all lines had similar survival rates despite having similar levels of *Ndb2* expression.

To investigate the physiological response of MLD-stressed plants, a number of transgenics were again exposed to MLD conditions and assessed physiologically across the full seven days of MLD exposure. Fresh and dry weights were measured from destructive harvesting from triplicates across each day under both conditions. Fresh weights between control and MLD conditions were not significantly different at the beginning of the MLD treatment but separated as plants succumbed to the stress (Figure 4.22A). Plants began to differ in fresh weight after day 2 of MLD and increased in difference across the seven days. Very little difference was seen between lines under either control or MLD conditions (Figure 4.22). Interestingly, dry weight didn't appear to differ across either condition or between any lines despite plants appearing severely stressed compared to their control counterparts (Figure 4.22 and 4.23). Furthermore, MLD plants increased in DW over the seven days and maintained similar biomass to their control counterparts. It appears that any weight lost during MLD is a result of a loss of water content and not biomass. Water content was measured under both conditions by combining measurements of fresh, dry and turgid weights to determine both the water content and the relative water content. All control lines maintained a consistent ~75% RWC under control conditions. RWC of line 5.2 under MLD was

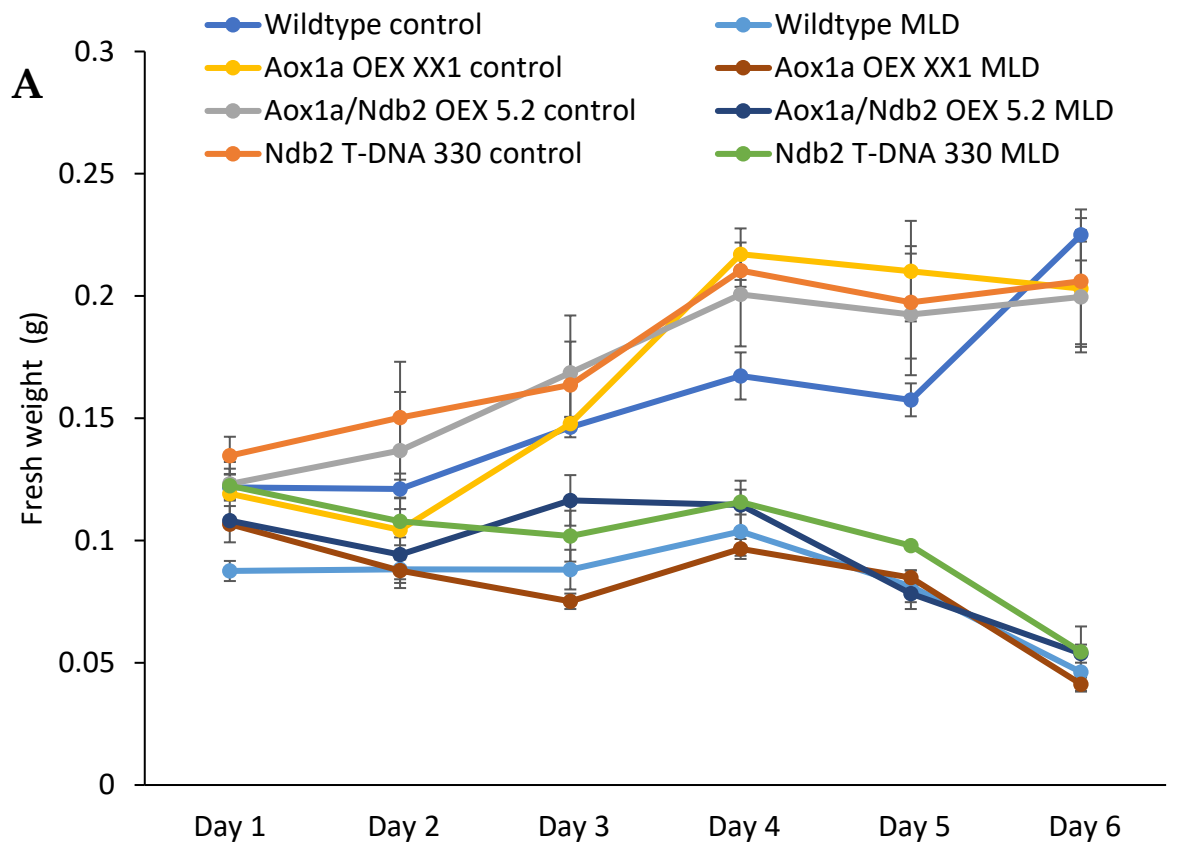
A
Wildtype control
Wildtype MLD
Aox1a OEX XX1 control
Aox1a OEX XX1 MLD
Aox1a/Ndb2 OEX 5.2 control
Aox1a/Ndb2 OEX 5.2 MLD
Ndb2 T-DNA 330 control
Ndb2 T-DNA 330 MLD
Fresh weight (g)
0.3
0.25
0.2
0.15
0.1
0.05
0
Day 1
Day 2
Day 3
Day 4
Day 5
Day 6

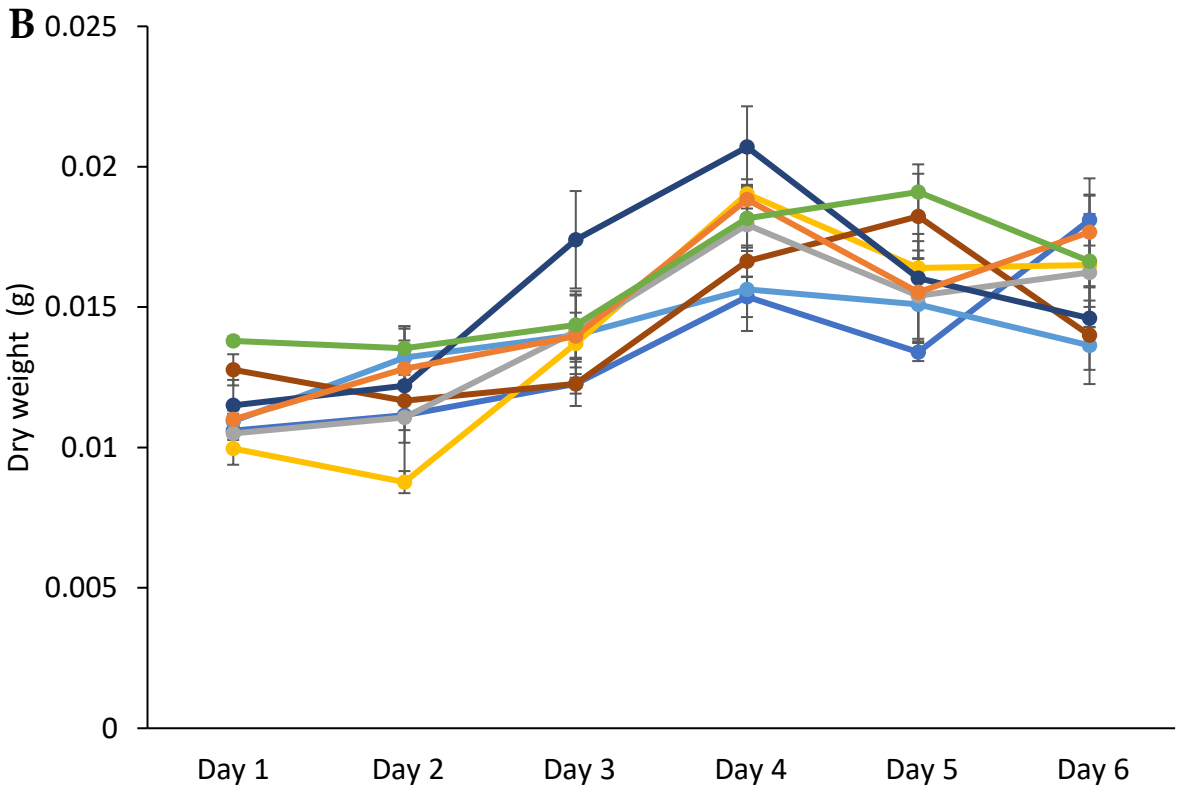
B
Dry weight (g)
0.025
0.02
0.015
0.01
0.005
0
Day 1
Day 2
Day 3
Day 4
Day 5
Day 6

Figure 4.22 Fresh and dry weights of rosettes in transgenic OEX and T-DNA lines grown in soil exposed to MLD or control conditions

Plants were grown in soil 28 days under well-watered conditions according to section 2.5.2. Water was then withheld for 6 days, followed by another 7 days of drought with a moderate light exposure of 300 μmol m^{-2} s^{-1}. Days are numbered from the beginning of seven days of MLD exposure. Each time point consists of triplicates of each line in each condition. Shoots fresh weights (A) were measured immediately and dry weights (B) were taken from tissue incubated at >80°C for 48 hours. Values are mean +/- S.E. N=3, FW control day 2, XX1 <0.05; FW control day 4, 330 and XX1 <0.05; FW MLD day 2, XX1 <0.05; FW MLD day 4, 330 and XX1 <0.05; DW control day 1, 5.2 <0.05; 330 <0.01; DW MLD day 1, 330 <0.05. Significance was determined via unpaired, two-tailed t-test against wild type

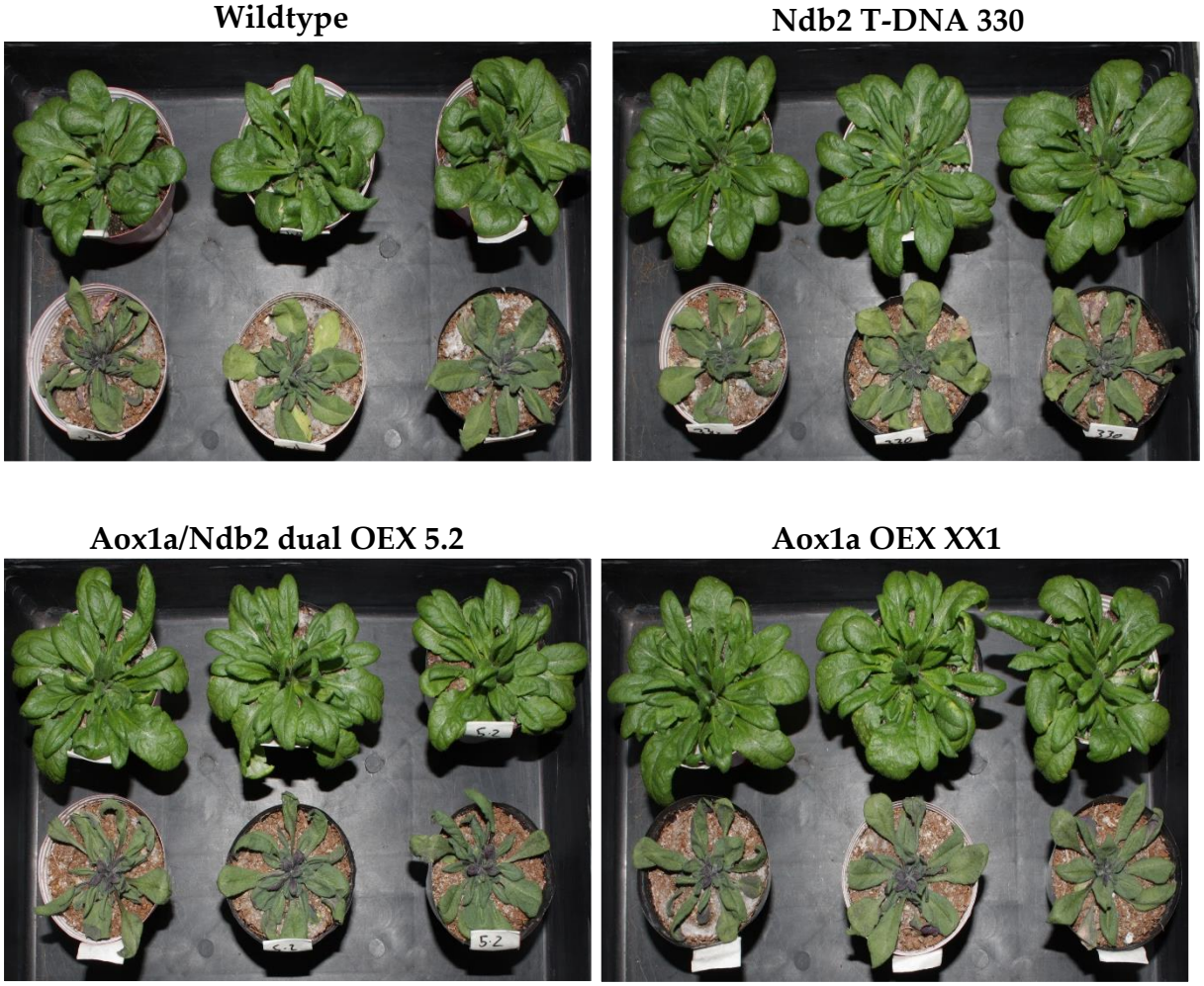

Figure 4.23 Control and MLD plants after either 41 days of optimal growth conditions or 28 days optimal growth and 6 days drought + 7 days MLD.

significantly less beginning day 2 compared to wildtype control samples, while other lines maintained similar values to the wildtype control (Figure 4.24A). Post day 4, control and MLD lines begun to separate and became significantly different from each other but maintained similar values between lines. It was only between the period of day 4 and 5 that any significant difference between lines under MLD conditions occurred, with the *ndb2* T-DNA line having significantly higher RWC than the wildtype MLD sample. However, this affect was not seen post day 5, with all samples having very similar RWC at the end of the MLD experiment. It seems that the plant relative water content is only affected 7-9 days into the simulated drought compared to control and that the transgenic expression of the alternative respiratory pathway has minimal effect on RWC under either condition. Looking at the water content of each line reaffirms what was seen in RWC; there were minimal differences between lines but large differences between control and MLD samples (Figure 4.24B). From what was seen in the previous experiment, (Figure 4.20B) it seems reliable and consistent measurements of water content under drought stress conditions are difficult to obtain. Thus, it seems that the altered AP expression and its effects on plant water content were not conclusive.

Anthocyanin levels were quantified to determine whether a difference exists between lines that could reflect changes relating to stress. Under control conditions, there were no differences or deviations between lines (Figure 4.25). Under MLD conditions, anthocyanin production is starkly increased. Initially, both the XX1 and 330 lines produce significantly less anthocyanin content while the 5.2 also trends

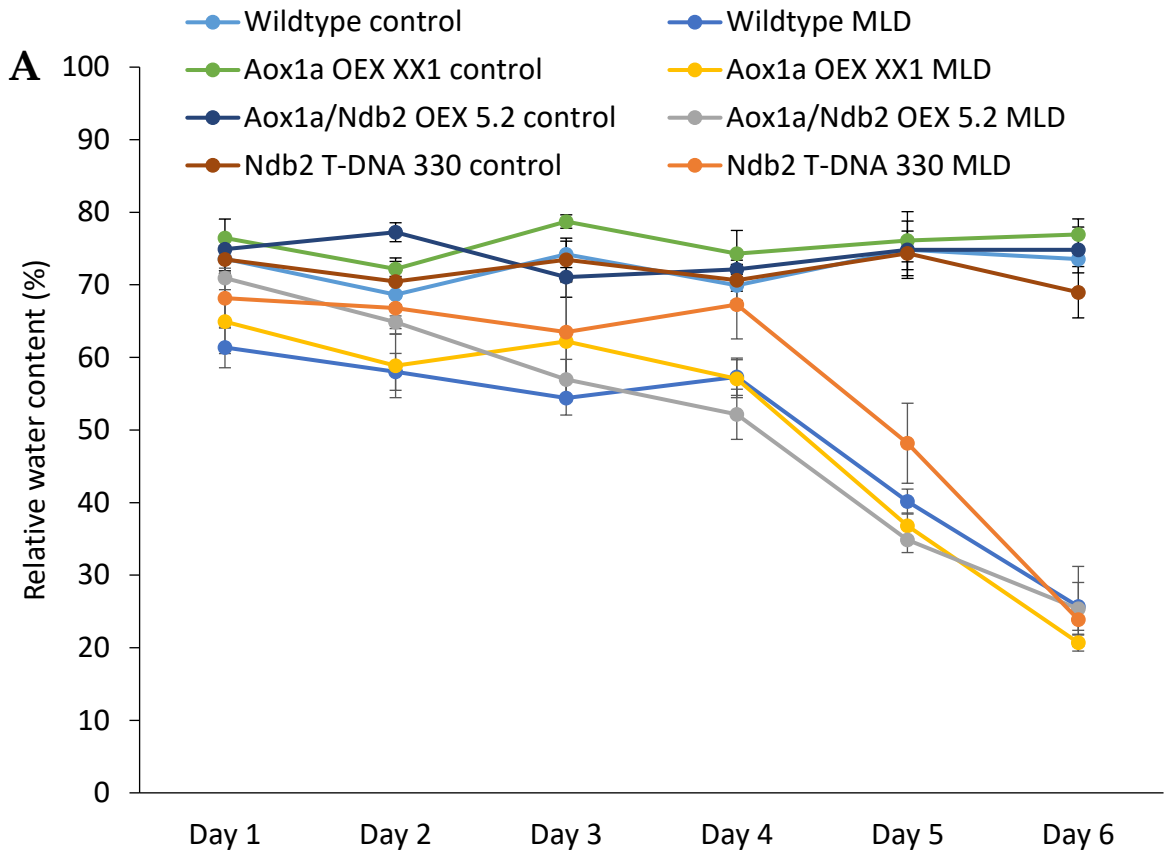
A
Wildtype control
Wildtype MLD
Aox1a OEX XX1 control
Aox1a OEX XX1 MLD
Aox1a/Ndb2 OEX 5.2 control
Aox1a/Ndb2 OEX 5.2 MLD
Ndb2 T-DNA 330 control
Ndb2 T-DNA 330 MLD
Relative water content (%)
100
90
80
70
60
50
40
30
20
10
0
Day 1
Day 2
Day 3
Day 4
Day 5
Day 6

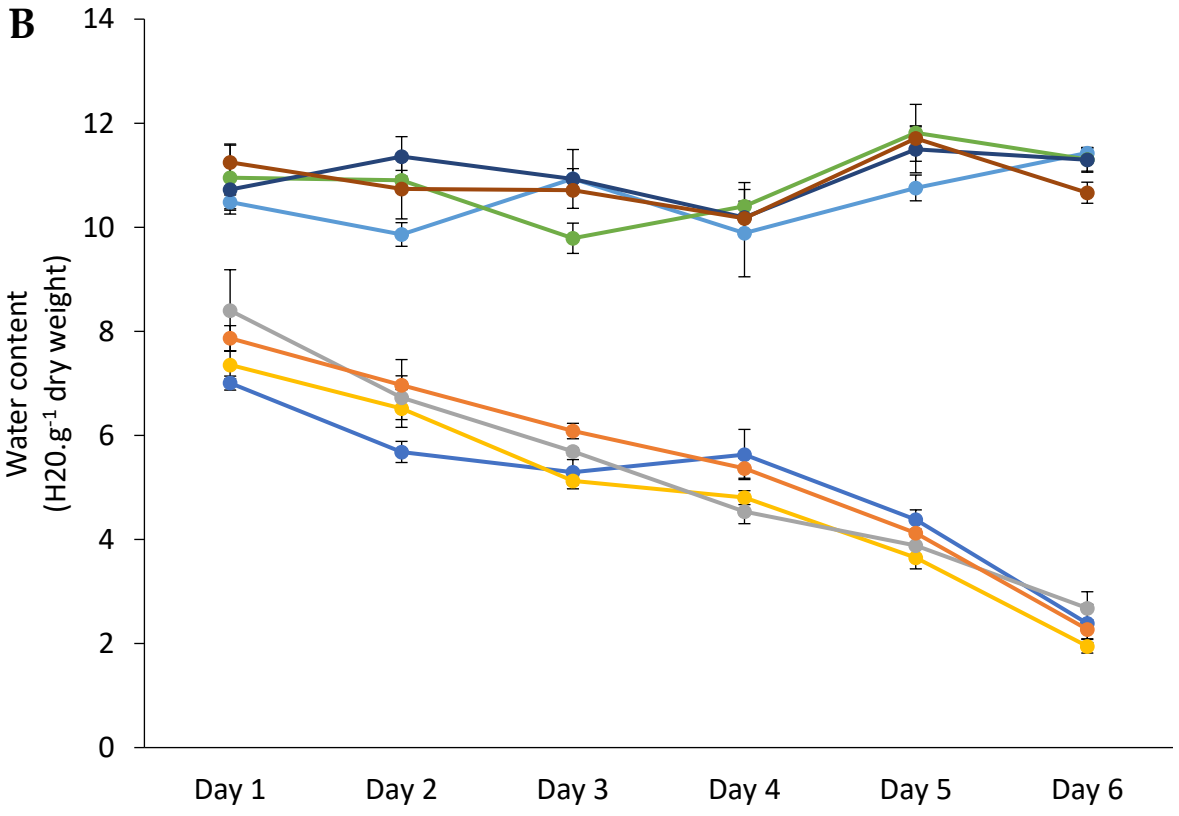
B
Water content
(H20.g-1 dry weight)
14
12
10
8
6
4
2
0
Day 1
Day 2
Day 3
Day 4
Day 5
Day 6

Figure 4.24 Water content in transgenic OEX and T-DNA lines exposed to moderate light and drought over a 6-day period

Plants were grown in soil 28 days under well-watered conditions according to section 2.5.2. Water was then withheld for 6 days, followed by another 7 days of drought with a moderate light exposure of 300 μmol m^{-2} s^{-1}. Days listed in the figure are from the seven days of MLD exposure. Each time point consists of triplicates of each line in each condition. Relative water content (A) is expressed as the percentage of water in fresh tissue compared to turgid tissue and water content (B) was the water content per g dry weight. Values are mean +/- S.E N=3. RWC Day 2 control, 5.2 <0.05; Water content Day 1 MLD, 330 <0.05; Day 2 control, 5.2 and XX1 <0.05; Day 3 control, XX1 <0.05; Day 5 control, 330 <0.05; Day 6 control, 330 <0.05 determined via unpaired, two-tailed t-test against wild type of the same growth conditions.

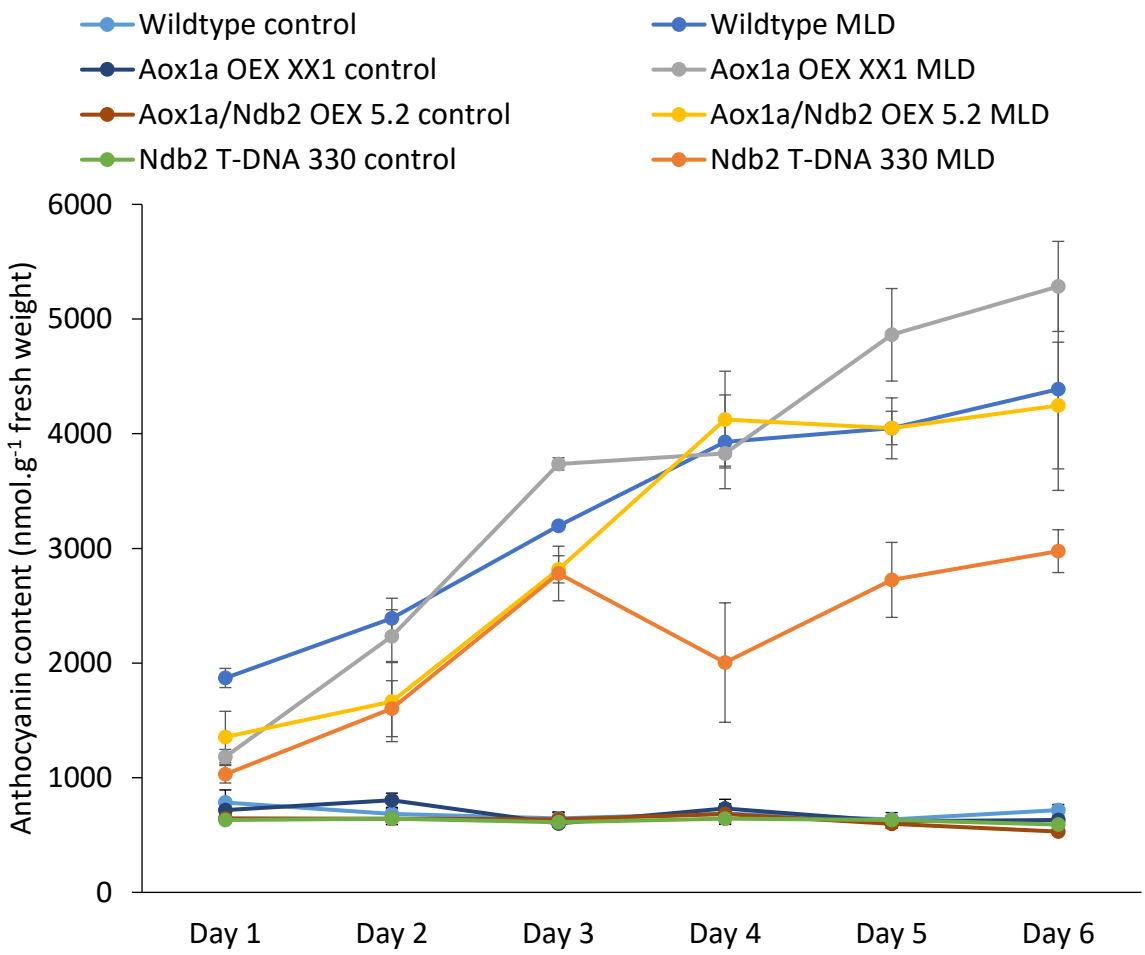

Figure 4.25 Anthocyanin content in transgenic OEX and T-DNA lines exposed to moderate light and drought

Anthocyanin content was determined spectrophotometrically from shoot tissue sampled daily after exposure to moderate light and drought stressed. Values are mean +/- S.E N=3. Day 1 MLD, XX1 and 330 <0.01; Day 3 MLD, XX1 <0.01; Day 4 MLD, 330 <0.05; Day 5 MLD, 330 <0.05 determined via unpaired, two-tailed t-test against wild type

towards a decrease. However, post day 2, this trend becomes weaker in both the XX1 and 5.2 line but continues to be significantly lower in *ndb2* T-DNA line 330, finishing with significantly less anthocyanin content than all lines tested.

Thiobarbituric acid reactive substances (TBARS) were measured as a proxy for oxidative damage to the cell. TBARS or the specific product they are expected to react with, malondialdehyde (MDA), are a by-product of the oxidation of lipid molecules, resulting from damage through ROS. Wildtype TBARS content under control conditions was significantly higher on several days, especially compared to XX1 and 5.2 (Figure 4.26A). There were little overall changes to TBARS content over the seven days measured in each line, although by the end of the seven days, both XX1 and 5.2 were still significantly lower in terms of TBARS compared to wildtype. When measuring TBARS under MLD conditions, substantial difficulties arose. Not only were a number of measurements significantly lower than control conditions values, there were significant variations and several negative values recorded (Figure 4.26B). Due to the fact the TBARS is measured at a very similar wavelength to anthocyanins, there is significant overlap when attempting to measure TBARS in tissue exposed to prolonged stress. Even though the TBARS method utilises a control sample that isn't reacted with thiobarbituric acid to offset the contribution of anthocyanins, the small contribution of TBARS relative to anthocyanin prevents accurate measurements in tissues with high concentrations of anthocyanins. From the recovery experiments performed on a number of lines, the dual OEX lines as well as the single *Aox1a* OEX

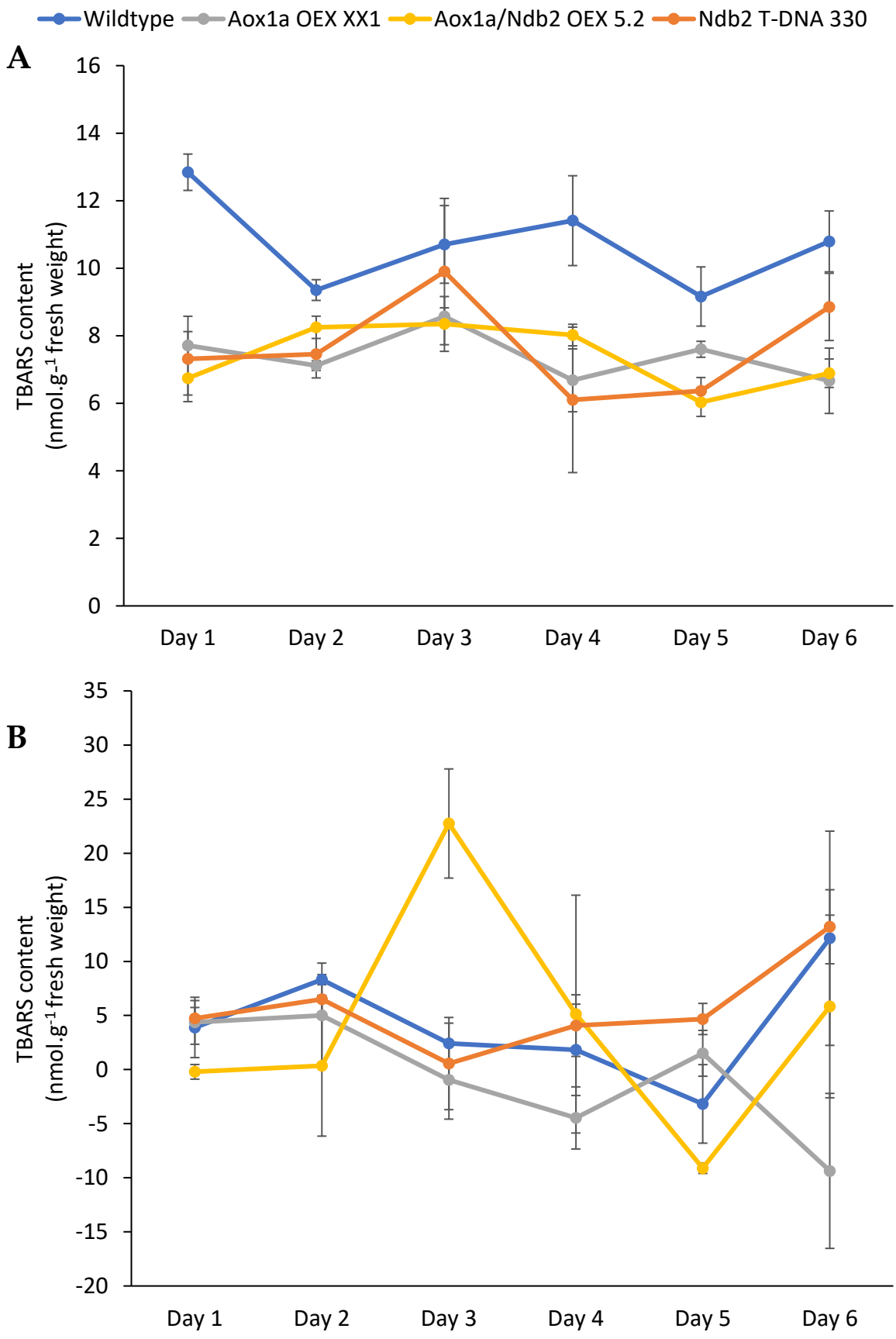
Wildtype
Aox1a OEX XX1
Aox1a/Ndb2 OEX 5.2
Ndb2 T-DNA 330
A
TBARS content (nmol.g-1 fresh weight)
16
14
12
10
8
6
4
2
0
Day 1
Day 2
Day 3
Day 4
Day 5
Day 6
B
TBARS content (nmol.g-1 fresh weight)
35
30
25
20
15
10
5
0
-5
-10
-15
-20
Day 1
Day 2
Day 3
Day 4
Day 5
Day 6

Figure 4.26 TBARS in transgenic OEX and T-DNA lines exposed to moderate light and drought

TBARS content was determined spectrophotometrically from shoot tissue sampled daily after exposure to (A) control conditions or (B) moderate light and drought stress. Values are mean +/- S.E N=3. Day 1 control, XX1, 330 and 5.2 <0.05; Day 2 control, XX1 <0.05; Day 4 control, XX1 <0.05; Day 6 control, XX1 and 5.2; Day 3 MLD, 5.2 <0.05 determined via unpaired, two-tailed t-test against wild type

XX1 showed an increase in the ability to recover from MLD stress. However, this is not reflected in the MDA and biomass measurements. Although one experiment showed (Figure 4.20C) a difference in water content between both XX1 and 5.2 compared to wildtype under MLD, these results were not reproducible in other experiments (Figure 4.16 and 4.24B). Moreover, none of the gas exchange measurements nor anthocyanin measurements were able to differentiate between the lines. However, MDA content was significantly higher in wildtype samples than in the transgenics under control conditions, suggesting less oxidative stress in the latter. Whether this contributed to the improved recovery of the transgenics after exposure to MLD, could not be determined.

4.4 Discussion

4.4.1 Sucrose is a crucial carbon source in MS media

From the experiments performed on MS media agar, sucrose is clearly a requirement for consistent germination and growth of both rosette and roots in Arabidopsis. In plates without sucrose, the germination was less than 50% and those that did germinate had very large growth differences. These differences were characterised by a lack of rosette emergence and little to no root growth. This phenotype was not restricted to a specific line, suggesting that the cause is systemic and not a result of transgene expression.

The intended role of sucrose is to provide an alternative carbon source than atmospheric CO_2. The reason for including the alternative carbon source is due to the limitation of growing seedlings on a semi-sealed agar plate. Due to the ideal nutrient content and lack of antibiotic, the MS media is highly susceptible to bacterial and fungal contamination and must be kept in a sterile environment. These contaminants are kept at bay through a semi-sealed agar plate, utilising 3M Micropore™ tape to allow gas exchange. Regardless, plants are still maintained in a stagnant air environment and as such require an alternative source of carbon to grow adequately. Unusually, the method outlined by Boyes et al. (2001) explicitly states that no supplemental sucrose is added. It should be noted that the plants that did manage to germinate and grow successfully produced similar sized rosettes and roots to those grown on sucrose. Additionally, it also appears that in most plates, approximately four to five plants would grow to a similar size as those on sucrose. It is suggested that

these plants are germinating and utilising the limited CO_2 available before other plants, providing them with the initial carbon required to develop optimally. It seems that the alternative carbon source is requirement for consistent early germination and growth but has minimal to no significant effect on plants growth past this stage. Furthermore, it may be possible to grow plants with consistent growth on agar if the number of seeds sowed is limited, although this was not tested. However, if maximising efficiency of the MS medium is crucial, sucrose should be used and allows for a maximum of 12 plants per 10x10x2 cm petri dishes. It does seem unusual, however, that plants are most affected earliest in development when CO_2 assimilation and photosynthesis is likely lowest but are not affected in later development when CO_2 assimilation and photosynthesis are at their highest. Regardless, experiments on MS media containing sucrose were used for interpretation because growth without was too inconsistent to interpret. This does limit the interpretation of the results, as any potential differences relating to carbon assimilation may be masked with the addition of an external carbon source. At the same time, growing seeds on MS media without sucrose clearly has a media-dependent effect which would have confused analysis of the transgenic lines.

4.4.2 Altering AP expression delays early growth milestones

Investigation into the phenotype of newly generated transgenics has identified consistent unique differences specific to early development within each line (where multiple lines were available). The OEX of *Aox1a* and/or *Ndb2* results in an early developmental growth delay that differs depending on single or dual OEX . Both

single OEX lines (XX1 and P3) were characterised by a delay in development of rosette tissue in both agar and soil, whereas this phenotype was not present in the dual OEX lines. A trend consistent across other measurements, including root length, developmental milestones, rosette size and stem height, was that the observed delay occurred early in rosette development, but the effect was carried through to the later stages of the growth study. That is, roots and rosettes maintained similar growth rates after the initial delay. Why OEX of either *Ndb2* or *Aox1a* alone, but not dual OEX, has such an effect is not clear but may point to an imbalance between inputs and outputs in the mETC that affect the metabolism of emerging seedlings or signalling pathways that regulate growth It should be noted that the dual OEX lines were also delayed in cotyledon development, but otherwise growth was similar to wildtype.

There are very few reports with phenotypical data on the effects of *Aox1a* or *Ndb2* OEX on *Arabidopsis* under control conditions, although Tarasenko et al. (2012) studied a similar *Aox1a* OEX line (XX2) (Umbach et al. 2005). This group found that the single *Aox1a* OEX tested showed both delayed rosette and flowering but almost no difference in cotyledon development, which is exactly what was observed in these experiments. The researchers who generated the single *Aox1a* OEX lines also performed preliminary phenotype characterisation, with some overlapping results. Fiorani et al. (2005) found that the rosette diameter of XX2 lines were smaller in size but weren't significantly different. Comparing the two datasets, there are differences in the sampling times that could explain the differences seen. From the results presented here, the significant differences seen in rosette radius were between days

14 and 22, with any differences disappearing by day 24. The measurements by Fiorani et al. (2005), on the other hand, were made 42 days after germination, which could explain why only small but insignificant differences were seen between the rosette sizes of *Aox1a* OEX and wildtype. It is interesting to note that the growth delay early in development of single OEX lines does not negatively affect final biomass, rosette size or stem height at the completion of measurements. The dual OEX lines 9.1 and 20.1, however, were significantly smaller in terms of both fresh and dry weight compared to wildtype. Although there were delays in early development of dual OEX lines, only the 5.2 and 9.1 lines were affected, making the drop in biomass shown in Figure 20.1 particularly unexpected.

There are some significant limitations and concerns of the Boyes et al. (2001) growth analysis method that may have impacted on the results. When taking measurements of biomass, the Boyes et al. (2001) method prompts users to harvest samples not on the same day but based on when they achieve a particular milestone. In the above cases these are when the first flower buds become visible (5.10) and when the plant height begins to plateau (6.50). The differences seen in fresh and dry weights of 9.1 and 20.1 are not a result of this sampling method, as they were mostly sampled on the same day as all other lines. However, as previously mentioned, both the single OEX lines have delayed flowering, (even more so for P3) and as such were harvested later in the second round of fresh and dry weight measurements compared to other lines. As a result, it could be argued that the significant differences in biomass seen between the P3 and wildtype lines are simply due to an extended period of growth

for the P3 lines. The fact that the other single OEX (XX1) biomass is not affected does not diminish this hypothesis, as the XX1 line flowering time was significantly less delayed than P3. Further to this, the P3 line spends more time than any other line in the vegetative phase of growth, which may explain why these lines have greater rosette biomass but have no significant differences in stem biomass. The growth rates seen for P3 were significantly higher than all other lines while XX1 was the same as wildtype. This does not rule out the possibility that the differences seen in biomass are a result of sampling times, as the growth rates of plants are sigmoidal (Liu et al. 2018) and as such are susceptible to errors if sampling times aren't the same. In repeated experiments, these results varied, with one repeated experiment in agreement with the increased P3 fresh weight (Figure 4.15), while the other experiment exhibited a decreased dry weight in P3 but no difference in fresh weight (Figure 4.20). These results highlight the difficulties in achieving consistent growth under differing conditions and with different experimenters, as was previously pointed out by Massonnet et al. (2010). This brings attention to the importance of multiple experiments to confirm tentative results. As such, not all measurements provided here can be regarded with the same confidence. However, there are several results that are reproducible and consistent amongst lines with the same construct. The delays seen in development, specifically rosette development, were mostly replicated in a phenotype analysis containing other *Ndb2* OEX lines (Sweetman et al. 2019). Results with root length were also supported by other experiments (Sweetman et al. 2019), but rosette radius was only partially supported as discussed above (Fiorani

et al. 2005). Again, the plant height and secondary root measurements were supported by other experiments (Sweetman et al. 2019). Bringing this altogether, it seems that both *Ndb2* and *Aox1a* single OEX lines are characterised by an initially slower growing phenotype but catch up with wildtype after a few weeks of growth. Overexpressing both *Ndb2* and *Aox1a* together, however, seems to rescue this delayed growth phenotype, with growth almost entirely the same as wildtype. The only noticeable differences between wildtype and the dual OEX lines was a slight delay in cotyledon development and reduction in biomass of 9.1 and 20.1 after approximately 22-24 days. However, after 43 days, this phenotype was only present in the 9.1 line. The very small growth differences in the OEX lines were not completely unexpected. The AOX enzyme is tightly controlled by numerous regulatory mechanisms including post-translational (Vanlerberghe 2013a) (Figure 1.2) and may not be (very) active in the OEX lines under control conditions. These mechanisms are likely an important control to prevent the potentially wasteful nature of the AP. Although this may explain why all these lines do not suffer from a severe growth penalty, it does not explain the differences between the single OEX lines and the dual OEX lines. It may be that the single OEX of either gene results in an imbalance in the input or output of the ETC. This could then manifest itself early in development by altering metabolism and/or signalling pathways.

4.4.3 Dual OEX of *Aox1a* and *Ndb2* improves stress tolerance above that of wildtype and single OEX

Several studies with a specific focus on moderate light and/or drought stress have utilised RNAi or T-DNA constructs to knockout or disrupt expression of *Aox1a.* These studies tend to focus towards biochemical and gas exchange characterisation with limited phenotyping data available (Bartoli et al. 2005; Giraud et al. 2008; Zhang et al. 2010; Yoshida et al. 2011b; Wang & Vanlerberghe 2013; Dahal et al. 2014; Dahal & Vanlerberghe 2017). A small number of studies however have highlighted the importance of *Aox1a* under a drought and/or light stress. Without *Aox1a*, plants are subject to photobleaching (Zhang et al. 2010), reduced recovery post stress (Wang & Vanlerberghe 2013) and accumulate anthocyanins at levels far above wildtype (Giraud et al. 2008). Our study aimed to test the effect of dual OEX of *Aox1a* and *Ndb2* on tolerance to moderate light and drought stress. From the results presented here, it is clear that both the dual OEX lines as well as the single *Aox1a* OEX show improved post-stress recovery over wildtype. This is evidenced by a significant proportion of plants able to recover after the MLD stress, whereas only one of 12 wildtype plants survived. However, from the combination of phenotypical, biochemical and gas exchange data collected, no single key trait was identified that confers the improved tolerance. Importantly, both *aox1a* and *ndb2* T-DNA lines showed a reduced capacity to recover post-stress as compared to wildtype.

Measurements of biomass were found to be inconclusive and varied amongst replicate experiments. Comparing across three separate MLD experiments, P3 FW and

DW under control conditions were up and down respectively in two different experiments, but together with P9, were both down under MLD but only in a single experiment. None of the more resilient lines showed any differences in biomass across either condition. Measurements of water content were more informative with both 5.2 and 20.1 having significantly higher water content that wildtype, although not seen under MLD. However, in other experiments in the same laboratory, 5.2 and XX1 were shown to contain significantly more water under both MLD and control when compared to wildtype (Sweetman et al. 2019). But again, a replicate experiment failed to repeat either findings. Though it should be noted that there is significantly difficulty in this particular experimental approach. Though all efforts were made to maintain consistent levels of water in each pot, the positioning within the growth cabinet meant that each pot was subjected to slightly different levels of light and movement of air, causing differences in rates of drying in the soil. This meant obtaining consistent data on small differences between lines was difficult and could explain why we saw some differences in water content in one experiment but not the other. In future, where time allows, a more detailed growth analysis should be performed over a greater period of time as well as different stresses. This may allow for more consistent data that could help identify phenotypic traits that have aided the OEX lines in recovery. Though it should be noted that none of the literature involving AOX transgenics and drought and/or light stress have reported differences in biomass and water content of transgenics (Wang & Vanlerberghe 2013; Dahal et al. 2014; Dahal & Vanlerberghe 2017) apart from one T-DNA experiment (Giraud et al. 2008). However, these

experiments did identify a number of traits relating to *Aox1a.* Maximal quantum yield of photosystem II became compromised during drought in *aox1a* lines and strongly increased oxidative damage (Dahal & Vanlerberghe 2017) and respiration rates slow in *aox1a* lines creating a lack of electron sink resulting in limited photosynthetic capacity (Dahal et al. 2014).

Gas exchange measurements in my hands, showed for the most part that transgenic modification of the AP components has minimal to no significant effect on CO_2 assimilation under control conditions. The lines showing significant decreases in CO_2 assimilation compared to wildtype were the dual OEX lines and *aox1a* T-DNA line. A similar drop in net CO_2 assimilation was also reported in the same *aox1a* line (Gandin et al. 2012). In other literature, an *aox1a* T-DNA line showed no difference under saturating irradiance, albeit with a much lower saturation irradiance and a different *aox1a* T-DNA line (Yoshida et al. 2011b). In partial agreement with our results, the CO_2 assimilation of an *aox1a* RNAi line measured by Dahal et al. (2014) was significantly lower than wildtype but another was not. Majority of lines used here tended towards a decrease in CO_2 assimilation though. The large variation amongst replicates, however, prevented a statistically significant difference from being measured. Unfortunately, these comparisons rely on experiments that utilise different methodology including different transgenic lines, different organisms and different saturating irradiance. Despite this, it is fascinating that all the dual OEX lines showed a reduced capacity to assimilate CO_2. We saw no difference in CO_2 assimilation in either single *Aox1a* or *Nbd2* OEX lines, suggesting that *Ndb2* OEX requires a

concomitant up-regulation of *Aox1a* to affect CO_2 assimilation, at least under saturating irradiance. Counter to what was seen in tobacco MLD (Dahal et al. 2014), OEX of *Aox1a* did not lead to increased CO_2 assimilation above wildtype, but due to numerous problems, my confidence in measurements under MLD conditions are low. The majority of plant lines (excluding wildtype, XX1, 20.1 and 084) did not reach CO_2 assimilation rates above 0 whereas both Dahal and Vanlerberghe (2017) and Dahal et al. (2014) demonstrated positive assimilation rates in both OEX and RNAi lines under MLD. Furthermore, the maximum assimilation rates for wildtype were no more than 0.5, whereas in the hands of Dahal et al. (2014), wildtype was closer to 5 μmol CO_2 m^{-2} s^{-1}. Assimilation rates above 120 PAR were mostly seen to plateau with rates below 120 PAR showing large variation. It is likely that in these experiments, the plants had been affected too badly by drought, resulting in plants so severely affected that it was difficult to achieve consistent CO_2 assimilation rates. These experiments need to be repeated earlier in the stress timeline. Regardless, it appears that the CO_2 assimilation rate under control conditions is not a reliable indicator of MLD resilience, at least in these transgenic *Arabidopsis* lines.

Mitochondrial respiration in the light (day respiration) was deduced from CO_2 assimilation rates using the method outlined by Kok (1948) and Sharp et al. (1984). Very similar to the results found by Dahal et al. (2014) and Dahal and Vanlerberghe (2017), respiration of the *Aox1a* OEX and T-DNA lines did not differ from wildtype under control conditions and showed similar rates between experiments. However, it is interesting to note that both T-DNA lines tested as well as the dual OEX lines all

trended towards a higher rate of respiration. This was more prevalent in the single *Ndb2* OEX lines where majority of the lines tested showed significant increases in day respiration. Activity measurements of the *Ndb2* OEX lines have demonstrated that NDB2 is not active unless there was a concomitant expression of AOX1a (Sweetman et al. 2019). This appears to conflict with respiration measurements, indicating that the activity of NDB2 in the single *Ndb2* OEX lines is engaged *in vivo* but not in isolated mitochondria. However, when compared to respiration measurements monitored in the dark, there were few differences between lines, highlighting the importance of light in combination with *Ndb2* OEX in changing respiration. Also noteworthy is the finding that day respiration trended faster in the dual OEX lines although this was not statistically significant. This may suggest that the effects caused by *Ndb2* on respiration are limited by expression of *Aox1a.* In future experiments it would be of value to measure the contribution of photorespiration to total respiration using a limited O_2 environment in conjunction with the LICOR6400-XT gas exchange analyser. This could help identify whether the increase in *Ndb2* OEX is a result of increased photorespiration (Sharkey 1988).

Transpiration was monitored over several different light intensities and showed significant differences between transgenics and wildtype. These differences were also consistent across lines, with *Ndb2* and dual OEX lines grouping together but separated based on lines. Under control conditions, plants more resilient to MLD stress tended to show reduced transpiration while those less resistant were much higher than wildtype. Under MLD conditions this effect was somewhat reversed.

Single *Ndb2* OEX lines and the *aox1a* T-DNA had the lowest transpiration while the dual OEX lines and *Aox1a* OEX were much higher albeit lower than the wildtype line. In contrast, Dahal and Vanlerberghe (2017) reported that transpiration in transgenic tobacco was generally reversed, whereby the single *Aox1a* OEX lines had higher transpiration rates under control. Only when drought was applied, did the single OEX lines produce similar rates to wildtype. In my experiments, under MLD conditions, lines measured on the same day tended to group with each other. Due to the sampling methodology used, only two plant lines could be measured per day. Despite trying to ensure that plants were grown under the same conditions for the same periods of time, there does appear to be a systemic effect specific to the time of sowing. In future experiments it would be advisable to make all plant lines available on the same day, to prevent different growth conditions affecting the results. Further to this, taking measurements earlier in the drought period with larger plants may increase the values seen and minimise errors caused by difficulty in gauging small rates.

Anthocyanins are consistently up-regulated in response to drought and light stress (Efeoğlu et al. 2009; Sperdouli & Moustakas 2012) and are useful in mitigating oxidative and drought stress within the cell (Steyn et al. 2002; Nakabayashi et al. 2014). As such, anthocyanins were monitored over several days to determine whether the increased resilience seen in the transgenics is correlated with an increase in anthocyanins. Under control conditions, the basal levels between lines did not differ. However, anthocyanin content in XX1 line was significantly increased across a number of time points while that in the 330 line was significantly less. Although the

reduced anthocyanin content could explain the reduced resilience of the *ndb2* T-DNA line it does not appear that the increase correlates with increased resilience. Dual OEX lines maintain similar levels of anthocyanins as wildtype and lower than XX1 despite being more resilient than both those lines. It seems that *Arabidopsis* requires an appropriate amount of anthocyanin for an adequate response to MLD but further increasing that beyond required, provides no additional benefit to MLD resilience and may even reduce fitness.

A number of studies have highlighted the importance of AOX in regulating the accumulation of ROS (Purvis 1997; Maxwell et al. 1999; Sweetlove et al. 2002) including situations of drought and excess light (Wang & Vanlerberghe 2013). Typically, an increase in ROS results in an increase in oxidative damage markers MDA and protein carbonyl groups as highlighted by Watanabe et al. (2008); Wang and Vanlerberghe (2013); Dahal et al. (2014); Dahal and Vanlerberghe (2017). Evidence for the effects of suppression or OEX of *Aox* is conflicting. Suppression has been shown to increase, decrease or have no effect on oxidative damage, while OEX apparently had no effect on oxidative damage (Watanabe et al. 2008; Wang & Vanlerberghe 2013; Dahal et al. 2014; Dahal & Vanlerberghe 2017). However, accumulation of MDA in *Arabidopsis*, in the presence of cyanide, is clearly mitigated by OEX or exacerbated by suppression of *Aox1a* (Umbach et al. 2005). Monitoring TBARS under both control and MLD over several days highlighted two important effects: under control conditions, basal levels of TBARS were significantly higher in wildtype than any of the transgenics tested. Secondly, TBARS measurements are not suitable for stressors that are applied

over several days in Arabidopsis, because of interference by anthocyanin accumulation. Although the methodology used makes an attempt to subtract interference away from the true value (Hodges et al. 1999), high levels of anthocyanins results in high variation and negative values. Thus, this method is not suitable where there are high ratios of interfering compounds relative to TBARS, a point made by Hodges et al. (1999). This method seems most appropriate to short term stressors that don't result in accumulation of anthocyanins.

The work presented in this chapter has highlighted phenotypes specific to the individual OEX of *Aox1a* or *Ndb2,* which results in delays in reaching growth milestones related to rosette and bolting or flowering. These delays ultimately do not affect biomass or water content further into development, but interestingly, the delayed phenotype is rescued by concomitant expression of *Ndb2 and Aox1a.* Most importantly, in this chapter it is demonstrated that the concomitant OEX of *Aox1a* and *Ndb2* further increased the stress tolerance of *A.thaliana* lines exposed to MLD above that of XX1 and wildtype. Gas exchange analysis revealed a reduced capacity to assimilate CO_2 at saturating irradiance in the dual OEX lines, possibly a result of stomatal aperture closure as the transpiration rates were also less in these lines. This may partially explain how the dual OEX lines are more resilient to the combined MLD stress. Unexpectedly, the single *Ndb2* OEX lines had increased respiration in the light despite measurements with isolated mitochondria showing minimal engagement of NDB2. The lack of difference seen in respiration measured in the dark suggests the importance of light in engaging NDB2. The concomitant expression of *Aox1a* also

reduced respiration in the light compared to the *Ndb2* OEX lines. However, it must be pointed out that the relative contribution of the AP to respiration in these plants *in vivo*, has not be determined and it is not possible to say whether the differences in whole plant respiration rates were a result of changes in AP or cytochrome path activity.

Unfortunately, neither measurements of TBARS or anthocyanins yielded any conclusive correlations to MLD tolerance. As such, there is a focus on transcriptomics in the next chapter with the aim to identify key genes contributing to the improved MLD resilience in dual OEX lines.

Chapter 5

A transcriptomic analysis of *Arabidopsis* plants with altered respiratory properties

5 A transcriptomic analysis of *Arabidopsis* plants with altered respiratory properties

5.1 The transcriptional networks in plant mitochondria

In *A thaliana*, the *Aox* family consists of five isoforms, each expressed differently according to location, life cycle and external stimuli (Clifton et al. 2006a). Similarly, the seven type II NAD(P)H dehydrogenase isoforms present in *A.thaliana*, are localised to different organs and organelles (Carrie et al. 2008) and respond to stimuli differently (Michalecka et al. 2003; Escobar et al. 2004). With each enzyme's unique position, differing substrate, activation cofactor, and expression timing, a complex transcriptional regulatory network coupled with numerous signalling molecules is required to regulate the AP (Elhafez et al. 2006; Selinski et al. 2018).

Signalling can come from multiple organelles in many forms and the ability to detect the origin of the signals and apply an appropriate response is crucial. A dysregulated pathway can utilise its own impairment to signal for action. An example of this is ROS in the mitochondria. Dysregulated concentrations of ROS can lead to cellular damage of proteins, lipids and DNA but can also signal the cell to counteract the oxidative damage. The most common ROS are singlet oxygen, hydrogen peroxide and the hydroxyl radical. However, as explained by Møller and Sweetlove (2010), it is unlikely that either the singlet oxygen or hydroxyl radical can travel far enough to carry the signal outside the organelle. Hydrogen peroxide in comparison is relatively stable, and able to pass membranes through aquaporins (Bienert et al. 2007). Due to

its simplistic structure and inability to store information, any hydrogen peroxide produced will be identical regardless of its origins. Lacking the ability to detect the source of ROS molecules, nuclear encoded genes cannot be selectively regulated with only ROS. A study by Ng et al. (2013b) has shown, partly, a mechanism that could be responsible for selective induction in localised organelles based on ROS signalling. ROS activated proteolytic activation of an endoplasmic reticulum (ER) bound transcription factor (ANAC017) which induces *Aox1a* expression in mitochondria, and ANAC017 was located at points where the ER intersected with the mitochondrial outer membrane. More recently Meng et al. (2019) demonstrated that the OEX of this transcription factor resulted in plants that were severely stunted and aligned more with a plant senescing. Meng et al. (2019) noted this and suggested ANAC017 upregulation of many genes was suggestive of a master regulator type role. A twin cysteine protein partially characterised by Wang et al. (2016) At12Cys-2 (At5g09570) is an example of how AOX1a could export a signalling molecule with the origin of stress embedded in the protein itself.

5.1.1 A transcriptomic approach to understanding the AP

All AP members have been identified as stress responsive to at least one stressor/treatment (Clifton et al. 2005; Elhafez et al. 2006; Feng et al. 2013). Some of these appear to be co-regulated together as well, particularly *Aox1a* and *Ndb2* in *Arabidopsis* (Clifton et al. 2005; Ho et al. 2008). Ho et al. (2008) identified 6 overlapping cis-acting regulatory elements (CAREs) in the upstream regions of *AtAox1a* and

AtNdb2 responding to stress, indicating the whole pathway was engaged in response to some stressors and not just *Aox1a.* On top of this, Clifton et al. (2006a) in a meta-analysis using Genevestigator, noted a number of interesting details, one of which was that the in lines tested with altered levels of *Aox*, more genes encoding proteins outside of the mitochondria than were altered than those inside. This demonstrates the wide-reaching effects AOX has on plant function, at least in *Arabidopsis*. Clearly, a global approach to determine the effects of altered AP proteins, as in the transgenics described in this thesis, have on the transcriptome needs to be considered.

Our previous measurements of our newly generated transgenics had highlighted differences in their ability to recover from a combined MLD stress. Measurements of phenotype and biochemistry failed to identify traits that were clearly beneficial to the plant's resilience. As such, a more comprehensive approach was required. RNA-seq allows for quick comparisons of relative transcript amounts of thousands of unique transcripts all at once. In combination with a series of software tools, genes can be categorised according to biological process, molecular function and cellular compartment. These were used in conjunction with mapping software to help visualise and understand the complex transcript profiles.

5.2 Aims

The aim of the experiments described in this chapter was to identify potential stress resilience transcripts present in the more tolerant overexpressing lines to help elucidate the positive effects the AP has on MLD resilience. It was hypothesised that

increasing the expression of *Aox1a* and *Ndb2* would induce expression of stress-responsive genes leading to a pre-stress/priming response that would adapt the plant to the stress prior to it occurring.

5.3 Results

5.3.1 qRT-PCR of Arabidopsis plants under a novel drought and light stress system

A new technique for simulating repeatable drought stress studies without the use of hydroponics and mannitol was adapted from Wang and Vanlerberghe (2013) by Sweetman et al. (2019). Using this system, plants were prevented access to water for 6 days and then exposed to ~300 $\mu mol\, m^{-2}\, s^{-1}$ light and a further 7 days of drought. This level of light exposure is similar to previously published methods. (Giraud et al. 2008). Plants were harvested everyday over the next six days and stored at -80°C. To determine when *Aox1a* was being upregulated in response to drought and light stress, qRT-PCR was performed at all timepoints, beginning at the start of MLD. It was expected this would be useful in determining changes coinciding with the *Aox1a* upregulation.

Aox1a transcripts under control conditions in wildtype and *ndb2* T-DNA were unaltered (Figure 5.1A). Only at day six of MLD was there a significant increase in expression in wildtype (5.73-fold). The initial upregulation, however, occurred on day five of MLD in wildtype with a 1.68-fold increase. Interestingly, the *ndb2* T-DNA line saw a slightly higher and earlier increase in expression compared to wildtype. The single *Aox1a* OEX and the dual *Aox1a* and *Ndb2* OEX produced significantly higher basal *Aox1a* expression than the wildtype and *ndb2* T-DNA line but did not see any significant increases when compared to their control. counterparts. Day two and five

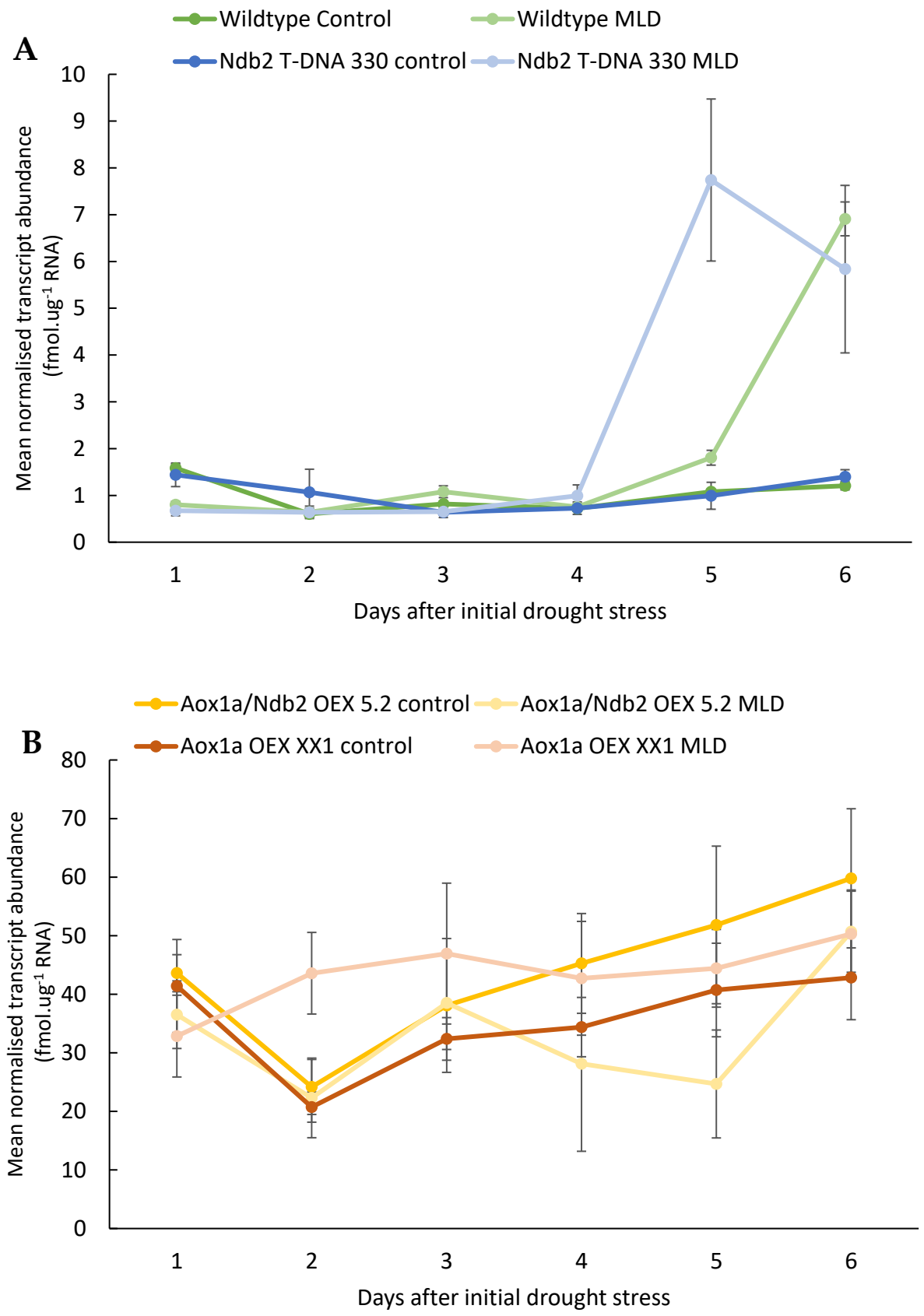
A
Wildtype Control
Wildtype MLD
Ndb2 T-DNA 330 control
Ndb2 T-DNA 330 MLD
Mean normalised transcript abundance (fmol.ug-1 RNA)
0
1
2
3
4
5
6
7
8
9
10
1
2
3
4
5
6
Days after initial drought stress
B
Aox1a/Ndb2 OEX 5.2 control
Aox1a/Ndb2 OEX 5.2 MLD
Aox1a OEX XX1 control
Aox1a OEX XX1 MLD
Mean normalised transcript abundance (fmol.ug-1 RNA)
0
10
20
30
40
50
60
70
80
1
2
3
4
5
6
Days after initial drought stress

Figure 5.1 Changes in mean normalised transcript abundance of *AtAox1a* in shoots under control and MLD conditions over six days

Transcript abundance was measured through QRT-PCR and normalised against *AtUbq* and *AtPDF2*. Wildtype and *ndb2* T-DNA (A) values are plotted separately from XX1 and 5.2 (B) due to large differences in transcript abundance. Values are mean +/- S.E N=3. Day 1 control, XX1 and 5.2 <0.001; Day 2 control, XX1 and 5.2 <0.001; Day 3 control, XX1 <0.001, 5.2 <0.01; Day 4 control, XX1 and 5.2 <0.001; Day 5 control, XX1 <0.001, 5.2 <0.01; Day 6 control, XX1 and 5.2 <0.001; Day 1 MLD, 5.2 <0.001, XX1 <0.01; Day 2 MLD, XX1 and 5.2 <0.001; Day 3 MLD, XX1 and 5.2 <0.01, 330 <0.05; Day 4 MLD, XX1 <0.01, 5.2 <0.05; Day 5 MLD, XX1 <0.001, 330 <0.01; 5.2 <0.05; Day 6 MLD, 5.2 <0.001 determined via unpaired, two-tailed t-test against wild type

were selected for RNA-seq analysis from both control and MLD conditions with the assumption that these time points in wildtype capture a 'prior' and 'current' *Aox1a* upregulation scenario.

5.3.2 Pre-processing analysis of control RNA-seq data

RNA SEQ was performed on several different comparator groups, (all performed in triplicate). Both the dual OEX and single *Aox1a* OEX lines were chosen for RNA seq as their response in previous experiments (Sweetman et al. 2019) showed increases in recovery ability over that of the wildtype. Variance highlighted in the PCA plots shows that the treatment and time of sampling were the biggest factors in determining the clustering of samples (Figure 5.2). The day 2 control and day 5 MLD samples had very tightly clustered groups that showed no difference between genotypes. There was no visible difference in clustering based on genotype under any groupings, but larger variation between replicates was seen in day 5 control and day 2 MLD samples. The clustering of samples appears to form only in response to the growth condition and the time of sampling. The close clustering of the replicates suggests that the response to time and condition were consistent among the three genotypes.

5.3.3 Filtering and analysis of RNA seq data within lines and across conditions

Prior to analysis of the RNA seq data, a significant proportion of the data was filtered out due to a) having low read counts in at least one sample group and therefore low confidence, b) an insignificant change in expression (this was arbitrarily

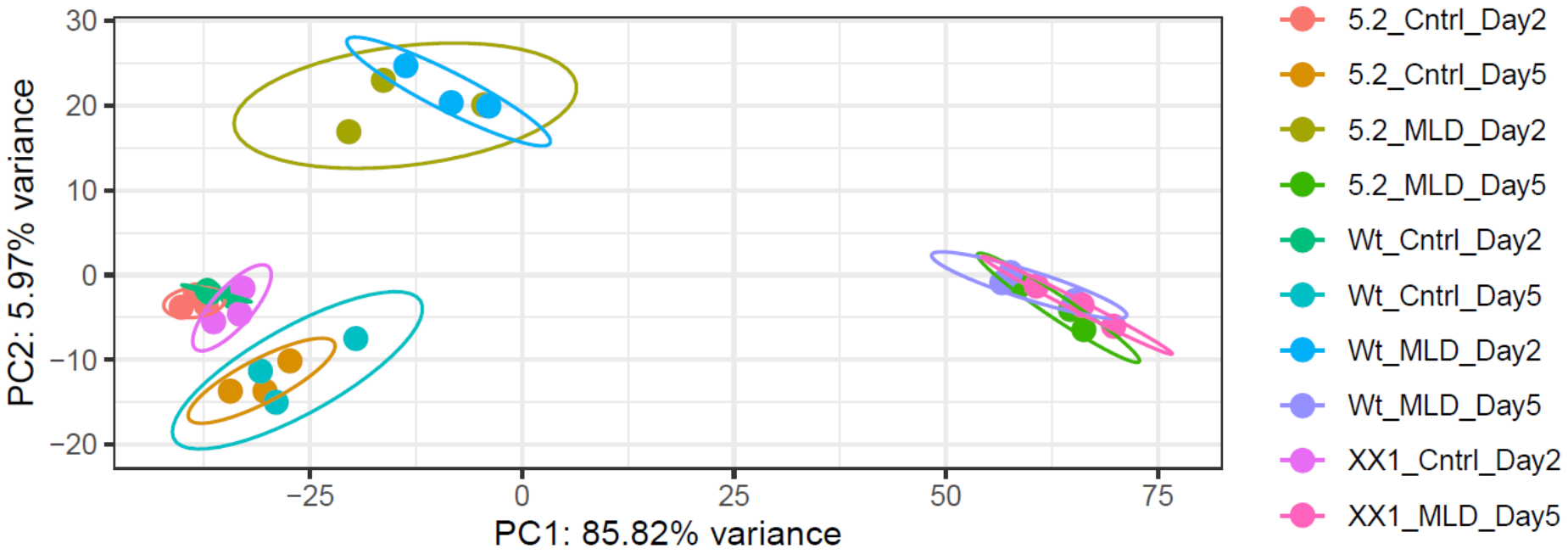

Figure 5.2 RNA-seq PCA outlining the variation between treatment groups, day sampled and wildtype, XX1 and 5.2

set as <1 or >-1 log_2 fold change) or c) where genes were filtered based on a p-adjusted value of <0.01. The greatest number of genes with altered expression were seen in comparisons between control and MLD samples between lines with expression being significantly altered in 3738, 4195 and 5482 transcripts in wildtype, dual and single OEX respectively. Upon interrogating the volcano plots it is clear that there are many more genes that have greater fold-changes with high significance in the OEX lines (Figure 5.3). These differences persist even when comparing between the OEX lines, with the single OEX line showing far more gene expression changes with greater significance. The distribution of up and downregulated regulated genes appears very similar within lines.

Many of the expression changes resulting from MLD seen across the lines were not unique, with 2752 changes being shared between all three lines and another 1163 duplicated across any two comparisons (Figure 5.4). Unsurprisingly the single *Aox1a* OEX had the greatest number of unique gene changes as this had substantially more genes that were significantly altered in total. The single and dual OEX lines shared markedly more expression changes compared to wildtype comparisons while the comparisons of wildtype to the transgenic lines displayed relatively similar number of shared genes.

The alternative respiratory pathway profiles of each lines exhibited overlap of some genes, although with some interesting differences. As expected, the wildtype

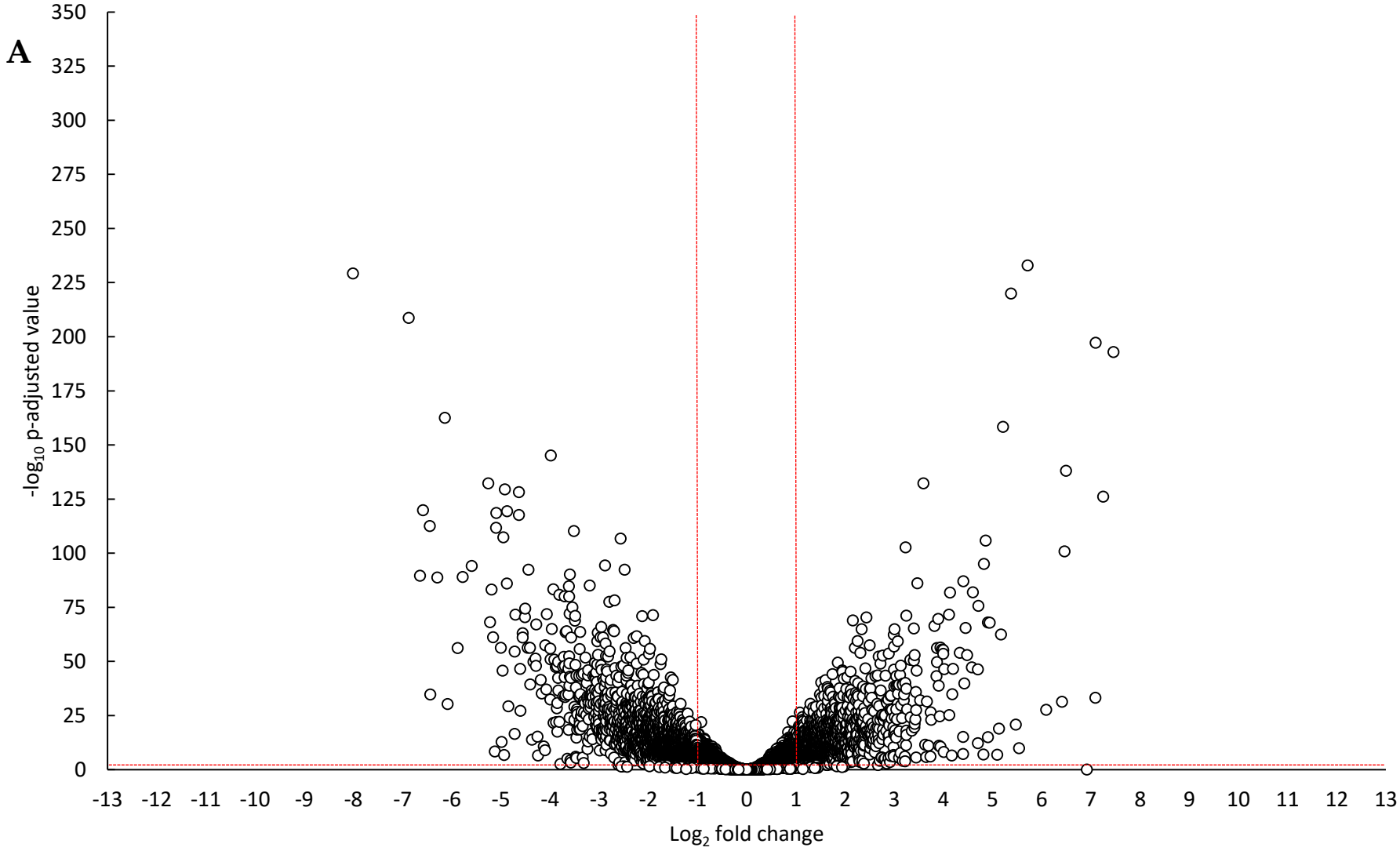
A
350
325
300
275
250
225
200
175
150
125
100
75
50
25
0
-log10 p-adjusted value
-13 -12 -11 -10 -9 -8 -7 -6 -5 -4 -3 -2 -1 0 1 2 3 4 5 6 7 8 9 10 11 12 13
Log2 fold change

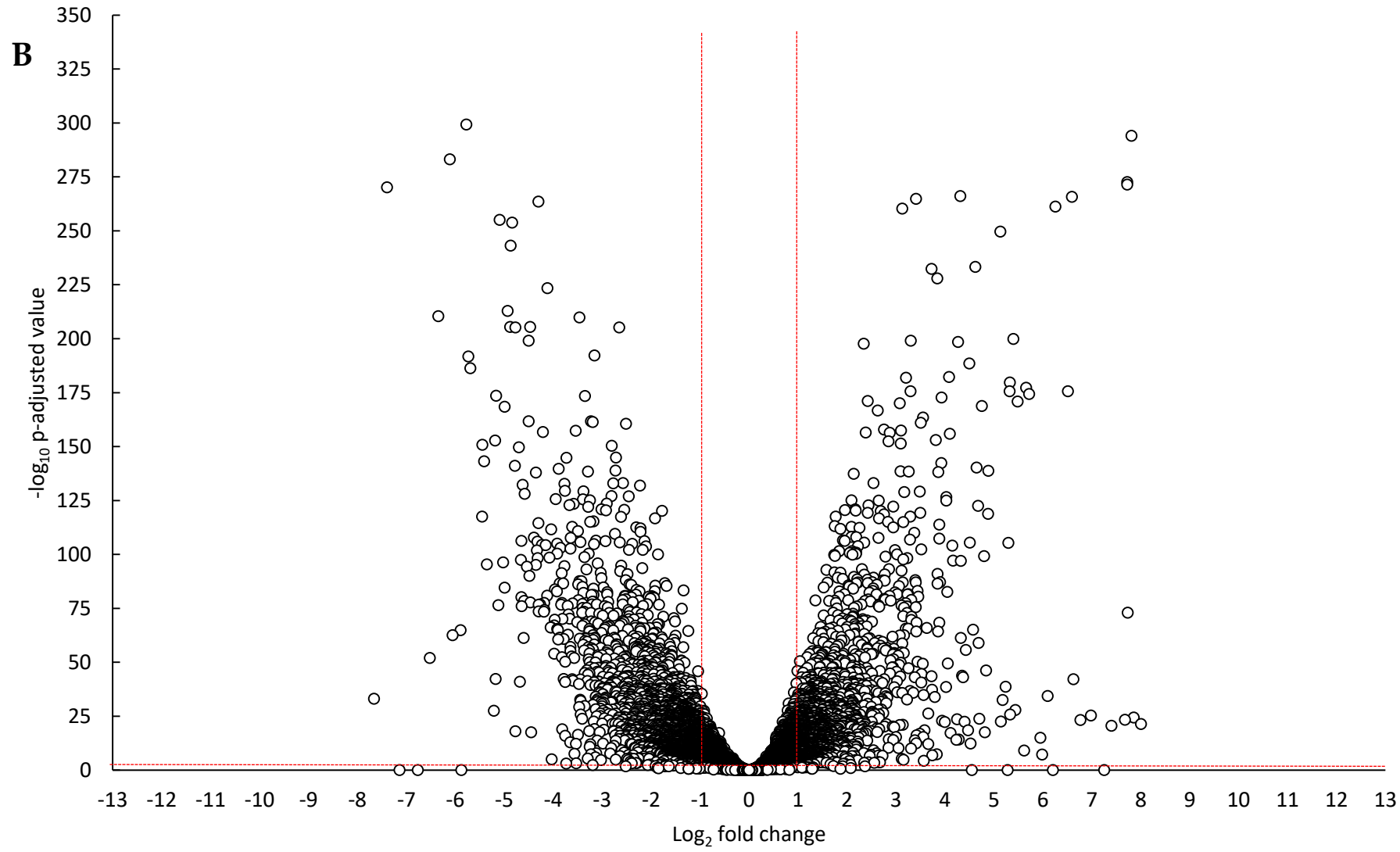
B
350
325
300
275
250
225
200
175
150
125
100
75
50
25
0
-log10 p-adjusted value
-13 -12 -11 -10 -9 -8 -7 -6 -5 -4 -3 -2 -1 0 1 2 3 4 5 6 7 8 9 10 11 12 13
Log2 fold change

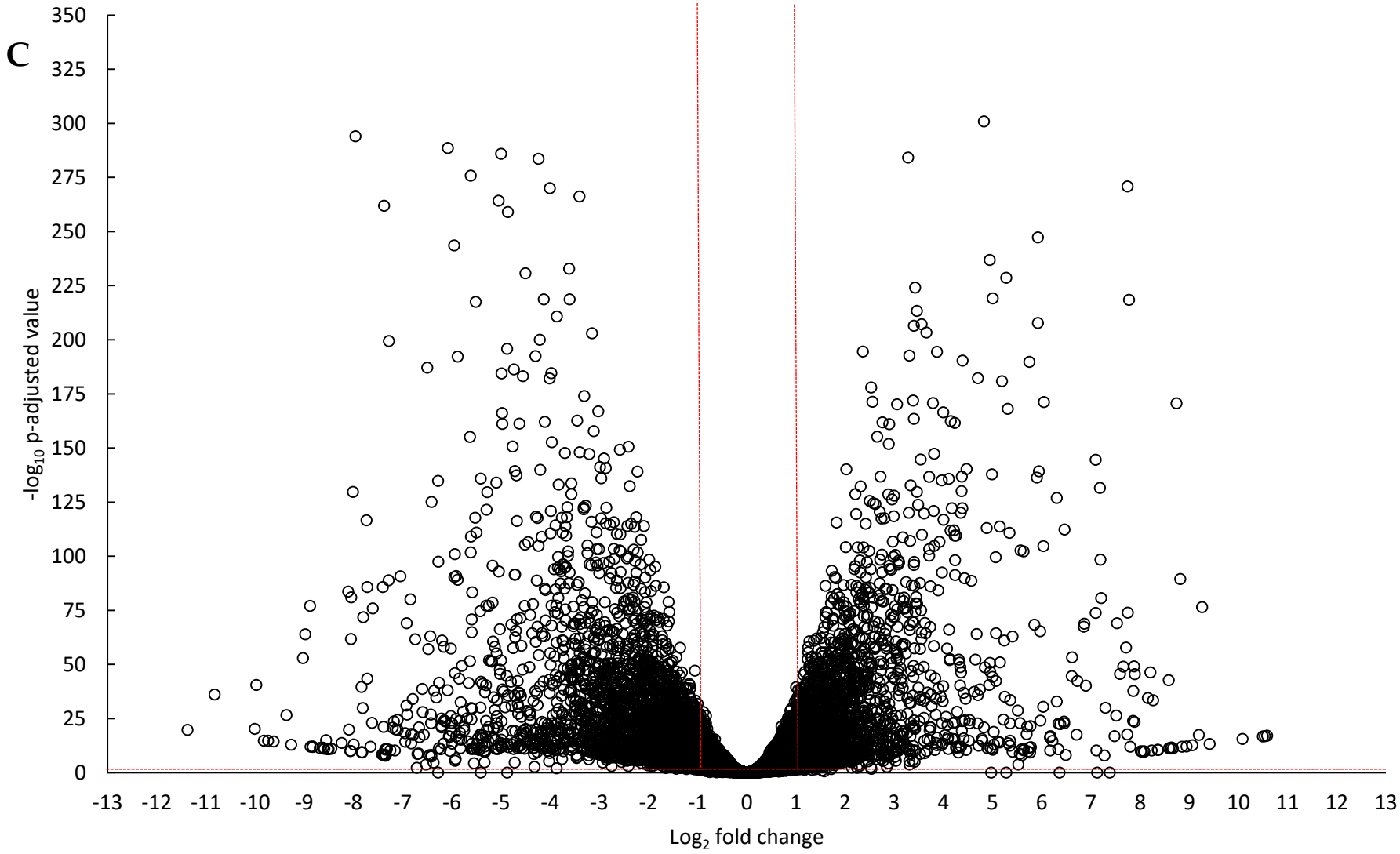
C
350
325
300
275
250
225
200
175
150
125
100
75
50
25
0
-log10 p-adjusted value
-13 -12 -11 -10 -9 -8 -7 -6 -5 -4 -3 -2 -1 0 1 2 3 4 5 6 7 8 9 10 11 12 13
Log2 fold change

Figure 5.3 Volcano plot distribution of differentially expressed genes in day 5 control comparisons against MLD of (A) wildtype (B) 5.2 and (C) XX1

Genes that had a base mean of <25 were removed from the dataset. A total of 3738, 4195 and 5482 genes were differently expressed in figures A, B and C respectively

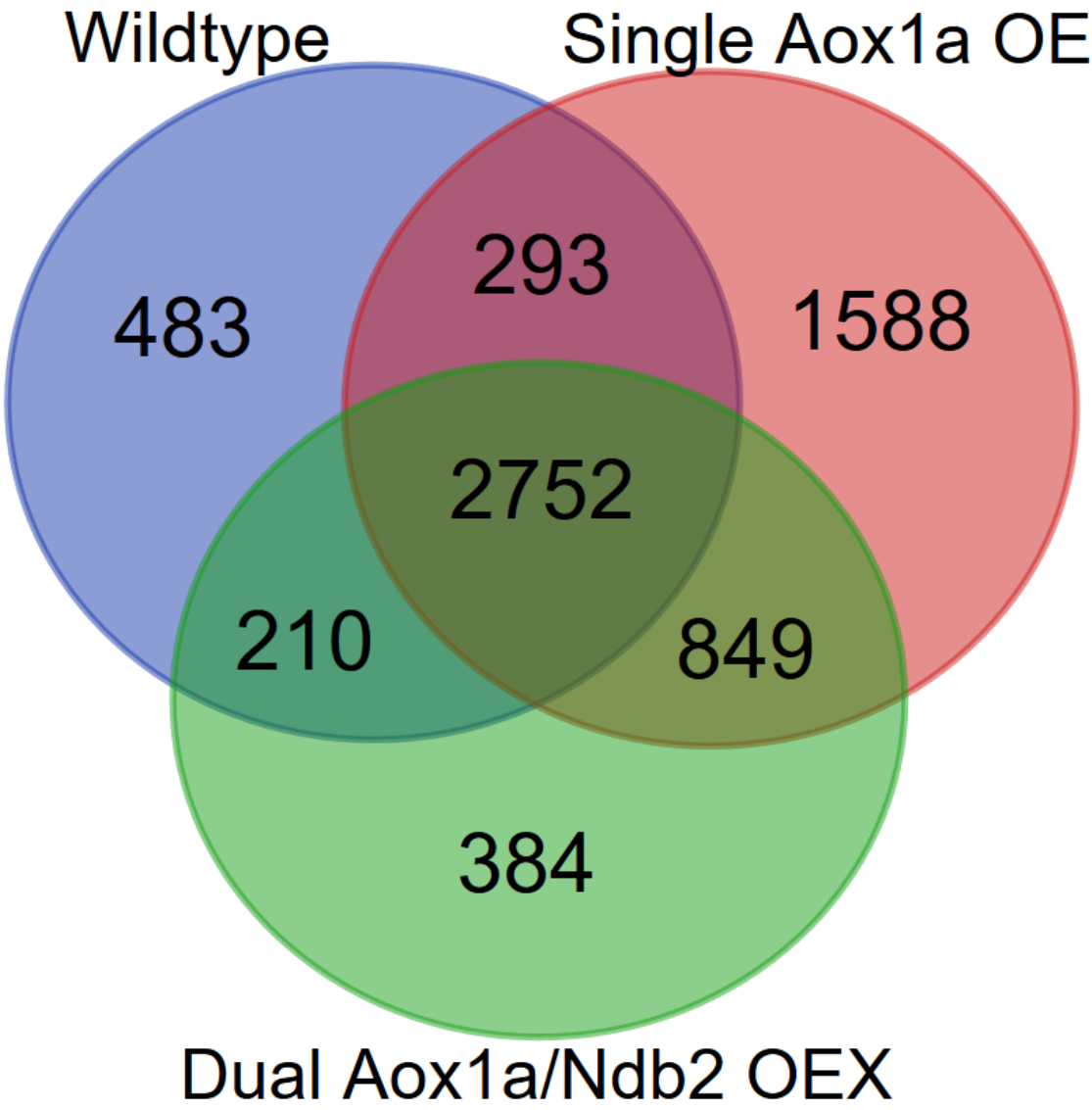

Figure 5.4 Significant unique and overlapping expression changes shared between lines in comparison of day 5 control and day 5 MLD within each line

A total of 3738, 4195 and 5482 genes were differently expressed in wildtype, single *Aox1a* OEX and dual *Aox1a*/*Ndb2* OEX respectively

line showed significant upregulation of *Aox1a* and *Ndb2* genes while also upregulating *Ptox*. *Ptox* and *Ndb2* were also upregulated in the single *Aox1a* OEX (Table 5.1). Although not significant, there was a trend of upregulation of *Ndb2* even in the dual OEX line. The dual OEX was the only line to significantly upregulate *Nda1.* All lines showed upregulation of *Aox1d* (although wildtype wasn't significant), with the dual OEX showing a large increase of over 3 $\log_2$ fold increase. Additionally, all lines showed downregulation of *Ndb1.*

Thirteen of the topmost upregulated genes in the dual OEX and wildtype were shared, with 10 also being shared in the highest downregulated gene list (Table A7.5, A7.6). Four of these upregulated genes were late embryogenesis abundant (*Lea)* transcripts with similar changes in fold changes. Others included sucrose and lipid transporters, ABA responsive and stress-induced/associated transcripts. Although not presented, both lines also share changes in many other isoforms of these genes including the sucrose efflux transporter family (*Sweet),* cytochrome p450 family (*Cyp450)* and pentatricopeptide repeat family (*Ppr)* of genes as well as numerous other gene families. Genes with downregulated expression included a light harvesting complex subunit (*Lhc)*, a number of stress tolerance/sensing and a cell wall protein, among others. However, there weren't any family groupings in the downregulated top 15 gene list. As previously seen, many gene families were also shared in the complete downregulation list These included the ATP binding cassette family (*Abcc*), *Cyp450* family, RAB GTPase family (*Rab)* as well as numerous *Lhc*

Table 5.1 Alternative respiratory pathway expression profile under MLD conditions compared to control conditions on day 5

All data with a * represents significant differences (P-adjusted value <0.01 and log_2 fold change greater than 1 or less than -1)

	Log_2 fold change		
Gene Name	Wildtype	Dual *Aox1a*/*Ndb2* OEX	Single *Aox1a* OEX
Aox1a	**1.157***	-0.283	0.328
Aox1d	1.303	**3.142***	**2.226***
Ptox	**1.068***	0.778	**1.126***
Nda1	-0.0399	**1.134***	0.460
Nda2	0.413	0.170	0.661
Ndb1	**-1.179***	**-1.012***	**-1.095***
Ndb2	**1.530**	0.827	**1.847**

genes and many other gene families. Interestingly, none of highest 15 up or down expression changes in the single OEX showed any overlap with either the wildtype or dual OEX (Table A7.7). Interestingly, this line also contained one *Lea* gene that was not shared with any other line tested. A number of metal-related genes were upregulated as well as an ABA induced gene. Similar to the upregulation list, there were no families of genes that were significantly downregulated in the top 15 list. However, when investigating the complete list of altered expression changes, the single OEX also had major changes to gene families of *Sweet, Cyp450* and *Ppr,* highlighting the shared expression changes to MLD albeit with different levels of regulation. This was also replicated in the downregulation list with *Abcc, Cyp450, Rab* and *Lhc* gene families being significantly downregulated.

Despite the majority of expression changes being shared between lines, a number of distinct gene family groupings were identified in some of the lines. Although *Ppr* expression changes were seen across all lines, larger groupings were distinct within these families. There were 21 unique *Ppr* transcripts found in wildtype and another 19 found in the single OEX, while only one other was found in the dual OEX, all with significant upregulation. The single OEX line also had eight different heat shock proteins (*Hsp)* and another 11 UDP-glucosyl transferase (*Ugt*) also significantly upregulated. The dual OEX line had 11 different ribosomal plastid transcripts significantly downregulated while wildtype had no changes and the single OEX had only one of these transcripts. Again, the single OEX had greater changes

with four large gene family groups being altered, including eight RING/U-box, 11 cyclin, 9 *Cyp450* and eight small auxin downregulated transcripts. The wildtype line had no large unique family groupings downregulated.

5.3.4 Filtering and analysis of RNA seq control data across lines

From over 33,000 genes detected, gene lists were whittled down to less than a 1,000 on the basis of fold changes (Figure 5.5). Analysis of the difference in comparisons made between XX1 and 5.2 to wildtype showed, a clear shift in the number of significant genes with altered expression is apparent in XX1. Additionally, there is an increased trend towards higher significance in XX1. When comparing XX1 to 5.2, there is a clear change in the distribution of genes with altered expression. XX1 has far more genes with increased abundance over that of 5.2. This highlights a clear change in transcriptional profile when *Ndb2* is overexpressed together with *Aox1a.*

Initially, the first set of genes considered in the control comparisons was the AP members (Table 5.2). None of the other AP members' expression was significantly altered in response to the transgenic single or dual OEX of *Aox1a* and/or *Ndb2*. It is interesting to note that the *Aox1d* isoform was consistently higher in the XX1 line even compared to 5.2, albeit insignificantly.

The next step was to consider the most altered genes from each comparison (Table A7.8, A7.9, A7.10). Starting with the control groups, 15 of the most altered transcripts were selected from both pools of increased and decreased abundance. An

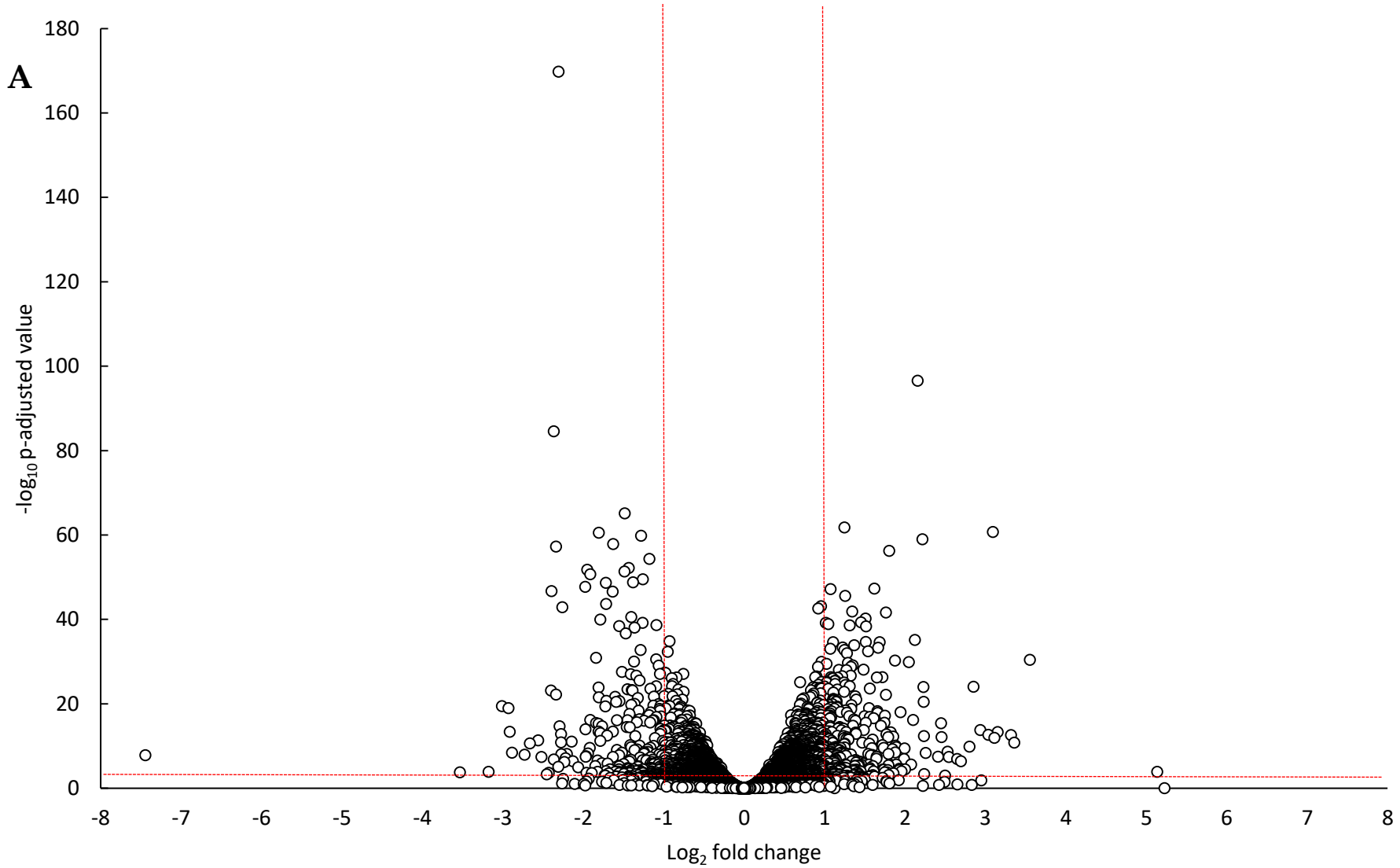
A
180
160
140
120
100
80
60
40
20
0
-log10 p-adjusted value
-8
-7
-6
-5
-4
-3
-2
-1
0
1
2
3
4
5
6
7
8
Log2 fold change

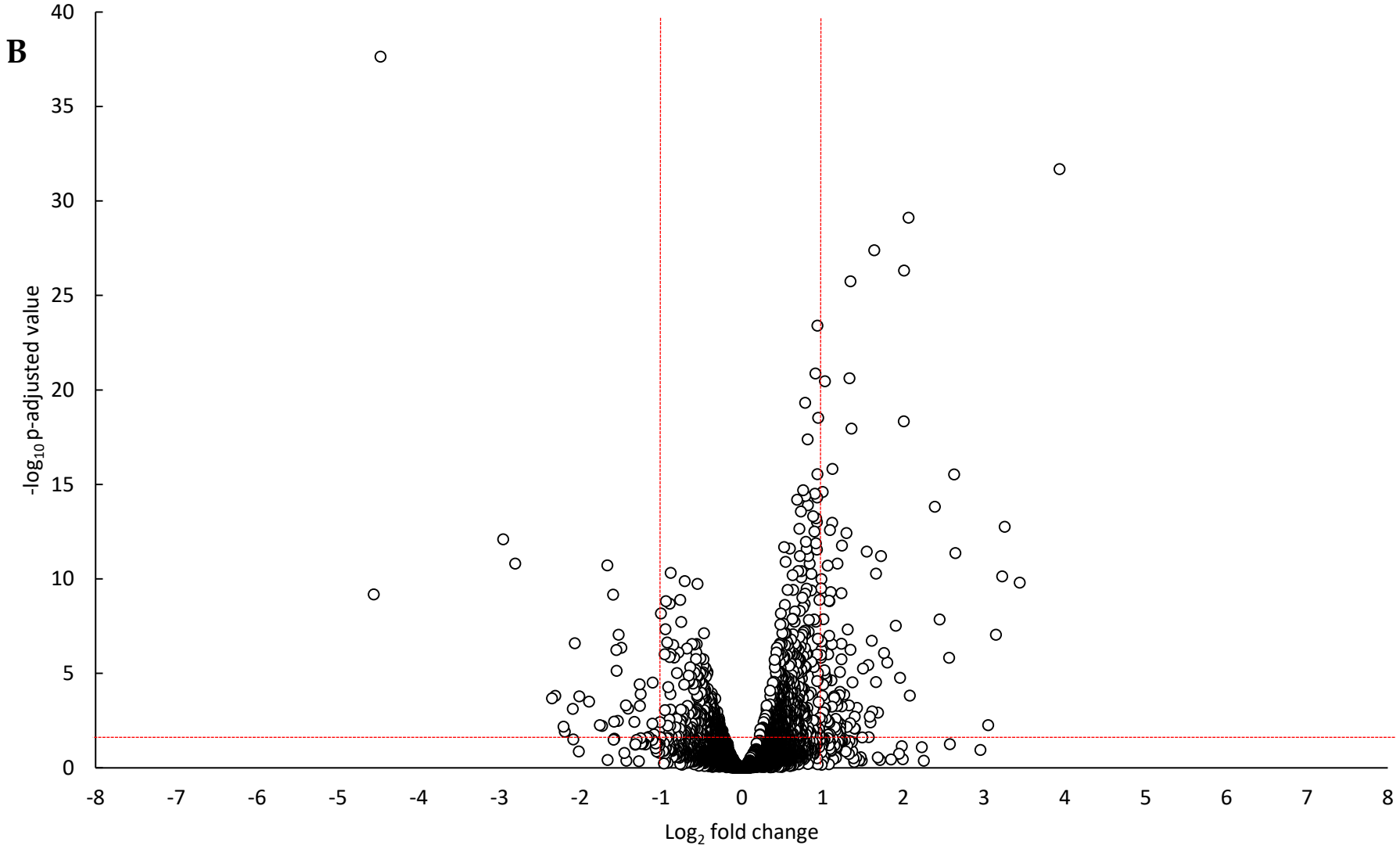
B
40
35
30
25
20
15
10
5
0
-log10 p-adjusted value
-8
-7
-6
-5
-4
-3
-2
-1
0
1
2
3
4
5
6
7
8
Log2 fold change

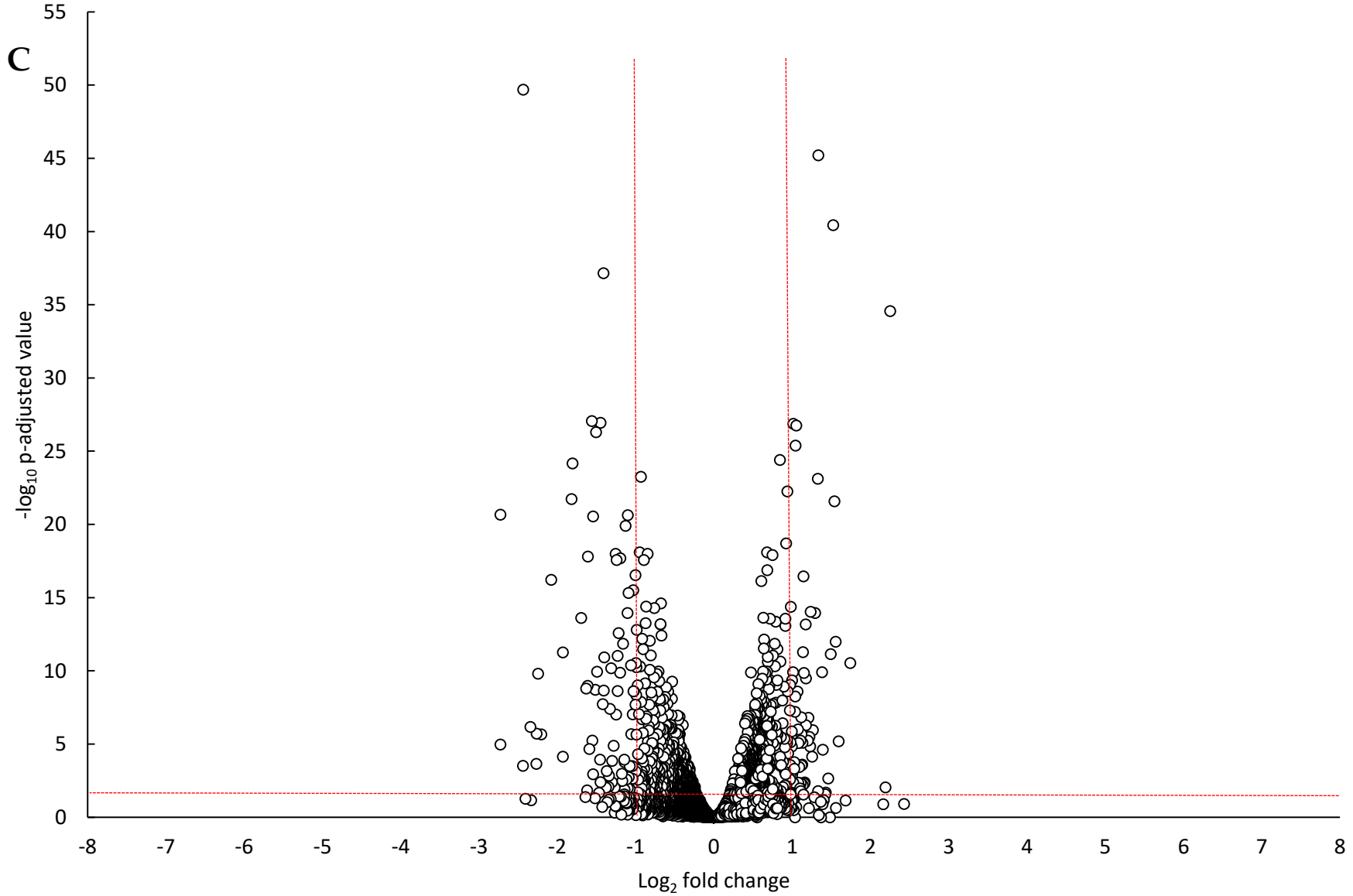
C
55
50
45
40
35
30
25
20
15
10
5
0
-log10 p-adjusted value
-8
-7
-6
-5
-4
-3
-2
-1
0
1
2
3
4
5
6
7
8
Log2 fold change

Figure 5.5 Volcano plot distribution of differentially expressed genes in day 2 control comparisons of (A) wildtype to XX1, (B) XX1 to 5.2 and (C) wildtype to 5.2

Genes that had a base mean of <25 were removed from the dataset. A total of 615, 125 and 142 genes were differently expressed in figures A, B and C respectively

Table 5.2 Alternative respiratory pathway expression profile of transgenics relative to wildtype under control conditions

All data with a * represents significant differences (P-adjusted value <0.01 and log_2 fold change greater than 1 or less than -1)

	Log_2 fold change		
Gene Name	5.2 relative to wildtype	XX1 relative to wildtype	XX1 relative to 5.2
Aox1a	**5.071***	**5.228***	0.135
Aox1d	-0.387	0.992	1.417
Ptox	0.064	0.242	0.176
Nda1	-0.379	-0.611	-0.209
Nda2	-0.196	-0.238	-0.037
Ndb1	0.055	0.089	0.045
Ndb2	**4.491***	0.065	**-4.473***

azelaic acid lipid transfer protein AZI3 was the only upregulated gene present in both XX1 and 5.2 compared to wildtype. In contrast, there were six genes shared between comparisons that were downregulated. Of these, there were glutamine-dependent asparagine synthetase 1 (*Asn1*), myo-inositol oxygenase (*Miox2*), xyloglucan endotransglucosylase/hydrolase (*Xth25*) and several genes with rudimentary characterisation. Although not represented in the topmost altered genes, of the 142 genes that were altered in 5.2 relative to wildtype, 103 of these are also present in the comparison between XX1 and wildtype.

5.3.5 Gene ontology term enrichment analysis of control plants

The filtered differential expression gene (DEG) list was subjected to a number of web tools useful for visualising, analysing and interpreting RNA-seq data, one of these being PantherGO. PantherGO allowed for the classification of genes into categories using the gene ontology system of classification. Gene ontology is comprised of three domains. These are defined into broad categories of cellular component (location at the subcellular structure), molecular function (the fundamental function of the gene product and not the purpose of the function) and biological process (the collection of molecular functions). To aid in interpreting these data, values were graphed according to their fold enrichment as a measure of their overrepresentation in comparison to what is expected under normal conditions in a wildtype plant A significant number of GO enriched terms in the category of biological function were significantly enriched across both XX1 and 5.2 (Figure 5.6).

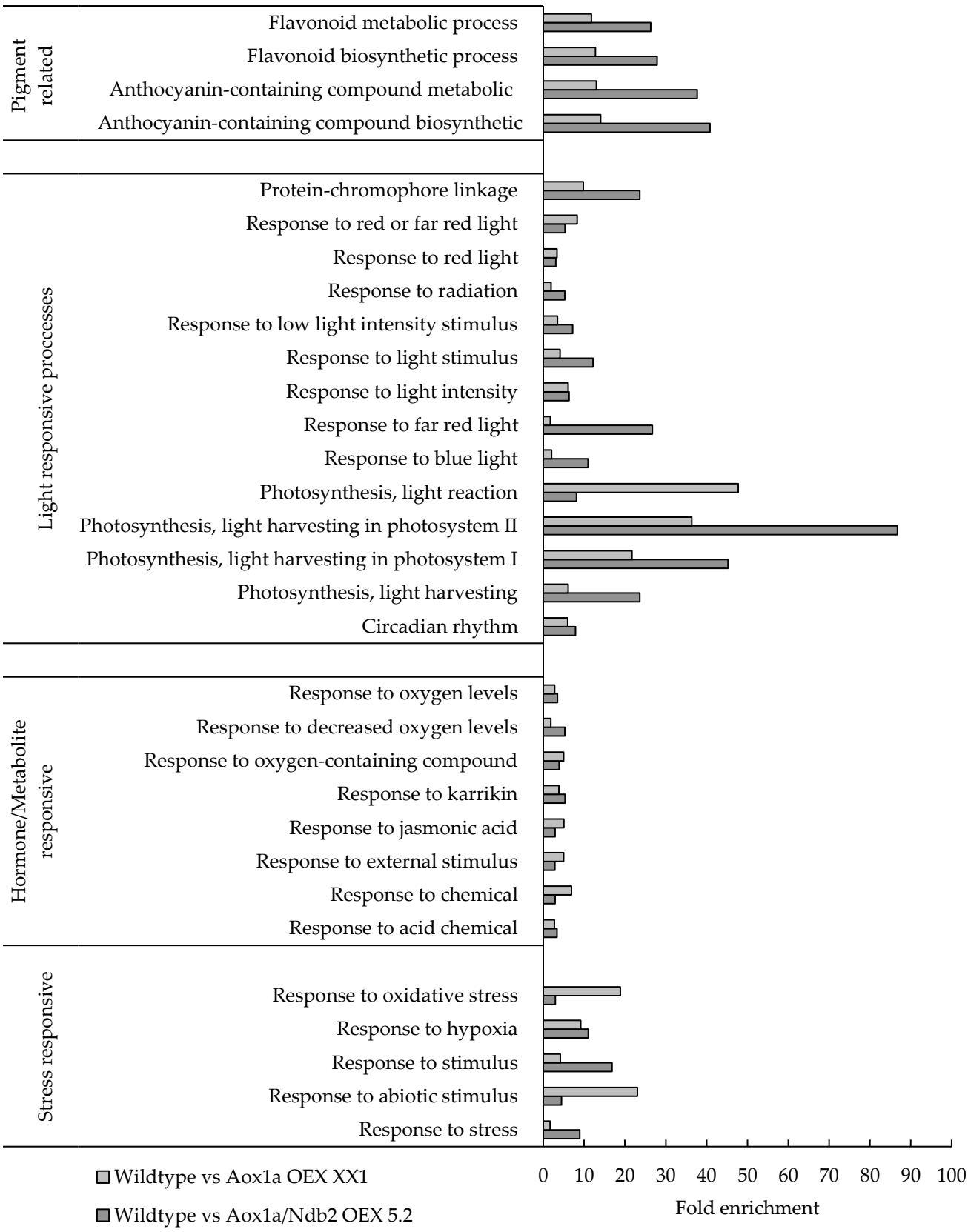

Figure 5.6 GO Term enrichment of biological processes found in the comparisons between wildtype and 5.2 or XX1 under control conditions

These were related to categories of stress responsive, hormone/metabolite responsive, light processes and pigment related. 5.2 is more overrepresented in pigment and light related processes than XX1 but maintains a similar hormonal/metabolic response. Interestingly, the XX1 line shows a greater representation under stress responsive categories of abiotic stimulus and oxidative stress.

5.3.6 KEGG pathway analysis of control plants

KEGG pathway analysis was used as a method to help visualise and categorise changes within the RNA-seq data set. KEGG allows the mapping of individual genes to pathways and aids in highlighting groups of genes related in sequence or function for which expression was altered together. Expression of several photosynthetic genes was altered across both XX1 and 5.2 relative to wildtype (Figure 5.7). Transcripts that were altered across both samples are present only in the PSII light-harvesting complex and all show downregulation. Conversely, only the XX1 line showed downregulation of PSI light harvesting complex subunits (Table 5.3)

Flavonoid biosynthesis was also significantly altered with a multitude of pathways affected (Figure 5.8). A number of shared transcripts were significantly altered (TT5, CHIL, FLS1)(Table 5.4). From the pathway mapping, it seems that these lines had induced expression of flavonoid synthesis, particularly for flavonols, (galangin, kaempferol, quercetin, myricetin) or flavononols (garbanzol, dihydrofisetin) (Figure 5.8) The downregulation of DFR in 5.2 (Table 5.4) could result

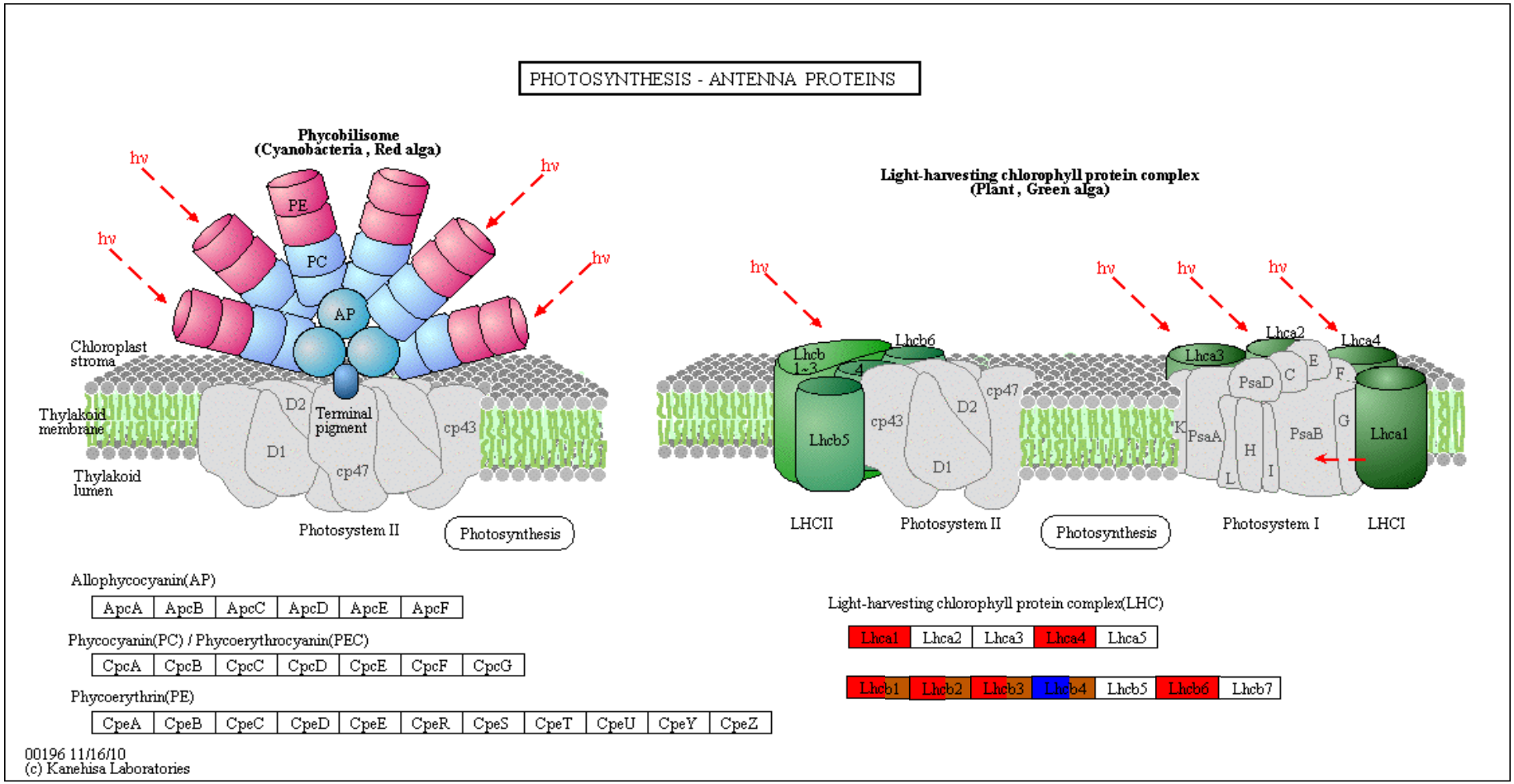

Figure 5.7 Expression changes in the photosynthetic apparatus of XX1 and 5.2 compared to wildtype under control conditions

Expression was mapped using KEGG and colours assigned based on increases or decreases. 5.2 upregulation, green; 5.2 downregulation, brown; XX1 upregulation, blue; XX1 downregulation, red.

Table 5.3 Gene list contributing to the photosynthetic KEGG pathway

N.S. : not significant

Gene I.D.	Gene name	Description	Log_2Fold Change in 5.2 relative to wildtype	Log_2Fold Change in XX1 relative to wildtype
AT2G05070	LHCB2.2	Photosystem II light harvesting complex protein 2.2	-1.346	-1.809
AT2G05100	LHCB2.1	Photosystem II light harvesting complex protein 2.1	-1.366	-1.786
AT2G34420	LHB1B2	Photosystem II light harvesting complex protein B1B2	-1.064	-1.719
AT3G08940	LHCB4.2	Light harvesting complex photosystem II	-1.023	-1.487
AT3G27690	LHCB2.3	Photosystem II light harvesting complex protein 2.3	-1.280	-1.362
AT5G54270	LHCB3	Light-harvesting chlorophyll B-binding protein 3	-1.084	-1.552
AT1G15820	LHCB6	light harvesting complex photosystem II subunit 6	N.S.	-1.046
AT1G29910	CAB3	chlorophyll A/B binding protein 3	N.S.	-1.433
AT1G29920	CAB2	chlorophyll A/B-binding protein 2	N.S.	-1.403
AT2G34430	LHB1B1	light-harvesting chlorophyll-protein complex II subunit B1	N.S.	-1.276
AT2G40100	LHCB4.3	light harvesting complex photosystem II	N.S.	1.053
AT3G47470	LHCA4	light-harvesting chlorophyll-protein complex I subunit A4	N.S.	-1.381
AT3G54890	LHCA1	chlorophyll a-b binding protein 6	N.S.	-1.263

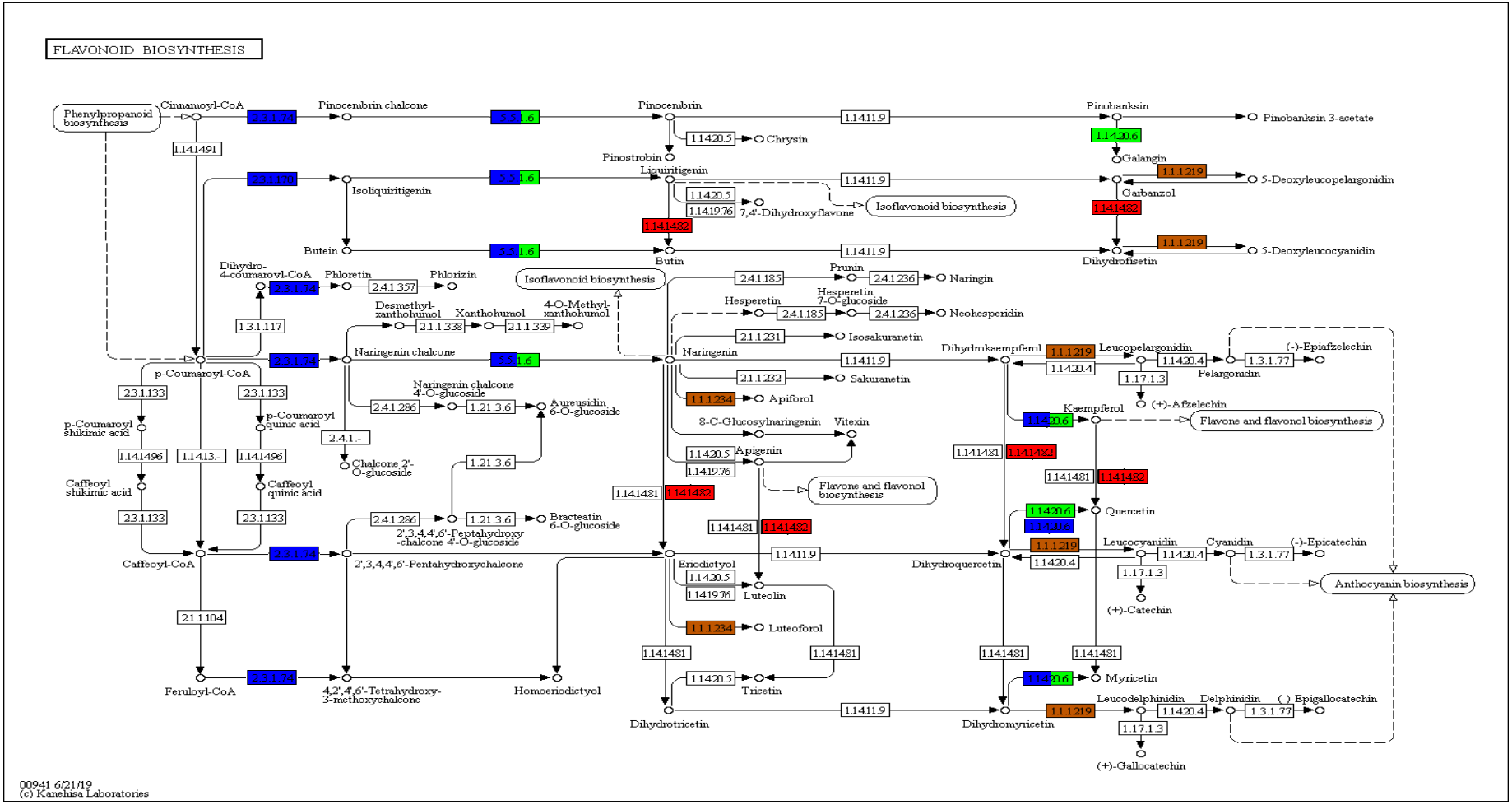

Figure 5.8 KEGG pathway mapping to flavonoid biosynthesis of XX1 and 5.2 compared to wildtype under control conditions

Expression was mapped using KEGG and colours assigned based on increases or decreases. 5.2 upregulation, green; 5.2 downregulation, brown; XX1 upregulation, blue; XX1 downregulation, red

Table 5.4 Gene list contributing to the flavonoid biosynthesis KEGG pathway

N.S. : not significant

Gene I.D.	Gene name	Description	Log_2Fold Change in 5.2 relative to wildtype	Log_2Fold Change in XX1 relative to wildtype
AT3G55120	CHIL	Chalcone-flavanone isomerase family protein	1.132	1.295
AT5G05270	CHIL	Chalcone-flavanone isomerase family protein	1.091	1.562
AT5G08640	FLS1	Flavonol synthase 1	1.633	1.762
AT5G42800	DFR	Dihydroflavonol 4-reductase	-1.929	N.S.
AT5G07990	TT7	Cytochrome P450 superfamily protein	N.S.	-1.156
AT5G13930	CHS	Chalcone and stilbene synthase family protein	N.S.	1.445

in the reduction of six enzyme products that contribute to the production of anthocyanins (pinobanksin-3- acetate, 5-deoxyleucopelargonidin, 5-deoxyleucocyanidin, leucopelargonidin, leucocyanidin, leucodelphinidin) as well as flavanols apiforol and luteoforol.

The phenylpropanoid pathway showed several differing alterations to expression profiles (Figure 5.9). While both XX1 and 5.2 shared similar upregulation to a number of transcripts involved in the formation of several coenzyme A metabolites (cinnamoyl COA, p-coumaroyl-COA, caffeoyl -COA, feruloyl CoA, 5-hydroxy-feruloyl CoA, sinapoyl CoA) there were differences in expression in the downstream pathway. XX1 showed upregulation of transcripts involved in the downstream formation of phenylpropanoid alcohols (coumarine, p-coumaryl alcohol, caffeyl-aldehyde, coniferyl- alcohol, 5-hydroxy-coniferyl alcohol, sinapyl alcohol) while 5.2 did not. The downstream final product of these alcohols is the formation of lignins. In XX1, genes relating to the formation of lignins were downregulated while the opposite was true for 5.2 (Figure 5.9, Table 5.5)

Plant hormone signalling was another pathway that was identified as having multiple transcripts that were altered and shared between lines (Table 5.6). In all cases where expression was significantly altered, both lines shared similar responses. Expression relating to cell growth and enlargement, as well as stomatal closure, were all altered in the same manner. The differences were present only in the zeatin and diterpenoid biosynthesis pathway as well as the phenylalanine metabolism pathway

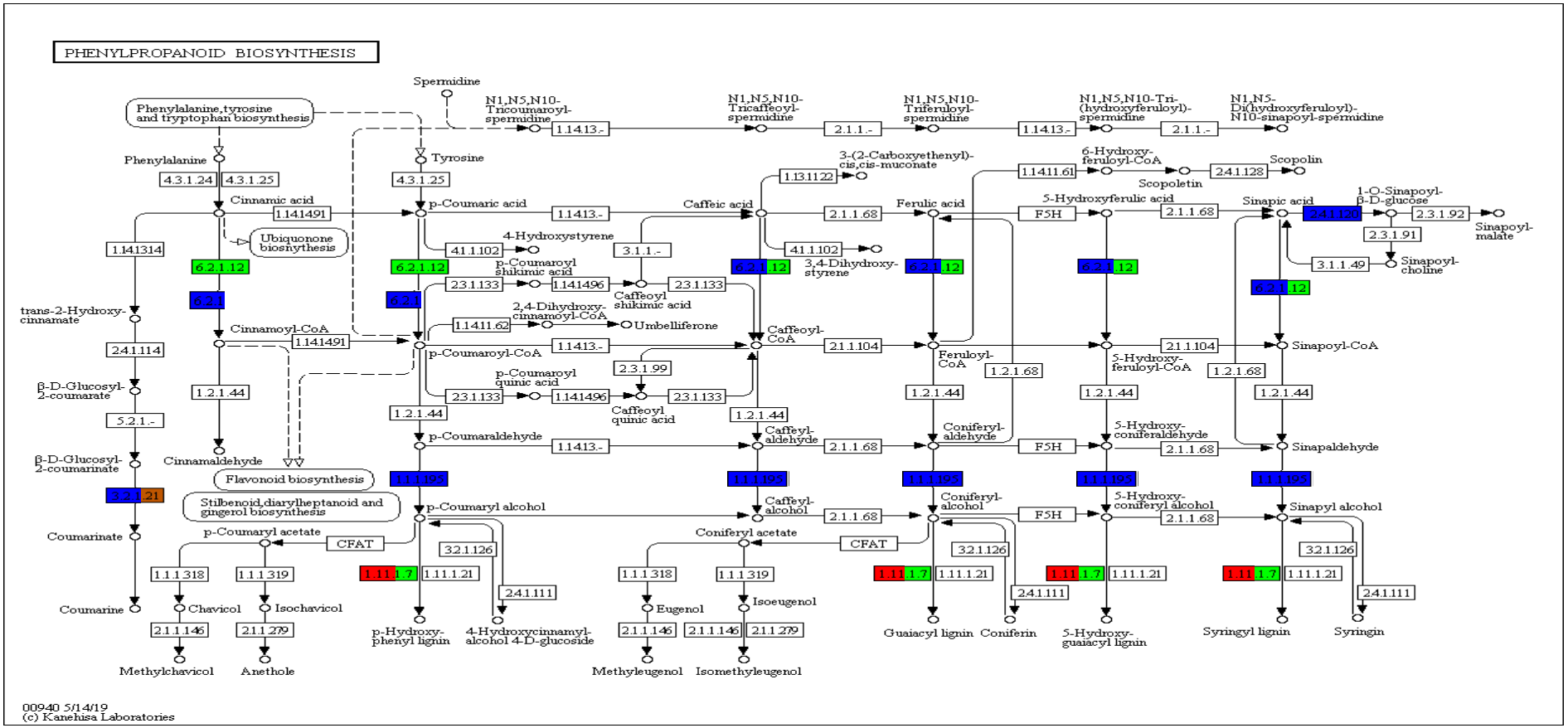

Figure 5.9 KEGG pathway mapping to phenylpropanoid biosynthesis of XX1 and 5.2 compared to wildtype under control conditions

Expression was mapped using KEGG and colours assigned based on increases or decreases. 5.2 upregulation, green; 5.2 downregulation, brown; XX1 upregulation, blue; XX1 downregulation, red

Table 5.5 Gene list contributing to the phenylpropanoid biosynthesis KEGG pathway

N.S. : not significant

Gene I.D.	Gene name	Description	Log_2Fold Change in 5.2 relative to wildtype	Log_2Fold Change in XX1 relative to wildtype
AT1G65060	4CL3	4-Coumarate:CoA ligase 3	1.547	N.S.
AT3G09260	PYK10	Glycosyl hydrolase superfamily protein	-2.266	N.S.
AT5G05340	PRX52	Peroxidase superfamily protein	1.462	N.S.
AT3G19450	ATCAD4	Groes-like zinc-binding alcohol dehydrogenase family protein	N.S.	1.078
AT3G21560	UGT84A2	UDP-Glycosyltransferase superfamily protein	N.S.	1.235
AT3G21770	AT3G21770	Peroxidase superfamily protein	N.S.	-1.092
AT3G60140	DIN2	Glycosyl hydrolase superfamily protein	N.S.	2.239
AT4G37530	AT4G37530	Peroxidase superfamily protein	N.S.	-1.263
AT4G39330	CAD9	Cinnamyl alcohol dehydrogenase 9	N.S.	1.076

Table 5.6 Gene list contributing to the plant hormone signalling KEGG pathway

N.S. : not significant

Gene I.D.	Gene name	Description	Log_2Fold Change in 5.2 relative to wildtype	Log_2Fold Change in XX1 relative to wildtype
AT1G78290	SNRK2-8	Protein kinase superfamily protein	1.532	2.046
AT4G27260	WES1	Auxin-responsive GH3 family protein	-1.447	-1.765
AT4G37390	BRU6	Auxin-responsive GH3 family protein	-1.159	N.S.
AT5G54510	DFL1	Auxin-responsive GH3 family protein	-1.425	-1.460
AT1G07430	HAI2	Highly ABA-induced PP2C protein 2	N.S.	-1.421
AT1G75590	SAUR	Auxin-responsive protein family	N.S.	-1.426
AT1G77920	TGA7	Bzip transcription factor family protein	N.S.	1.269
AT2G01760	RR14	Response regulator 14	N.S.	1.012
AT2G40670	RR16	Response regulator 16	N.S.	1.089
AT3G48100	RR5	Response regulator 5	N.S.	1.496
AT2G43010	PIF4	Phytochrome interacting factor 4	N.S.	-1.485
AT5G17490	RGL3	RGA-like protein 3	N.S.	-1.156

(Figure 5.10). The auxin responsive GH3 protein family was overrepresented in the gene lists with three family members present in 5.2 and four in XX1.

5.3.7 Filtering and analysis of RNA seq MLD data

The MLD dataset derived from the same experiment as the controls had the same filtering criteria imposed. Comparing the distribution of altered transcripts to control samples, there are some minor differences. XX1 relative to wildtype has decreased noticeably in the level of significance and the number of significantly altered transcripts (from 615 genes down to 331) (Figure 5.11A). The same trend was present in the comparison of XX1 to 5.2 but also maintaining a skewed distribution, favouring upregulated genes (Figure 5.11B). Again, the number of significantly altered transcripts was down from 125 to 88. 5.2 relative to wildtype was the only comparison that showed an increase in the number of significant transcripts (from 142 to 374). The distribution of transcripts also appeared very similar to that of the control sample (Figure 5.11C).

As was done previously, all AP members detected were assessed. In all comparisons presented, there were no differences seen between MLD samples and control in terms of AP members expression (Table 5.7). The only notable difference was the detection of *Aox1c* in XX1 but not in 5.2 samples, albeit with no significance. Expression of *Aox1a* and *Ndb2* did, however, drop in both XX1 and 5.2 comparisons to wildtype, indicating the upregulation of both genes in wildtype.

The most altered transcripts were seen in the comparisons made between both

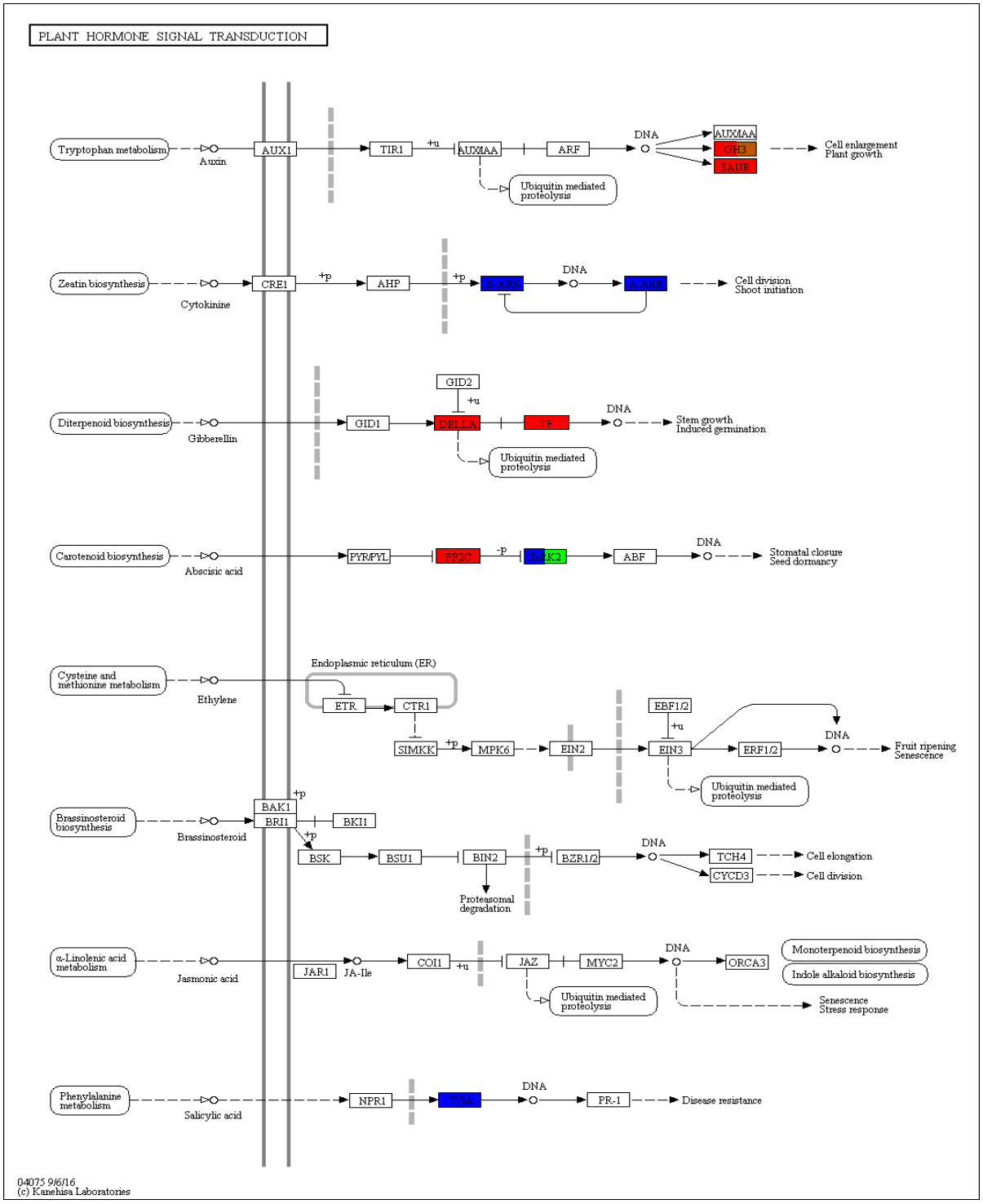

Figure 5.10 KEGG pathway mapping to plant hormone signalling of XX1 and 5.2 compared to wildtype under control conditions

Expression was mapped using KEGG and colours assigned based on increases or decreases. 5.2 upregulation, green; 5.2 downregulation, brown; XX1 upregulation, blue; XX1 downregulation, red

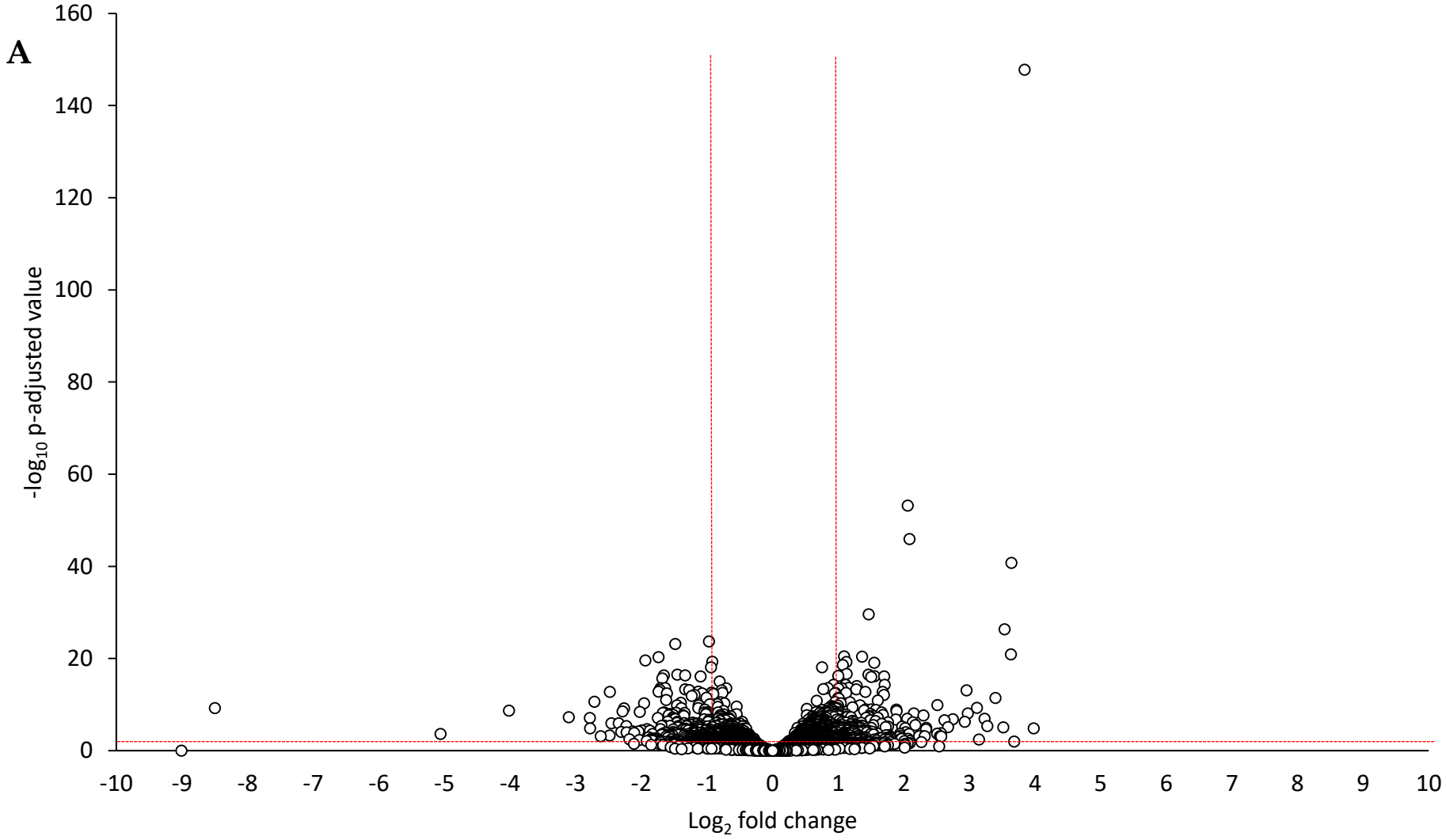
A
160
140
120
100
80
60
40
20
0
-log10 p-adjusted value
-10
-9
-8
-7
-6
-5
-4
-3
-2
-1
0
1
2
3
4
5
6
7
8
9
10
Log2 fold change

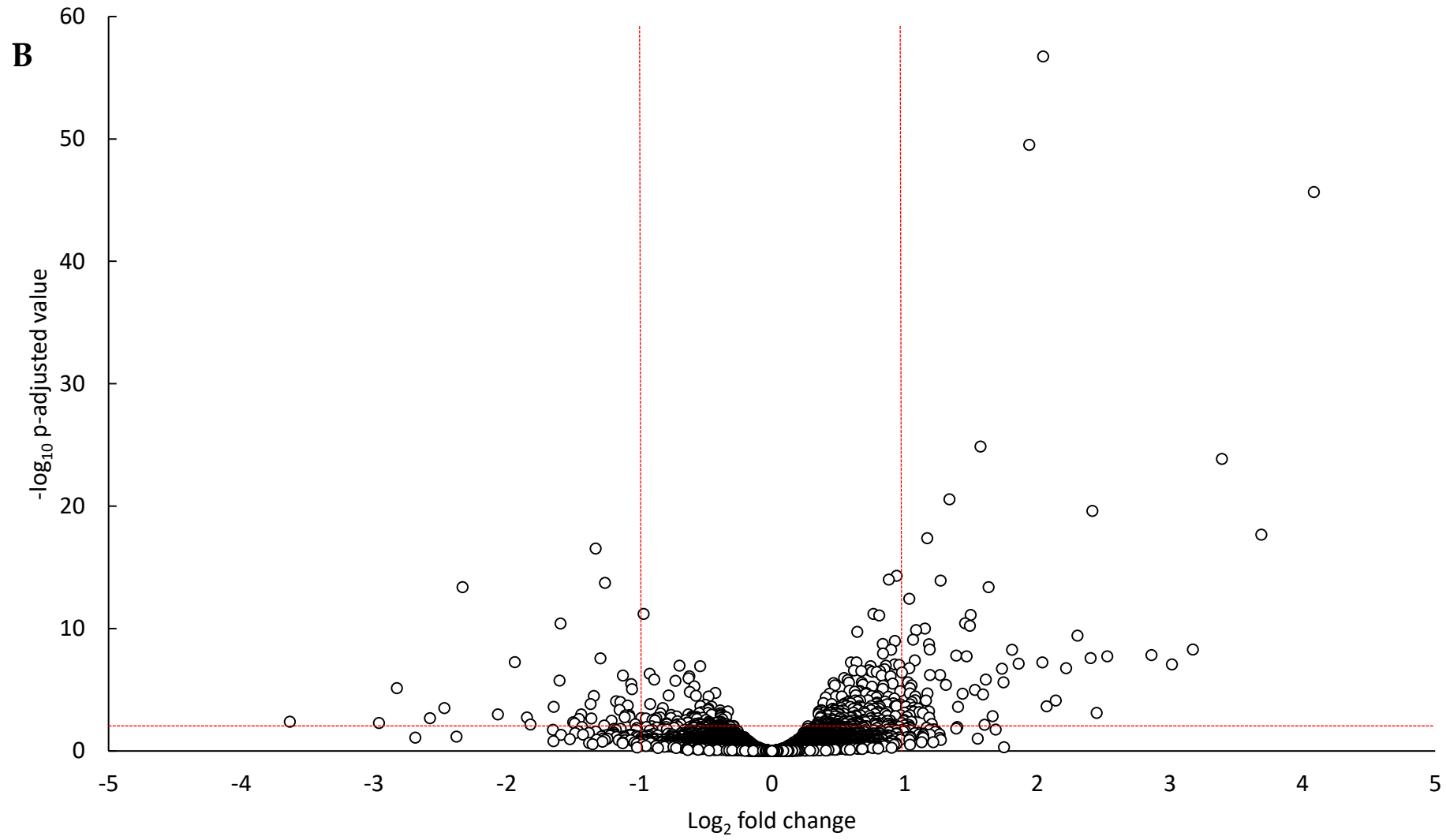
B
60
50
40
30
20
10
0
-log10 p-adjusted value
-5
-4
-3
-2
-1
0
1
2
3
4
5
Log2 fold change

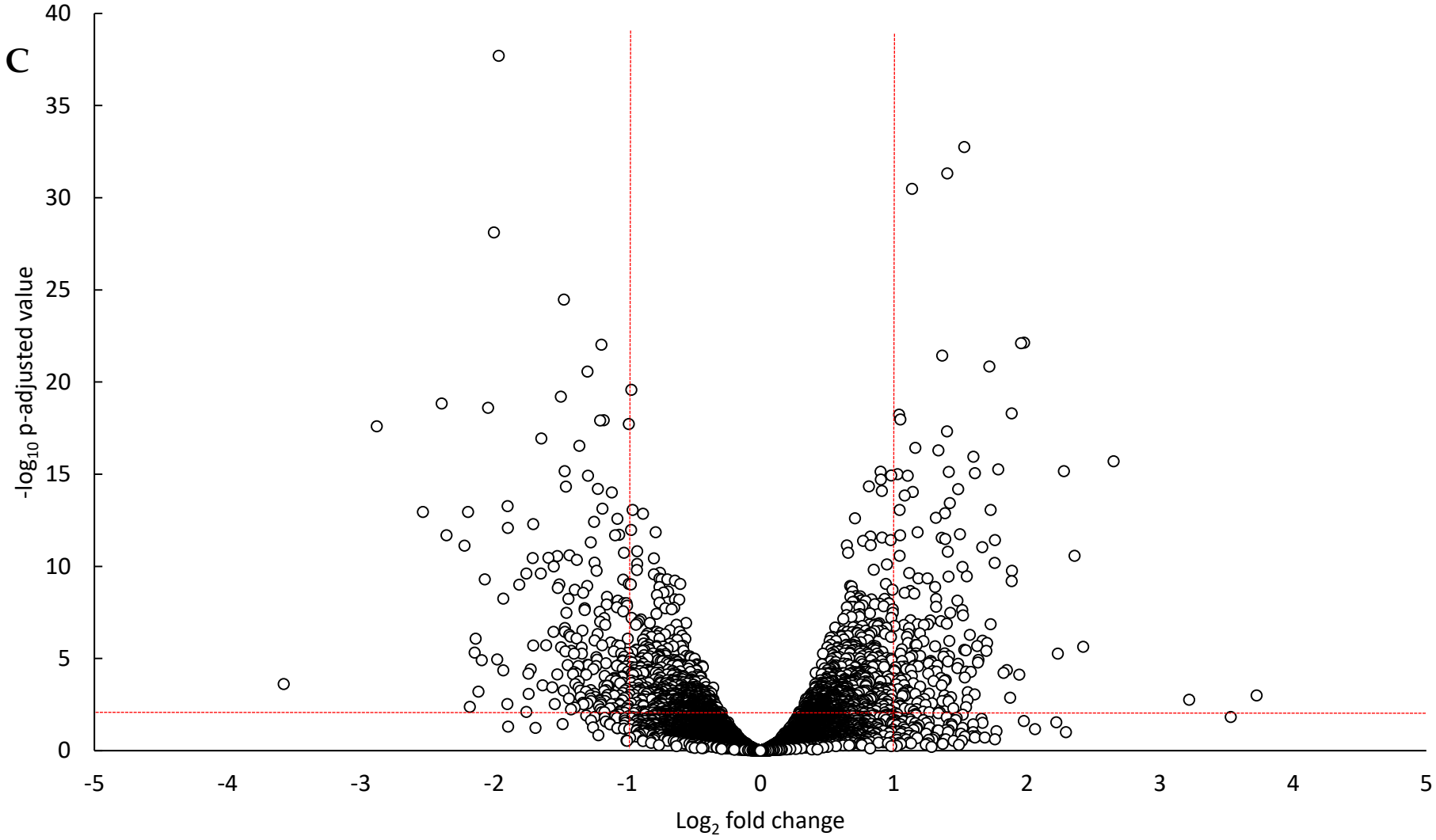
C
40
35
30
25
20
15
10
5
0
-log10 p-adjusted value
-5
-4
-3
-2
-1
0
1
2
3
4
5
Log2 fold change

Figure 5.11 Volcano plot distribution of differentially expressed genes in day 5 MLD comparisons of (A) wildtype to XX1, (B) XX1 to 5.2 and (C) wildtype to 5.2

Genes that had a base mean of <25 were removed from the dataset. A total of 331, 88 and 374 genes were differently expressed in figures A, B and C respectively

Table 5.7 Alternative respiratory pathway profile under MLD conditions

All data with a * represents significant differences (P-adjusted value <0.01 and log_2 fold change greater than 1 or less than -1) Gene expression listed as B.T. are beneath the threshold of base mean read count >25

	Log_2 fold change		
Gene Name	5.2 relative to wildtype	XX1 relative to wildtype	XX1 relative to 5.2
Aox1a	**3.219***	**3.840***	0.589
Aox1c	B.T.	-0.475	B.T.
Aox1d	0.886	0.456	-0.423
Ptox	0.105	0.264	0.146
Nda1	0.004	-0.199	-0.206
Nda2	0.505	0.482	-0.006
Ndb1	0.111	0.037	-0.066
Ndb2	**3.724***	0.139	**-3.634***

XX1 and 5.2 to wildtype under MLD (Table A7.11, A7.12, A7.13). Several genes are shared between both XX1 and 5.2. None of the transcripts found to be upregulated in either line was seen under control conditions. However, in the downregulated transcript list, the plant specific protease inhibitor *AtDR4,* was present in both MLD lines but only in XX1 under control conditions. This was the only transcript shared between MLD and control samples. A total of eight transcripts were shared equally between both up- and downregulated lists. These included *Aox1a,* jasmonoyl-isoleucine-12-hydroxylase (*Cyp94b3*), DREB2 transcription factor (*Dreb2c)* and cytidine triphosphate synthase (AT4G20320) in the upregulated list. While ammonium transporter protein (*Amt12),* plasma membrane intrinsic protein (*Pip2-2),* plant-specific protease inhibitor (*AtDr4)* and asparagine synthetase (*Asn2)* were found in the downregulated list. It is interesting to note that under control conditions, both lines upregulated the asparagine synthetase isoform *Asn1* while under MLD conditions they both upregulate the other isoform *Asn2.*

5.3.8 Gene ontology term enrichment analysis of MLD plants

The MLD differentially expressed transcript list was again run through the GO Panther analysis**.** In comparison to control samples, there was a shift away from light responsive and pigment related genes towards glucosinolate biosynthesis (Figure 5.12). This was present in both XX1 and 5.2 comparisons to wildtype, though the XX1 line did appear to have greater overrepresentation than the 5.2 line. A larger number of hormone/metabolic GO terms were present in MLD than in control, although the

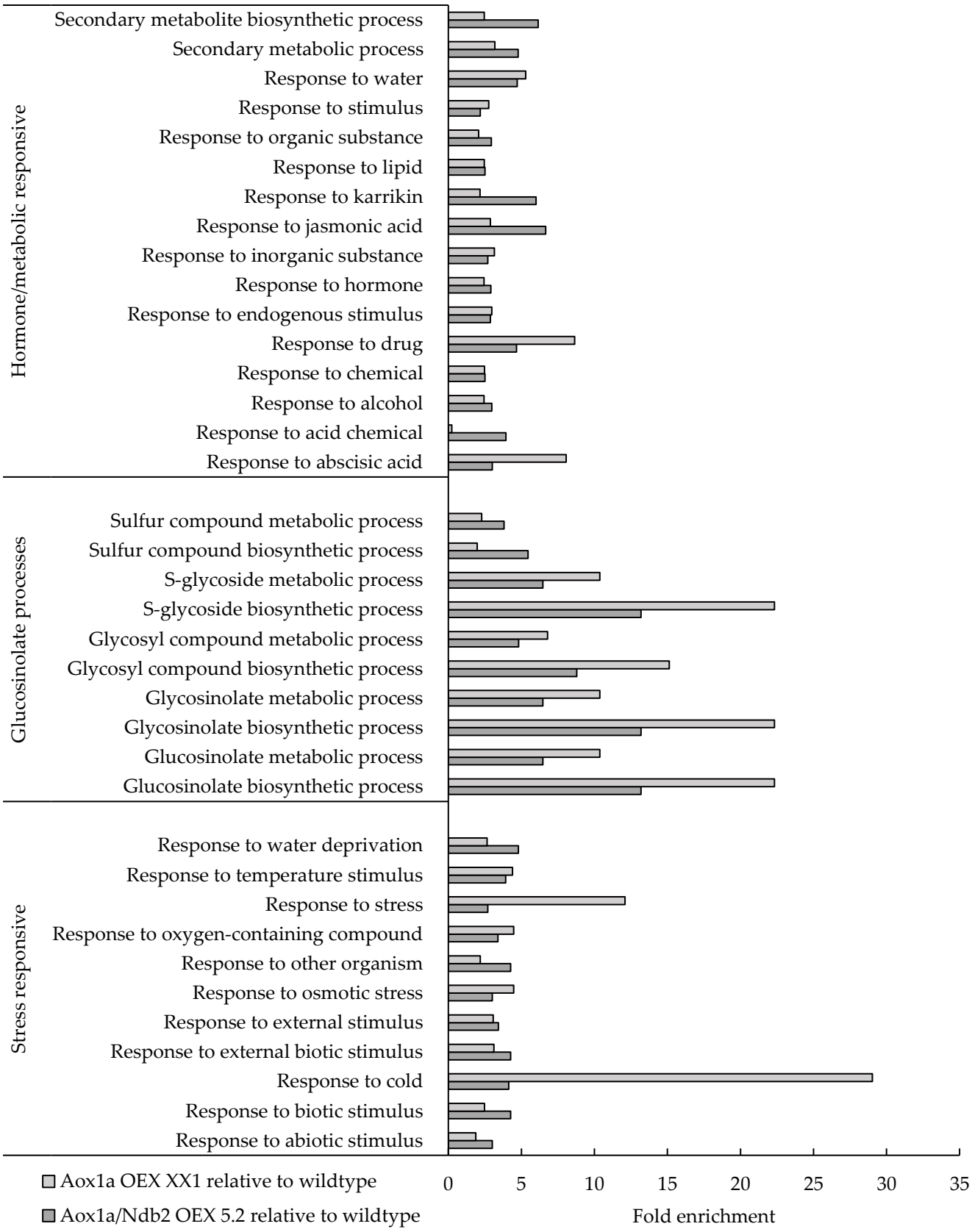

Figure 5.12 GO Term enrichment of biological processes found in the comparisons between wildtype and 5.2 or XX1 under MLD conditions

shared GO terms had similar fold changes. There were also larger numbers of GO terms present in the stress responsive classification, albeit again with very similar fold changes. It was interesting to note that despite both lines showing improved recovery to MLD stress, neither line was overrepresented in categories specific to the stress or enzymes altered i.e. high light stress or oxidative stress, although both lines are represented under water deprivation stress.

5.3.9 KEGG pathway analysis of control plants

KEGG pathways were again utilised to aid in interpretation of the MLD dataset. The plant hormone signalling pathway again featured prominently in terms of over-representation (Figure 5.13), although only *Rr5* and *Wes1* were shared between controls and MLD, leaving nine other unique genes. Under MLD conditions, the majority of the transcripts listed under plant hormone signalling are auxin responsive (Table 5.8), similar to what was seen under control conditions, although with different isoforms. Both lines show similar up- and downregulation of shared genes. The dual OEX, however, had upregulation of a few jasmonate and ethylene responsive proteins that were not seen in the single OEX.

Compared to control conditions, several new pathways became more prominent under MLD. One of these was the nitrogen metabolism pathway, a pathway not highlighted under control conditions (Figure 5.14). Interestingly, both lines do not share transcripts, but have downregulation of numerous transcripts related to the pathway (Table 5.9). The dual OEX saw downregulation of glutamate

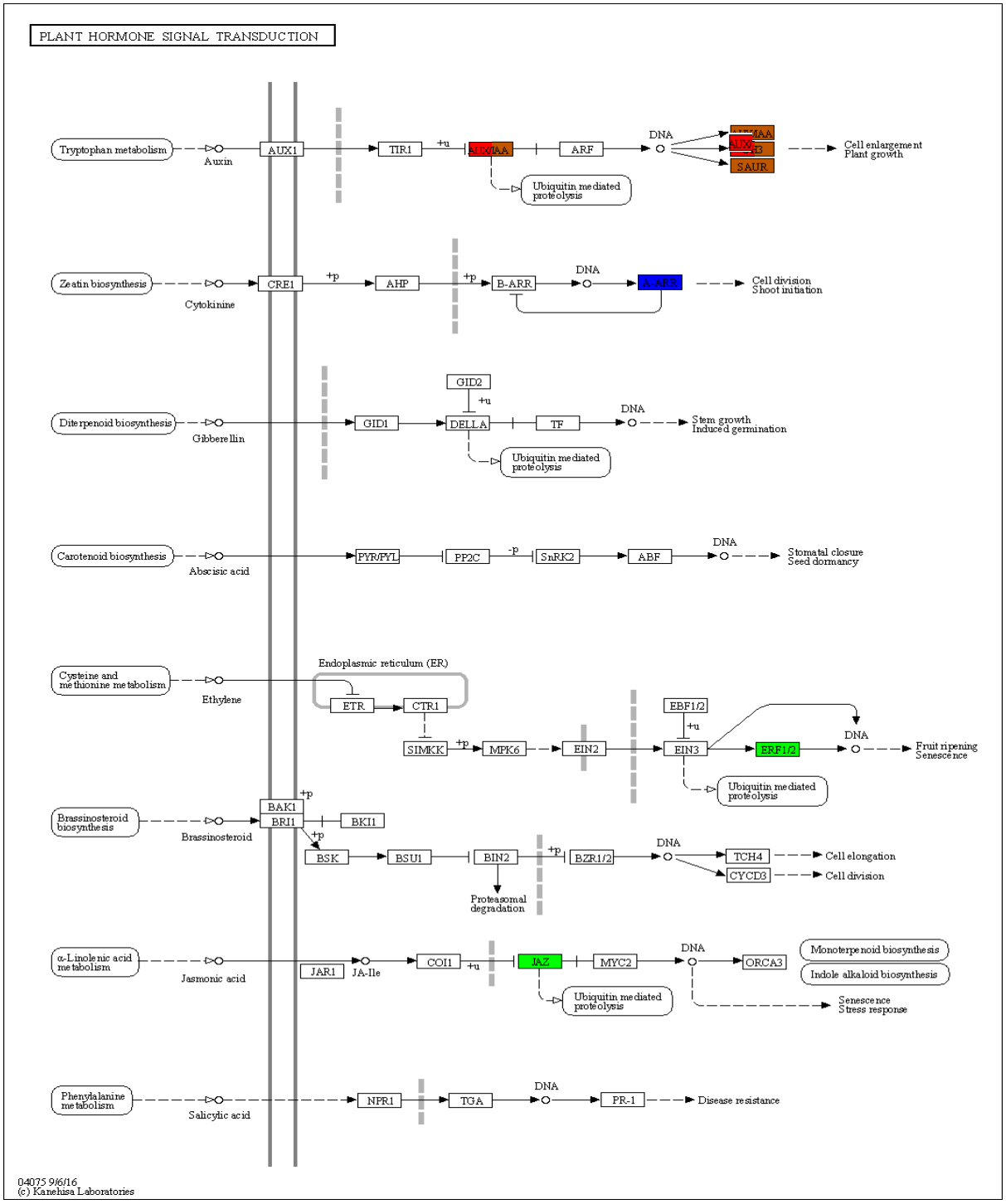

Figure 5.13 KEGG pathway mapping to plant hormone signalling of XX1 and 5.2 compared to wildtype under MLD conditions

Expression was mapped using KEGG and colours assigned based on increases or decreases. 5.2 upregulation, green; 5.2 downregulation, brown; XX1 upregulation, blue; XX1 downregulation, red

Table 5.8 Gene list contributing to the plant hormone signalling KEGG pathway

N.S. : not significant

Gene I.D.	Gene name	Description	Log_2Fold Change in 5.2 relative to wildtype	Log_2Fold Change in XX1 relative to wildtype
AT1G04250	AXR3	Aux/IAA transcriptional regulator family protein	-1.036	-1.310
AT1G17380	JAZ5	Jasmonate-zim-domain protein 5	1.074	N.S.
AT1G19180	JAZ1	Jasmonate-zim-domain protein 1	1.153	N.S.
AT2G01200	IAA32	Indole-3-acetic acid inducible 32	1.231	1.187
AT2G21210	SAUR6	Saur-like auxin-responsive protein family	-1.225	N.S.
AT3G23050	IAA7	Indole-3-acetic acid 7	-1.203	N.S.
AT4G14550	IAA14	Indole-3-acetic acid inducible 14	-1.054	N.S.
AT4G27260	WES1	Auxin-responsive gh3 family protein	-1.158	-1.282
AT4G38840	SAUR14	Saur-like auxin-responsive protein family	-1.341	N.S.
AT5G47220	ERF2	Ethylene responsive element binding factor 2	1.184	N.S.
AT3G48100	RR5	Response regulator 5	N.S.	1.120

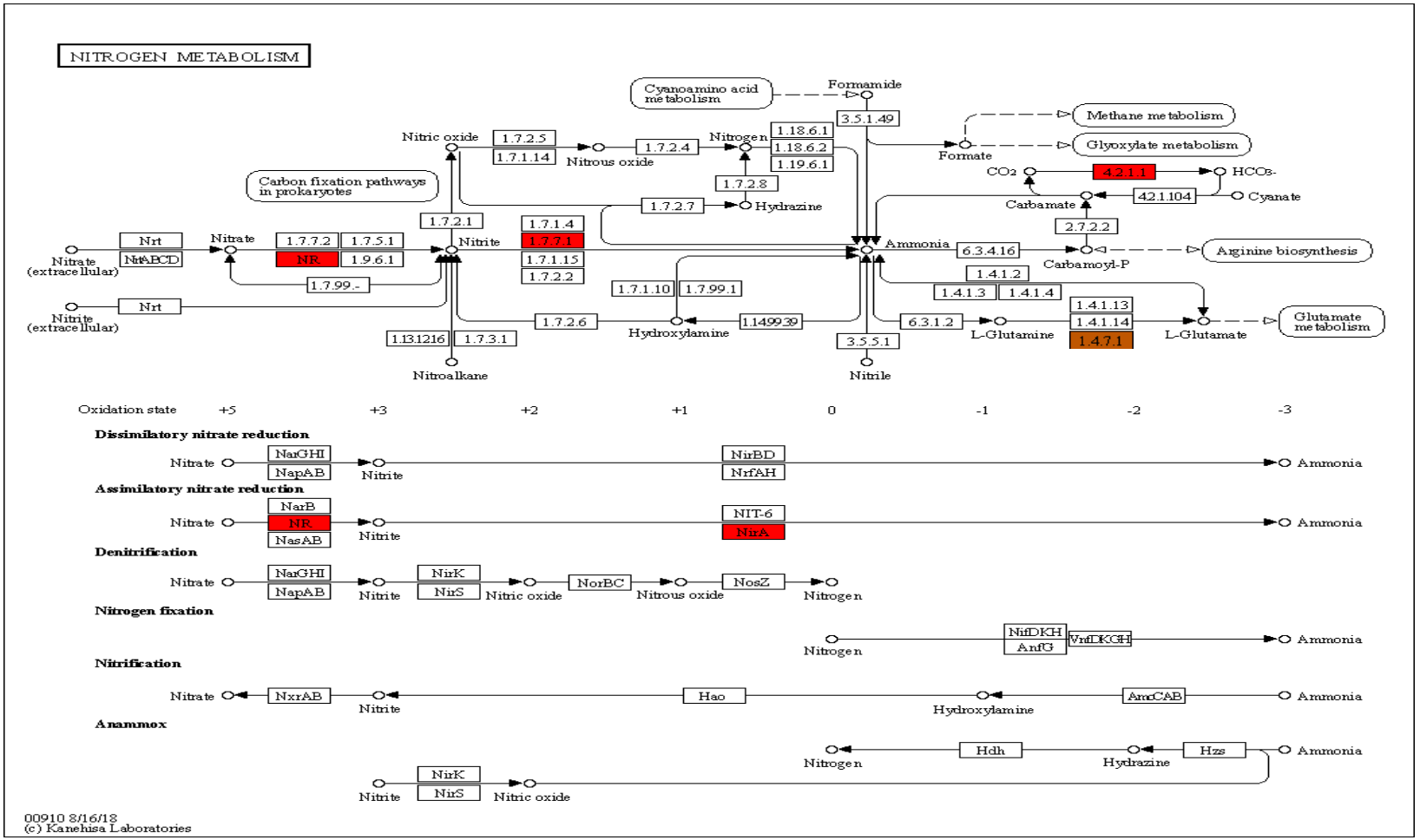

Figure 5.14 KEGG pathway mapping to nitrogen metabolism of XX1 and 5.2 compared to wildtype under MLD conditions

Expression was mapped using KEGG and colours assigned based on increases or decreases. 5.2 upregulation, green; 5.2 downregulation, brown; XX1 upregulation, blue; XX1 downregulation, red.

Table 5.9 Gene list contributing to the nitrogen metabolism KEGG pathway

N.S. : not significant

Gene I.D.	Gene name	Description	Log_2Fold Change in 5.2 relative to wildtype	Log_2Fold Change in XX1 relative to wildtype
AT5G04140	GLU1	Glutamate synthase 1	-1.029	N.S.
AT1G77760	NIA1	Nitrate reductase 1	N.S.	-1.483
AT2G15620	NIR1	Nitrite reductase 1	N.S.	-1.037
AT3G52720	ACA1	Alpha carbonic anhydrase 1	N.S.	-2.457

synthase, responsible for the conversion of glutamine to glutamate; a loosely related nitrogen metabolism gene. The single OEX had nitrite and nitrate reductases, responsible for the assimilation of nitrite into ammonia, downregulated. A protein responsible for assimilation of CO_2 into solution, alpha carbonic anhydrase, was also heavily downregulated. But again, the ties to nitrogen metabolism is loose, seemingly more associated with carbon catabolism.

Another overrepresented pathway unique to the MLD dataset was glucosinolate biosynthesis (Figure 5.15). A number of transcripts all relating to side chain elongation were all downregulated to a similar extent in both lines. The majority of these transcripts were shared between lines except for two (Table 5.10). It is worth pointing out that *Ipmi2*, a protein that is repeatedly involved in the side chain elongation, was not altered in the single OEX line. Likewise, the *Cyp79f1* gene responsible for conversion into glucosinolate, was altered in the single OEX line but not the OEX line (Figure 5.15).

Of significant interest in the carbon metabolism pathway was the downregulation of a number of RUBISCO subunits in the dual OEX line, an effect not seen under control conditions in either OEX line (Table 5.11). Likewise, the pentose phosphate pathway enzyme, glucose-6-phosphate dehydrogenase was again, only downregulated in the dual OEX line under MLD. Only two genes were shared between lists. One of those, fructose-bisphosphate aldolase 1, is another glycolytic enzyme, but also shared in the gluconeogenesis and pentose phosphate pathways. The

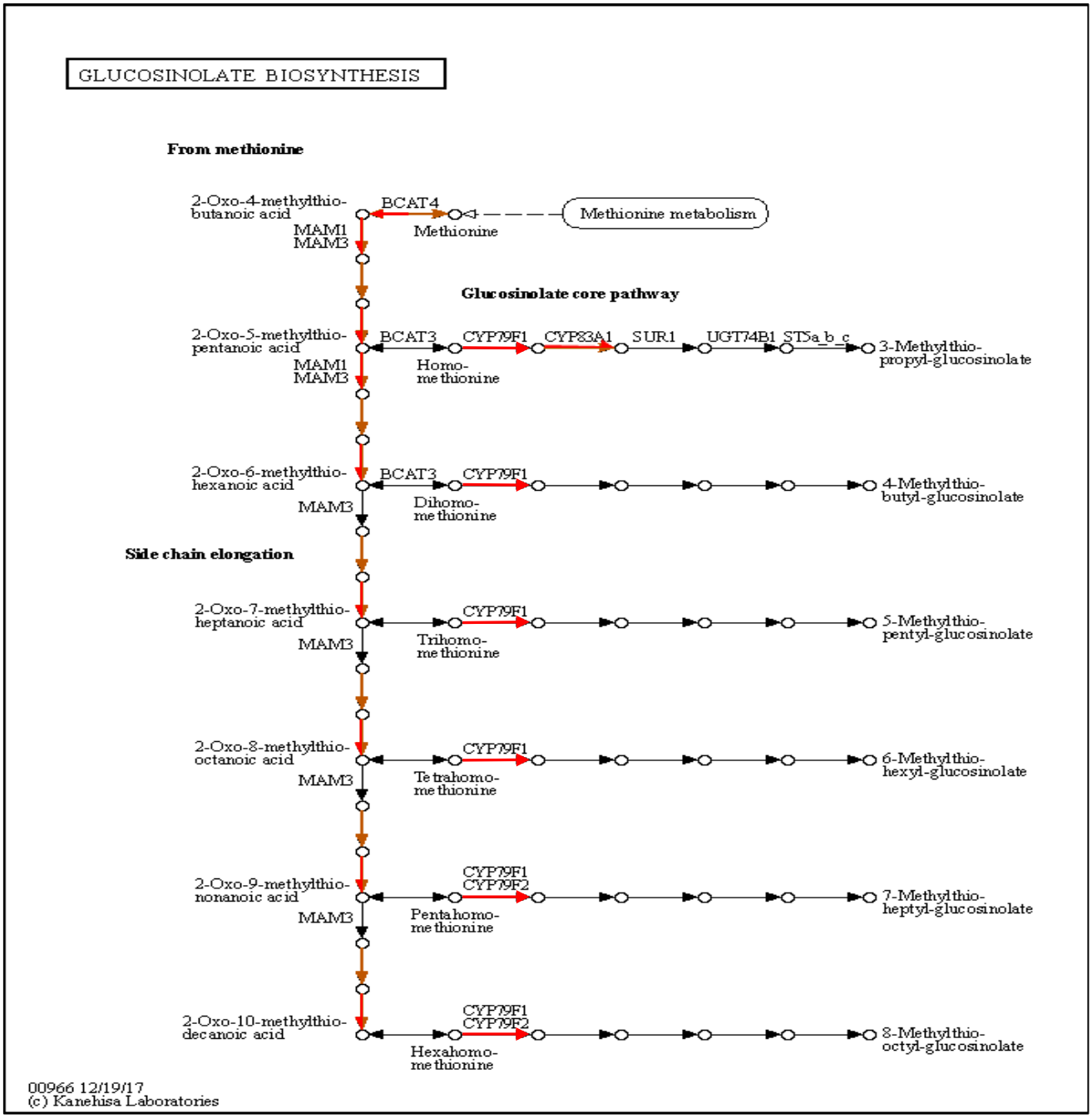

Figure 5.15 KEGG pathway mapping to glucosinolate biosynthesis of XX1 and 5.2 compared to wildtype under MLD conditions

Expression was mapped using KEGG and colours assigned based on increases or decreases. 5.2 upregulation, green; 5.2 downregulation, brown; XX1 upregulation, blue; XX1 downregulation, red.

Table 5.10 Gene list contributing to glucosinolate biosynthesis KEGG pathway under MLD conditions

N.S. : not significant

Gene I.D.	Gene name	Description	Log_2Fold Change in 5.2 relative to wildtype	Log_2Fold Change in XX1 relative to wildtype
AT2G43100	IPMI2	Isopropyl-malate isomerase 2	-1.034	N.S.
AT3G19710	BCAT4	Branched-chain aminotransferase 4	-1.426	-1.229
AT4G13770	CYP83A1	Cytochrome P450, family 83, subfamily A, polypeptide 1	-1.231	-1.131
AT5G14200	IMD1	Isopropylmalate dehydrogenase 1	-1.463	-1.221
AT5G23010	MAM1	Methylthioalkylmalate synthase 1	-1.436	-1.194
AT1G16410	CYP79F1	Cytochrome p450 79f1	N.S.	-1.323

Table 5.11 Gene list contributing to carbon metabolism KEGG pathway under MLD conditions

N.S. : not significant

Gene I.D.	Gene name	Description	Log_2Fold Change in 5.2 relative to wildtype	Log_2Fold Change in XX1 relative to wildtype
AT1G24280	G6PD3	Glucose-6-phosphate dehydrogenase 3	-1.068	N.S.
AT1G67090	RBCS1A	Ribulose bisphosphate carboxylase small chain 1A	-1.044	N.S.
AT2G21330	FBA1	Fructose-bisphosphate aldolase 1	-1.294	-1.028
AT5G28020	CYSD2	Cysteine synthase D2	-1.341	-1.014
AT5G38410	RBCS3B	Ribulose bisphosphate carboxylase (small chain) family protein	-1.477	N.S.
AT5G38420	RBCS2B	Ribulose bisphosphate carboxylase (small chain) family protein	-1.757	N.S.
AT5G38430	RBCS1B	Ribulose bisphosphate carboxylase (small chain) family protein	-1.328	N.S.
AT5G28030	DES1	L-cysteine desulfhydrase 1	N.S.	-1.637

other, cysteine synthase, is involved in the conversion of acetylserine to cysteine (Figure 5.16). Additionally, the single OEX line has another cysteine desulfhydrase involved in the same reaction that was not present in the dual OEX.

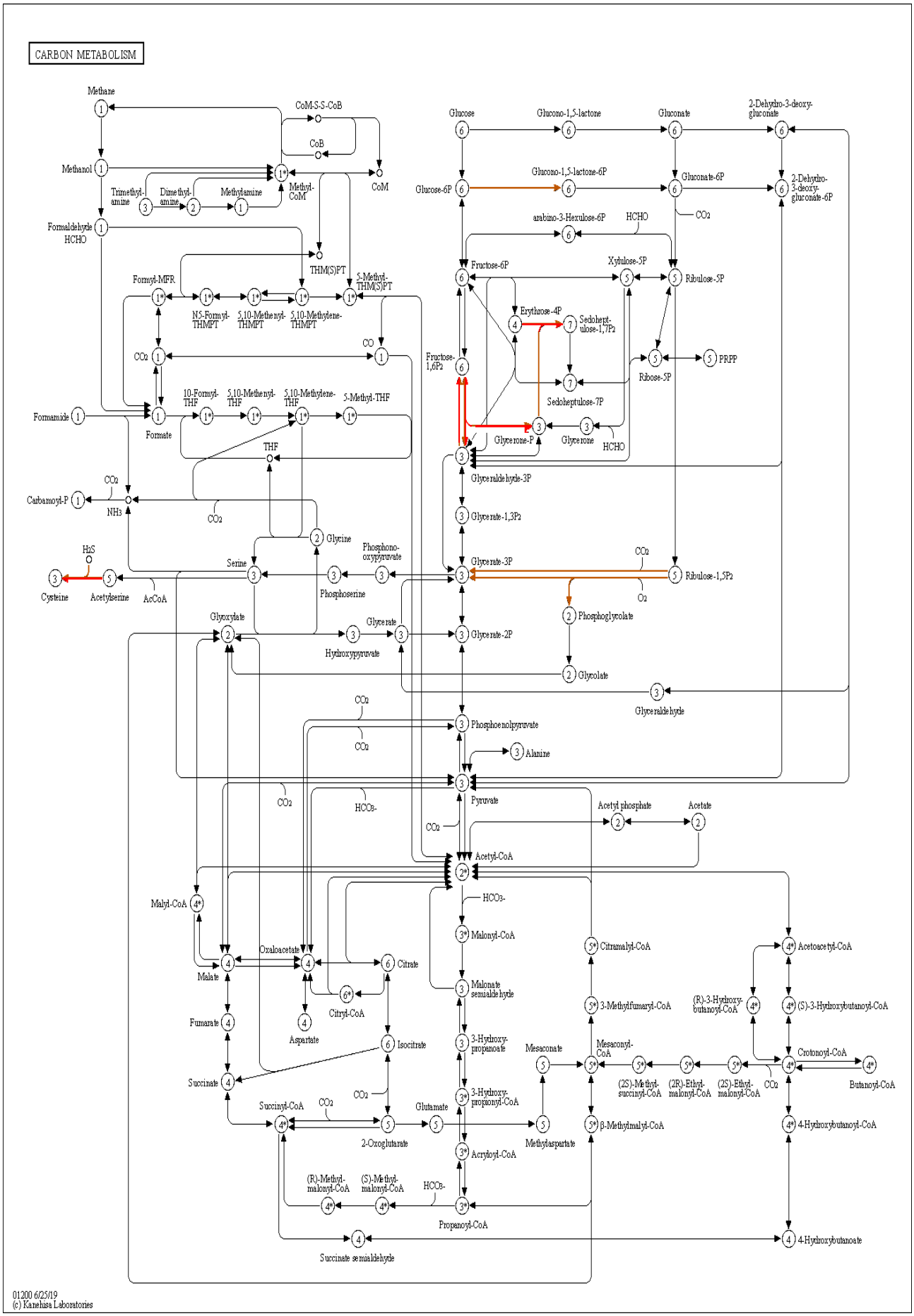
CARBON METABOLISM
Methane
CoM-S-S-CoB
CoB
Methanol
Trimethyl-amine
Dimethyl-amine
Methylamine
Methyl-CoM
CoM
Formaldehyde HCHO
THM(S)PT
Formyl-MFR
5-Methyl-THM(S)PT
N5-Formyl-THMPT
5,10-Methenyl-THMPT
5,10-Methylene-THMPT
CO
CO2
Formamide
Formate
10-Formyl-THF
5,10-Methenyl-THF
5,10-Methylene-THF
5-Methyl-THF
THF
Carbamoyl-P
NH3
Glycine
Serine
Phosphono-oxypyruvate
H2S
Cysteine
Acetylserine
AcCoA
Phosphoserine
Glyoxylate
Glycerate
Hydroxypyruvate
Glycerate-2P
Glycerate-3P
Glycerate-1,3P2
Glyceraldehyde-3P
Phosphoglycolate
Glycolate
Glyceraldehyde
Phosphoenolpyruvate
Alanine
Pyruvate
HCO3-
Acetyl phosphate
Acetate
Acetyl-CoA
Malyl-CoA
Malonyl-CoA
Oxaloacetate
Citrate
Malate
Citryl-CoA
Fumarate
Aspartate
Isocitrate
Malonate semialdehyde
3-Hydroxy-propanoate
Succinate
Succinyl-CoA
2-Oxoglutarate
Glutamate
3-Hydroxy-propionyl-CoA
Acryloyl-CoA
Propanoyl-CoA
(R)-Methyl-malonyl-CoA
(S)-Methyl-malonyl-CoA
Succinate semialdehyde
Mesaconate
Methylaspartate
Citramalyl-CoA
3-Methylfumaryl-CoA
Mesaconyl-CoA
β-Methylmalyl-CoA
(2S)-Methyl-succinyl-CoA
(2R)-Ethyl-malonyl-CoA
(2S)-Ethyl-malonyl-CoA
(R)-3-Hydroxy-butanoyl-CoA
Acetoacetyl-CoA
(S)-3-Hydroxybutanoyl-CoA
Crotonoyl-CoA
Butanoyl-CoA
4-Hydroxybutanoyl-CoA
4-Hydroxybutanoate
Glucose
Glucono-1,5-lactone
Gluconate
2-Dehydro-3-deoxy-gluconate
Glucose-6P
Glucono-1,5-lactone-6P
Gluconate-6P
2-Dehydro-3-deoxy-gluconate-6P
arabino-3-Hexulose-6P
HCHO
CO2
Fructose-6P
Xylulose-5P
Ribulose-5P
Erythrose-4P
Sedoheptulose-1,7P2
Fructose-1,6P2
Ribose-5P
PRPP
Sedoheptulose-7P
Glycerone-P
Glycerone
HCHO
Ribulose-1,5P2
O2
01200 6/25/19
(c) Kanehisa Laboratories

Figure 5.16 KEGG pathway mapping to carbon metabolism of XX1 and 5.2 compared to wildtype under MLD conditions

Expression was mapped using KEGG and colours assigned based on increases or decreases. 5.2 upregulation, green; 5.2 downregulation, brown; XX1 upregulation, blue; XX1 downregulation, red.

5.4 Discussion

5.4.1 Transcriptomic profiles of the individual lines in response to MLD

From the work performed in the previous chapter, it was curious to note that the overexpression of *Aox1a* with or without *Ndb2* resulted in minimal growth differences compared to wildtype under control conditions, but major improvements to recovery under MLD. To elucidate how overexpression of these genes affected these responses, a global transcriptomic approach was applied. The principal component analysis (PCA) highlighted the consistency between replicates and the lack of major differences between lines, showing limited variance of transcriptomic profiles of each line. The replicates of each genotype produced tightly clustered grouping which gave me confidence in the reproducibility of the data.

However, further interrogation of the data using volcano plots highlighted some significant differences in the number of expression changes seen in transgenic OEX lines. Both the transgenic OEX lines showed a greater number of genes with significant changes in expression at an even greater level of significance. While both lines had substantially more significantly altered genes, the single *Aox1a* OEX line had even greater fold-changes than the dual OEX line, with close to 1300 more significantly altered genes. This highlights the substantial effects that altering AP expression has on downstream global gene expression changes and also shows that the additional introduction of *Ndb2* in the dual OEX line had a rebalancing effect with respect to the transcriptomic profile. Nonetheless, the transgenic OEX lines shared many of the same

transcriptional responses as the wildtype with the majority of the expression changes overwhelmingly shared, albeit with different intensity.

Interestingly, the response of AP genes to the MLD treatment was notably different between the OEX lines and wildtype. As expected, the wildtype line saw increases to both the *Aox1a* and *Ndb2* transcripts, demonstrating the response these two enzymes play to an MLD stress. Wildtype and the single *Aox1a* OEX also saw increased expression of *Ptox*, which had also been documented by Quiles (2006) under high light conditions in oat leaves. In a review by Rumeau et al. (2007), it was proposed that PTOX may be able to fine tune the redox state of the chloroplast, allowing cyclic electron flow to function more optimally under stress. They also suggested that similar to the proposed mechanism of AOX1a, PTOX may act as an electron safety valve, protecting overreduction of the photosystem complexes and further photo inhibitory damage, a statement backed up by experiments in which overexpression of *Ptox* in *A.thaliana* resulted in a protective effect on PSI photoinhibition (Rosso et al. 2006). It is interesting to note that upregulation of *Ptox* was not seen in the dual OEX line, hinting that the co-overexpression of the NDB2 enzyme altered photosynthetic signalling under stress. Notably, all three lines tested showed similarly significant downregulation of the *Ndb1* transcript. Previous experimenters found that NDB1 was not upregulated in response to a variety of chemical stressors (Clifton et al. 2005) and another report even found improvements to ammonium toxicity stress experiments in *ndb1* RNAi supressed lines (Podgórska et al. 2018). Wallström et al. (2014a) noted that *ndb1* RNAi suppression lines had a significant effect on metabolism and

vegetative growth suggesting its importance to these pathways. NDB1 suppression may thus be a strategy applied under stress conditions by prioritising NADPH for the stress response rather than through the ETC. Regardless, it appears that neither the single nor dual OEX lines seem to modify this approach. *Aox1d* upregulation also seemed to occur consistently across all lines, although not significantly in wildtype. The dual OEX line had the greatest increase, with upwards of a $\log_2$ fold change of 3. *Aox1d* is a stress responsive AOX isoform known to be co-expressed with *Aox1a* under stress (Pu et al. 2015) and may be responding to changes in plant hormone signalling as its responses to senescence (a complex hormonal signalling pathway) has been documented (Clifton et al. 2006a). It is not clear why *Aox1d* appears to have greater upregulation in the dual OEX, especially compared with the single *Aox1a* OEX. It may be that the differences seen in nitrogen metabolism related genes between the two transgenics lines contribute to this, as *Aox1d* has previously been seen to be altered by nitrogen status (Escobar et al. 2006). Also unique to the dual OEX line was the significant upregulation of *Nda1. Nda1* is known to be upregulated diurnally in potato leaves (Svensson & Rasmusson 2001). It may be that the dual OEX lines are able to maintain greater levels of photorespiration and as such produce higher levels of mitochondrial NADH from glycine decarboxylase, resulting in the need for NDA1 to consume excess NADH. This might agree with what was seen with *Ptox* upregulation as the dual OEX is in a more advantageous position to allow greater photorespiration.

When assessing the topmost altered transcripts across the three lines tested, a number of trends were apparent. Firstly, both the wildtype and dual OEX line showed

high levels of similarity in the expression changes seen whereas the single OEX shared none of the genes present in either the up or downregulated lists. As is highlighted later in the discussion this may indicate a rebalancing effect of the NDB2 enzyme on signalling, altering the effects of *Aox1a* OEX and softening some of its negative effects, thereby allowing for better recovery from MLD stress. It was interesting to note that a majority of the largest expression changes that occurred were shared between the wildtype and dual OEX line, but a clear recovery advantage was present for the dual OEX. Many of the gene changes were also shared with the single OEX line, but not with the same level of expression change.

5.4.2 A transcriptomic analysis of the alternative OEX lines under optimal growth conditions

Volcano plots were used to evaluate the distribution of significance and expression changes. Despite growing similarly under control conditions, the single OEX line had over four times the amount of significantly altered genes compared to wildtype and the dual OEX line. The expression of these genes also tended to have a larger fold change and far greater statistical significance than the dual OEX. This could indicate that the larger changes to gene expression caused by OEX of *Aox1a* alone are attenuated by co-overexpression of *Ndb2*. This agrees with the phenotyping data where changes seen in the single OEX were no longer present in the dual OEX lines. As suggested in the previous chapter, rebalancing of the input/output of the electron

transport chain could affect signalling and affect further downstream expression changes.

The AP members were investigated for changes to their expression. Neither OEX lines showed significant changes to expression of any of the other AP members. The 2-fold increase in *Aox1d* transcripts in the single OEX line was interesting to note, an effect also seen by the creators of this line (Umbach et al. 2005). A previous microarray analysis highlighted *Aox1d* as stress responsive (Clifton et al. 2006a) and was upregulated in *aox1a* T-DNA lines in the presence of antimycin A (Strodtkötter et al. 2009). *Aox1d* upregulation did not occur in the dual OEX and it was even even marginally downregulated, highlighting the effect of concomitant *Ndb2* upregulation on AP members and its effect on stress signalling.

GO term analysis involves assigning dysregulated genes to categories relating to their biological function, molecular process or organelle location, and then making an assessment on whether the number of genes altered in expression suggests over or under representation in that category. These GO terms were further grouped based on four different categories. Making comparisons between the dual and single OEX lines and wildtype highlighted a number of shared categories, but with different levels of enrichment. The dual OEX has close to double the enrichment in light harvesting associated with PSI and PSII as well responses to far-red and blue light. In contrast, the single OEX only shows greater enrichment in the light reaction category. However, it's difficult to interpret and understand the enrichment seen in figure 5.6 when compared with the data seen in table 5.3. More genes relating to PSII and especially

PSI were altered in the single OEX than in the dual OEX line. Since no changes to genes directly relating to PSI were apparent in the dual OEX lines, it seems the annotation of PSI and PSII includes a broader array of genes than just those involved in light harvesting. Regardless of this, it is interesting to see that both OEX lines had significant downregulation of genes involved in the photosynthetic apparatus under control conditions, relative to wildtype, with the single OEX being unique in its downregulation of PSI. Mutant *aox1a* lines have previously been shown by numerous studies to influence PSII function especially under high light and drought conditions (Bartoli et al. 2005; Yoshida et al. 2011b; Watanabe et al. 2016). Watanabe et al. (2016) suggested that when the cytochrome pathway becomes limited or inhibited, excess reductants can flow through the AP, minimising excess ROS/RNS production. Zhang et al. (2011) suggested that the effects dealt by AOX1A inhibition are also felt through PSI, as excess reducing equivalents build up and PSI becomes over-reduced. Our experiments suggest that OEX of AOX1a can alter signalling that affects the expression of both PSI and PSII. Interestingly, with the addition of *Ndb2* OEX, PSI expression was no longer affected. The reduced downregulation of PSII expression and lack of changes in PSI expression in the dual expression lines is further evidence that co-overexpression of NDB2 balances the overexpression of just AOX1a. In particular, overexpression of both enzymes would allow more rapid oxidation of excess reducing power exported from the chloroplast under the photo-inhibitory conditions of drought and increased light intensity.

Pigment related processes including flavonoid and anthocyanin related processes were significantly enriched across both single and dual OEX lines. From the pathway mapping performed in KEGG, the expression of AOX in both lines seems to result in upregulation of the production of particular flavonoids including but not limited to kaempferol, quercetin and myricetin. Work performed by Shimoji and Yamasaki (2005) demonstrated quercetin and myricetin to have strong inhibitory effects on alternative respiration, similar to that of the commonly used AOX inhibitor n-propyl gallate. Kaempferol showed minimal inhibitory effects. It should also be noted that *Fls1* (flavonol synthase 1) was one of the most significantly altered genes in the dual OEX line and *Fls1* contributes to all of the above listed flavonoids. Similarly, upregulation of *Chs* (chalcone synthase) was also found in another single *Aox1a* OEX experiment (using XX2 rather than XX1). It could be suggested that in *Aox1a* OEX lines and under control conditions, the activity of AOX1a is partially regulated through the upregulation of these flavonoids to minimise wasteful activity. However, this is at odds with a study of drought and light stressed *aox1a* lines where a very strong upregulation of the flavonoid related genes was observed(Giraud et al. 2008). Additionally, plants exposed to either a UV-B or NaCl stress after four days show a strong accumulation of quercetin 3-O-glycosides (Fini et al. 2011). It may be that the regulators of these flavonoid genes, MYB transcription factors, which are known to be affected by redox status (Dubos et al. 2010), are affected by the changes to photosynthetic redox status as demonstrated by Akhtar et al. (2010), brought on by the changes in AP expression. Asparagine synthetase 1 was the most significantly

downregulated gene under control conditions in the dual OEX and also highly downregulated in the single OEX, a gene that also has been shown to contain MYB transcription factor binding sites (Canales et al. 2012). Three different MYB transcription factors were significantly altered in both OEX lines (AT1G71030, AT5G49330 and AT1G57560) giving credence to this hypothesis.

Genes relating to the phenylpropanoid biosynthesis pathway show the greatest differences between the single and dual OEX, with none of the genes mapped shared between either line. Additionally, genes belonging to the same gene families show opposite levels of expression in the two lines. Both lines show changes in genes that belong to either the glycosyl hydrolase superfamily or the peroxidase superfamily. Work performed by Sircar et al. (2012) demonstrated a positive correlation between the activity of AOX and phenylpropanoid biosynthesis, backed up by work from Macedo et al. (2012). In a review by Sharma et al. (2019), 4-Coumarate:CoA ligase 3 (*4cl3)* was shown to alter the activity and transcription of numerous genes in the phenylpropanoid pathway. *4cl3* was only altered in the dual OEX and was one of the most highly expressed genes in the dual OEX. This could partly explain the differences in transcription between the two pathways. Many of the genes involved in the phenylpropanoid pathway are stress responsive and react to a broad range of stressors. A number of these genes also work in sync with genes from the flavonoid pathway in response to stress. It could be that the alteration to the AP, with its broad ranging effects on signalling, have modified the signalling between the mitochondria and/or the chloroplast resulting in adjustments to downstream secondary metabolite

pathways such as the flavonoid and phenylpropanoid biosynthesis pathways. This also may explain in part, why these plants were able to recover when exposed to the MLD stress.

A major role of plant hormone signalling is the regulation of development and growth. Plants continually adjust their metabolism and growth to their surrounding environment. One example of this is the auxin responsive GH3 proteins that mediate auxin homeostasis (Park et al. 2007). The GH3 gene *Wes1* is responsive to not just auxin, but stress hormones salicylic acid and abscisic acid. Park et al. (2007) demonstrated that OEX of *Wes1* was negatively correlated with growth and positively correlated with stress resistance. They suggested it was acting to balance resource allocation to improve stress fitness. In our experiments, both OEX lines saw significant downregulation of this gene under both conditions, giving reason to why these lines both perform better under recovery after MLD exposure, but it doesn't explain the similarities in growth phenotype under control conditions. The suppression of auxin signalling has previously been demonstrated by antimycin A induction of alternative oxidase, and the induction of *Aox1a* was reciprocally inhibited by auxin analogues, showing how these two components can function antagonistically (Ivanova et al. 2014). Similar negative growth correlations were also found for *Dfl1* although it was not tested for stress response alterations (Nakazawa et al. 2001). Whether the downregulation of these GH3 genes benefit the stress response of these OEX lines or are simply a downstream effect of the upregulation *Aox1a* is not known.

Another highly upregulated gene was the sucrose non-fermenting-related kinase 2 (*Snrk2-8)* gene. One of the more highly expressed genes, *Snrk2-8* is an important kinase involved in the phosphorylation of drought stress signalling transcription factor NTL6 (Kim et al. 2012) and other important drought and osmotic regulating genes (Umezawa et al. 2004; Fujita et al. 2009; Yoshida et al. 2015). Furthermore, its correlation with plant growth regulation through phosphorylation of metabolic processes is interesting, (Shin et al. 2007) as the strongly downregulated *bzip63* transcription has a number of metabolic related target proteins that are present in both gene lists (Tomé et al. 2014; Mair et al. 2015). It should be noted that *Snrk2-8* has not been identified as a regulator of *Bzip63*, but has been shown to alter other *bzip* transcription factors (Furihata et al. 2006) and the closely related homologue *Snrk1* is a well-known regulator of *bzip63* (Tomé et al. 2014). *Bzip63* is a key regulator of the starvation response and can significantly alter primary metabolism, being downregulated synergistically by ABA and glucose (Matiolli et al. 2011). *Bzip63* transcriptionally regulates a number of genes present in the gene lists including the some of the most highly downregulated genes in the dual OEX, including *Asn1* (Baena-González et al. 2007a), proline dehydrogenase 1 (*Pox1)*(Dietrich et al. 2011), raffinose synthase 6/dark-inducible 10 (*Rfs6*/*Din10)*(Matiolli et al. 2011) and senescence 1/dark-inducible 1(*Str15*/*Din1)*(Matiolli et al. 2011). The downregulation of *bzip63* may indicate the plant signalling network is responding to a high-energy status within the cell. This may indicate that OEX of *Aox1a* alters the energy signalling from the mitochondria through the AP. This is further backed up by the downregulation of

myo-inositol oxygenase 2 (Miox2), another gene downregulated by high glucose conditions (Alford et al. 2012). Alteration of signalling doesn't just appear to be isolated to carbon metabolism, with *Asn1,* a key enzyme in nitrogen catabolism, also very significantly affected. An important question to ask is why the plant signalling network is responding to a state of excess energy/nutrients when a potentially wasteful pathway is overexpressed. It may be that the alterations to ROS levels, caused by the altered expression of the AP and affected indirectly by the energy status of the cell, are contributing to the change in signalling.

Our transcriptomic analysis of these AP OEX lines has highlighted the wide-ranging effects the AP can have on signalling networks and the downstream knock on effects these have. It is interesting that these alterations to signalling have minimal effects on phenotype under control conditions but provide a significant advantage under stress conditions. It may be that the post-transcriptional regulation of these pathways limits the effects it has on phenotype under control conditions but primes the plant for stress conditions, providing the benefit seen under MLD recovery.

5.4.3 A transcriptomic analysis of AP OEX lines under moderate light and drought conditions

In contrast with what was seen across comparisons under control conditions, the single and dual OEX compared to wildtype were similar in terms of numbers of significant genes and levels of fold change under MLD. Both lines showed lower numbers of significantly altered genes, but the numbers were similar. Despite the

similarity in the number of genes expressed, of the 331 and 364 significant genes found in XX1 and 5.2 respectively, more than half of the genes were unique to each line demonstrating significant transcriptional changes between the two lines.

Expression of other AP members was not altered in either line. In comparison to control conditions where *Aox1d* looked to be upregulated in the single OEX and marginally downregulated in the dual OEX, the numbers were partially reversed, but still not statistically significant. There didn't appear to be any difference in transcriptional regulation of *Ndb2* between the single OEX and wildtype although both lines had smaller differences in fold-change compared to control conditions implying that *Ndb2* was upregulated in both lines.

As was seen under control conditions, GO terms relating to hormone/metabolic responses and stress responses were significantly enriched in both lines. Both lines share mostly similar levels of enrichment in the majority of hormone/metabolic responses GO terms, with the dual OEX showing greater enrichment in response to karrikin and jasmonic acid while the single OEX shows stronger enrichment in response to abscisic acid. All three of these hormone/plant growth regulators are especially important in response to abiotic/biotic stressors. Not represented in the GO term analysis was the significant downregulation of several auxin related/inducible genes highlighted by the KEGG pathway analysis, which was only present in the dual OEX, although there were similar responses in three auxin related genes shared between the pair. A number of the auxin related genes are significantly downregulated while the jasmonic and ethylene related genes are strongly

upregulated, highlighting a shift from plant growth and enlargement to stress tolerance. The majority of the genes shared weren't present under control conditions barring *Wes1* and *Rr5*, suggesting both genes are regulated independently of stress conditions.

Transcripts relating to assimilation of nitrate and nitrite into ammonia were significantly downregulated in the single OEX line. We also see downregulation of alpha carbonic anhydrase 1, the first step in carbon assimilation and asparagine synthetase 1, an important nitrogen catabolic enzyme (Gaufichon et al. 2010), suggesting an alteration to the carbon/nitrogen status from *Aox1a* OEX. Other experimenters have demonstrated alterations to carbon/nitrogen balance in mutant *aox1a* lines (Sieger et al. 2005). This has also been found in other plant species, where limited nitrogen availability altered the expression and capacity of AOX (Noguchi & Terashima 2006). It was suspected that due to the inhibitive effects on photosynthesis caused by limited nitrogen availability, AOX was employed to expend excess carbohydrates and maintain cellular redox and carbon balance. However, in this case it may be that there is an excess output of ammonia resulting from photorespiration in the single OEX line, causing the downregulation of the nitrate assimilatory pathway transcripts as ammonia has previously been seen to exert feedback inhibition on nitrate influx (King et al. 1993). It is interesting to see that the included OEX of *Ndb2* in our experiments eliminated downregulation of these genes. We also saw downregulation of glutamate synthase specifically in the dual OEX line. Glutamate

synthase is partially responsible for the breakdown of ammonia from photorespiration into glutamates. It could be that the dual OEX lines have an improved capacity to deal with the excess NADH resulting from glycine decarboxylation in the mitochondria, improving the efficiency of the photorespiratory pathway and lessening the need for additional glutamine synthase. Further to this, the dual OEX lines may provide relief to the photosynthetic electron transport chain (pETC) as Giordano et al. (2005) demonstrated that nitrate reductase expression can be significantly downregulated as a result of pETC redox poise being disrupted.

In assessing carbon metabolism, four different RUBISCO small-subunit genes were downregulated specifically in the dual OEX line, while no changes were detected in the single OEX, consistent with Dahal et al. (2014)'s work with single *Aox1a* OEX lines. The downregulation of these subunits may indicate that *Ndb2* OEX has significant effects on photosynthetic performance during drought. Whether this indirectly improves the recovery ability after drought is not known, but it may provide a conservation of energy during peak stress conditions. Glucose-6-phosphate dehydrogenase (*G6pdh*) is a key enzyme in the pentose phosphate pathway and its production of NADPH has been linked to the maintenance of the antioxidant pool of glutathione and can be regulated through redox poise (Salvemini et al. 1999; Née et al. 2009). The down regulation of *G6pdh* in the dual OEX may indicate that the inclusion of *Ndb2* OEX alongside *Aox1a* alters the redox and/or oxidative stress signalling.

A number of glucosinolate biosynthesis genes were significantly downregulated across both lines. Glucosinolates in the Brassicales order are typically associated with biotic stress defence and innate immune response (Sønderby et al. 2010). Cytochrome p450 has been shown to regulate these genes through changes in auxin production (Bak et al. 2001). The downregulation of two different p450 genes could explain why we see downregulation of this pathway and also downregulation in auxin hormone signalling. This may be a result of modification in signalling of WRKY transcription factors that are known to regulate transcription of both cytochrome p450 (Narusaka et al. 2004) and alternative oxidase (Dojcinovic et al. 2005a; Vanderauwera et al. 2012a; Van Aken et al. 2013). This may explain why there are minimal differences in transcription in this pathway between the dual and single OEX lines. In addition to this, a number of different MYB transcription factors were detected with significant dysregulation in both OEX lines. These particular MYB transcription factors have all be shown to affect glucosinolate biosynthesis (Gigolashvili et al. 2007; Hirai et al. 2007).

5.4.4 Concluding remarks

In summary, this RNA-seq experiment has identified a number of pathways and transcripts both shared and unique to the transgenic OEX lines across both control and stress conditions. In both of the lines tested we found large changes to expression of hundreds of genes that we suspect are due to modification in signalling stemming from changes to redox poise. Despite such a broad alteration of

genes in both lines, they share a similar phenotype compared to wildtype under control conditions. This is an important facet of transgenic modifications, as implementing these modifications in real world commercial settings must not affect their growth under control conditions. The transcripts measured under MLD were also wide-ranging and included alterations in the balance between carbon/nitrogen and hormone signalling, highlighting the importance the AP has on maintaining balance across many far-reaching pathways.

Chapter 6

Summary and future directions

6 General Discussion

The main aim of this study was to further elucidate the function and role of the commonly co-expressed AP members *Aox1a* and *Ndb2* and test their proposed enhanced performance with dual OEX under a combined drought and light stress. This was realised through three smaller aims. Initially, three dual OEX lines were generated in *A.thaliana* and changes to both transcript and protein expression were determined. From there, we were then able to assess changes to activity levels, substrate specificity, calcium activation, AOX activation and the combined effects of forming a complete bypass through the mETC using the AP. Secondly, we then assessed the phenotype of these plant lines using a comprehensive analysis laid out by Boyes et al. (2001). These newly generated lines were then subjected to a combined light and drought stress along with the parent line to determine whether any benefits would be gained from overexpressing *Ndb2* alongside *Aox1a*. The improvements seen in the dual OEX lines ability to recover were then investigated using a number of methods including gas exchange, phenotype and biochemical. Finally, these lines were subjected to RNA-seq and the whole transcriptome characterised under both control and stress conditions.

Geisler et al. (2007) had previously shown the NDB2 protein to be NADH specific and stimulated by calcium using a heterologous expression system in *E.coli* but this does not necessarily mean that NDB2 is the main external NADH dehydrogenase *in planta*. This was further backed up by evidence provided by Smith et al. (2011) who

found increases *in planta* in NDB4 knockdown lines which resulted in increased levels of NDB2. However other isoforms were also upregulated in Smith et al. (2011) case and the heterologous expression needed further evidence *in planta.* From the direct OEX of *Ndb2* in the current experiments, the previous results were found to be accurate, with NDB2 being NADH specific and calcium stimulated. Interestingly, work previously performed in our lab (unpublished) with single *Ndb2* OEX lines, showed no change in mitochondrial NADH oxidation in three separate lines. Only with concomitant *Aox1a* OEX was there a significant increase. This is the first example of another AP member being regulated by AOX1a. It was proposed that these enzymes were complexing, forming a bridge across the inner mitochondrial membrane. Mitochondrial complexome profiling performed by Senkler et al. (2017) gives credence to this hypothesis as they showed both AOX1a and NDB2 formed complexes around 140-150 kDa which is near the theoretical size 129 kDa size for the complexing of the AOX1a dimer and NDB2 monomer. A combination of cross-linking, co-immunoprecipitation and western blotting could validate this hypothesis and shed light on the interactions of the AP (Herrmann et al. 2001).

Minimal phenotypic data exists for the single *Aox1a* OEX lines especially under control conditions (Fiorani et al. 2005). As such, a comprehensive phenotypic analysis including the newly generated dual OEX lines was performed. We found the single OEX lines (*Aox1a* or *Ndb2*) were delayed in their growth milestones, with seedlings, roots, rosettes and flowering showing delays. Interestingly, nearing the end of the

measurement period, these lines were not significantly different from the wildtype lines, highlighting an initial deficit in growth rate early in development, but at the same time managing to maintain a faster growth rate in the later stages of growth. Unlike either of the single OEX lines, the dual OEX lines were mostly unaffected with small delays in seedling development that did not result in further delays later in the growth analysis. It was hypothesised that the addition of NDB2 was balancing out the effects of excess AOX1a and mitigating the changes to the metabolic balance. It is interesting to note that despite AOX1a being so heavily regulated post transcriptionally i.e. through carbon (pyruvate), energy (ADP:ATP) and redox status, the presence of additional AOX1a protein can still alter plant growth significantly. Stress resistant dual OEX lines in a commercial crop could potentially be useful, where stunting of growth under optimal conditions is unfavourable.

Clifton et al. (2005) highlighted the co-expression of *Aox1a* and *Ndb2* under a number of mitochondrial/plastid inhibition and abiotic stress treatments and showed there are a number of shared common sequence elements present upstream. By chance, Smith et al. (2011) had found that when they knocked down *Ndb4* they saw increases in *Aox1a* and *Ndb2* in response. This also led to improvements in salinity tolerance and improvements in response to oxidative stress. While there were also changes to other AP members (among other non-AP related genes), it was hypothesised that upregulation of these two members had provided improved stress tolerance. Previous experimenters had already highlighted the importance of *Aox1a* in

both drought and light stress (Giraud et al. 2008; Wang & Vanlerberghe 2013) and the potential for improvements in *A.thaliana* (Dahal et al. 2015a). The data presented in this thesis confirm these results but further highlight the importance of the external type II dehydrogenase NDB2 in stress tolerance and recovery under MLD. Dual OEX in two of the three lines generated conveyed significantly greater ability to recover from the MLD stress. Under MLD stress, these lines were able to recover with a rate of 92 and 75% whereas only 9% of wildtype plants were recoverable. Other works have identified the APs capability in minimising ROS production when the cytochrome c pathway becomes inhibited (Maxwell et al. 1999; Fiorani et al. 2005). In our experiments, the oxidative damage marker TBARS was also reduced in both single and dual OEX lines under control conditions, compared to wildtype. However, due to interference caused by increased synthesis of anthocyanins that absorb at a similar wavelength, oxidative damage changes could not be confirmed in MLD samples, although protein carbonylation experiments in drought experiments by Dahal and Vanlerberghe (2017) would suggest these would be decreased. A potentially shorter MLD stress experiment may allow teasing out of oxidative damage changes without the interference of anthocyanins. Additionally, protein carbonylation combined with western blotting may also allow measurements of oxidative damage without hinderance of other compounds sharing similar maximal absorbance wavelengths. A more time consuming approach could include the insertion of ROS-specific biosensors, that fluoresce in response to H_2O_2 (Choi et al. 2012). However, these sensors are limited by their spatial expression, exclusive to the cytosol or peroxisome.

More recent work with mitochondrial specific H_2O_2 biosensors in mammalian cell cultures is promising (Zhang et al. 2018), but requires testing *in planta.*

Previous gas exchange measurements of the single *Aox1a* OEX strongly correlated respiration rate in the light with the reduction state of the photosynthetic ETC and maintenance of leaf water use efficiency under drought conditions (Dahal & Vanlerberghe 2017). In our experiments, we saw trends across all dual OEX lines of increased respiration in the light under control conditions while there were no changes to the single *Aox1a* OEX. This could indicate that the presence of NDB2 is able to engage the ETC pathway, increasing respiration. Notably, all single *Ndb2* OEX lines saw even greater increases in respiration. This suggests that the flux through NDB2 may be regulated through the presence of AOX1a, reducing rates of respiration. Although measurements of respiration under MLD were not possible in these experiments due to difficulty obtaining gas exchange measurements under severe drought conditions, it is suggested that the increased respiration under control conditions may have carried through under these conditions. A further experiment using the leaf clamp technique instead of whole rosette measurements and additionally under less severe drought will provide further insight into the ability of NDB2 to alter and adapt the photosynthetic system to drought.

Regulating stomatal aperture during drought is important in minimising water loss and maintaining photosynthetic function (Nilson & Assmann 2007). During drought, closing of the stomatal aperture allows the plant to reduce excess

transpiration by reducing loss of water through gas exchange. Measurements of transpiration were significantly reduced in all dual OEX lines compared to both the wildtype and *Aox1a* OEX lines, but they were similar in water content compared to all other lines under MLD. This further indicates that these lines may have a higher water use efficiency, maximising photosynthetic ability while also minimising water loss.

To provide further insight into the changes in gene expression brought on by altering the AP and how this improved recovery response, the use of transcriptomics was employed. Under both control and MLD conditions, both the single and dual OEX lines tested saw significant changes in thousands of genes. Under control conditions, the number of genes were significantly more altered in the single *Aox1a* OEX line. We also saw much more similar responses in the topmost altered genes in the dual OEX and wildtype in response to MLD compared to the single OEX. Relating this with what was seen previously in the phenotype experiments, the addition of *Ndb2* seems to provide a balancing effect to the changes in signalling brought on by *Aox1a* OEX. Additionally, upregulation of different AP members in response to the MLD stress especially in the dual OEX line, demonstrates the effects NDB2 can have on signalling affecting gene expression. It was suspected that the changes to AP expression were also having additional effects in redox balance affecting numerous other systems including photosynthesis, flavonoid, phenylpropanoid biosynthesis and a number of transcription factors.

Interestingly, there were a number of genes related to carbon/nitrogen balance

that suggested the plants were under an excess of energy. Genes such as *Bzip63*, *Miox2* and *Asn1* all play a role in this balance and were all significantly downregulated. It was argued that most of these genes were likely affected downstream of regulators *Snrk2-8* and a number of different MYB transcription factors that all show the ability to be regulated by redox status (Dubos et al. 2010; Zhu et al. 2017). Thus, it seems that altering AP expression has the ability to significantly alter redox state and result in significant downstream changes including the significant downregulation of a number of photosynthetic genes. With the addition of *Ndb2* to the single *Aox1a* OEX line, we see a mitigation of this effect, with significantly less genes altered, especially in the light harvesting complexes of the chloroplast. Even with such wide changes to transcription and likely redox balance, both lines manage to behave very similarly to the wildtype while under control conditions. It's only when exposed to the MLD stress that these expression changes become apparent. It may be that the decreased expression of these light harvesting and other photosynthetic genes in the transgenics, has provided an advantage while under high light intensities. By minimising the levels of photo damage, this could partly explain the improved recovery rates while under MLD. Additionally, the photo-inhibitive effects brought on by MLD could be mitigated by *Aox1a* and *Ndb2* OEX by equipping the plants with the extra capacity to deal with excess reductants exported by the chloroplast. Although the RNA-seq analysis has allowed us to gain an insight into the transcriptional changes and signalling alteration that led to improved recovery in the OEX lines, it doesn't provide any information on the potential metabolic changes that may have occurred as a result.

As such it may be useful to identify how these changes have altered the metabolomic profile and how this could have potentially improved the recovery ability. A potential avenue for investigation is the metabolites directly affected by the AP. Measurements of ADP:ATP and NADP:NADP(H) specific to the mitochondria are notoriously hard to obtain due to the contribution by the chloroplasts that would overwhelm any differences seen between lines. Additionally, these would not allow the origin of the difference to be known. A likely better option would be the use of biosensors that are mitochondrial specific, allowing insight into the differences seen in organelles (Vevea et al. 2013; Voon et al. 2018). These would require the insertion of these genes into the established lines that would take significant amount of time but could be a worthwhile endeavour. Other future works could also include further comprehensive analysis of the cell using proteomics and metabolomics. As was previously established in the transcriptomic data, many changes occurred that could have significantly altered the levels of many metabolic proteins and their derivatives. Without the direct measurement of these proteins and compounds, it is unknown how the transcriptomic data correlates with changes downstream and whether these changes have provided an additional benefit at the proteomic and ultimately metabolic level.

Appendix

7 Appendix

A7.1 Plant growth conditions

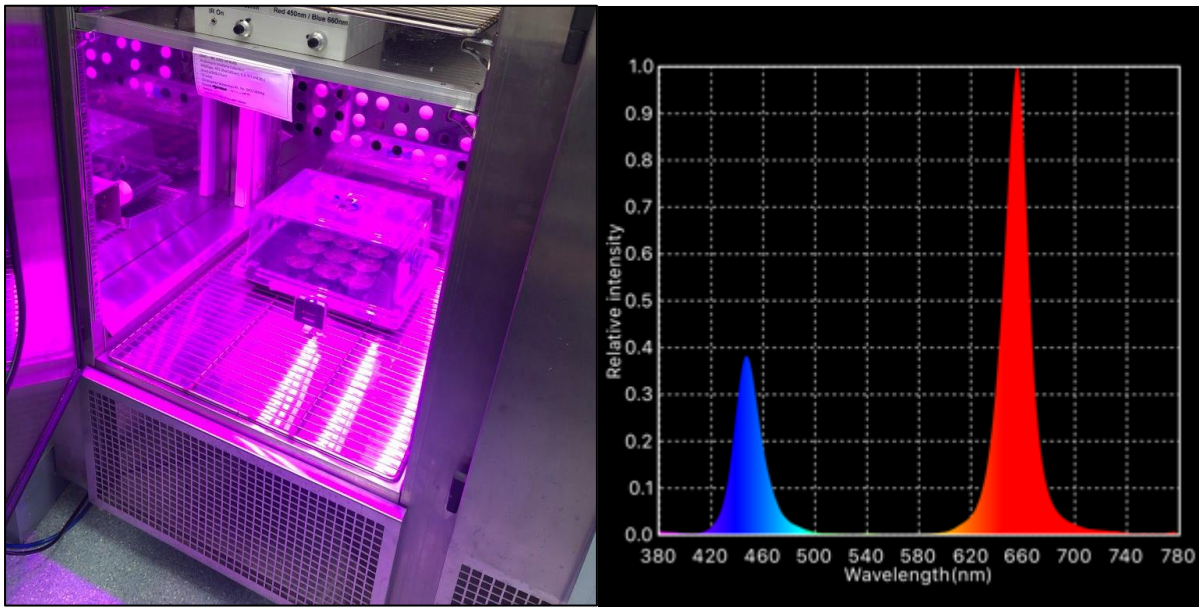

Figure A7.1 Lighting spectra used in growth cabinets

Relative intensity was measured using the AsenseTek Essence Lighting Passport light analyser in combination with the Spectrum Genius Essence Application. Sample photograph shows positioning of Lighting Passport

Table A7.1 Soil composition used in growth of A.thaliana

Soil pH was 5.7 to 5.8.

Bulk Ingredients	**Volume (L)**
Sand	200
Perlite	200
Peatmoss	200

Fertilizers	**Weight (g/kg soil)**
Iron Sulphate	500
Osmocote+	1500
Dolomite	1000
Gypsum	250
Ag Lime	500
Hydrated lime	200

A7.2 Buffers/Reagents/Solutions/Media

All reagents were of molecular grade and supplied by Sigma Aldrich (Australia) unless otherwise stated. Sterilisation of solutions was performed in an autoclave on a fluid cycle at 121°C for 15 minutes.

A7.2.1 Gel Electrophoresis

50X TAE buffer

1.98M Tris Base, 50mM EDTA *pH 8*, 22.8% (v/v) Glacial Acetic Acid

Diluted to 1x and used in the preparation of agarose gels and as running buffer in gel tanks.

A7.2.2 DNA extraction

DNA extraction buffer

100mM Tris adjusted to *pH 8* with HCl, 50mM EDTA *pH 8*, 500mM NaCl, 10mM β-mercaptoethanol

A7.2.3 RNA extraction

TRIzol-like reagent

38 % (v/v) phenol solution saturated with 0.1 M citrate buffer (pH 4.3), 62.5mM guanidine thiocyanate, 62.5 mM ammonium thiocyanate, 100.2 mM sodium acetate, 5 % (v/v) glycerol

A7.2.4 LB broth/agar

0.1% (w/v) Tryptone, 0.5% (w/v) Yeast Extract, 0.5% (w/v) NaCl, 1.5% (w/v) Agar (exclude agar for broth solutions), adjusted to pH 7 and autoclaved

A7.2.5 Mitochondrial isolation and assays

Isolation media

0.45 M mannitol, 10 mM TES, 10 mM KH_2PO_4, 2 mM EDTA, 0.6 % PVP-40 (v/v), 0.5 % (w/v) BSA, 10 mM L-ascorbic acid, 5 mM DTT and pH to 7.4 using NaOH

Wash media

450 mM mannitol, 10 mM TES, 1 mM EDTA and adjust pH to 7.2 with NaOH

Wash media with BSA

450 mM mannitol, 10 mM TES, 1 mM EDTA, 0.25 % (w/v) BSA and adjust pH to 7.2 with NaOH

Table A7.2 Percoll Gradient mixtures

Vol (ml)	60 % (v/v)	45 % (v/v)	28 % (v/v)	5% (v/v)
Per gradient	6	8	10	10
TOTAL	40	50	32.5 (x2)	32.5 (x2)
2.5x Wash Media +BSA	16	20	13	13
Percoll	24	22.5	9.1	1.625
MQ	0	7.5	10.4	17.85

Standard Reaction Media

0.3 M Sucrose, 10mM TES, 10mM KH2PO4, 2mM MgCl2, pH 7.2

A7.2.6 SDS-PAGE Gel Electrophoresis and Western Blots

2x Denaturing Loading Buffer

125mM Tris-HCl *pH 6.8*, 2% (w/v) SDS, 40% (w/v) Glycerol, 0.006% (w/v) Bromophenol Blue, 6M Urea. *Added 100mM DTT to a small aliquot prior to use*

Resolving Gel 10%

375mM Tris-HCl *pH 8.8*, 0.1% (w/v) SDS, 10% (w/v) Acrylamide, 0.4% (v/v) TEMED, 0.05% (w/v) Ammonium persulphate

Stacking Gel 4%

125mM Tris-HCl *pH 6.8*, 0.1% (w/v) SDS, 4% (w/v) Acrylamide, 0.1% (w/v) TEMED, 0.05% (w/v) Ammonium persulphate

Running Buffer

192mM Glycine, 25mM Trizma-Base, 0.01% SDS

Transfer Buffer

152mM Glycine, 25mM Trizma-base

Blocking Buffer

5% (w/v) Skim Milk Powder, 20mM Trizma-base *pH7.4*, 0.1% (v/v) Polyoxyethylene Sorbitan Monolaurate (Tween-20), 150mM NaCl

Table A7.3 Antibody dilutions used for western blotting

Protein probed	Primary dilution	Secondary antibody	Secondary dilution
AOX	1:1,000	Anti-mouse	1:10,000
NDB2	1:10,000	Anti-rabbit	1:10,000
PORIN	1:10,000	Anti-mouse	1:10,000

1x TBST Buffer

25mM Trizma-base, 0.1% (v/v) Polyoxyethylene Sorbitan Monolaurate (Tween-20), 150mM NaCl

A7.2.7 TBARS assay

TBA+ solution

20% (w/v) Trichloroacetic acid, 0.01% (w/v) β-Hydroxybutyric acid, 0.01% (w/v) Thiobarbituric acid

TBA- solution

20% (w/v) Trichloroacetic acid, 0.01% (w/v) β-Hydroxybutyric acid

A7.3 Primers

Table A7.4 Primer table used for PCR and qRT-PCR

Primers used in this project were manufactured by Life Technologies (U.S.A.) and Sigma Aldrich (U.S.A.) or sourced from previous projects which had employed Geneworks (Australia).

Primer name	Primer sequence (5'>3')	Tm	Product size (bp)		Application
		(^{0}C)	cDNA	gDNA	
Aox1aOVERcDNAFWDScreen	GATGATAACTCGCGGTGGAGCCAA	58	1100	1500	Screening *Aox1a* transgenics prior to transformation
Aox1aOVERcDNARWDScreen	GCCGAATCCAAGTATGGCTTAAGC				
AtNdb2Fw	CCGAAACTGATGATGTATCTAAG	60	172	271	Screening pEarlygate *Ndb2* OEX construct and *Ndb2* putative transformants. qRT-PCR for *Ndb2*
AtNdb2Rv	TTCTCACACTCTTCCATACGG				
AtAox1aFw	CTGGACCACGTTTGTTC	58	277	277	qRT-PCR for *Aox1a*
AtAox1aRv	ACACCCCAATAGCTCG				
AtPdf2Fw	ATTCCGATAGTCGACCAAGC	58	84	No product	qRT-PCR for *Pdf2*
AtPdf2Rv	AACATCAACATCTGGGTCTTCA				
AtUbiqFw	GACAGAGCAGAGAACATAAGG	58	184	292	qRT-PCR for *Ubq*
AtUbiqRv	TGGGGATTGGGTAAAGAGG				

A7.4 RNA Seq top highest altered gene lists

Table A7.5 Top 15 increased and decreased differentially expressed genes in wildtype MLD relative to wildtype under control conditions

Gene I.D.	Gene name	Description	Log_2 fold change relative to 5.2
AT3G02480	LEA	Late embryogenesis abundant protein	7.458
AT1G52690	LEA7	Late embryogenesis abundant protein	7.249
AT3G17520	LEA	Late embryogenesis abundant protein	7.099
AT5G13170	SWEET15	SWEET sucrose efflux transporter	7.01
AT5G59310	LTP4	Lipid transfer protein	6.917
AT5G06760	LEA4-5	Late embryogenesis abundant protein	6.5
AT4G24000	CSLG2	Cellulose synthase like g2	6.466
AT2G47770	TSPO	Tryptophan-rich sensory membrane protein	6.415
AT5G66400	RAB18	Responsive to ABA	6.091
AT4G15910	ATDI21	Drought-induced 21 protein	5.713
AT5G52300	LTI65	Low-temperature-induced 65 protein	5.538
AT1G05340	CYSTM1	cysteine-rich TM module stress tolerance protein	5.475
AT4G21320	HSA32	Heat-stress-associated 32 protein	5.378
AT4G23680	AT4G23680	Polyketide cyclase/dehydrase and lipid transport superfamily protein	5.212
AT5G50360	AIRT5	ABA-induced transcription repressor 5	5.173
AT3G22231	PCC1	Pathogen and circadian controlled 1 protein	-8.010
AT3G22235	CYSTM8	Cysteine-rich TM module stress tolerance protein	-6.877
AT4G14400	ACD6	Accelerated cell death 6 protein	-6.646
AT2G14560	LURP1	Late upregulated in response to *Hyaloperonospora parasitica* protein	-6.582
AT5G20630	GER3	Germin-like protein	-6.447
AT2G10940	AT2G10940	Bifunctional inhibitor/lipid-transfer protein	-6.437
AT5G44020	AT5G44020	HAD superfamily protein	-6.294
AT2G41090	CML10	Cytoplasmic, calcium binding calmodulin variant protein	-6.140
AT3G27690	LHCB2.4	Light-harvesting chlorophyll b-binding 2 protein	-6.082
AT1G19960	AT1G19960	Unknown protein	-5.880
AT5G54190	PORA	Light-dependent NADPH:protochlorophyllide oxidoreductase A	-5.779
AT1G31580	ECS1	Cell wall protein	-5.593
AT1G04680	AT1G04680	Pectin lyase-like superfamily protein	-5.254
AT3G12610	DRT100	Plays a role in DNA-damage repair/toleration	-5.220
AT1G20010	TUBB5	Beta tubulin protein	-5.189

Table A7.6 Top 15 increased and decreased differentially expressed genes in 5.2 MLD relative to 5.2 under control conditions

Gene I.D.	Gene name	Description	Log_2 fold change relative to 5.2
AT5G13170	SWEET15	SWEET sucrose efflux transporter protein	8.007
AT1G52690	LEA7	Late embryogenesis abundant protein	7.858
AT2G47770	TSPO	Tryptophan-rich sensory membrane protein	7.812
AT5G52300	LTI65	Stress induced protein	7.735
AT5G66400	RAB18	Responsive to ABA	7.726
AT3G22840	ELIP1	Early light-inducible protein.	7.724
AT3G17520	LEA	Late embryogenesis abundant protein	7.678
AT3G02480	LEA	Late embryogenesis abundant protein	7.403
AT4G24000	CSLG2	Protein similar to cellulose synthase	7.254
AT5G06760	LEA4-5	Late embryogenesis abundant protein	6.984
AT5G59310	LTP4	Lipid transfer protein	6.767
AT1G05340	AT1G05340	Cysteine-rich TM module stress tolerance protein	6.627
AT4G15910	ATDI21	Drought induced protein	6.595
AT2G21820	AT2G21820	Seed maturation protein	6.514
AT3G56275	AT3G56275	Pseudogene of expressed protein	6.257
AT5G20630	GER3	Germin-like protein	-7.661
AT2G10940	AT2G10940	Bifunctional inhibitor/lipid-transfer protein	-7.397
AT4G14400	ACD6	Accelerated cell death 6 protein	-7.139
AT3G22231	PCC1	Pathogen and circadian controlled 1	-6.766
AT2G41090	CML10	Cytoplasmic, calcium binding calmodulin variant protein	-6.521
AT5G22580	AT5G22580	Stress responsive A/B Barrel Domain-containing protein	-6.345
AT2G14560	LURP1	Late upregulated in response to *Hyaloperonospora parasitica* protein	-6.114
AT3G27690	LHCB2.4	Light-harvesting chlorophyll b-binding 2	-6.054
AT1G31580	ECS1	Cell wall protein	-5.895
AT3G22235	AT3G22235	Cysteine-rich TM module stress tolerance protein	-5.875
AT1G52190	NPF1.2	Low affinity nitrate transporter	-5.773
AT1G15125	AT1G15125	S-adenosyl-L-methionine-dependent methyltransferases	-5.734
AT1G74670	GASA6	Gibberellin-regulated protein	-5.690
AT5G54190	PORA	Light-dependent NADPH:protochlorophyllide oxidoreductase A	-5.450
AT4G04570	CRK40	Cysteine-rich receptor-like protein kinase	-5.448

Table A7.7 Top 15 increased and decreased differentially expressed genes in XX1 MLD relative to XX1 under control conditions

Gene I.D.	Gene name	Description	Log_2 fold change relative to 5.2
AT5G22470	PARP3	Poly(ADP-ribose) polymerase 3	10.583
AT2G29380	HAI3	Highly ABA-induced PP2C protein	10.538
AT4G31830	AT4G31830	Transmembrane protein	10.499
AT2G18590	AT2G18590	Major facilitator superfamily protein	10.082
AT3G51810	EM1	Late embryogenesis abundant protein	9.416
AT3G13784	AtCWINV5	Cell wall invertase 5	9.261
AT4G10250	HSP22.0	Endomembrane-localized small heat shock protein	9.197
AT5G04380	AT5G04380	S-adenosyl-L-methionine-dependent methyltransferase	9.065
AT1G07540	TRP5	Telomere-binding protein	8.944
AT3G12960	AT3G12960	Seed maturation protein 1	8.852
AT4G08570	AT4G08570	Heavy metal transport/detoxification protein	8.819
AT3G46230	HSP17.4A	Heat shock protein 17.4	8.744
AT5G04010	NSFBX	F-box family protein	8.672
AT5G62800	AT5G62800	RING/U-box and TRAF-like domain protein	8.637
AT2G42000	AT2G42000	Type 4 metallothionein protein	8.623
AT4G12470	AZI1	Azelaic acid induced 1	-11.376
AT1G05135	AT1G05135	Unknown protein	-10.821
AT3G57240	BG3	B-1,3-glucanase 3	-10.004
AT1G66940	AT1G66940	Kinase-like protein	-9.974
AT3G05730	AT3G05730	Defensin-like (DEFL) protein	-9.819
AT3G53190	AT3G53190	Pectin lyase-like protein	-9.732
AT5G44568	AT5G44568	Secreted peptide which functions in plant growth and pathogen defence.	-9.622
AT3G58120	BZIP61	BZIP transcription factor	-9.360
AT1G06080	ADS1	Homologous to delta 9 acyl-lipid desaturases/acyl-coa desaturases	-9.267
AT1G66100	AT1G66100	Pathogenesis related protein	-9.022
AT2G40610	EXPA8	Alpha-Expansin protein	-8.980
AT5G62360	AT5G62360	Pectin methyl-esterase inhibitor 13	-8.881
AT3G51280	AT3G51280	Tetratricopeptide repeat protein	-8.870
AT4G25110	AMC2	Type I metacaspase	-8.832
AT5G28630	AT5G28630	Glycine-rich protein	-8.824

Table A7.8 Top 15 increased and decreased differentially expressed genes in 5.2 relative to wildtype under control conditions

Gene I.D.	Gene name	Description	Log_2 fold change relative to 5.2
AT3G22370	AOX1A	Alternative oxidase 1A	5.071
AT4G05020	NDB2	Type II NAD(P)H dehydrogenase	4.491
AT5G44430	PDF1.2C	Plant defensin 1.2C	2.375
AT5G44420	PDF1.2A	Plant defensin 1.2	2.077
AT4G12490	AZI3	AZI family of lipid transfer proteins	2.071
AT3G49340	AT3G49340	Cysteine proteinases	1.997
AT3G16670	AT3G16670	Pollen Ole e 1 allergen and extensin family	1.788
AT1G04600	XI-A	Myosin-like protein	1.718
AT1G04220	KCS17	3-Ketoacyl-CoA synthase	1.649
AT3G27400	AT3G27400	Pectate lyase	1.640
AT5G08640	FLS1	Flavonol synthase	1.633
AT2G02990	RNS1	Ribonuclease T2 family	1.619
AT1G65060	4CL3	4-Coumarate:CoA ligase	1.547
AT1G78290	SRK2C	SNF1-related protein kinase	1.533
AT1G60590	AT1G60590	Pectin lyase-like	1.496
AT3G47340	ASN1	Glutamine-dependent asparagine synthetase	-2.727
AT2G19800	MIOX2	Myo-inositol oxygenase	-2.727
AT4G36850	AT4G36850	PQ-loop repeat family protein	-2.439
AT5G65080	MAF5	MADS-domain protein	-2.434
AT5G24770	VSP2	Vegetative storage protein 2	-2.405
AT3G15450	AT3G15450	Aluminium induced protein with YGL and LRDR motifs	-2.344
AT5G20250	RFS6	Glycosyl hydrolase/ Raffinose synthase	-2.333
AT3G09260	BGLU23	Beta-glucosidase	-2.266
AT3G30775	POX1	Proline oxidase	-2.263
AT1G62510	AT1G62510	Expressed in the root cortex.	-2.243
AT2G20670	AT2G20670	Sugar phosphate exchanger	-2.202
AT5G57550	XTH25	Xyloglucan endotransglucosylase/hydrolase	-2.077
AT5G42800	DFRA	Dihydroflavonol 4-reductase	-1.930
AT5G41340	UBC4	Ubiquitin conjugating	-1.929
AT5G49360	BXL1	Bifunctional (beta) pala-D-xylosidase/(alpha)-L-arabinofuranosidase	-1.818

Table A7.9 Top 15 increased and decreased differentially expressed genes in XX1 relative to wildtype under control conditions

Gene I.D.	Gene name	Description	Log_2 fold change relative to 5.2
AT3G22370	AOX1A	Alternative oxidase 1A	5.228
AT1G29418	AT1G29418	Transmembrane protein	3.552
AT5G35480	AT5G35480	Hypothetical protein	3.092
ATCG00630	PSAJ	Subunit J of photosystem I	2.851
AT4G12490	AT4G12490	AZI family of lipid transfer proteins	2.497
AT3G28270	AT3G28270	Peripheral membrane protein associated with endomembranes and plasmamembrane	2.456
AT1G73600	NMT3	S-adenosyl-L-methionine-dependent phosphoethanolamine N-methyltransferase	2.448
AT2G41800	AT2G41800	Cell wall protein	2.412
AT3G60140	BGLU30	Beta-glucosidase	2.239
AT1G31173	MIR167D	MicroRNA that targets ARF6 and ARF8	2.237
AT4G13493	MIR850A	MicroRNA of unknown function	2.234
AT3G14770	SWEET2	Nodulin mtn3 family protein	2.230
AT1G72645	AT1G72645	Transmembrane protein	2.216
AT2G32690	ATGRP23	Glycine-rich protein similar in structure to GRP5	2.157
AT1G25098	AT1G25098	Natural antisense transcript overlaps with AT1G25097	2.124
AT5G37940	AT5G37940	Zinc binding dehydrogenase family	-3.534
AT2G19800	MIOX2	Myo-inositol oxygenase 2	-3.177
AT3G15450	AT3G15450	Aluminium induced protein with YGL and LRDR motifs	-3.012
AT3G47340	ASN1	Glutamine-dependent asparagine synthase 1	-2.931
AT1G73330	ATDR4	Plant-specific protease inhibitor	-2.915
AT2G01021	AT2G01021	Hypothetical protein	-2.885
AT5G22430	AT5G22430	Pollen Ole e 1 allergen and extensin	-2.731
AT4G36850	AT4G36850	PQ-loop repeat family protein / transmembrane family protein	-2.663
AT5G57550	XTH25	Xyloglucan endotransglucosylase/hydrolase 25	-2.561
ATCG01170	RRN4.5S.2	Ribosomal rna4.5s,	-2.519
ATCG00970	RRN5S	Ribosomal rna5s	-2.454
ATCG01160	RRN5S	Ribosomal rna5s	-2.428
ATCG00960	RRN4.5S.1	Ribosomal rna4.5s	-2.401
AT2G15880	PEX3	Leucine-rich repeat/extensin 10	-2.396
AT5G24770	VSP2	Vegetative storage protein 2,	-2.368

Table A7.10 Top 15 increased and decreased differentially expressed genes in XX1 relative to 5.2 under control conditions

Gene I.D.	Gene name	Description	Log_2 fold change relative to 5.2
AT1G29418	AT1G29418	Transmembrane protein	3.934
AT1G13609	AT1G13609	Defensin-like (DEFL) family protein	3.053
AT1G29950	BHLH144	Basic helix-loop-helix (bhlh) DNA-binding superfamily protein	2.646
ATCG00630	PSAJ	Subunit J of photosystem I.	2.630
AT1G31173	MIR167D	MicroRNA that targets ARF6 and ARF8.	2.391
AT1G72645	AT1G72645	Transmembrane protein	2.066
AT1G25098	AT1G25098	Natural antisense transcript overlaps with AT1G25097	2.011
AT5G35480	AT5G35480	Hypothetical protein	2.006
ATCG00530	CEMA	Cema-like proton extrusion protein	1.909
AT2G43375	AT2G43375	No data present	1.763
AT2G39675	TAS1C	Trans-acting sirna1c	1.726
AT4G13493	MIR850A	MicroRNA of unknown function.	1.662
AT1G34418	AT1G34418	Small open reading frame	1.640
AT2G14090	AT2G14090	Pseudogene of F-box/RNI-like protein	1.610
AT2G24040	AT2G24040	Low temperature and salt responsive protein family	1.568
AT4G05020	NDB2	Type II NAD(P)H dehydrogenase	-4.473
AT5G22430	AT5G22430	Zinc-binding dehydrogenase protein	-2.952
AT5G37940	AT5G37940	Zinc-binding dehydrogenase protein	-2.804
AT2G01021	AT2G01021	Hypothetical protein	-2.350
ATCG01170	RRN4.5S.2	Chloroplast-encoded 4.5S ribosomal RNA,	-2.308
ATCG01160	RRN5S	Chloroplast-encoded 5S ribosomal RNA,	-2.205
AT2G04070	DTXL2	Boron activated protein	-2.066
ATCG00960	RRN4.5S.1	Chloroplast-encoded 4.5S ribosomal RNA,	-2.010
ATMG00030	ORF107A	Hypothetical protein	-1.755
ATMG00020	RRN26	Mitochondrial 26S ribosomal RNA protein	-1.729
ATCG00930	TRNI.2	tRNA-Ile	-1.665
ATCG01190	TRNA.2	tRNA-Ala	-1.591
AT2G18193	AT2G18193	P-loop containing nucleoside triphosphate hydrolases	-1.551
AT4G01390	AT4G01390	TRAF-like family protein	-1.549
ATCG00940	TRNA.1	tRNA-Ala	-1.524

Table A7.11 Top 15 increased and decreased differentially expressed genes in 5.2 relative to wildtype under MLD conditions

Gene I.D.	Gene name	Description	Log_2 fold change relative to 5.2
AT4G05020	NDB2	Type II NAD(P)H dehydrogenase	3.724
AT3G22370	AOX1A	Alternative oxidase 1A	3.219
AT3G48520	CYP94B3	Jasmonoyl-isoleucine-12-hydroxylase	2.652
AT1G54020	AT1G54020	GDSL-motif esterase/acyltransferase/lipase	2.423
AT2G40340	DREB2C	DREB subfamily A-2 of ERF/AP2 transcription factor family	2.359
AT2G03760	SOT12	Brassinosteroid sulfotransferase	2.279
AT4G20320	AT4G20320	Cytidine triphosphate synthase.	2.233
AT1G68050	ADO3	Flavin-binding kelch repeat F box protein	1.980
AT1G32860	AT1G32860	Glycosyl hydrolase superfamily protein	1.957
AT1G02930	GSTF6	Glutathione transferase	1.943
AT3G45970	EXLA1	EXPANSIN-LIKE protein	1.887
AT5G26920	CBP60G	Calmodulin-binding protein	1.887
AT4G33980	AT4G33980	Cold-regulated gene 28	1.887
AT2G18690	AT2G18690	Transmembrane protein	1.876
AT3G50970	XERO2	Dehydrin protein family	1.851
AT5G65080	MAF5	MADS-domain protein	-3.579
AT1G64780	AMT1-2	Ammonium transporter protein	-2.881
AT2G37170	PIP2-2	Plasma membrane intrinsic protein subfamily	-2.534
AT2G36120	DOT1	Glycine rich protein	-2.394
AT5G27360	SFP2	Sugar-porter family protein	-2.357
AT1G47510	AT5PTASE11	Phosphatidylinositol polyphosphate 5-phosphatase	-2.222
AT1G53540	HSP17.6C	Small heat-shock protein	-2.195
AT5G48390	ZIP4	Defective in meiotic chromosome segregation	-2.181
AT1G73330	ATDR4	Plant-specific protease inhibitor	-2.146
AT5G65010	ASN2	Asparagine synthetase	-2.137
AT4G16590	ATCSLA01	Cellulose synthase	-2.117
AT2G29290	AT2G29290	NAD(P)-binding Rossmann-fold protein	-2.093
AT5G52900	MAKR6	MEMBRANE-ASSOCIATED KINASE REGULATOR gene family	-2.070
AT3G23930	AT3G23930	Troponin T, skeletal protein	-2.044
AT5G54490	PBP1	PINOID (PID)-binding protein	-2.000

Table A7.12 Top 15 increased and decreased differentially expressed genes in XX1 relative to wildtype under MLD conditions

Gene I.D.	Gene name	Description	Log_2 fold change relative to 5.2
AT3G22370	AOX1A	Alternative oxidase 1A	3.840
AT1G29418	AT1G29418	Transmembrane protein	3.639
AT4G02005	AT4G02005	No information available	3.635
AT5G28080	WNK9	WNK family of protein kinases	3.536
AT3G29000	CML30	Calcium-binding EF-hand family protein	3.148
AT3G05890	RCI2B	Low temperature and salt responsive protein	3.115
AT5G06165	AT5G06165	No information available	2.513
AT2G15390	FUT4	Alpha-(1,2)-fucosyltransferase	2.510
AT1G71000	AT1G71000	Chaperone DNA j-domain protein	2.300
AT4G20320	AT4G20320	Cytidine triphosphate synthase	2.285
AT2G38240	AT2G38240	2-oxoglutarate/Fe(II)-dependent oxygenases	2.178
AT3G48520	CYP94B3	Jasmonoyl-isoleucine-12-hydroxylase	2.152
AT1G25098	AT1G25098	Natural antisense transcript overlaps with AT1G25097	2.087
AT1G34418	AT1G34418	Small open reading frame	2.062
AT2G40340	DREB2C	DREB subfamily A-2 of ERF/AP2 transcription factor	2.053
AT5G19600	SULTR3;5	Sulfate transporter	-4.018
AT3G09260	BGLU23	Beta-glucosidase	-2.785
AT1G73330	ATDR4	Plant-specific protease inhibitor	-2.712
AT1G64780	AMT1-2	Ammonium transporter	-2.478
AT3G52720	ACA1	Alpha carbonic anhydrase	-2.457
AT2G37180	PIP2-3	Plasma membrane intrinsic protein	-2.285
AT2G37170	PIP2-2	Plasma membrane intrinsic protein	-2.261
AT3G28740	CYP81D11	Cytochrome p450 family	-2.228
AT2G31980	CYS2	Phytocystatin 2	-2.225
ATCG01160	RRN5S	Chloroplast-encoded 5S ribosomal RNA	-2.132
AT5G65010	ASN2	Asparagine synthetase	-2.107
AT4G17340	TIP2-2	Tonoplast intrinsic protein	-1.959
AT4G28040	AT4G28040	Nodulin mtn21-like transporter	-1.937
AT3G52780	PAP20	Purple acid phosphatases	-1.793
AT3G29644	AT3G29644	Natural antisense transcript overlaps with AT3G29642	-1.748

Table A7.13 Top 15 increased and decreased differentially expressed genes in 5.2 relative to XX1 under MLD conditions

Gene I.D.	Gene name	Description	Log_2 fold change relative to 5.2
AT1G29418	AT1G29418	Transmembrane protein	4.086
AT4G02005	AT4G02005	No information available	3.393
AT1G72645	AT1G72645	Transmembrane protein	2.415
AT5G06165	AT5G06165	No information available	2.303
AT1G25098	AT1G25098	Natural antisense transcript overlaps with AT1G25097	2.044
AT1G11785	AT1G11785	Transmembrane protein	2.039
AT1G34418	AT1G34418	Small open reading frame	1.940
AT2G43375	AT2G43375	No information available	1.860
AT1G19396	AT1G19396	Hypothetical protein	1.811
ATCG00800	RPS3	Chloroplast ribosomal protein S3	1.746
AT2G39675	TAS1C	Trans-acting sirna1c	1.735
AT5G10946	AT5G10946	Hypothetical protein	1.634
AT1G31173	MIR167D	MicroRNA that targets ARF family members ARF6 and ARF8	1.613
AT5G56520	AT5G56520	Hypothetical protein	1.573
AT2G01175	AT2G01175	Transmembrane protein	1.530
AT4G05020	NDB2	Type II NAD(P)H dehydrogenase	-3.634
AT2G14610	PR1	Pathogenesis-related gene	-2.963
AT2G24850	TAT3	Tyrosine aminotransferase	-2.577
AT4G39950	CYP79B2	Cytochrome P450	-2.332
AT4G16260	AT4G16260	Beta-1,3-endoglucanase	-1.937
AT4G11320	AT4G11320	Papain family cysteine protease	-1.820
AT5G38900	AT5G38900	Thioredoxin superfamily protein	-1.600
AT2G45220	PME17	Plant invertase/pectin methylesterase inhibitor	-1.593
AT1G13520	AT1G13520	Hypothetical protein	-1.498
AT2G07698	AT2G07698	ATPase, F1 complex, alpha subunit protein	-1.487
AT1G02920	GSTF7	Glutathione transferase	-1.367
AT1G69140	AT1G69140	Hypothetical protein	-1.341
ATCG00350	PSAA	Psaa protein comprising the reaction center for photosystem I	-1.329
AT1G75040	PR5	Thaumatin-like protein involved in response to pathogens	-1.292
AT4G37390	YDK1	IAA-amido synthase	-1.263

8 References

Affourtit, C, Krab, K, Leach, GR, Whitehouse, DG & Moore, AL 2001, 'New insights in the regulation of the plant succinate dehydrogenase-on the role of the protonmotive force', *Journal of Biological Chemistry*, vol. 276, no. 35, pp. 32567-74.

Akhtar, TA, Lees, HA, Lampi, MA, Enstone, D, Brain, RA & Greenberg, BM 2010, 'Photosynthetic redox imbalance influences flavonoid biosynthesis in Lemna gibba', *Plant, Cell & Environment*, vol. 33, no. 7, pp. 1205-19.

Albury, MS, Affourtit, C, Crichton, PG & Moore, AL 2002, 'Structure of the plant alternative oxidase site-directed mutagenesis provides new information on the active site and membrane topology', *Journal of Biological Chemistry,* vol. 277, no. 2, pp. 1190-4.

Alford, SR, Rangarajan, P, Williams, SP & Gillaspy, GE 2012, 'myo-Inositol oxygenase is required for responses to low energy conditions in Arabidopsis thaliana', *Frontiers in plant science*, vol. 3, p. 69.

Apel, K & Hirt, H 2004, 'Reactive oxygen species: metabolism, oxidative stress, and signal transduction', *Annu. Rev. Plant Biol*, vol. 55, pp. 373-99.

Araujo, WL, Nunes-Nesi, A, Nikoloski, Z, Sweetlove, LJ, Fernie, A.R 2012, 'Metabolic control and regulation of the tricarboxylic acid cycle in photosynthetic and heterotrophic plant tissues', *Plant, cell & environment,* vol. 35, no. 1, pp. 1-21.

Atkin, O, Millar, A, Gardeström, P & Day, D 2000, 'Photosynthesis, carbohydrate metabolism and respiration in leaves of higher plants', *Photosynthesis*, Springer, pp. 153-75.

Baena-González, E, Rolland, F, Thevelein, JM & Sheen, J 2007a, 'A central integrator of transcription networks in plant stress and energy signalling', *Nature*, vol. 448, no. 7156, p. 938.

Baena-González, E, Rolland, F, Thevelein, JM & Sheen, J 2007b, 'A central integrator of transcription networks in plant stress and energy signalling', *Nature,* vol. 448, no. 7156, p. 938.

Baena-González, E & Sheen, J 2008, 'Convergent energy and stress signaling', *Trends in plant science,* vol. 13, no. 9, pp. 474-82.

Bak, S, Tax, FE, Feldmann, KA, Galbraith, DW & Feyereisen, R 2001, 'CYP83B1, a cytochrome P450 at the metabolic branch point in auxin and indole glucosinolate biosynthesis in Arabidopsis', *The Plant Cell*, vol. 13, no. 1, pp. 101-11.

Bartoli, CG, Gomez, F, Gergoff, G, Guiamét, JJ & Puntarulo, S 2005, 'Up-regulation of the mitochondrial alternative oxidase pathway enhances photosynthetic electron transport under drought conditions', *Journal of Experimental Botany*, vol. 56, no. 415, pp. 1269-76.

Behal, RH, Oliver, DJJ 1997, 'Biochemical and molecular characterization of fumarase from plants: purification and characterization of the enzyme—cloning, sequencing, and expression of the gene', *Archives of biochemistry and biophysics,* vol. 348, no. 1, pp. 65-74.

Bénit, P, Slama, A, Rustin, P 2008, 'Decylubiquinol impedes mitochondrial respiratory chain complex I activity', *Molecular and cellular biochemistry,* vol. 314, no. 1-2, p. 45.

Benz, R 1994, 'Permeation of hydrophilic solutes through mitochondrial outer membranes: review on mitochondrial porins', *Biochimica et Biophysica Acta (BBA)-Reviews on Biomembranes*, vol. 1197, no. 2, pp. 167-96.

Berardini, TZ, Reiser, L, Li, D, Mezheritsky, Y, Muller, R, Strait, E & Huala, E 2015, 'The Arabidopsis information resource: making and mining the "gold standard" annotated reference plant genome', *genesis,* vol. 53, no. 8, pp. 474-85.

Biagini, GA, Viriyavejakul, P, O'Neill, PM, Bray, PG, Ward, SA 2006, 'Functional characterization and target validation of alternative complex I of Plasmodium falciparum mitochondria', *Antimicrobial agents and chemotherapy,* vol. 50, no. 5, pp. 1841-51.

Bienert, GP, Møller, AL, Kristiansen, KA, Schulz, A, Møller, IM, Schjoerring, JK & Jahn, TP 2007, 'Specific aquaporins facilitate the diffusion of hydrogen peroxide across membranes', *Journal of Biological Chemistry,* vol. 282, no. 2, pp. 1183-92.

Bogeski, I, Gulaboski, R, Kappl, R, Mirceski, V, Stefova, M, Petreska, J & Hoth, M 2011, 'Calcium binding and transport by coenzyme Q', *Journal of the American Chemical Society,* vol. 133, no. 24, pp. 9293-303.

Boyes, DC, Zayed, AM, Ascenzi, R, McCaskill, AJ, Hoffman, NE, Davis, KR & Görlach, J 2001, 'Growth stage–based phenotypic analysis of Arabidopsis: a model for high throughput functional genomics in plants', *The Plant Cell,* vol. 13, no. 7, pp. 1499-510.

Bradford, MM 1976, 'A rapid and sensitive method for the quantitation of microgram quantities of protein utilizing the principle of protein-dye binding', *Analytical biochemistry*, vol. 72, no. 1-2, pp. 248-54.

Brand, MD, Affourtit, C, Esteves, TC, Green, K, Lambert, AJ, Miwa, S, Pakay, JL, Parker, N 2004, 'Mitochondrial superoxide: production, biological effects, and activation of uncoupling proteins', *Free Radical Biology and Medicine,* vol. 37, no. 6, pp. 755-67.

Bricker, DK, Taylor, EB, Schell, JC, Orsak, T, Boutron, A, Chen, Y-C, Cox, JE, Cardon, CM, Van Vranken, JG, Dephoure, N, Redin, C 2012, 'A mitochondrial pyruvate carrier required for pyruvate uptake in yeast, Drosophila, and humans', *Science,* vol. 337, no. 6090, pp. 96-100.

Bunik, VI & Fernie, AR 2009, 'Metabolic control exerted by the 2-oxoglutarate dehydrogenase reaction: a cross-kingdom comparison of the crossroad between energy production and nitrogen assimilation', *Biochemical Journal,* vol. 422, no. 3, pp. 405-21.

Canales, J, Rueda-López, M, Craven-Bartle, B, Avila, C, Cánovas, FM 2012, 'Novel insights into regulation of asparagine synthetase in conifers', *Frontiers in plant science*, vol. 3, p. 100.

Carré, J, Affourtit, C & Moore, AL 2011, 'Interaction of purified alternative oxidase from thermogenic Arum maculatum with pyruvate', *FEBS letters,* vol. 585, no. 2, pp. 397-401.

Carrie, C, Murcha, MW, Kuehn, K, Duncan, O, Barthet, M, Smith, PM, Eubel, H, Meyer, E, Day, DA & Millar, AH, Whelan, J 2008, 'Type II NAD (P) H dehydrogenases are targeted to mitochondria and chloroplasts or peroxisomes in Arabidopsis thaliana', *FEBS letters,* vol. 582, no. 20, pp. 3073-9.

Chai, T-T, Colmer, TD, Finnegan, PM 2010a, 'Alternative oxidase, a determinant of plant gametophyte fitness and fecundity', *Plant signalling & behavior,* vol. 5, no. 5, pp. 604-6.

Chai, T-T, Simmonds, D, Day, DA, Colmer, TD & Finnegan, PM 2010b, 'Photosynthetic performance and fertility are repressed in GmAOX2b antisense soybean', *Plant physiology,* vol. 152, no. 3, pp. 1638-49.

Choi, WG, Swanson, SJ & Gilroy, S 2012, 'High-resolution imaging of Ca2+, redox status, ROS and pH using GFP biosensors', *The Plant Journal*, vol. 70, no. 1, pp. 118-28.

Clayton, EE 1919, 'Hydrogen cyanide fumigation', *Botanical Gazette,* vol. 67, no. 6, pp. 483-500.

Clifton, R, Lister, R, Parker, KL, Sappl, PG, Elhafez, D, Millar, AH, Day, DA & Whelan, J 2005, 'Stress-induced co-expression of alternative respiratory chain components in Arabidopsis thaliana', *Plant molecular biology,* vol. 58, no. 2, p. 193.

Clifton, R, Millar, AH & Whelan, J 2006a, 'Alternative oxidases in Arabidopsis: a comparative analysis of differential expression in the gene family provides new insights into function of non-phosphorylating bypasses', *Biochimica et Biophysica Acta (BBA)-Bioenergetics*, vol. 1757, no. 7, pp. 730-41.

Clifton, R, Millar, AH & Whelan, J 2006b, 'Alternative oxidases in Arabidopsis: a comparative analysis of differential expression in the gene family provides new insights into function of non-phosphorylating bypasses', *Biochimica et Biophysica Acta (BBA)-Bioenergetics,* vol. 1757, no. 7, pp. 730-41.

Clough, SJ & Bent, AF 1998, 'Floral dip: a simplified method for Agrobacterium-mediated transformation of Arabidopsis thaliana', *The plant journal,* vol. 16, no. 6, pp. 735-43.

Considine, MJ, Holtzapffel, RC, Day, DA, Whelan, J & Millar, AH 2002, 'Molecular distinction between alternative oxidase from monocots and dicots', *Plant Physiology* vol. 129, no. 3, pp. 949-53.

Corpas, FJ, Gupta, DK & Palma, JM 2015, 'Production sites of reactive oxygen species (ROS) in organelles from plant cells', *Reactive oxygen species and oxidative damage in plants under stress*, Springer, pp. 1-22.

Costa, JH, McDonald, AE, Arnholdt-Schmitt, B, de Melo, DF 2014, 'A classification scheme for alternative oxidases reveals the taxonomic distribution and evolutionary history of the enzyme in angiosperms', *Mitochondrion,* vol. 19, pp. 172-83.

Cvetkovska, M & Vanlerberghe, GC 2012, 'Alternative oxidase modulates leaf mitochondrial concentrations of superoxide and nitric oxide', *New Phytologist,* vol. 195, no. 1, pp. 32-9.

Dahal, K, Martyn, GD & Vanlerberghe, GC 2015a, 'Improved photosynthetic performance during severe drought in Nicotiana tabacum overexpressing a nonenergy conserving respiratory electron sink', *New Phytologist*, vol. 208, no. 2, pp. 382-95.

Dahal, K, Martyn, GD & Vanlerberghe, GC 2015b, 'Improved photosynthetic performance during severe drought in Nicotiana tabacum overexpressing a nonenergy conserving respiratory electron sink', *New Phytologist,* vol. 208, no. 2, pp. 382-95.

Dahal, K & Vanlerberghe, GC 2017, 'Alternative oxidase respiration maintains both mitochondrial and chloroplast function during drought', *New Phytologist*, vol. 213, no. 2, pp. 560-71.

Dahal, K, Wang, J, Martyn, GD, Rahimy, F & Vanlerberghe, GC 2014, 'Mitochondrial alternative oxidase maintains respiration and preserves photosynthetic capacity during moderate drought in Nicotiana tabacum', *Plant Physiology,* vol. 166, no. 3, pp. 1560-74.

Davletova, S, Schlauch, K, Coutu, J & Mittler, R 2005, 'The zinc-finger protein Zat12 plays a central role in reactive oxygen and abiotic stress signaling in Arabidopsis', *Plant physiology,* vol. 139, no. 2, pp. 847-56.

Dehio, C & Schell, J 1994, 'Identification of plant genetic loci involved in a posttranscriptional mechanism for meiotically reversible transgene silencing', *Proceedings of the National Academy of Sciences,* vol. 91, no. 12, pp. 5538-42.

Del-Saz, N. F., Ribas-Carbo, M., McDonald, A. E., Lambers, H., Fernie, A. R., & Florez-Sarasa, I. 2018, 'An in vivo perspective of the role (s) of the alternative oxidase pathway', *Trends in Plant Science*, vol. 23, no.3, pp. 206-219.

Dietrich, K, Weltmeier, F, Ehlert, A, Weiste, C, Stahl, M, Harter, K & Dröge-Laser, W 2011, 'Heterodimers of the Arabidopsis transcription factors bZIP1 and bZIP53 reprogram amino acid metabolism during low energy stress', *The Plant Cell*, vol. 23, no. 1, pp. 381-95.

Djajanegara, I, Finnegan, PM, Mathieu, C, McCabe, T, Whelan, J & Day, DA 2002, 'Regulation of alternative oxidase gene expression in soybean', *Plant molecular biology,* vol. 50, no. 4-5, pp. 735-42.

Dojcinovic, D, Krosting, J, Harris, AJ, Wagner, DJ & Rhoads, DM 2005a, 'Identification of a region of the Arabidopsis AtAOX1a promoter necessary for mitochondrial retrograde regulation of expression', *Plant molecular biology*, vol. 58, no. 2, pp. 159-75.

Dojcinovic, D, Krosting, J, Harris, AJ, Wagner, DJ & Rhoads, DM 2005b, 'Identification of a region of the Arabidopsis AtAOX1a promoter necessary for mitochondrial retrograde regulation of expression', *Plant molecular biology,* vol. 58, no. 2, pp. 159-75.

Douce, R, Mannella, CA & Bonner Jr, WD 1973, 'The external NADH dehydrogenases of intact plant mitochondria', *Biochimica et Biophysica Acta (BBA)-Bioenergetics,* vol. 292, no. 1, pp. 105-16.

Dubos, C, Stracke, R, Grotewold, E, Weisshaar, B, Martin, C & Lepiniec, L 2010, 'MYB transcription factors in Arabidopsis', *Trends in plant science*, vol. 15, no. 10, pp. 573-81.

Earley, KW, Haag, JR, Pontes, O, Opper, K, Juehne, T, Song, K & Pikaard, CS 2006, 'Gateway-compatible vectors for plant functional genomics and proteomics', *The Plant Journal,* vol. 45, no. 4, pp. 616-29.

Efeoğlu, B, Ekmekci, Y & Cicek, N 2009, 'Physiological responses of three maize cultivars to drought stress and recovery', *South African Journal of Botany*, vol. 75, no. 1, pp. 34-42.

Eisenhut, M, Bräutigam, A, Timm, S, Florian, A, Tohge, T, Fernie, AR, Bauwe, H & Weber, AP 2017, 'Photorespiration is crucial for dynamic response of photosynthetic metabolism and stomatal movement to altered CO2 availability', *Molecular plant,* vol. 10, no. 1, pp. 47-61.

Elhafez, D, Murcha, MW, Clifton, R, Soole, KL, Day, DA, Whelan, J 2006, 'Characterization of mitochondrial alternative NAD (P) H dehydrogenases in Arabidopsis: intraorganelle location and expression', *Plant and Cell Physiology* , vol. 47, no. 1, pp. 43-54.

Elmayan, T & Vaucheret, H 1996, 'Expression of single copies of a strongly expressed 35S transgene can be silenced post-transcriptionally', *The Plant Journal,* vol. 9, no. 6, pp. 787-97.

English, JJ, Mueller, E & Baulcombe, DC 1996, 'Suppression of virus accumulation in transgenic plants exhibiting silencing of nuclear genes', *The Plant Cell,* vol. 8, no. 2, pp. 179-88.

Escobar, MA, Franklin, KA, Svensson, ÅS, Salter, MG, Whitelam, GC & Rasmusson, AG 2004, 'Light regulation of the Arabidopsis respiratory chain. Multiple discrete photoreceptor responses contribute to induction of type II NAD (P) H dehydrogenase genes', *Plant Physiology,* vol. 136, no. 1, pp. 2710-21.

Escobar, MA, Geisler, DA & Rasmusson, AG 2006, 'Reorganization of the alternative pathways of the Arabidopsis respiratory chain by nitrogen supply: opposing effects of ammonium and nitrate', *The Plant Journal*, vol. 45, no. 5, pp. 775-88.

Eslake, S 2018, *The economic impact of farm drought in rural Australia*, Australian Institute of Public Directors, viewed 27 August 2019, <http://aicd.companydirectors.com.au/membership/company-director-magazine/2018-back-editions/october/economist-the-big-dry>.

Estavillo, GM, Crisp, PA, Pornsiriwong, W, Wirtz, M, Collinge, D, Carrie, C, Giraud, E, Whelan, J, David, P & Javot, H, Brearley, C, 2011, 'Evidence for a SAL1-PAP chloroplast retrograde pathway that functions in drought and high light signaling in Arabidopsis', *The Plant Cell,* vol. 23, no. 11, pp. 3992-4012.

Evans, GC 1972, *The quantitative analysis of plant growth*, vol. 1, Univ of California Press.

Falk, KL, Behal, RH, Xiang, C & Oliver, DJ 1998, 'Metabolic bypass of the tricarboxylic acid cycle during lipid mobilization in germinating oilseeds: regulation of NAD+-dependent isocitrate dehydrogenase versus fumarase', *Plant Physiology,* vol. 117, no. 2, pp. 473-81.

Feng, H, Guan, D, Sun, K, Wang, Y, Zhang, T & Wang, R 2013, 'Expression and signal regulation of the alternative oxidase genes under abiotic stresses', *Acta Biochim Biophys Sin*, vol. 45, no. 12, pp. 985-94.

Fini, A, Brunetti, C, Di Ferdinando, M, Ferrini, F & Tattini, M 2011, 'Stress-induced flavonoid biosynthesis and the antioxidant machinery of plants', *Plant signaling & behavior*, vol. 6, no. 5, pp. 709-11.

Finnegan, PM, Soole, KL & Umbach, AL 2004, 'Alternative mitochondrial electron transport proteins in higher plants', in *Plant mitochondria: from genome to function*, Springer, pp. 163-230.

Fiorani, F, Umbach, AL & Siedow, JN 2005, 'The alternative oxidase of plant mitochondria is involved in the acclimation of shoot growth at low temperature. A study of Arabidopsis AOX1a transgenic plants', *Plant physiology,* vol. 139, no. 4, pp. 1795-805.

Flexas, J & Medrano, H 2002, 'Energy dissipation in C3 plants under drought', *Functional Plant Biology,* vol. 29, no. 10, pp. 1209-15.

Florez-Sarasa, I, Flexas, J, Rasmusson, AG, Umbach, AL, Siedow, JN, Ribas-Carbo, M 2011, 'In vivo cytochrome and alternative pathway respiration in leaves of Arabidopsis thaliana plants with altered alternative oxidase under different light conditions', *Plant, Cell & Environment,* vol. 34, no. 8, pp. 1373-83.

Foyer, CH, Lelandais, M & Kunert, KJ 1994, 'Photooxidative stress in plants', *Physiologia plantarum,* vol. 92, no. 4, pp. 696-717.

Foyer, CH & Noctor, G 2003, 'Redox sensing and signalling associated with reactive oxygen in chloroplasts, peroxisomes and mitochondria', *Physiologia plantarum,* vol. 119, no. 3, pp. 355-64.
Frederico, AM, Zavattieri, MA, Campos, MD, Cardoso, HG, McDonald, AE & Arnholdt-Schmitt, B 2009, 'The gymnosperm Pinus pinea contains both AOX gene subfamilies, AOX1 and AOX2', *Physiologia Plantarum,* vol. 137, no. 4, pp. 566-77.

Fu, A, Liu, H, Yu, F, Kambakam, S, Luan, S & Rodermel, S 2012, 'Alternative oxidases (AOX1a and AOX2) can functionally substitute for plastid terminal oxidase in Arabidopsis chloroplasts', *The Plant Cell,* vol. 24, no. 4, pp. 1579-95

Fujita, Y, Nakashima, K, Yoshida, T, Katagiri, T, Kidokoro, S, Kanamori, N, Umezawa, T, Fujita, M, Maruyama, K & Ishiyama, K 2009, 'Three SnRK2 protein kinases are the main positive regulators of abscisic acid signaling in response to water stress in Arabidopsis', *Plant and Cell Physiology*, vol. 50, no. 12, pp. 2123-32.

Furihata, T, Maruyama, K, Fujita, Y, Umezawa, T, Yoshida, R, Shinozaki, K & Yamaguchi-Shinozaki, K 2006, 'Abscisic acid-dependent multisite phosphorylation regulates the activity of a transcription activator AREB1', *Proceedings of the National Academy of Sciences*, vol. 103, no. 6, pp. 1988-93.

Gadjev, I, Stone, JM, Gechev, TS 2008, 'Programmed cell death in plants: new insights into redox regulation and the role of hydrogen peroxide', *International review of cell and molecular biology,* vol. 270, pp. 87-144.

Gandin, A, Duffes, C, Day, DA, Cousins, AB 2012, 'The absence of alternative oxidase AOX1A results in altered response of photosynthetic carbon assimilation to increasing CO2 in Arabidopsis thaliana', *Plant and Cell Physiology,* vol. 53, no. 9, pp. 1627-37.

Gaufichon, L, Reisdorf-Cren, M, Rothstein, SJ, Chardon, F & Suzuki, A 2010, 'Biological functions of asparagine synthetase in plants', *Plant Science*, vol. 179, no. 3, pp. 141-53.

Gechev, TS, Van Breusegem, F, Stone, JM, Denev, I & Laloi, C 2006, 'Reactive oxygen species as signals that modulate plant stress responses and programmed cell death', *Bioessays,* vol. 28, no. 11, pp. 1091-101.

Geisler, DA, Broselid, C, Hederstedt, L & Rasmusson, AG 2007, 'Ca2+-binding and Ca2+-independent respiratory NADH and NADPH dehydrogenases of Arabidopsis thaliana', *Journal of Biological Chemistry,* vol. 282, no. 39, pp. 28455-464

Gelhaye, E, Rouhier, N, Gérard, J, Jolivet, Y, Gualberto, J, Navrot, N, Ohlsson, P-I, Wingsle, G, Hirasawa, M, Knaff, D, Wang, H 2004, 'A specific form of thioredoxin h occurs in plant mitochondria and regulates the alternative oxidase', *Proceedings of the National Academy of Sciences,* vol. 101, no. 40, pp. 14545-50.
Gigolashvili, T, Berger, B, Mock, HP, Müller, C, Weisshaar, B & Flügge, UI 2007, 'The transcription factor HIG1/MYB51 regulates indolic glucosinolate biosynthesis in Arabidopsis thaliana', *The Plant Journal*, vol. 50, no. 5, pp. 886-901.

Giordano, M, Chen, Y-B, Koblizek, M & Falkowski, PG 2005, 'Regulation of nitrate reductase in Chlamydomonas reinhardtii by the redox state of the plastoquinone pool', *European Journal of Phycology*, vol. 40, no. 4, pp. 345-52.

Giraud, E, Ho, LH, Clifton, R, Carroll, A, Estavillo, G, Tan, Y-F, Howell, KA, Ivanova, A, Pogson, BJ & Millar, AH, Whelan, J 2008, 'The absence of ALTERNATIVE OXIDASE1a in Arabidopsis results in acute sensitivity to combined light and drought stress', *Plant physiology,* vol. 147, no. 2, pp. 595-610.

Giraud, E, Van Aken, O, Ho, LH & Whelan, J 2009, 'The transcription factor ABI4 is a regulator of mitochondrial retrograde expression of ALTERNATIVE OXIDASE1a', *Plant physiology,* vol. 150, no. 3, pp. 1286-96.

Grant, N, Onda, Y, Kakizaki, Y, Ito, K, Watling, J & Robinson, S 2009, 'Two cys or not two cys? That is the question; alternative oxidase in the thermogenic plant sacred lotus', *Plant Physiology,* vol. 150, no. 2, pp. 987-95.

Gupta, KJ & Igamberdiev, AU 2015, 'Compartmentalization of reactive oxygen species and nitric oxide production in plant cells: an overview', in *Reactive Oxygen and Nitrogen Species Signaling and Communication in Plants*, Springer, pp. 1-14.

Guy, RD & Vanlerberghe, GC 2005, 'Partitioning of respiratory electrons in the dark in leaves of transgenic tobacco with modified levels of alternative oxidase', *Physiologia Plantarum*, vol. 125, no. 2, pp. 171-80.

Hansford, RG, Hogue, BA, Mildaziene, V 1997, 'Dependence of H 2 O 2 formation by rat heart mitochondria on substrate availability and donor age', *Journal of bioenergetics and biomembranes,* vol. 29, no. 1, pp. 89-95.

Hao, M-S, Jensen, AM, Boquist, A-S, Liu, Y-J & Rasmusson, AG 2015, 'The Ca2+-regulation of the mitochondrial external NADPH dehydrogenase in plants is controlled by cytosolic pH', *PLoS One,* vol. 10, no. 9, p. e0139224.

Herrmann, JM, Westermann, B & Neupert, W 2001, 'Analysis of protein-protein interactions in mitochondria by coimmunoprecipitation and chemical cross-linking', *Methods in cell biology*, vol. 65, pp. 217-30.

Herzig, S, Raemy, E, Montessuit, S, Veuthey, J-L, Zamboni, N, Westermann, B, Kunji, ER & Martinou, J-C 2012, 'Identification and functional expression of the mitochondrial pyruvate carrier', *Science,* vol. 337, no. 6090, pp. 93-6.

Hirai, MY, Sugiyama, K, Sawada, Y, Tohge, T, Obayashi, T, Suzuki, A, Araki, R, Sakurai, N, Suzuki, H & Aoki, K 2007, 'Omics-based identification of Arabidopsis Myb transcription factors regulating aliphatic glucosinolate biosynthesis', *Proceedings of the National Academy of Sciences*, vol. 104, no. 15, pp. 6478-83.

Ho, LH, Giraud, E, Uggalla, V, Lister, R, Clifton, R, Glen, A, Thirkettle-Watts, D, Van Aken, O & Whelan, J 2008, 'Identification of regulatory pathways controlling gene expression of stress-responsive mitochondrial proteins in Arabidopsis', *Plant physiology,* vol. 147, no. 4, pp. 1858-73.

Hodges, DM, DeLong, JM, Forney, CF & Prange, RK 1999, 'Improving the thiobarbituric acid-reactive-substances assay for estimating lipid peroxidation in plant tissues containing anthocyanin and other interfering compounds', *Planta,* vol. 207, no. 4, pp. 604-11.

Hoefnagel, MH, Wiskich, JT 1998, 'Activation of the plant alternative oxidase by high reduction levels of the Q-pool and pyruvate', *Archives of Biochemistry and Biophysics,* vol. 355, no. 2, pp. 262-70.

Hoffmann, WA & Poorter, H 2002, 'Avoiding bias in calculations of relative growth rate', *Annals of botany,* vol. 90, no. 1, pp. 37-42.

Holtorf, S, Apel, K & Bohlmann, H 1995, 'Comparison of different constitutive and inducible promoters for the overexpression of transgenes in Arabidopsis thaliana', *Plant molecular biology,* vol. 29, no. 4, pp. 637-46.

Holtzapffel, RC, Castelli, J, Finnegan, PM, Millar, AH, Whelan, J & Day, DA 2003, 'A tomato alternative oxidase protein with altered regulatory properties', *Biochimica et Biophysica Acta (BBA)-Bioenergetics,* vol. 1606, no. 1-3, pp. 153-62.

Igamberdiev, AU & Gardeström, P 2003, 'Regulation of NAD-and NADP-dependent isocitrate dehydrogenases by reduction levels of pyridine nucleotides in mitochondria and cytosol of pea leaves', *Biochimica et Biophysica Acta (BBA)-Bioenergetics,* vol. 1606, no. 1-3, pp. 117-25.

Ingelbrecht, I, Van Houdt, H, Van Montagu, M & Depicker, A 1994, 'Posttranscriptional silencing of reporter transgenes in tobacco correlates with DNA methylation', *Proceedings of the National Academy of Sciences,* vol. 91, no. 22, pp. 10502-6.
Ivanova, A, Law, SR, Narsai, R, Duncan, O, Lee, J-H, Zhang, B, Van Aken, O, Radomiljac, JD, van der Merwe, M & Yi, K 2014, 'A functional antagonistic relationship between auxin and mitochondrial retrograde signaling regulates alternative oxidase1a expression in Arabidopsis', *Plant Physiology*, vol. 165, no. 3, pp. 1233-54.

Jackson, TZ, Kirk; Hatfield-Dodds,Steve 2018, *Snapshot of Australian Agriculture*, Department of Agriculture and Water Resources, viewed 27 August 2019, <http://www.agriculture.gov.au/abares/Documents/snapshot-australian-agriculture.pdf>.

James, WO & Beevers, H 1950, 'The respiration of Arum spadix. A rapid respiration, resistant to cyanide', *The New Phytologist,* vol. 49, no. 3, pp. 353-74.

Juszczuk, IM, Flexas, J, Szal, B, Dąbrowska, Z, Ribas-Carbo, M & Rychter, AM 2007, 'Effect of mitochondrial genome rearrangement on respiratory activity, photosynthesis, photorespiration and energy status of MSC16 cucumber (Cucumis sativus) mutant', *Physiologia Plantarum,* vol. 131, no. 4, pp. 527-41.

Kanehisa, M 2019, 'Toward understanding the origin and evolution of cellular organisms', *Protein Science*, vol. 28, no. 11, pp. 1947-51.

Kanehisa, M & Goto, S 2000, 'KEGG: kyoto encyclopedia of genes and genomes', *Nucleic acids research*, vol. 28, no. 1, pp. 27-30.

Kanehisa, M, Sato, Y, Furumichi, M, Morishima, K & Tanabe, M 2019, 'New approach for understanding genome variations in KEGG', *Nucleic acids research*, vol. 47, no. D1, pp. D590-D5.

Kano, H, Kageyama, M 1977, 'Effects of cyanide on the respiration of musk melon (Cucumis melo L.) roots', *Plant and cell physiology,* vol. 18, no. 5, pp. 1149-53.

Karpinski, S, Escobar, C, Karpinska, B, Creissen, G & Mullineaux, PM 1997, 'Photosynthetic electron transport regulates the expression of cytosolic ascorbate peroxidase genes in Arabidopsis during excess light stress', *The Plant Cell,* vol. 9, no. 4, pp. 627-40.

Kim, MJ, Park, M-J, Seo, PJ, Song, J-S, Kim, H-J & Park, C-M 2012, 'Controlled nuclear import of the transcription factor NTL6 reveals a cytoplasmic role of SnRK2. 8 in the drought-stress response', *Biochemical Journal*, vol. 448, no. 3, pp. 353-63.

King, AD, Karoly, DJ & Henley, BJ 2017, 'Australian climate extremes at 1.5 C and 2 C of global warming', *Nature,* vol. 7, no. 6, p. 412.

King, BJ, Siddiqi, MY, Ruth, TJ, Warner, RL & Glass, AD 1993, 'Feedback regulation of nitrate influx in barley roots by nitrate, nitrite, and ammonium', *Plant Physiology*, vol. 102, no. 4, pp. 1279-86.

Kok, B 1948, *A Critical consideration of the quantum yield of Chlorella-photosynthesis*, W. Junk.

Korshunov, SS, Skulachev, VP & Starkov, AA 1997, 'High protonic potential actuates a mechanism of production of reactive oxygen species in mitochondria', *FEBS letters,* vol. 416, no. 1, pp. 15-8.

Kowaltowski, AJ, de Souza-Pinto, NC, Castilho, RF & Vercesi, AE 2009, 'Mitochondria and reactive oxygen species', *Free Radical Biology and Medicine*, vol. 47, no. 4, pp. 333-43.

Kozaki, A & Takeba, G 1996, 'Photorespiration protects C3 plants from photooxidation', *Nature,* vol. 384, no. 6609, p. 557.

Kudin, AP, Bimpong-Buta, NY-B, Vielhaber, S, Elger, CE & Kunz, WS 2004, 'Characterization of superoxide-producing sites in isolated brain mitochondria', *Journal of Biological Chemistry,* vol. 279, no. 6, pp. 4127-35.

Kussmaul, L & Hirst, J 2006, 'The mechanism of superoxide production by NADH: ubiquinone oxidoreductase (complex I) from bovine heart mitochondria', *Proceedings of the National Academy of Sciences,* vol. 103, no. 20, pp. 7607-12.

Lam, E, Kato, N & Lawton, M 2001, 'Programmed cell death, mitochondria and the plant hypersensitive response', *Nature,* vol. 411, no. 6839, p. 848.

Lee, CP, Eubel, H, Millar, AH 2010, 'Diurnal changes in mitochondrial function reveal daily optimization of light and dark respiratory metabolism in Arabidopsis', *Molecular & Cellular Proteomics*, vol. 9, no. 10, pp. 2125-39.

Li, C, Liang, D, Xu, R, Li, H, Zhang, Y, Qin, R, Li, L, Wei, PC, Yang, JB 2013, 'Overexpression of an alternative oxidase gene, OsAOX1a, improves cold tolerance in Oryza sativa L', *Genet Mol Res,* vol. 12, no. 4, pp. 5424-32.

Li, Z, Wakao, S, Fischer, BB & Niyogi, KK 2009, 'Sensing and responding to excess light', *Annual review of plant biology,* vol. 60, pp. 239-60.

Liu, J-H, Yan, Y, Ali, A, Yu, M-F, Xu, Q-J, Shi, P-J & Chen, L 2018, 'Simulation of crop growth, time to maturity and yield by an improved sigmoidal model', *Scientific reports*, vol. 8, no. 1, p. 7030.
Liu, J, Li, Z, Wang, Y & Xing, D 2014, 'Overexpression of ALTERNATIVE OXIDASE1a alleviates mitochondria-dependent programmed cell death induced by aluminium phytotoxicity in Arabidopsis', *Journal of experimental botany,* vol. 65, no. 15, pp. 4465-78.

Liu, Y-J, Norberg, FE, Szilágyi, A, De Paepe, R, Åkerlund, HE, Rasmusson, AG 2008, 'The mitochondrial external NADPH dehydrogenase modulates the leaf NADPH/NADP+ ratio in transgenic Nicotiana sylvestris', *Plant and cell physiology,* vol. 49, no. 2, pp. 251-63.

Macedo, ES, Sircar, D, Cardoso, H, Peixe, A & Arnholdt-Schmitt, B 2012, 'Involvement of alternative oxidase (AOX) in adventitious rooting of Olea europaea L. microshoots is linked to adaptive phenylpropanoid and lignin metabolism', *Plant cell reports*, vol. 31, no. 9, pp. 1581-90.

MacRae, E 2007, 'Extraction of plant RNA', *Protocols for nucleic acid analysis by nonradioactive probes*, Springer, pp. 15-24.

Maier, A, Zell, MB & Maurino, VG 2011, 'Malate decarboxylases: evolution and roles of NAD (P)-ME isoforms in species performing C4 and C3 photosynthesis', *Journal of Experimental Botany*, vol. 62, no. 9, pp. 3061-9.

Mair, A, Pedrotti, L, Wurzinger, B, Anrather, D, Simeunovic, A, Weiste, C, Valerio, C, Dietrich, K, Kirchler, T & Nägele, T 2015, 'SnRK1-triggered switch of bZIP63 dimerization mediates the low-energy response in plants', *Elife*, vol. 4, p. e05828.

Massonnet, C, Vile, D, Fabre, J, Hannah, MA, Caldana, C, Lisec, J, Beemster, GT, Meyer, RC, Messerli, G & Gronlund, JT 2010, 'Probing the reproducibility of leaf growth and molecular phenotypes: a comparison of three Arabidopsis accessions cultivated in ten laboratories', *Plant Physiology*, vol. 152, no. 4, pp. 2142-57.

Matiolli, CC, Tomaz, JP, Duarte, GT, Prado, FM, Del Bem, LEV, Silveira, AB, Gauer, L, Corrêa, LGG, Drumond, RD & Viana, AJC 2011, 'The Arabidopsis bZIP gene AtbZIP63 is a sensitive integrator of transient abscisic acid and glucose signals', *Plant Physiology*, vol. 157, no. 2, pp. 692-705.

Maxwell, DP, Wang, Y & McIntosh, L 1999, 'The alternative oxidase lowers mitochondrial reactive oxygen production in plant cells', *Proceedings of the National Academy of Sciences,* vol. 96, no. 14, pp. 8271-6.

McDonald, AE, Vanlerberghe, GC & Staples, JF 2009, 'Alternative oxidase in animals: unique characteristics and taxonomic distribution', *Journal of Experimental Biology,* vol. 212, no. 16, pp. 2627-34.
Melo, AM, Bandeiras, TM, Teixeira, M 2004, 'New insights into type II NAD (P) H: quinone oxidoreductases', *Microbiology and Molecular Biology Reviews,* vol. 68, no. 4, pp. 603-16.

Meng, X, Li, L, De Clercq, I, Narsai, R, Xu, Y, Hartmann, A, Claros, DL, Custovic, E, Lewsey, MG & Whelan, J, Berkowitz, O 2019, 'ANAC017 coordinates organellar functions and stress responses by reprogramming retrograde signaling', *Plant Physiology,* vol. 180, no. 1, pp. 634-53.

Meteorology, ABo 2019, *Drought*, Australian Bureau of Meteorology, viewed 27 August 2019, <http://www.bom.gov.au/climate/drought/>.

Michalecka, AM, Agius, SC, Møller, IM & Rasmusson, AG 2004, 'Identification of a mitochondrial external NADPH dehydrogenase by overexpression in transgenic Nicotiana sylvestris', *The Plant Journal,* vol. 37, no. 3, pp. 415-25.

Michalecka, AM, Svensson, ÅS, Johansson, FI, Agius, SC, Johanson, U, Brennicke, A, Binder, S & Rasmusson, AG 2003, 'Arabidopsis genes encoding mitochondrial type II NAD (P) H dehydrogenases have different evolutionary origin and show distinct responses to light', *Plant Physiology,* vol. 133, no. 2, pp. 642-52.

Millar, AH, Atkin, OK, Menz, RI, Henry, B, Farquhar, G & Day, DA 1998, 'Analysis of respiratory chain regulation in roots of soybean seedlings', *Plant Physiology*, vol. 117, no. 3, pp. 1083-93.

Millar, AH, Hoefnagel, MH, Day, DA & Wiskich, JT 1996, 'Specificity of the organic acid activation of alternative oxidase in plant mitochondria', *Plant Physiology,* vol. 111, no. 2, pp. 613-8.

Millar, AH, Whelan, J, Soole, KL & Day, DA 2011, 'Organization and regulation of mitochondrial respiration in plants', *Annual review of plant biology*, vol. 62, pp. 79-104.

Millar, AH, Wiskich, JT, Whelan, J & Day, DA 1993, 'Organic acid activation of the alternatlve oxidase of plant mitochondria', *FEBS letters,* vol. 329, no. 3, pp. 259-62.

Millar, H, Bergersen, F & Day, DA 1994, 'Oxygen affinity of terminal oxidases in soybean mitochondria', *Plant physiology and biochemistry (Paris)*, vol. 32, no. 6, pp. 847-52.

Møller, IM & Sweetlove, LJ 2010, 'ROS signalling–specificity is required', *Trends in plant science,* vol. 15, no. 7, pp. 370-4.

Moore, AL & Albury, MS 2008, *Further insights into the structure of the alternative oxidase: from plants to parasites*, Portland Press Limited, 0300-5127.

Moore, AL, Bonner Jr, WD, Rich, PR 1978, 'The determination of the proton-motive force during cyanide-insensitive respiration in plant mitochondria', *Archives of Biochemistry and Biophysics,* vol. 186, no. 2, pp. 298-306.

Moore, AL, Umbach, AL & Siedow, JN 1995, 'Structure-function relationships of the alternative oxidase of plant mitochondria: a model of the active site', *Journal of bioenergetics and biomembranes*, vol. 27, no. 4, pp. 367-77.

Murakami, Y & Toriyama, K 2008, 'Enhanced high temperature tolerance in transgenic rice seedlings with elevated levels of alternative oxidase, OsAOX1a', *Plant biotechnology,* vol. 25, no. 4, pp. 361-4.

Murphy, MP 2009, 'How mitochondria produce reactive oxygen species', *Biochemical journal,* vol. 417, no. 1, pp. 1-13.

Nakabayashi, R, Mori, T & Saito, K 2014, 'Alternation of flavonoid accumulation under drought stress in Arabidopsis thaliana', *Plant signaling & behavior*, vol. 9, no. 8, pp. 29518.

Nakata, M, Mitsuda, N, Herde, M, Koo, AJ, Moreno, JE, Suzuki, K, Howe, GA, Ohme-Takagi, M 2013, 'A bHLH-type transcription factor, ABA-INDUCIBLE BHLH-TYPE TRANSCRIPTION FACTOR/JA-ASSOCIATED MYC2-LIKE1, acts as a repressor to negatively regulate jasmonate signaling in Arabidopsis', *The Plant Cell,* vol. 25, no. 5, pp. 1641-56.

Nakazawa, M, Yabe, N, Ichikawa, T, Yamamoto, YY, Yoshizumi, T, Hasunuma, K & Matsui, M 2001, 'DFL1, an auxin-responsive GH3 gene homologue, negatively regulates shoot cell elongation and lateral root formation, and positively regulates the light response of hypocotyl length', *The Plant Journal*, vol. 25, no. 2, pp. 213-21.

Narusaka, M, Seki, M, Umezawa, T, Ishida, J, Nakajima, M, Enju, A & Shinozaki, K 2004, 'Crosstalk in the responses to abiotic and biotic stresses in Arabidopsis: analysis of gene expression in cytochrome P450 gene superfamily by cDNA microarray', *Plant molecular biology*, vol. 55, no. 3, pp. 327-42.

Née, G, Zaffagnini, M, Trost, P & Issakidis-Bourguet, E 2009, 'Redox regulation of chloroplastic glucose-6-phosphate dehydrogenase: A new role for f-type thioredoxin', *FEBS letters*, vol. 583, no. 17, pp. 2827-32.

Nelson, CJ, Li, L, Jacoby, RP & Millar, AH 2013, 'Degradation rate of mitochondrial proteins in Arabidopsis thaliana cells', *Journal of Proteome Research,* vol. 12, no. 7, pp. 3449-59.

Neuburger, M, Journet, E-P, Bligny, R, Carde, J-P, Douce, R 1982, 'Purification of plant mitochondria by isopycnic centrifugation in density gradients of Percoll', *Archives of Biochemistry and Biophysics,* vol. 217, no. 1, pp. 312-23.

Ng, S, Giraud, E, Duncan, O, Law, SR, Wang, Y, Xu, L, Narsai, R, Carrie, C, Walker, H & Day, DA 2013a, 'Cyclin-dependent kinase E1 (CDKE1) provides a cellular switch in plants between growth and stress responses', *Journal of Biological Chemistry*, vol. 288, no. 5, pp. 3449-59.

Ng, S, Ivanova, A, Duncan, O, Law, SR, Van Aken, O, De Clercq, I, Wang, Y, Carrie, C, Xu, L & Kmiec, B, Walker, H 2013b, 'A membrane-bound NAC transcription factor, ANAC017, mediates mitochondrial retrograde signaling in Arabidopsis', *The Plant Cell,* vol. 25, no. 9, pp. 3450-71.

Nilson, SE & Assmann, SM 2007, 'The control of transpiration. Insights from Arabidopsis', *Plant Physiology*, vol. 143, no. 1, pp. 19-27.

Noctor, G, De Paepe, R & Foyer, CH 2007, 'Mitochondrial redox biology and homeostasis in plants', *Trends in plant science,* vol. 12, no. 3, pp. 125-34.

Noguchi, K, Taylor, NL, Millar, AH, Lambers, H & Day, DA 2005, 'Response of mitochondria to light intensity in the leaves of sun and shade species', *Plant, Cell & Environment*, vol. 28, no. 6, pp. 760-71.

Noguchi, K & Terashima, I 2006, 'Responses of spinach leaf mitochondria to low N availability', *Plant, Cell & Environment*, vol. 29, no. 4, pp. 710-9.

Oancea, S, Stoia, M & Coman, D 2012, 'Effects of extraction conditions on bioactive anthocyanin content of Vaccinium corymbosum in the perspective of food applications', *Procedia Engineering,* vol. 42, pp. 489-95.

Oestreicher, G, Hogue, P, Singer, TP 1973, 'Regulation of succinate dehydrogenase in higher plants: II. Activation by substrates, reduced coenzyme Q, nucleotides, and anions', *Plant physiology,* vol. 52, no. 6, pp. 622-6.

Osakabe, Y, Osakabe, K, Shinozaki, K & Tran, L-SP 2014, 'Response of plants to water stress', *Frontiers in plant science,* vol. 5, p. 86.

Osmundsen, H 1981, 'Spectrophotometric procedure for measuring mitochondrial β-oxidation', *Methods in enzymology*, vol. 72, pp. 306-14.

Osmundsen, H & Bremer, J 1977, 'A spectrophotometric procedure for rapid and sensitive measurements of β-oxidation. Demonstration of factors that can be rate-limiting for β-oxidation', *Biochemical Journal,* vol. 164, no. 3, pp. 621-33.

Park, J-E, Park, J-Y, Kim, Y-S, Staswick, PE, Jeon, J, Yun, J, Kim, S-Y, Kim, J, Lee, Y-H & Park, C-M 2007, 'GH3-mediated auxin homeostasis links growth regulation with stress adaptation response in Arabidopsis', *Journal of Biological Chemistry*, vol. 282, no. 13, pp. 10036-46.

Pasqualini, S, Paolocci, F, Borgogni, A, Morettini, R, Ederli, L 2007, 'The overexpression of an alternative oxidase gene triggers ozone sensitivity in tobacco plants', *Plant, cell & environment,* vol. 30, no. 12, pp. 1545-56.

Petrov, V, Hille, J, Mueller-Roeber, B & Gechev, TS 2015, 'ROS-mediated abiotic stress-induced programmed cell death in plants', *Frontiers in plant science,* vol. 6, p. 69.

Podgórska, A, Ostaszewska-Bugajska, M, Borysiuk, K, Tarnowska, A, Jakubiak, M, Burian, M, Rasmusson, AG & Szal, B 2018, 'Suppression of External NADPH Dehydrogenase—NDB1 in Arabidopsis thaliana Confers Improved Tolerance to Ammonium Toxicity via Efficient Glutathione/Redox Metabolism', *International journal of molecular sciences*, vol. 19, no. 5, p. 1412.

Pu, X-j, Lv, X & Lin, H-H 2015, 'Unraveling the evolution and regulation of the alternative oxidase gene family in plants', *Development genes and evolution*, vol. 225, no. 6, pp. 331-9.

Purvis, AC 1997, 'Role of the alternative oxidase in limiting superoxide production by plant mitochondria', *Physiologia Plantarum*, vol. 100, no. 1, pp. 165-70.

Quiles, MJ 2006, 'Stimulation of chlororespiration by heat and high light intensity in oat plants', *Plant, Cell & Environment*, vol. 29, no. 8, pp. 1463-70.

Rabino, I, Mancinelli, AL 1986, 'Light, temperature, and anthocyanin production', *Plant Physiology,* vol. 81, no. 3, pp. 922-4.

Rasmusson, AG & Agius, SC 2001, 'Rotenone-insensitive NAD (P) H dehydrogenases in plants: immunodetection and distribution of native proteins in mitochondria', *Plant Physiology and Biochemistry*, vol. 39, no. 12, pp. 1057-66.

Rasmusson, AG & Escobar, MA 2007, 'Light and diurnal regulation of plant respiratory gene expression', *Physiologia Plantarum,* vol. 129, no. 1, pp. 57-67.

Rhoads, DM, Umbach, AL, Sweet, CR, Lennon, AM, Rauch, GS & Siedow, JN 1998, 'Regulation of the cyanide-resistant alternative oxidase of plant mitochondria identification of the cysteine residue involved in α-keto acid stimulation and intersubunit disulfide bond formation', *Journal of Biological Chemistry,* vol. 273, no. 46, pp. 30750-6.

Ribas-Carbo, M, Taylor, NL, Giles, L, Busquets, S, Finnegan, PM, Day, DA, Lambers, H, Medrano, H, Berry, JA, Flexas, J 2005, 'Effects of water stress on respiration in soybean leaves', *Plant Physiology*, vol. 139, no. 1, pp. 466-73.

Rossel, JB, Walter, PB, Hendrickson, L, Chow, WS, Poole, A, Mullineaux, PM, Pogson, BJ 2006, 'A mutation affecting ASCORBATE PEROXIDASE 2 gene expression reveals a link between responses to high light and drought tolerance', *Plant, Cell & Environment,* vol. 29, no. 2, pp. 269-81.

Rosso, D, Ivanov, AG, Fu, A, Geisler-Lee, J, Hendrickson, L, Geisler, M, Stewart, G, Krol, M, Hurry, V, Rodermel, SR 2006, 'IMMUTANS does not act as a stress-induced safety valve in the protection of the photosynthetic apparatus of Arabidopsis during steady-state photosynthesis', *Plant Physiology*, vol. 142, no. 2, pp. 574-85.

Royo, B, Moran, JF, Ratcliffe, RG & Gupta, KJ 2015, 'Nitric oxide induces the alternative oxidase pathway in Arabidopsis seedlings deprived of inorganic phosphate', *Journal of experimental botany,* vol. 66, no. 20, pp. 6273-80.

Rumeau, D, Peltier, G & Cournac, L 2007, 'Chlororespiration and cyclic electron flow around PSI during photosynthesis and plant stress response', *Plant, Cell & Environment*, vol. 30, no. 9, pp. 1041-51.

Rychter, AM, Chauveau, M, Bomsel, JL & Lance, C 1992, 'The effect of phosphate deficiency on mitochondrial activity and adenylate levels in bean roots', *Physiologia Plantarum,* vol. 84, no. 1, pp. 80-6.

Saha, B, Borovskii, G & Panda, SK 2016, 'Alternative oxidase and plant stress tolerance', *Plant signaling & behavior*, vol. 11, no. 12, p. e1256530.

Saisho, D, Nakazono, M, Lee, K-H, Tsutsumi, N, Akita, S, Hirai, A 2001, 'The gene for alternative oxidase-2 (AOX2) from Arabidopsis thaliana consists of five exons unlike other AOX genes and is transcribed at an early stage during germination', *Genes & genetic systems,* vol. 76, no. 2, pp. 89-97.

Salvemini, F, Franzé, A, Iervolino, A, Filosa, S, Salzano, S & Ursini, MV 1999, 'Enhanced glutathione levels and oxidoresistance mediated by increased glucose-6-phosphate dehydrogenase expression', *Journal of Biological Chemistry*, vol. 274, no. 5, pp. 2750-7.

Sambrook, J, Fritsch, EF & Maniatis, T 1989, *Molecular cloning: a laboratory manual*, Cold spring harbor laboratory press.

Schell, JC, Rutter, J 2013, 'The long and winding road to the mitochondrial pyruvate carrier', *Cancer & metabolism,* vol. 1, no. 1, p. 6.

Schneider, CA, Rasband, WS & Eliceiri, KW 2012, 'NIH Image to ImageJ: 25 years of image analysis', *Nature,* vol. 9, no. 7, p. 671.

Selinski, J, Scheibe, R, Day, DA & Whelan, J 2018, 'Alternative oxidase is positive for plant performance', *Trends in plant science*, vol. 23, no. 7, pp. 588-97.

Senkler, J, Senkler, M, Eubel, H, Hildebrandt, T, Lengwenus, C, Schertl, P, Schwarzländer, M, Wagner, S, Wittig, I & Braun, HP 2017, 'The mitochondrial complexome of Arabidopsis thaliana', *The Plant Journal*, vol. 89, no. 6, pp. 1079-92.

Sharkey, TD 1988, 'Estimating the rate of photorespiration in leaves', *Physiologia Plantarum*, vol. 73, no. 1, pp. 147-52.

Sharma, A, Shahzad, B, Rehman, A, Bhardwaj, R, Landi, M & Zheng, B 2019, 'Response of phenylpropanoid pathway and the role of polyphenols in plants under abiotic stress', *Molecules*, vol. 24, no. 13, p. 2452.

Sharma, P, Jha, AB, Dubey, RS & Pessarakli, MJJob 2012, 'Reactive oxygen species, oxidative damage, and antioxidative defense mechanism in plants under stressful conditions', *Journal of botany,* vol. 2012.

Sharp, RE, Matthews, MA & Boyer, JS 1984, 'Kok effect and the quantum yield of photosynthesis: light partially inhibits dark respiration', *Plant Physiology,* vol. 75, no. 1, pp. 95-101.

Shen, LC & Atkinson, DE 1970, 'Regulation of pyruvate dehydrogenase from Escherichia coli interactions of adenylate energy charge and other regulatory parameters', *Journal of Biological Chemistry*, vol. 245, no. 22, pp. 5974-8.

Shiba, T, Kido, Y, Sakamoto, K, Inaoka, DK, Tsuge, C, Tatsumi, R, Takahashi, G, Balogun, EO, Nara, T & Aoki, T 2013, 'Structure of the trypanosome cyanide-insensitive alternative oxidase', *Proceedings of the National Academy of Sciences*, vol. 110, no. 12, pp. 4580-5.

Shimoji, H & Yamasaki, H 2005, 'Inhibitory effects of flavonoids on alternative respiration of plant mitochondria', *Biologia plantarum*, vol. 49, no. 1, pp. 117-9.

Shin, R, Alvarez, S, Burch, AY, Jez, JM & Schachtman, DP 2007, 'Phosphoproteomic identification of targets of the Arabidopsis sucrose nonfermenting-like kinase SnRK2. 8 reveals a connection to metabolic processes', *Proceedings of the National Academy of Sciences*, vol. 104, no. 15, pp. 6460-5.

Siedow, JN & Umbach, AL 1995, 'Plant mitochondrial electron transfer and molecular biology', *The Plant Cell*, vol. 7, no. 7, p. 821.

Sieger, SM, Kristensen, BK, Robson, CA, Amirsadeghi, S, Eng, EW, Abdel-Mesih, A, Møller, IM & Vanlerberghe, GC 2005, 'The role of alternative oxidase in modulating carbon use efficiency and growth during macronutrient stress in tobacco cells', *Journal of Experimental Botany*, vol. 56, no. 416, pp. 1499-515.

Singh, S, Gupta, A, Kaur, N 2012, 'Differential responses of antioxidative defence system to long-term field drought in wheat (Triticum aestivum L.) genotypes differing in drought tolerance', *Journal of Agronomy and Crop Science,* vol. 198, no. 3, pp. 185-95.

Sircar, D, Cardoso, HG, Mukherjee, C, Mitra, A & Arnholdt-Schmitt, B 2012, 'Alternative oxidase (AOX) and phenolic metabolism in methyl jasmonate-treated hairy root cultures of Daucus carota L', *Journal of plant physiology*, vol. 169, no. 7, pp. 657-63.

Smith, C, Barthet, M, Melino, V, Smith, P, Day, D, Soole, KL 2011, 'Alterations in the mitochondrial alternative NAD (P) H dehydrogenase NDB4 lead to changes in mitochondrial electron transport chain composition, plant growth and response to oxidative stress', *Plant and cell physiology,* vol. 52, no. 7, pp. 1222-37.

Smith, CA 2010, *Altered Expression of The Non-Phosphorylation Electron Transport Chain Effects Growth and Stress Tolerance in Arabidopsis thaliana*, Flinders University, School of Biological Sciences.

Smith, CA, Melino, VJ, Sweetman, C & Soole, KL 2009, 'Manipulation of alternative oxidase can influence salt tolerance in Arabidopsis thaliana', *Physiologia Plantarum*, vol. 137, no. 4, pp. 459-72.

Smith, SM, Fulton, DC, Chia, T, Thorneycroft, D, Chapple, A, Dunstan, H, Hylton, C, Zeeman, SC, Smith, AM 2004, 'Diurnal changes in the transcriptome encoding enzymes of starch metabolism provide evidence for both transcriptional and posttranscriptional regulation of starch metabolism in Arabidopsis leaves', *Plant physiology*, vol. 136, no. 1, pp. 2687-99.

Sønderby, IE, Geu-Flores, F, Halkier, BA 2010, 'Biosynthesis of glucosinolates–gene discovery and beyond', *Trends in plant science*, vol. 15, no. 5, pp. 283-90.

Sperdouli, I, Moustakas, M 2012, 'Interaction of proline, sugars, and anthocyanins during photosynthetic acclimation of Arabidopsis thaliana to drought stress', *Journal of plant physiology*, vol. 169, no. 6, pp. 577-85.

Steyn, W, Wand, S, Holcroft, D, Jacobs, G 2002, 'Anthocyanins in vegetative tissues: a proposed unified function in photoprotection', *New Phytologist*, vol. 155, no. 3, pp. 349-61.

Strodtkötter, I, Padmasree, K, Dinakar, C, Speth, B, Niazi, PS, Wojtera, J, Voss, I, Do, PT, Nunes-Nesi, A & Fernie, AR, Linke, V 2009, 'Induction of the AOX1D isoform of alternative oxidase in A. thaliana T-DNA insertion lines lacking isoform AOX1A is insufficient to optimize photosynthesis when treated with antimycin A', *Molecular Plant*, vol. 2, no. 2, pp. 284-97.

Studart-Guimaraes, C, Gibon, Y, Frankel, N, Wood, CC, Zanor, MI, Fernie, AR, Carrari, F 2005, 'Identification and characterisation of the α and β subunits of succinyl CoA ligase of tomato', *Plant molecular biology*, vol. 59, no. 5, pp. 781-91.

Svensson, ÅS & Rasmusson, AG 2001, 'Light-dependent gene expression for proteins in the respiratory chain of potato leaves', *The Plant Journal*, vol. 28, no. 1, pp. 73-82.

Sweetlove, L, Heazlewood, J, Herald, V, Holtzapffel, R, Day, D, Leaver, C & Millar, A 2002, 'The impact of oxidative stress on Arabidopsis mitochondria', *The Plant Journal*, vol. 32, no. 6, pp. 891-904.

Sweetlove, LJ, Taylor, NL & Leaver, CJ 2007, 'Isolation of intact, functional mitochondria from the model plant Arabidopsis thaliana', *Mitochondria*, pp. 125-36.

Sweetman, C, Waterman, CD, Rainbird, BM, Smith, PMC, Jenkins, CL, Day, DA & Soole, KL 2019, 'AtNDB2 is the main external NADH dehydrogenase in mitochondria

and is important for tolerance to environmental stress', *Plant physiology,* vol. 181, no. 2, pp. 774-88

Tarasenko, V, Garnik, EY, Shmakov, V & Konstantinov, YM 2012, 'Modified alternative oxidase expression results in different reactive oxygen species contents in Arabidopsis cell culture but not in whole plants', *Biologia plantarum*, vol. 56, no. 4, pp. 635-40.

Thomas, PD, Campbell, MJ, Kejariwal, A, Mi, H, Karlak, B, Daverman, R, Diemer, K, Muruganujan, A, Narechania, A 2003, 'PANTHER: a library of protein families and subfamilies indexed by function', *Genome research,* vol. 13, no. 9, pp. 2129-41.

Thomas, PD, Kejariwal, A, Guo, N, Mi, H, Campbell, MJ, Muruganujan, A & Lazareva-Ulitsky, B 2006, 'Applications for protein sequence–function evolution data: mRNA/protein expression analysis and coding SNP scoring tools', *Nucleic acids research,* vol. 34, no. 2, pp. 645-50.

Tomé, F, Nägele, T, Adamo, M, Garg, A, Marco-llorca, C, Nukarinen, E, Pedrotti, L, Peviani, A, Simeunovic, A & Tatkiewicz, A 2014, 'The low energy signaling network', *Frontiers in plant science*, vol. 5, p. 353.

Turrens, JF 2003, 'Mitochondrial formation of reactive oxygen species', *The Journal of physiology,* vol. 552, no. 2, pp. 335-44.

Umbach, AL, Fiorani, F & Siedow, JN 2005, 'Characterization of transformed Arabidopsis with altered alternative oxidase levels and analysis of effects on reactive oxygen species in tissue', *Plant Physiology,* vol. 139, no. 4, pp. 1806-20.

Umbach, AL, Ng, VS & Siedow, JN 2006, 'Regulation of plant alternative oxidase activity: a tale of two cysteines', *Biochimica et Biophysica Acta (BBA)-Bioenergetics* , vol. 1757, no. 2, pp. 135-42.

Umbach, AL & Siedow, JN 1993, 'Covalent and noncovalent dimers of the cyanide-resistant alternative oxidase protein in higher plant mitochondria and their relationship to enzyme activity', *Plant physiology,* vol. 103, no. 3, pp. 845-54.

Umezawa, T, Yoshida, R, Maruyama, K, Yamaguchi-Shinozaki, K & Shinozaki, K 2004, 'SRK2C, a SNF1-related protein kinase 2, improves drought tolerance by controlling stress-responsive gene expression in Arabidopsis thaliana', *Proceedings of the National Academy of Sciences*, vol. 101, no. 49, pp. 17306-11.

Van Aken, O, Zhang, B, Law, S, Narsai, R & Whelan, J 2013, 'AtWRKY40 and AtWRKY63 modulate the expression of stress-responsive nuclear genes encoding mitochondrial and chloroplast proteins', *Plant Physiology*, vol. 162, no. 1, pp. 254-71.

Vanderauwera, S, Vandenbroucke, K, Inzé, A, Van De Cotte, B, Mühlenbock, P, De Rycke, R, Naouar, N, Van Gaever, T, Van Montagu, MC & Van Breusegem, F 2012a, 'AtWRKY15 perturbation abolishes the mitochondrial stress response that steers osmotic stress tolerance in Arabidopsis', *Proceedings of the National Academy of Sciences*, vol. 109, no. 49, pp. 20113-8.

Vanderauwera, S, Vandenbroucke, K, Inzé, A, Van De Cotte, B, Mühlenbock, P, De Rycke, R, Naouar, N, Van Gaever, T, Van Montagu, MC & Van Breusegem, F 2012b, 'AtWRKY15 perturbation abolishes the mitochondrial stress response that steers osmotic stress tolerance in Arabidopsis', *Proceedings of the National Academy of Sciences,* vol. 109, no. 49, pp. 20113-8.

Vanlerberghe, GC 2013a, 'Alternative oxidase: a mitochondrial respiratory pathway to maintain metabolic and signaling homeostasis during abiotic and biotic stress in plants', *International journal of molecular sciences*, vol. 14, no. 4, pp. 6805-47.

Vanlerberghe, GC, Day, DA, Wiskich, JT, Vanlerberghe, AE & McIntosh, L 1995, 'Alternative oxidase activity in tobacco leaf mitochondria (dependence on tricarboxylic acid cycle-mediated redox regulation and pyruvate activation)', *Plant Physiology,* vol. 109, no. 2, pp. 353-61.

Vanlerberghe, GC 2013b, 'Alternative oxidase: a mitochondrial respiratory pathway to maintain metabolic and signaling homeostasis during abiotic and biotic stress in plants', *International Journal of Molecular Sciences,* vol. 14, no. 4, pp. 6805-47.

Vaucheret, H, Béclin, C, Elmayan, T, Feuerbach, F, Godon, C, Morel, JB, Mourrain, P, Palauqui, JC & Vernhettes, S 1998, 'Transgene-induced gene silencing in plants', *The Plant Journal,* vol. 16, no. 6, pp. 651-9.

Verniquet, F, Gaillard, J, Neuburger, M & Douce, R 1991, 'Rapid inactivation of plant aconitase by hydrogen peroxide', *Biochemical Journal,* vol. 276, no. 3, pp. 643-8.

Vevea, JD, Wolken, DMA, Swayne, TC, White, AB & Pon, LA 2013, 'Ratiometric biosensors that measure mitochondrial redox state and ATP in living yeast cells', *Journal of Visualized Experiments*, no. 77, pp. 50633.

Vishwakarma, A, Bashyam, L, Senthilkumaran, B, Scheibe, R, Padmasree, K 2014, 'Physiological role of AOX1a in photosynthesis and maintenance of cellular redox

homeostasis under high light in Arabidopsis thaliana', *Plant Physiology and Biochemistry,* vol. 81, pp. 44-53.

Voon, CP, Guan, X, Sun, Y, Sahu, A, Chan, MN, Gardeström, P, Wagner, S, Fuchs, P, Nietzel, T, Versaw, WK 2018, 'ATP compartmentation in plastids and cytosol of Arabidopsis thaliana revealed by fluorescent protein sensing', *Proceedings of the National Academy of Sciences*, vol. 115, no. 45, pp. 10778-87.

Wagner, AM, Krab, K, Wagner, MJ & Moore, AL 2008, 'Regulation of thermogenesis in flowering Araceae: the role of the alternative oxidase', *Biophysica Acta (BBA)-Bioenergetics,* vol. 1777, no. 7-8, pp. 993-1000.

Wallström, SV, Florez-Sarasa, I, Araújo, WL, Aidemark, M, Fernández-Fernández, M, Fernie, AR, Ribas-Carbó, M & Rasmusson, AG 2014a, 'Suppression of the external mitochondrial NADPH dehydrogenase, NDB1, in Arabidopsis thaliana affects central metabolism and vegetative growth', *Molecular plant,* vol. 7, no. 2, pp. 356-68.

Wallström, SV, Florez-Sarasa, I, Araújo, WL, Escobar, MA, Geisler, DA, Aidemark, M, Lager, I, Fernie, AR, Ribas-Carbó, M, Rasmusson, AG 2014b, 'Suppression of NDA-type alternative mitochondrial NAD (P) H dehydrogenases in Arabidopsis thaliana modifies growth and metabolism, but not high light stimulation of mitochondrial electron transport', *Plant and Cell Physiology,* vol. 55, no. 5, pp. 881-96.

Wang, J & Vanlerberghe, GC 2013, 'A lack of mitochondrial alternative oxidase compromises capacity to recover from severe drought stress', *Physiologia Plantarum*, vol. 149, no. 4, pp. 461-73.

Wang, Y, Lyu, W, Berkowitz, O, Radomiljac, JD, Law, SR, Murcha, MW, Carrie, C, Teixeira, PF, Kmiec, B, Duncan, O, Van Aken, O 2016, 'Inactivation of mitochondrial complex I induces the expression of a twin cysteine protein that targets and affects cytosolic, chloroplastidic and mitochondrial function', *Molecular plant,* vol. 9, no. 5, pp. 696-710.

Watanabe, CK, Hachiya, T, Terashima, I, Noguchi, K 2008, 'The lack of alternative oxidase at low temperature leads to a disruption of the balance in carbon and nitrogen metabolism, and to an up-regulation of antioxidant defence systems in Arabidopsis thaliana leaves', *Plant, Cell & Environment*, vol. 31, no. 8, pp. 1190-202.

Watanabe, CK, Yamori, W, Takahashi, S, Terashima, I & Noguchi, K 2016, 'Mitochondrial alternative pathway-associated photoprotection of photosystem II is related to the photorespiratory pathway', *Plant and Cell Physiology*, vol. 57, no. 7, pp. 1426-31.

Whelan, J, Millar, AH & Day, DA 1996, 'The alternative oxidase is encoded in a multigene family in soybean', *Planta*, vol. 198, no. 2, pp. 197-201.

Wilson, PB, Estavillo, GM, Field, KJ, Pornsiriwong, W, Carroll, AJ, Howell, KA, Woo, NS, Lake, JA, Smith, SM, Millar H 2009, 'The nucleotidase/phosphatase SAL1 is a negative regulator of drought tolerance in Arabidopsis', *The Plant Journal,* vol. 58, no. 2, pp. 299-317.

Xu, L, Law, SR, Murcha, MW, Whelan, J & Carrie, C 2013, 'The dual targeting ability of type II NAD (P) H dehydrogenases arose early in land plant evolution', *BMC plant biology*, vol. 13, no. 1, p. 100.

Yoshida, K, Noguchi, KO 2009, 'Differential gene expression profiles of the mitochondrial respiratory components in illuminated Arabidopsis leaves', *Plant and cell physiology,* vol. 50, no. 8, pp. 1449-62.

Yoshida, K, Watanabe, CK, Hachiya, T, Tholen, D, Shibata, M, Terashima, I, Noguchi, KO 2011a, 'Distinct responses of the mitochondrial respiratory chain to long-and short-term high-light environments in Arabidopsis thaliana', *Plant, cell & environment,* vol. 34, no. 4, pp. 618-28.

Yoshida, K, Watanabe, CK, Terashima, I, Noguchi, KO 2011b, 'Physiological impact of mitochondrial alternative oxidase on photosynthesis and growth in Arabidopsis thaliana', *Plant, Cell & Environment,* vol. 34, no. 11, pp. 1890-9.

Yoshida, T, Fujita, Y, Maruyama, K, Mogami, J, Todaka, D, Shinozaki, K & Yamaguchi-Shinozaki, K 2015, 'Four A rabidopsis AREB/ABF transcription factors function predominantly in gene expression downstream of SnRK2 kinases in abscisic acid signalling in response to osmotic stress', *Plant, Cell & Environment*, vol. 38, no. 1, pp. 35-49.

Zhang, DW, Xu, F, Zhang, ZW, Chen, YE, Du, JB, Jia, SD, Yuan, S, Lin, HH 2010, 'Effects of light on cyanide-resistant respiration and alternative oxidase function in Arabidopsis seedlings', *Plant, cell & environment*, vol. 33, no. 12, pp. 2121-31.

Zhang, L-T, Zhang, Z-S, Gao, H-Y, Meng, X-L, Yang, C, Liu, J-G & Meng, Q-W 2012a, 'The mitochondrial alternative oxidase pathway protects the photosynthetic apparatus against photodamage in Rumex K-1 leaves', *BMC Plant Biology,* vol. 12, no. 1, p. 40.

Zhang, L, Gao, H, Zhang, Z, Xue, Z, Meng, QW 2012b, 'Multiple effects of inhibition of mitochondrial alternative oxidase pathway on photosynthetic apparatus in Rumex K-1 leaves', *Biologia plantarum,* vol. 56, no. 2, pp. 365-8.

Zhang, LT, Zhang, ZS, Gao, HY, Xue, ZC, Yang, C, Meng, XL & Meng, QW 2011, 'Mitochondrial alternative oxidase pathway protects plants against photoinhibition by alleviating inhibition of the repair of photodamaged PSII through preventing formation of reactive oxygen species in Rumex K-1 leaves', *Physiologia Plantarum*, vol. 143, no. 4, pp. 396-407.

Zhang, X, Gibhardt, CS, Cappello, S, Zimmermann, KM, Vultur, A, Bogeski, I 2018, 'Measuring Mitochondrial ROS in Mammalian Cells with a Genetically Encoded Protein Sensor', *BIO-PROTOCOL*, vol. 8, no. 2.

Zhao, C, Wang, X, Wang, X, Wu, K, Li, P, Chang, N, Wang, J, Wang, F, Li, J, Bi, Y 2015, 'Glucose-6-phosphate dehydrogenase and alternative oxidase are involved in the cross tolerance of highland barley to salt stress and UV-B radiation', *Journal of plant physiology*, vol. 181, pp. 83-95.

Zhu, M, Zhang, T, Ji, W, Silva-Sanchez, C, Song, W-y, Assmann, SM, Harmon, AC, Chen, S 2017, 'Redox regulation of a guard cell SNF1-related protein kinase in Brassica napus, an oilseed crop', *Biochemical Journal*, vol. 474, no. 15, pp. 2585-99.